

Graduation Thesis

XBeach-G as a Design Tool for Rock on mild slopes under wave loading.



XBeach-G as a Design Tool for Rock on mild slopes under wave loading.

Master of Science Thesis

M.G. Postma (Mark Germ)

Delft, July 1st 2016

+31 6 207 373 94



Graduation Committee:

Prof. Dr. ir. M.J.F. Stive

Ing. C. Kuiper

Dr. ir. M. Zijlema

Ir. D. Jumelet

Delft University of Technology - Hydraulic Engineering

Delft University of Technology - Hydraulic Engineering

Witteveen + Bos

Delft University of Technology – Environmental fluid mechanics

de Vries & van de Wiel Dredging & Environmental Solutions



**de Vries
& van de Wiel**

Dredging & Environmental Solutions

Faculty of Civil Engineering and Geosciences
Section Hydraulic Engineering
Stevingweg 1
2600 GA Delft
The Netherlands

Toetsenbordweg 11
1033 MZ Amsterdam
The Netherlands

PREFACE

This thesis is written to obtain the Master of Science degree at the Delft University of Technology. It is written for the contractor de Vries & van de Wiel which is a Dutch contractor with as core activity Hydraulic Engineering, Environmental engineering and Sand exploitation. De Vries & van de Wiel is part of the DEME group (Dredging, Environmental Marine Engineering) which is a Belgium dredging company with works all over the world.

The daily supervising is done by Daan Jumelet from de Vries & van de Wiel and the tutoring from the TU Delft came from Marcel Stive, Coen Kuiper and Marcel Zijlema.

In this preface I want to take the opportunity to thank all the people who support me during my graduation. During my thesis I felt enormously supported by my graduation committee who helped me with their advices. I always felt welcome to come along and ask my questions.

From de Vries & van de Wiel I want to thank Daan Jumelet for the daily supervision and warm welcome at the company. I want to thank Coen Kuiper for keeping me on track and his unconditional trust and enthusiasm. Marcel Zijlema helped me with understanding the model and Marcel Stive for giving his thoughts on the matter. From Deltares I want to thank Robert McCall for helping me with XBeach-G.

Finally I want to thank my family, friends and girlfriend who kept believing in me.

Mark Postma

Delft, July 2016

ABSTRACT

This study describes the stability of rock on a mild slope (e.g. milder than 1:6) under wave loading. This is done because an increasing number of situations occur where mild foreshores are protected from the wave and currents. The empirical stability formula, designed by VAN DER MEER [1988], is not valid for these kind of slopes. Nonetheless, an extrapolation of this VAN DER MEER [1988] formula is currently used to design for these mild slopes. Recent research shows that an optimisation is possible as the extrapolated VAN DER MEER [1988] formula seems to overestimate the erosion. This research tests XBeach-G on mild slopes to verify its applicability as a design method for mild slopes. XBeach-G is a process based 1D numerical model, designed to model the physics occurring on mild gravel beaches.

To verify the potential XBeach-G as a design tool, some of the VAN DER MEER [1988] tests are reproduced and the occurred damage is compared to two sediment transport formulas, the VAN RIJN, [2007] and NIELSEN, [2006]. Because the VAN DER MEER [1988] tests are executed on relative steep slopes, the slope angle is changed to more mild slopes. The observed trend is analysed on several hydrodynamic and morphodynamic parameters, such as the velocity, the acceleration, the shear stress and the sediment transport rate. Beside the slope, several other parameters such as the stone size; the phase lag angle and layer thickness are changed as well.

A comparison of the test results to the formulas show that neither of the two formulas are able to predict the trend of damage levels as is found in the tests. The NIELSEN, [2006] formula gives unexpected results for steeper slopes, and the VAN RIJN, [2007] formula for mild slopes. This report proposes to use the VAN RIJN, [2007] formula for steeper slopes and to use the NIELSEN, [2006] formula for mild slopes. (milder than 1:6). Considerable attention should be given to the calibration factors in the NIELSEN, [2006] formula as these have a significant effect on the formed erosion.

The model functions well enough for less detailed erosion profile estimations. The overall erosion depths and profile do not deflect that much and can be used for more dynamic profile descriptions.

Because there is not a lot of data for comparison, it is recommended to do additional tests to verify the observed results. The test programme should focus on the point of incipient motion for coarse sediment under an angle. Both formulas are designed for horizontal sandy beds. Adjustments have been made to use them for rocks on slopes. Further research should focus on these correction factors as these do not yet seem to be correct.

Keywords:

Xbeach-G
Rock protection
mild slopes
Gravel modelling
VAN DER MEER [1988]
VAN RIJN, [2007]
NIELSEN, [2006]
sediment transport

LIST OF FIGURES

Figure 1: Homogeneous and impermeable dike structures.....	4
Figure 2: Difference between statically stable and dynamic profiles for both mild as steep slopes.....	4
Figure 3: Experimental results G .J. Schiereck & Verhagen, [2012] and VAN DER MEER [1988] formula.	6
Figure 4: Statically stable results of XBeach-G for a homogeneous structure. Wit [2015].....	7
Figure 5: Left: Eroded area and maximum eroded depth versus the grain size. ; Right: Profile collapse from crest to bar. Wit [2015]	8
Figure 6: Iribarren number for different breaker types.	14
Figure 7: Overview experimental conditions wave flume.....	14
Figure 8: Typical Damage curve used by VAN DER MEER [1988]	15
Figure 9: VAN DER MEER [1988] formula for homogeneous and inhomogeneous structures with experimental data.	16
Figure 10: SCHIERECK & FONTIJN [1996], Design rule & VAN DER MEER [1988] formulae.....	17
Figure 11: Step at the wave breaking point and a berm at the high water mark.	18
Figure 12: Concept of the effect of breaking of a plunging breaker. (ADRIAN PEDROZO-ACUÑA ET AL., [2008])	19
Figure 13: Left: Uprush effects; Right: Downrush effects BUTT ET AL., [2001].....	21
Figure 14: Left; Effect of gravitational force; Right; Angle of repose per stone size G .J. SCHIERECK & VERHAGEN, [2012].	23
Figure 15: velocity and boundary layer in time. NIELSEN, [2006].....	25
Figure 16: Forces acting on a particle.....	27
Figure 17: Shields parameter adjusted by VAN RIJN, [1984].	28
Figure 18: Damage level; Left: Method of Wit; Right: Alternative method	32
Figure 19: Left: Influence initial profile VAN DER MEER [1988]; Right: Influence hydr. Forcing Wit [2015].....	33
Figure 20: Overview of the process based model XBeach-G.	35
Figure 21: groundwater; surface water and their interaction.	36
Figure 22: Beach erosion validation tests	43
Figure 23: Spectrum at different locations along the slope.....	43
Figure 24: Input limitations wave period vs. offshore water depth.....	45
Figure 25: Modelled profile.....	49
Figure 26: Executed tests with variation in slope and stone diameter visualised in the stability vs. iribarren graph.....	50
Figure 27: From left to right model size a, b and c respectively.	52
Figure 28: Calculated damage vs. relative erosion depth for both NIELSEN, [2006] as VAN RIJN, [2007] transport formula.	56
Figure 29: Test series C with test 1 for both the NIELSEN, [2006] as the VAN RIJN, [2007] method.....	57
Figure 30: Test series C with test 2 for both the NIELSEN, [2006] as the VAN RIJN, [2007] method.....	57
Figure 31: Slope effect with the VAN RIJN, [2007] transport formula for both tests series A as B.	59
Figure 32: Slope effect with the NIELSEN, [2006] transport formula for both tests series A as B.....	60
Figure 33: Test series B; Calculated Damage level vs. Iribarren number.	60
Figure 34: Damage in time for test 10.....	61

Figure 35: Test series A and B with different layer thickness for the VAN RIJN, [2007] transport formula	62
Figure 36: Test series B with changing slope and the VAN RIJN, [2007] transport formula	64
Figure 37: Test series B with changing slope and the NIELSEN, [2006] transport formula.....	65
Figure 38: Test series B with changing phase lag angle.	66
Figure 39: Slope effect with a bigger hydraulic conductivity.	67
Figure 40: velocity for test 10 with Van Rijn, [2007]; Nielsen, [2006] and no morphological updating	70
Figure 41: Acceleration for test 10 with the Van Rijn; NIELSEN, [2006] and the case without morphological updating.	72
Figure 42: Infiltration effects for test 10 for the three cases: NIELSEN, [2006]; VAN RIJN, [2007] and no morph. updating.....	74
Figure 43: shear stresses for test 10 with the VAN RIJN, [2007], the NIELSEN, [2006] and the VAN RIJN, [2007] with no morphological updating.....	76
Figure 44: Shear velocity for test 10 with the Nielsen and the case without no morphological updating	77
Figure 45: Shields parameter for test 10 with the VAN RIJN, [2007], the NIELSEN, [2006] and the case with no morphological updating.	79
Figure 46: Sediment transport rates for the VAN RIJN, [2007] and NIELSEN, [2006] transport method.	80
Figure 47: Sediment transport rates for test 10 with the VAN RIJN, [2007], the NIELSEN, [2006] transport formula	81

LIST OF TABLES

Table 1: 4 types of permeability described by VAN DER MEER [1988]/	12
Table 2: Allowed damage level for different slopes.....	13
Table 3: Number of tests executed by VAN DER MEER [1988].....	15
Table 4: Sediment classification (Chadwick, n.d.)	18
Table 5: Influence slope angle and internal angle of repose on the slope effect.	24
Table 6: Experimental test results WATANABE AND SATO [2004] used by NIELSEN, [2006]	31
Table 7: : Validation location and characteristics. (MCCALL, [2015])	42
Table 8: Wave height transformation from offshore to nearshore (MCCALL, [2015])	44
Table 9: Run-up validation results.....	44
Table 10: Overview current available data and model validation area.	46
Table 11: Overview used experimental test series.	47
Table 12: Overview Model input	49
Table 13: Stage B Tests executed for different parameters.....	51
Table 14: Calculated damage for Model a, Model b and Model c.	53
Table 15: Measured damage levels for tests series A and B.	53
Table 16: Relative erosion depth for tests series A and B.....	55
Table 17: Test series A and B with different layer thickness for the NIELSEN, [2006] transport formula	63
Table 18: Damage level of 1:6 slope tests with two different phase lag angles.	66
Table 19: Influence of the infiltration term.....	74
Table 20: critical shear stress according to VAN RIJN, [2007].....	78

LIST OF SYMBOLS

Symbol	Unit	Description
A_e	$[m^2]$	Eroded cross sectional area
α	$[-]$	Ratio seepage factor surface and bed
β	$[-]$	Groundwater head parabolic curvature coefficient
$c_{f,0}$	$[-]$	Bed friction coefficient(KOBAYASHI, OTTA, & ROY, [1987])
c_f	$[-]$	Bed friction coefficient plus ventilation effects
c_m	$[-]$	Coefficient of mass
c_v	$[-]$	Volume shape factor
c_n	$[-]$	Coefficient of grain density per unit of surface area
c_i	$[-]$	Inertia parameter set at $c_i = 1.0$
c_s	$[-]$	Smagorinsky constant ($c_s = 0.1$)
C'	$[m^{1/2}s]$	Chezy bed friction coefficient
D^*	$[-]$	Particle parameter
D_{n50}	$[m]$	Median nominal grain size
D_{50}	$[m]$	Median grain size from sieve analysis
D_{90}	$[m]$	Grain size that exceeds by size 90% of the sediment distribution
$\partial u / \partial t$	$[m/s^2]$	Acceleration
d_i	$[m]$	Infiltration wetting front thickness
Δ	$[-]$	Relative submerged weight
Δi	$[-]$	Relative submerged weight including effect of infiltration
f_c	$[-]$	Friction due to currents
f_w	$[-]$	Friction due to waves
f_s	$[-]$	Friction factor Nielsen
g	$[m/s^2]$	Gravity constanty (9.81)
\bar{H}	$[m]$	Depth – averaged hydraulic head
h_{gw}	$[m]$	Groundwater height
h	$[m]$	Waterdepth
H_s	$[m]$	Significant wave height
K	$[ms^{-1}]$	Hydraulic conductivity
L_0	$[m]$	Deep water wave length
n_p	$[-]$	Porosity
N	$[-]$	Number of waves
ξ	$[m]$	Free surface elevation
ξ_b	$[m]$	Bed level
ξ_{gw}	$[m]$	Groundwater level
ρ	$[kgm^{-3}]$	Density water
ρ_s	$[kgm^{-3}]$	Density stones
P	$[-]$	Notional permeability, specified by VAN DER MEER [1988]
P_b	$[kgm^{-1}s^{-2}]$	Surfance water pressure at the bed
θ	$[-]$	Shields parameter
θ_{cr}	$[-]$	Critical shields parameter
θ	$[-]v$	Phase lag angle
T_m	$[s]$	Mean wave period from time series
$T_{m,1-0}$	$[s]$	Spectral mean period
T_P	$[s]$	Peak period
T	$[s]$	Transport stage parameter
ζ_m	$[-]$	Iribarren number, using T_m
\bar{q}	$[m^2s^{-2}]$	Depth – averaged dynamic pressure
q_b	$[m^3s^{-1}m^{-1}]$	Bed sediment transport
Re	$[-]$	Reynolds number
s	$[-]$	Wave steepness

S	$[-]$	Damage level
S_s	$[ms^{-1}]$	Submarine water exchange
S_i	$[ms^{-1}]$	Infiltration water exchange
S_e	$[ms^{-1}]$	Exfiltration water exchange
$\tan(\beta)$	$[-]$	Local angle of the bed
$\tan(\alpha)$	$[-]$	Slope
τ_b	$[kgm^{-1}s^{-2}]$	Bed shear stress
$\tau_{b,inertia}$	$[kgm^{-1}s^{-2}]$	Bed shear stress due to inertia
$\tau_{b,cr}$	$[kgm^{-1}s^{-2}]$	Critical bed shear stress
$\tau_{b,drag}$	$[kgm^{-1}s^{-2}]$	Bed shear stress due to drag
$\tau_{b,c}$	$[kgm^{-1}s^{-2}]$	Shear stress due to currents
$\tau_{b,w}$	$[kgm^{-1}s^{-2}]$	Shear stress due to waves
$\tau_{b,cw}$	$[kgm^{-1}s^{-2}]$	Shear stress due to currents and waves
u	$[ms^{-1}]$	Velocity
u_*	$[ms^{-1}]$	Shear velocity
$u_{*,cr}$	$[ms^{-1}]$	Critical shear velocity
u_{gw}	$[ms^{-1}]$	Groundwater velocity
ν_h	$[m^2s^{-1}]$	Horizontal viscosity
γ	$[-]$	Correction factor
\emptyset	$[^\circ]$	Internal angle of repose
Φ	$[-]$	Dimensionless ventilation parameter of CONLEY AND INMAN [1994]

TABLE OF CONTENTS

PREFACE.....	IV
ABSTRACT	VI
LIST OF FIGURES	VIII
LIST OF TABLES.....	IX
LIST OF SYMBOLS	X
TABLE OF CONTENTS	XII
INTRODUCTION & PROBLEM DEFINITION	2
1.1 BACKGROUND INFORMATION.....	2
1.2 GOAL & RESEARCH QUESTIONS	2
1.3 SCOPE DEFINITION	3
1.4 REPORT OUTLINE	3
1.5 TERMINOLOGY	3
MOTIVATION FOR THE RESEARCH.....	6
2.1 EXPERIMENTAL TESTS - SCHIERECK & FONTIJN [1996],	6
2.2 XBEACH-G RESULTS - WIT [2015].....	7
2.2.1 <i>Statically stable results</i>	7
2.2.2 <i>Dynamically stable results</i>	7
THEORETICAL BACKGROUND INFORMATION.....	10
3.1 CURRENT AVAILABLE DESIGN FORMULAS.....	10
3.1.1 <i>Historic overview</i>	10
3.1.2 <i>Design formula of VAN DER MEER [1988]</i>	11
3.1.3 <i>Design Rule of SCHIERECK & FONTIJN [1996],</i>	16
3.2 GRAVEL CHARACTERISTICS	18
3.2.1 <i>Sediment classification</i>	18
3.2.2 <i>Gravel -profile</i>	18
3.3 HYDRODYNAMICS	19
3.3.1 <i>Plunging Breaker</i>	19
3.3.2 <i>Swash zone</i>	20
3.4 MORPHODYNAMICS	22
3.4.1 <i>Types of transport</i>	22
3.4.2 <i>Incipient motion</i>	22
3.4.3 <i>Sediment transport due to Acceleration</i>	24
3.4.4 <i>Bed Shear stress</i>	25
3.4.5 <i>VAN RIJN, [2007] transport formula</i>	27
3.4.6 <i>NIELSEN, [2006] transport formula</i>	30
3.5 DAMAGE QUANTIFICATION METHODS	32
3.5.1 <i>Eroded Area</i>	32
3.5.2 <i>Erosion profile</i>	33
SELECTED NUMERICAL MODEL.....	34
4.1 WHY XBEACH-G	34
4.2 ALTERNATIVES	34
4.3 HOW DOES XBEACH-G WORK?	35
4.3.1 <i>Model Overview</i>	35
4.3.2 <i>Model Hydrodynamics</i>	36

4.3.3	Model Morphodynamics	40
4.4	MODEL VALIDATION	42
4.4.1	Validation Locations	42
4.4.2	Morphological validation	42
4.4.3	Hydrodynamic validation	43
4.4.4	Groundwater validation	44
4.5	MODEL LIMITATIONS	45
	DATA ANALYSIS	46
5.1	AVAILABLE DATA.....	46
5.2	USED EXPERIMENTAL DATA.....	47
	TEST SETUP	48
6.1	INPUT MODEL.....	48
6.1.1	Parameter conversion	48
6.1.2	Hydrodynamics.....	48
6.1.3	Model bathymetry.....	48
6.1.4	Grid distance	49
6.1.5	Overview Model input	49
6.2	MODEL TEST STAGES	50
6.2.1	Stage 1: Model size.....	50
6.2.2	Stage 2: NIELSEN, [2006] vs. VAN RIJN, [2007].....	50
6.2.3	Stage 3: Variation parameters	50
6.2.4	Stage 4: Hydrodynamics and Morphodynamics	51
	RESULTS.....	52
7.1	STAGE 1: MODEL SIZE	52
7.2	STAGE 2: NIELSEN, [2006] vs. VAN RIJN, [2007].....	53
7.2.1	Damage level.....	53
7.2.2	Erosion depth.....	55
7.2.3	Damage level vs. Relative erosion depth.....	56
7.2.4	Erosion profile shape	57
7.2.5	Recap stage 2	58
7.3	STAGE 3: VARIATION PARAMETERS	59
7.3.1	Slope effect.....	59
7.3.2	Layer thickness	62
7.3.3	Stone size.....	64
7.3.4	Phase lag angle ϕ	65
7.3.5	Hydraulic conductivity	67
7.3.6	Recap stage 3	68
7.4	STAGE 4: HYDRO- AND MORPHODYNAMICS	69
7.4.1	Hydrodynamics.....	69
7.4.2	Morphodynamics.....	75
7.4.3	Recap stage 4	82
	CONCLUSIONS & RECOMMENDATIONS	84
8.1	CONCLUSIONS.....	84
8.2	RECOMMENDATIONS.....	86
	DISCUSSION	87
	REFERENCES.....	88

1 INTRODUCTION & PROBLEM DEFINITION

- Background information
- Goal & Research question
- Scope definition
- Report outline
- Terminology

1.1 Background information

The stability of rock slopes under wave loading has been the subject of many researchers, e.g. VAN DER MEER [1988]. The stability of rock on steep slopes (slopes steeper than 1:6) is well understood and several design methods exist for these types of slopes. Typical applications are breakwaters, sloped embankments and sea defences.

The stability of rocks on mild slopes under wave loading is less well understood. Typical applications are foreshore protections at sea defences, pipeline protection at landings and artificial gravel beaches. The foreshore has an important aspect in the protection, as it determines the wave behaviour in front of the protection. Rocks are installed to make sure no erosion due to the waves (or currents) will take place.

Recently de Vries & van de Wiel has been assigned to install a rock protection on the mild foreshores of the Eastern Scheldt River to protect the sandy foreshores. During the project it appeared that the current design methods were not sufficient to design an economic protection. This is why de Vries & van de Wiel is interested in finding a more effective design solutions for the protection of mild slopes with rocks or gravel.

This research report continues with the work done by WIT [2015], which describes the stability of gravel on mild slopes in breaking waves using the numerical model Xbeach-G. Earlier studies by GROTE [1994], P.G.J. SISTERMANS [1993] and YE [1996] already performed small scale physical model tests for mild slopes and WIT [2015] identified some recommendations which formed the basis for this report.

1.2 Goal & Research questions

As the current empirical design methods seem to over predict the stone sizes, this thesis focus on researching the possibilities for a more effective design method for rock/gravel on mild slopes (more gentle than 1:6). More specific, the goal of this study is to find out if the numerical model XBeach-G is appropriate as a design tool for the design of the protection of mild slopes with stones. This goal is achieved with the following research questions.

- 1) How do the Xbeach-G model results, using the transport formulae developed by NIELSEN [2006] and VAN RIJN [2007], relate to the experimental data done by VAN DER MEER [1988]. Which of the two transport formulas reproduces the results of the experiments the best?

- 2) How well are the hydrodynamics modelled and are these translated correctly to the morphodynamics?
- 3) How can the amount of erosion/damage for mild slopes best be quantified, such that the safety requirements are still assured?

1.3 Scope definition

The research of WIT [2015] focuses on a uniform slope with a constant water level; no extra effects due to changing bed slope will occur. The research uses hydraulic conditions which resembles the situation along the Eastern Scheldt. The test conditions are based on an irregular wave field using a standard JONSWAP type wave spectrum. De Vries & van de Wiel contractually had to design a statically stable structure, which means that only minor damage may occur during the lifetime of the structure. This report focuses mainly on statically stable designs. The report of WIT [2015] provided new thoughts on damage definition for mild slopes, taking into account dynamically stable structures with allowable erosion depth. This definition is used in this report and explained in the section 'Terminology'.

The 2015 release of XBeach-G is used for this thesis. This version includes compared with previous versions more functions, such as the sediment transport formula of VAN RIJN, [2007], compared to the previous version

This study looks at homogeneous structures (structures with only rock material) as well as structures with rock on an impermeable core (sand). The impermeable core is modelled as an aquifer, which should model the situation correct.

1.4 Report outline

The chapter following this introduction describes the motivation for this research and its importance. It elaborates on the results of WIT [2015] and G. SCHIERECK ET AL. [1994] which formed the basis for this thesis.

Chapter 3 explains the theory necessary to understand this report. This theoretical framework is divided in a part about the current design formula's, the hydrodynamics and the morphodynamics in the cross-shore.

The next chapter focuses on the model XBeach-G and how it incorporates the hydrodynamics and morphodynamics discussed in the theoretical framework. The input data and model setup are described in chapter 5 and 6.

The model results are presented in chapter 7 followed by the conclusions & recommendations in chapter 8 and a discussion in chapter 9.

1.5 Terminology

There is no general definition for mild and steep slopes. The term 'mild slopes' is used for slopes milder than 1:6. The 1:6 slope is used as boundary as the VAN DER MEER [1988] empirical design formulae has a validity range between 1:1.5 and 1:6. The homogeneous structures are validated till a 1:3 slope. When in this report the term gravel is used, the cobble kind of gravel is meant. The difference between the types of gravel is explained in the theoretical framework in the chapter gravel characteristics.

Homogeneous structures consists of only the same gravel material (i.e. no layers are present). Impermeable structures have a gravel layer installed on an impermeable core, e.g. sand. VAN DER MEER [1988] started with this approach and used a permeability factor. For homogeneous structures this permeability factor is 0.6 and for impermeable structures this permeability factor is 0.1. This means more stability for increasing permeability of the construction. (See Figure 1)

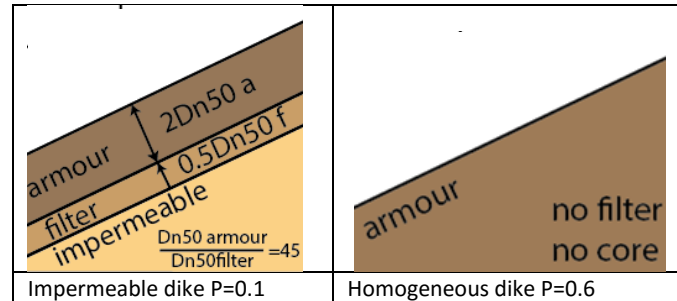


Figure 1: Homogeneous and impermeable dike structures

Another not yet well formulated situation occurs when talking about a stable structure. VAN DER MEER [1988] used the terms statically stable profiles and Dynamic profiles. When a profile is stable or unstable is arbitrary and discussable. For milder slopes maybe more erosion is tolerated, as VAN DER MEER [1988] also mentioned in his research.

Literature mentions statically stable slopes when only minor damage may occur during design conditions. VAN DER MEER [1988] describes the damage level between $S=2 - 3$. Statically stable structures usually have stability numbers $H_s/\Delta D_{n50} < 4$. Dynamically stable profiles are slopes which may reshape during design conditions until a kind of equilibrium profile is established. In this case there is movement of stones, but the transport of material is minimised. Dynamically stable structures have stability numbers which are larger than statically stable structures with stability numbers $H_s/\Delta D_{n50} > 6$. The difference is schematised in Figure 2.

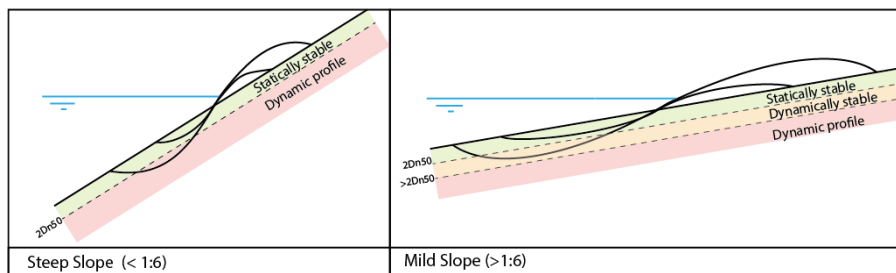


Figure 2: Difference between statically stable and dynamic profiles for both mild as steep slopes.

2

MOTIVATION FOR THE RESEARCH

- Experimental tests
- XBeach-G Results

The chapter motivation for the research indicates the starting point and the intention for this research. This chapter describes experiments executed by SCHIERECK & FONTIJN [1996], and work done by WIT [2015].

2.1 Experimental tests - SCHIERECK & FONTIJN [1996],

G. SCHIERECK ET AL. [1994] investigated the stability relations for rock on mild slopes for the protection of a pipeline in the surf zone. G. SCHIERECK ET AL. [1994] The experimental tests done by P.G.J. SISTERMANS [1993] and YE [1996], were used to derive the stability relations. The experiments are performed for both irregular as regular waves on a 1:10 and 1:25 slope and during the tests the number of displaced stones were counted. The measured damage was formulated as Equation 2–1 G. SCHIERECK ET AL. [1994] assumed that incipient motion occurs if S_n is larger than 0.5%, so it can be compared with the statically stable VAN DER MEER [1988] formula. (Equation 2–1)

$$S_n = n_{tot} * \frac{D_{n50}^2}{A} \quad (S_n = 0.5 \rightarrow \text{incipient motion}) \quad \text{Equation 2-1}$$

The experimental results of incipient motion used by GERRIT J SCHIERECK & FONTIJN [1996] are compared with the VAN DER MEER [1988] formula in Figure 3. It can be observed that for mild slopes, with a low iribarren number, the stability increases for both formulae. The experimental results, used by SCHIERECK & FONTIJN [1996], however show an increased stability compared to the predicted stability according to the VAN DER MEER [1988] formula . The type of wave breaking changes into a spilling breaker, which results in more stable structures than the assumed plunging wave breaking in the VAN DER MEER [1988] formula.

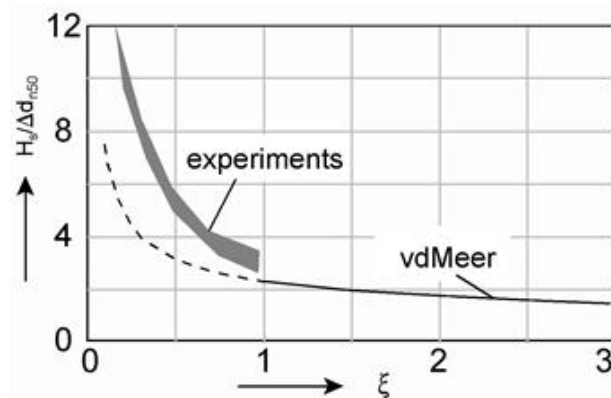


Figure 3: Experimental results G. J. Schiereck & Verhagen, [2012] and VAN DER MEER [1988] formula.

2.2 XBeach-G results - WIT [2015]

In the research of WIT [2015], the numerical model XBeach-G was used to investigate how well it predicts morphodynamic response compared to the VAN DER MEER [1988] results (both statically and dynamically stable structures were compared). This is done for homogeneous structures, with a uniform slope and the transport formula of NIELSEN, [2006].

2.2.1 Statically stable results

The statically stable Xbeach-G results of WIT [2015], with $S \approx 2$, clearly confirms the results from GERRIT J SCHIERECK & FONTIJN [1996] The mild slope results give higher stability values than when the VAN DER MEER [1988] formula is extended in the spilling breaker area.

Figure 4 shows the stability of gravel on homogeneous structures for $S = 2$ values. The figure has three regions. Region three is within the validity of the VAN DER MEER [1988] formula for plunging waves. Region one and two are outside the validity range. The dashed line indicates an extrapolation of his formula.

The red stars indicate the Xbeach-G results from WIT [2015]. These results confirm the higher stability numbers than can be expected from the extrapolated VAN DER MEER [1988] results.

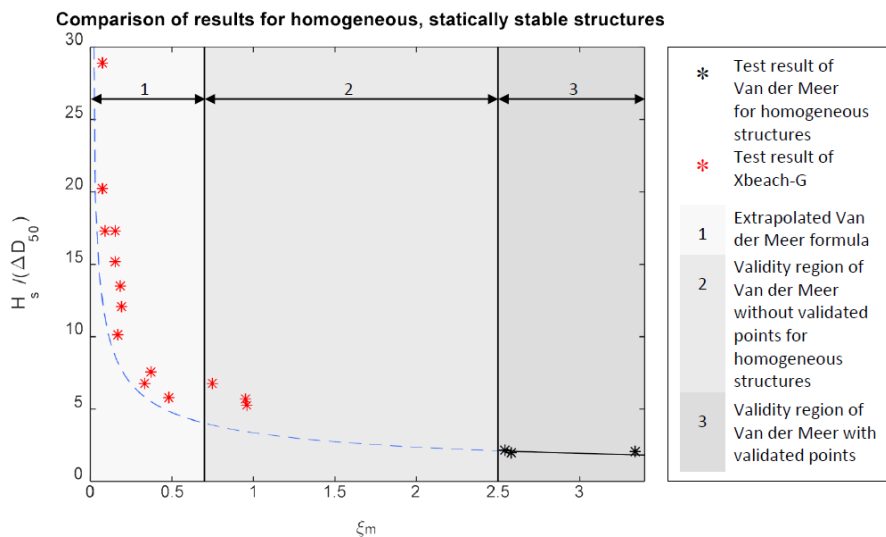


Figure 4: Statically stable results of XBeach-G for a homogeneous structure. WIT [2015]

For impermeable structures VAN DER MEER [1988] has executed tests in region two. VAN DER MEER [1988] assumes for region two the same difference between homogeneous and impermeable structures as he observed for region three. This difference is processed in the permeability factor.

2.2.2 Dynamically stable results

The figure below show some remarkable trends from the report of WIT [2015], which could not be explained. The orange line in the left image shows the result of three tests with three different grain sizes with a constant wave height of 1m, a deep water wave steepness of $s_{op} = 0.01$ on a 1:10 slope. The eroded area for these tests is increases for an increasing grain size. This implies that increasing the grain size causes more erosion and vice versa a smaller grain size gives less erosion. This is very counterintuitive and thus interesting. Especially because in the middle figure the green line shows for

the same tests the maximum eroded depth. In this case the eroded depth becomes smaller for increasing grain size. This arouses suspicion with respect to the formulation of the eroded area.

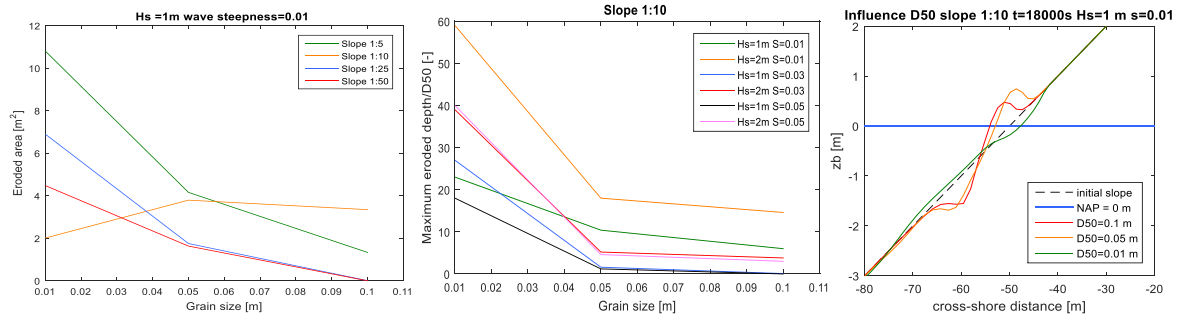


Figure 5: Left: Eroded area and maximum eroded depth versus the grain size. ; Right: Profile collapse from crest to bar. WIT [2015]

The erosion profile for this 1:10 slope, from which the eroded area and depth is derived, is also shown in Figure 5. This figure shows the trend that the profile collapses from a bar profile (accretion below the water line) to a crest profile (accretion above the water line) for the smallest grain sizes of $D50=0.01\text{m}$. Why this profile shape is changing and if these results might correlate with the results above is further investigated in this thesis.

3

THEORETICAL BACKGROUND INFORMATION

- Current available design formulas
- Gravel Characteristics
- Hydrodynamics
- Morphodynamics
- Damage quantification methods

The chapter theoretical background describes the necessary information, necessary for understanding this report. The background information contains literature research on most relevant aspects of gravel stability in breaking waves, i.e. describes the current design formulae, gravel characteristics and the hydrodynamic and morphological processes in the cross-shore.

3.1 Current available design formulas

3.1.1 Historic overview

Research has been conducted to find a suitable design formula for designing rocks on slopes under wave attack. Izbash made in 1938 a force balance for a particle on a horizontal bed in a turbulent flow. When the load was bigger than the strength the particle starts to move. Shields tried another approach where is assumed that the shear stress describes the destabilizing force in a uniform flow on a horizontal bed. This flow is compensated by the underwater weight of the particles. The result is a formula which gives an indication for which shear stress incipient motion occurs. SLEATH[1978] adjusted the Shields formula and implemented the orbital motion due to waves on a horizontal bed into it.

In 1938 Iribarren made a design formula for breakwaters which included beside the drag and resisting force also a slope correction factor. When rocks are placed on a slope the gravitational component of the resisting force is less effective. (Rocks are intended to roll down easier on a steep slope than a mild slope)

Because this formula did not describe all the processes HUDSON [1959] did experimental tests and made a quite similar formula with a stability factor (so called 'dustbin factor') K_d to account for all the not yet described processes. Values for this K_d factor are achieved with the experimental tests. The formula of HUDSON [1959] changed over the years.

VAN DER MEER [1988] published in 1988 his design formula for rock stability in waves, also achieved with experimental tests, which has a more physical understanding of the stability than the HUDSON [1959] formula. The VAN DER MEER [1988] formulae are most commonly used formula for current design works for rock slopes. Van Gent did a large number of additional experimental studies in 2003

to investigate the stability of rock slopes in (very) shallow water wave conditions. This research concluded that the effect of the wave period was not clear from his tests. This formula is achieved by curve fitting of many experimental data, but has less physical background than the VAN DER MEER [1988] formula.

The HUDSON [1959] and VAN DER MEER [1988] experiments are carried out on slopes ranging from 1:1.5 to 1: 4 for HUDSON [1959] and 1.1.5:1:6 for VAN DER MEER [1988]. Van Gent did his tests on 1:2 and 1:4 slopes, both for permeable and impermeable core.

This thesis focuses on the stability of stones on mild slopes (milder than 1:6). The current method for mild slopes is to extrapolate the VAN DER MEER [1988] formula. That is why only the VAN DER MEER [1988] formula is elaborated in this chapter. The other formulas are further elucidated in the appendix A: Design formula's.

3.1.2 Design formula of VAN DER MEER [1988]

The most accepted method for steep slopes is the formula of VAN DER MEER [1988]. The VAN DER MEER [1988] formula is obtained with experiments on slopes in the range from 1:1.5 till 1:6. Most tests are executed with impermeable underlayer. For 1:3 slopes also tests for permeable structures are executed. The final formula consists of two parts, for both surging as plunging breakers. Collapsing type of waves are present at the intersection of both curves.

$$\text{surging breaker: } \frac{H_s}{\Delta d_{n50}} = 1.0 * P^{-0.13} \left(\frac{S}{\sqrt{N}} \right)^{0.2} \sqrt{\cot(\alpha)} \cdot \xi_m^P \quad \text{Equation 3-1}$$

$$\text{plunging breaker: } \frac{H_s}{\Delta d_{n50}} = 6.2 * P^{0.18} \left(\frac{S}{\sqrt{N}} \right)^{0.2} \xi_m^{-0.5} \quad \text{Equation 3-2}$$

P = permeability factor
 N = number of waves
 Δ = Dimensionless density
 S = Damage factor

H_s = Significant wave height
 d_{n50} = Grain size diameter
 ξ_m = Iribarren related to mean wave period.

$$S = \frac{A}{d_{n50}^2}$$

$$\frac{H_s}{\Delta d_{n50}} = \text{stability parameter}$$

$$\xi_m = \frac{\tan(\alpha)}{s} \quad \text{with } s = \sqrt{\frac{H_s}{L_0}} = \sqrt{\frac{H_s}{\frac{g \cdot T_m^2}{2\pi}}}$$

Transition area between the plunging and surging formula

The transition between the surging and plunging breakers is gradually and lays between $\xi_m = 2.4 - 4$ according to VAN DER MEER [1988]. This transition can be derived from the equations above which results in Equation 3-3. According to this formula the transition point depends on the slope angle and the permeability of the structure.

$$\xi_{m,transition} = 6.2 * P^{0.31} \sqrt{\tan(\alpha)}^{\frac{1}{P+0.5}} \quad \text{Equation 3-3}$$

The surging formula has another shape than the plunging formula. The surging formula gives increasing stability for higher iribarren numbers, while the plunging formula gives lower stability for

higher irribarren numbers. That is why the minimum of the VAN DER MEER [1988] formula is at the transition point

Variables used in the plunging formula

Notional Permeability (P-value)

The structural built-up determines the permeability. Most permeable structures are homogeneous structures, which consist of one type of stone (core and armour). Less permeable structures are structures where the core is made of smaller stones or wider grading and thus less permeable. The amount of permeability is described by VAN DER MEER [1988] in the notional permeability factor, which describes the ratio in stone diameter between the core and the protective layers. VAN DER MEER [1988] derived P-values for four types of structures and their corresponding permeability, shown in Table 1.

Table 1: 4 types of permeability described by VAN DER MEER [1988]/

P-fact.	Description	Ratio filter	Ratio core	Shape
P=0.1	<ul style="list-style-type: none"> Impermeable core (sand or clay) 	$\frac{D_{n50 a}}{D_{n50 f}} = 45$	Imp. core	
P=0.4	<ul style="list-style-type: none"> permeable core; thicker filter layer 	$\frac{D_{n50 a}}{D_{n50 f}} = 2$	$\frac{D_{n50 f}}{D_{n50 c}} = 4$	
P=0.5	<ul style="list-style-type: none"> Permeable core; No filter layer 	No filter	$\frac{D_{n50 a}}{D_{n50 c}} = 32$	
P=0.6	<ul style="list-style-type: none"> Homogeneous; core material similar to armour; no filter 	No filter	$\frac{D_{n50 a}}{D_{n50 c}} = 1$	

The permeability factor is determined with experimental curve fitting for the different type of structures. The results show that a more permeable structure is more stable than an impermeable structure. This is because for a permeable structure the water can penetrate more easily through the structure, which gives a gradually dissipation and totally absorption of the wave energy. For longer wave periods, (higher ξ_m) the stability will increase, as more water can flow into the core. This effect, noticed by VAN DER MEER [1988] is included in the surging formula, where the permeability is related to the slope angle. This is not further elaborated in this report.

Damage level

The damage formed during the wave attack is described in the damage level as can be seen in Equation 3–4. The formula used by VAN DER MEER [1988] describes the damage as the eroded area divided by the D_{n50}^2 , which is about the same as the amount of square shaped stones that can be fit into the erosion hole. The shape of the stone is calculated as a square, but for a realistic indication of the amount of displaced stones, the damage level should be multiplied times 0.7.

$$S = \frac{A}{d_{n50}^2} \quad \text{Equation 3-4}$$

For a damage level of $S=2$ (approximately 2 stones replaced), the damage starts and this gives according to the tests VAN DER MEER [1988] a statically stable structure. For milder slopes more erosion can be tolerated. Table 2 gives an indication of the higher damage levels in the test range of VAN DER MEER [1988].

Table 2: Allowed damage level for different slopes.

	Damage Level: $S = \frac{A}{d_{n50}^2}$	
Slope	Start of damage	Filter layer visible (2 D_{n50} thick layer)
1.5	2	8
2	2	8
3	2	12
4	3	17
5	3	17

The damage level only describes the eroded area and not the erosion depth, so it does not give an indication if the filter layer is visible or not. The design criteria commonly used are based on a armour layer thickness of $2D_{n50}$.

Number of waves

The number of waves gives an idea about the storm duration. For north sea conditions it is common to use 3000 waves for a 5-6 hour storm situation. This thesis uses a fixed storm duration of 3000 waves. The report of WIT [2015] and VAN DER MEER [1988], already did some investigation of the effect on the amount of waves in the program XBeach-G and after 3000 waves most of the damage was already formed.

Stability parameter

$$\frac{H_s}{\Delta D_{n50}} \quad \text{Equation 3-5}$$

The stability parameter is a dimensionless parameter that describes the load and the strength on the stone. The load is determined by the wave height and the strength with the weight of the stones. This stability number is often used to describe the stability for different breaker parameters (Iribarren numbers)

In the research of GERRIT J SCHIERECK & FONTIJN [1996], the functioning the stability parameter and the breaker parameter is discussed for milder slopes. It is argued that this relation does not describe

the vertical velocities near the bottom occurring for plunging breakers; nor the influence of turbulence on a single stone.

Iribarren Number

$$\xi_m = \frac{\tan(\alpha)}{\sqrt{s}}$$

Equation 3-6

$$s = \frac{H_s}{L_0}$$

$$L_0 = \frac{g \cdot T_m^2}{2\pi}$$

The Iribarren number describes how the waves are breaking on the shore. This is done with the wave shape, formulated as the wave steepness [s] and the slope angle [tan(α)]. For mild slopes only the plunging breakers are important and eventually the spilling type of breaker, see Figure 6.

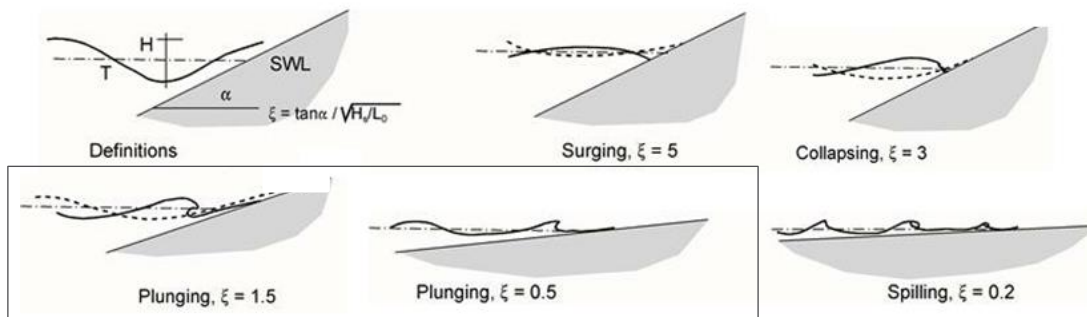


Figure 6: Iribarren number for different breaker types.

VAN DER MEER [1988] did his tests on different slopes ranging from 1:1.5-1:6 with corresponding Iribarren numbers in the range of 0.7-7.

Van der Meer Experiments

Experimental setup

VAN DER MEER [1988] did experimental tests for structures with an impermeable core; with a permeable core and for homogeneous structures. These tests were executed in a wave flume under different hydraulic and structural circumstances. The tests were almost all executed with a water depth of 0.8m which are, for the chosen wave heights, deep water conditions. The used wave board, was able to filter out the reflected waves and the wave height was measured at the toe of the structure with two wave gauges, placed $1/4L_0$ from each other. With these wave gauges the wave height at the toe is determined by filtering the reflected waves from the measured wave height. The formed profile is measured after 1000 waves and 3000 waves with a measuring rod that has an accuracy of about 0.04m. For impermeable structures, a layer thickness of 0.08m is used.

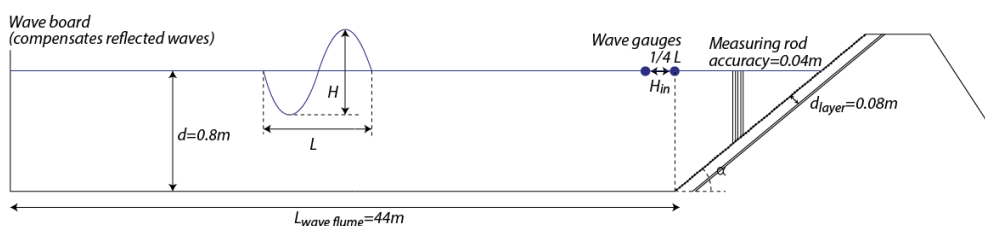


Figure 7: Overview experimental conditions wave flume.

Amount of performed experiments

Most tests were executed under the circumstances as is explained above. For the impermeable 1:3 slope and the permeable 1:2 & 1:3 slope also other tests are done where several parameters were changed, such as the water depth, the density of the stones, the spectrum and the crest height. The changed parameters and the number of tests that were executed for these situations are presented in Table 3.

Table 3: Number of tests executed by VAN DER MEER [1988].

Type of structure	Slope	Number of tests						Total
		Normal tests	Different tests					
			Depth	Dens.	Low crest	Large scale	Spec.	
Impermeable	1:2	18						18
	1:3	41				5	40	86
	1:4	46						46
	1:6	27						27
Permeable	1:1.5	21						21
	1:2	20	16	20	31			87
	1:3	19				6		25
Homogeneous	1:2	15						15
								325

Damage prediction method (damage curve)

The tests of VAN DER MEER [1988] are executed in series where the wave period was kept the same but the significant wave height is changed. For every test series a damage curve is made to estimate the values corresponding to other damage levels. A typical damage curve is shown in Figure 8 where it is also clear that this method has some inaccuracy, as the measured points are not exactly on the trend line.

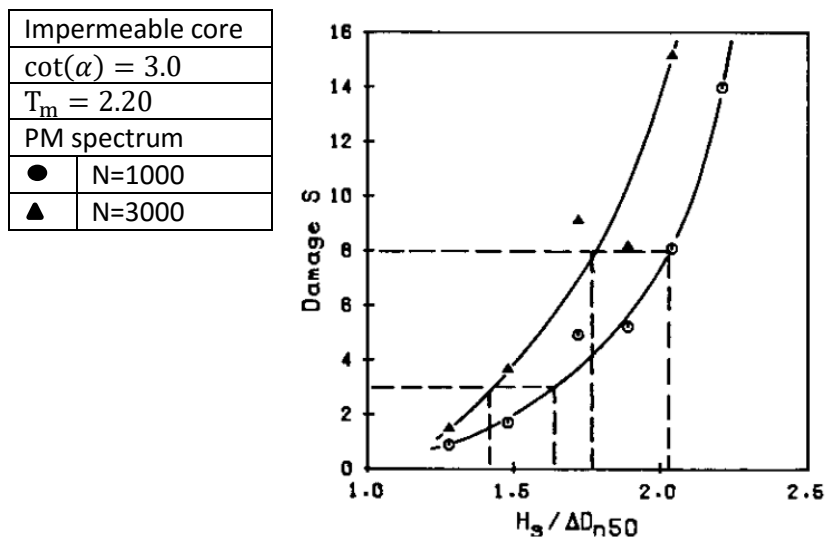


Figure 8: Typical Damage curve used by VAN DER MEER [1988]

In Figure 9, the VAN DER MEER [1988] formula for both a homogeneous as an inhomogeneous situation are displayed with the experimental data obtained with the damage curves and the real executed tests. Also the 5% exceedance line is shown, which shows the area of inaccuracy. The tests results, achieved with the damage curve seem less accurate than the results obtained with the real experiments with a damage level of $S \approx 2$.

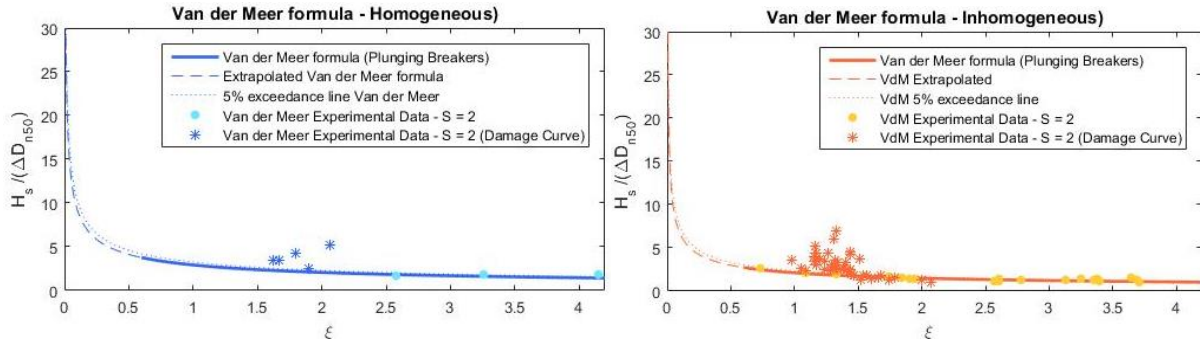


Figure 9: VAN DER MEER [1988] formula for homogeneous and inhomogeneous structures with experimental data.

3.1.3 Design Rule of SCHIERECK & FONTIJN [1996],

Experimental data

YE [1996], GROTE [1994] and P.G.J. SISTERMANS [1993] performed tests for mild slopes in a wave flume to obtain insight in the amount of damage under different hydrodynamic conditions. P.G.J. SISTERMANS [1993] start his research in 1993 and did tests for both regular as irregular waves with a Jonswap spectrum. The tests were performed on a 1:25 slope with a grain size of 9.9mm, so the slope and grain size were not varied. YE [1996] focused on irregular waves for 2 different slopes, 1:10 and 1:25, and for 4 different stone sizes with 2 different mass densities. GROTE, [1994] also did tests with smaller stones lower on the slope and bigger stones near MWL. In all tests the damage is described by the amount of stones displaced per unit width (Equation 3–7).

$$S_n = n_{tot} * \frac{D_{n50}}{\text{width wave flume}} \quad \text{Equation 3-7}$$

This damage determination is different than used by VAN DER MEER [1988]. He used a profiles to measure the profiles before and after a test to come to the damage level.

Design rule SCHIERECK & FONTIJN [1996],

With the test results of P.G.J. SISTERMANS [1993] and YE [1996], SCHIERECK & FONTIJN [1996], tried to make a provisional design formula. The paper G. SCHIERECK ET AL. [1994] assume that a damage level of 0.5% describes incipient motion. By interpolating the results of P.G.J. SISTERMANS [1993] and Ye, the stability and iribarren number for a damage level of $S_n = 0.5\%$ is determined. With this data SCHIERECK & FONTIJN [1996], tried to make a design formula for milder slopes. (Equation 3–8). This formula is made with the measurements of YE [1996] and P.G.J. SISTERMANS [1993] and is therefore only valid for a 1:25 slope.

$$\frac{H_{s0}}{\Delta d_{n50}} = 4.5 + 50 \cdot s_0 \quad \text{Equation 3-8}$$

$$s_0 = \left(\frac{\tan(\alpha)}{\xi} \right)^2$$

The design formula is compared with the obtained experimental data and the VAN DER MEER [1988] formula for $S = 2$, see Figure 10. It should be noted that the damage determination used by SCHIERECK & FONTIJN [1996], and VAN DER MEER [1988] was very different.

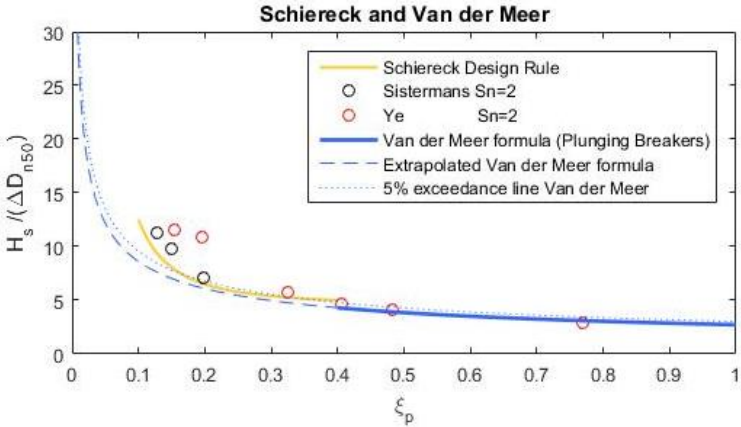


Figure 10: SCHIERECK & FONTIJN [1996], Design rule & VAN DER MEER [1988] formulae

3.2 Gravel characteristics

Most models and formulas are designed for sandy beds. The numerical model XBeach-G is designed for gravel beaches. Gravel has other characteristics than sand and in this part of the theoretical framework some of these characteristics are appointed.

3.2.1 Sediment classification

Gravel is more coarse material than for example sand. The transition area is commonly described according to the Wentworth scale where particles are classified according to their size. This is shown in Table 4. For larger particles the porosity increases. Commonly for gravel beaches the porosity is between 0.25 and 0.4. When talking about gravel in this report, the cobble kind of gravel is meant. The tests executed by VAN DER MEER [1988] are carried out with stones in the range of 10-30mm, which is according to this sediment classification called pebbles.

Table 4: Sediment classification (CHADWICK, [n.d.])

Sand	0.0625 -2mm	
Gravel	>2mm	
▪ Granular	2-4 mm	
▪ Pebble	4-64 mm	
▪ Cobble	64-256 mm	
▪ Boulder	>256 mm	
▪ Shingle	Rounded gravel (UK)	

3.2.2 Gravel -profile

Because the sediment of a gravel beach is more coarse, it can support steeper slopes. The internal angle of gravel is approximately 35° in air while in water it decreases to 30° . Gravel beaches also form another profile than sand beaches often do. Typically slopes in the area between 1:20 till 1:5 are found, which tend to create a reflective beach domain (MCCALL, [2015]). The general profile of a gravel beach has a berm at the high water mark and a step at the points where the waves break. ADRIÁN PEDROZO-ACUÑA, SIMMONDS, OTTA, & CHADWICK, [2006].

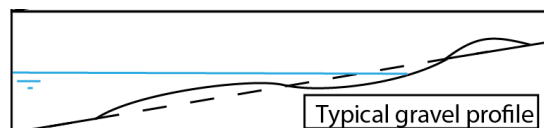


Figure 11: Step at the wave breaking point and a berm at the high water mark.

Another performance of gravel beaches under wave loading is the formation of cusps. Cusps are arc shaped patterns in the longshore direction of the beach. Because this research focusses on the cross-shore, no attention to this phenomena is given.

3.3 Hydrodynamics

The hydrodynamics in the cross shore are with the velocity and acceleration the input for the sediment transport formula's and the core of a numerical model. The nearshore processes can be divided in several regions. For this report the breaking process of a plunging wave and the swash zone are the main processes. Typical for both effects is the high interaction between the surface water and groundwater. The other processes from the offshore to nearshore transformation are explained in Appendix B: Hydrodynamics. The linear shallow water equations, used to model the offshore to nearshore transformation is also added in the Appendix B: Hydrodynamics.

3.3.1 Plunging Breaker

There are different forms of breaking which are described by Iribarren as is already explained in the chapter Iribarren Number. In this case the focus is on plunging breakers, so only this type of breaker is considered.

Plunging breakers occur on relative mild slopes where the upper part of the wave breaks over the lower part. Most energy is released in just one big splash. The influence of the impact of the plunging wave is often discussed as possible effect for sediment movement. This effect is investigated by ADRIAN PEDROZO-ACUÑA, SIMMONDS, & REEVE, [2008], who clearly shows a link between the impact of waves and the pressure on the bed. The research of ADRIAN PEDROZO-ACUÑA, SIMMONDS, & REEVE, [2008] divides the plunging breaker in three situations, which can be seen in Figure 12.

At the most left picture the wave is shown just before breaking. The infiltration and exfiltration effects due to up and down rush can be seen in the pressure diagram in the right top corner.

The picture in the middle shows the situation when the wave is just on the moment of breaking on the shore. The impact of this wave is clearly visible in the pressure diagram (top corner) and are in the range of 15-30kPa, which is big enough to influence the sediment transport. The peaked sudden pressure on the bed has as effect that the pore pressure between the grains increases, which reduces the intergranular stresses and thus reducing the strength of the stones. It is even found out that liquefaction for gravel beaches is possible. (ADRIAN PEDROZO-ACUÑA ET AL., [2008])

While the stones are still weakened by the pressure, the wave is rushing over the bed, as a kind of bore, taking all the particles to the upper part of the profile. This is shown in the most right picture.

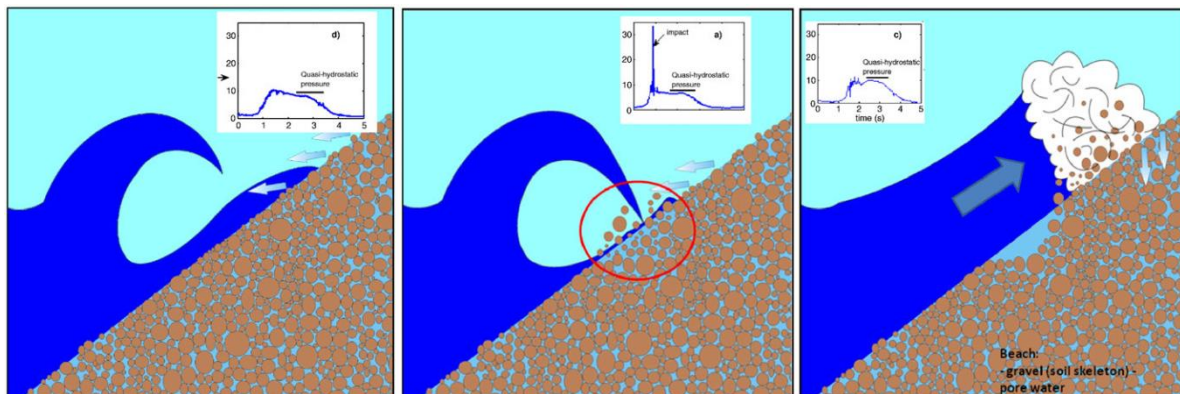


Figure 12: Concept of the effect of breaking of a plunging breaker. (ADRIAN PEDROZO-ACUÑA ET AL., [2008])

3.3.2 Swash zone

Especially for porous beaches with coarse material, such as the VAN DER MEER [1988] experiments, the groundwater and surface water exchange play an important role. These effects occur in the swash zone and determine the transport of sediment upslope and downslope and the formation of a bar.

During the run up and run down the water is flowing over the stones and between the stones due to the higher permeability of coarse beaches. Three main mechanisms are important during this process. (ADRIÁN PEDROZO-ACUÑA, SIMMONDS, CHADWICK, & SILVA, [2007]).

1. Reduction of backwash volume
2. Change in effective weight of particles (vertical pressure differences)
3. Change in shear force (boundary layer)

The investigation of BUTT, RUSSELL, & TURNER, [2001] is aimed at understanding the contrary processes that happen in the swash zone. In the swash zone there is a high interaction between the groundwater and the surface water and as consequence other processes happen during uprush than during backwash.

During uprush the infiltration has a stabilizing effect on the sediment transport as the water is causing a force directed downward on the stones. This has as consequence that the turbulent boundary layer is getting pressed towards the shore, giving a thinner boundary layer thickness during uprush. A thinner boundary layer gives higher bed shear stresses and thus more transport.

During downrush, exfiltration of the water particles is taking place with as consequence an upward directed destabilizing force. This effect has also as results a thickening of the boundary layer and thus a reduction of the bed shear stresses.

A secondary effect of the infiltration is the reduction of the backwash volume which creates less erosion. This process is especially important for situations with a hydraulic conductivity higher than $1 \cdot 10^{-1} \text{ m s}^{-1}$. The swash zone is found to be unsaturated for mild beaches and long wave periods and also for steep slopes the swash zone is also most of the time unsaturated. This indicates the effect and importance of the infiltration and exfiltration that is taking place on gravel beaches.

These processes which are explained above are summarized in Figure 13. The ratio between these stabilizing and destabilizing processes is important to give an approximation for the amount of sediment transport in the swash zone and the direction. The research of Butt to the infiltration and exfiltration effects show a decrease in uprush transport of 10.5% and an increase in backwash transport of 4.5% which implements more backwash transport than uprush transport. This effect due to infiltration and exfiltration can change in direction for different stone sizes. This research claims that there is a critical stone sizes for which the sediment transport changes from onshore to offshore. (BUTT ET AL., [2001]).

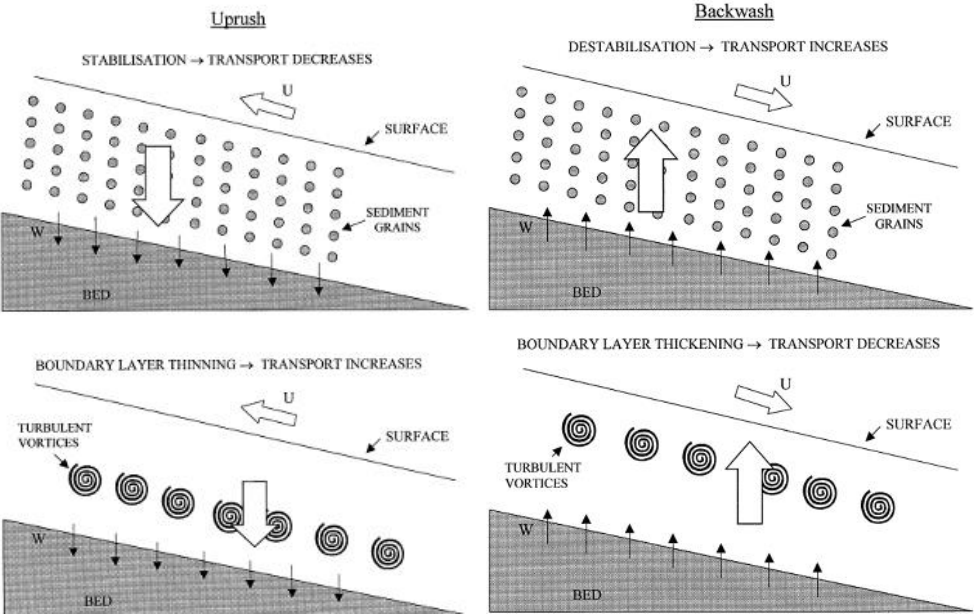


Figure 13: Left: Uprush effects; Right: Downrush effects BUTT ET AL., [2001]

3.4 Morphodynamics

The numerical model XBeach-G, that is used in this report, has the option for the VAN RIJN, [2007], transport formula and the NIELSEN, [2006] transport formula. That is why in this chapter these two transport formulas are elaborated.

The translation from the hydrodynamics to the morphodynamic response is still a not yet fully understood phenomena for rocky slopes. Most of the sediment transport formulas are derived for horizontal sandy beds. The validity has been extended by adding terms to include the effects for more coarse material and a slope.

3.4.1 Types of transport

The VAN RIJN, [2007], method clearly distinguishes several types of transport in his approach. For mathematical expressions, sediment transport can be divided into bed-load and suspended load transport. For bed-load transport two different type of particle motions are considered:

1. Rolling and sliding
2. Saltation

When the shear stress just exceeds the stabilizing force there is initiation of motion in the form of rolling and sliding of the particle. When this shear stress increases, more stones will move and this will look like jumps. This type of movement is called saltation and is also a form of bed load transport VAN RIJN, [1984].

If the occurring vertical turbulent forces are higher than the falling velocity, the particle will stay in the water column and it is in suspended mode. Suspended load is important for more fine sediments and can therefore be neglected, for gravel beaches. That is why in this chapter the focus is on bed load transport.

3.4.2 Incipient motion

The moment of incipient motion indicates for which load the particle starts to move. Most descriptions for the sediment transport are based on the principle of incipient motion. Both the VAN RIJN, [2007] and NIELSEN, [2006] method use the Shields parameter to describe the incipient motion in their formulation for the sediment transport.

Shields

The Shields shear formula is the most used formula to find a critical shear stress for which the particle starts to move. The shear is created by the current around the particle which is the driving force that causes the particle to move. The particle gets its stabilizing strength due to the underwater weight and the corresponding gravitational component. The Shields parameter is shown in Equation 3–9 where the nominator is the shear stress and the denominator the stabilizing weight component.

$$\theta_{cr} = \frac{\tau_{cr}}{(\rho_s - \rho_w)gD} = \frac{u_{*cr}^2}{\Delta gD} = \frac{load}{strength} \quad (\text{SHIELDS [1938]}) \quad \text{Equation 3–9}$$

Shields made this formula for horizontal sandy beds with a laminar flow, so this is without a slope and waves. The Shields criterion is often assumed to be 0.05 but laboratory studies from BREUSERS AND SCHUKKING[1971] and from PAINTAL[1971] show that for situations with a high Reynolds numbers

(turbulent flow) the shields criteria can range from $0.03 \leq \theta_{cr} \leq 0.07$. RESEARCH ET AL., [2007]. According to the RESEARCH ET AL., [2007] the following should be assumed when designing rock fill:

$$\begin{aligned} \theta_{cr} &= 0.03 - 0.035 && \text{First stones start to move} \\ \theta_{cr} &= 0.05 - 0.055 && \text{Limited movement} \end{aligned}$$

Bed slope effect

The Shields parameter and corresponding sediment transport formulations are originally developed for horizontal situations. To model the reality accurately the influence of the slope is included. The bed slope effect is the biggest for steep slopes but also for more mild slopes a correction is applied.

To correct this slope effect, the Shields parameter is often multiplied with a correction factor depending on the slope angle and the internal angle of repose of the material. The slope effect in Equation 3–10 is determined with a force balance, illustrated in Figure 14.

The destabilizing force is created by the current that creates a shear force. This shear force is compensated by the weight of the particle and the induced friction. Due to the slope the gravitational component is less efficient and less friction is created. (see force balance). The angle of repose in this formulation is difficult to determine as it is depended on multiple factors such as the stone size and the angularity. The graph in the right part of Figure 14 gives an indication for the angle of repose per stone size. VAN DER MEER [1988] uses in his experiments stones in the range of 10-30mm, which corresponds to an angle of repose of 35 to 40 degrees.

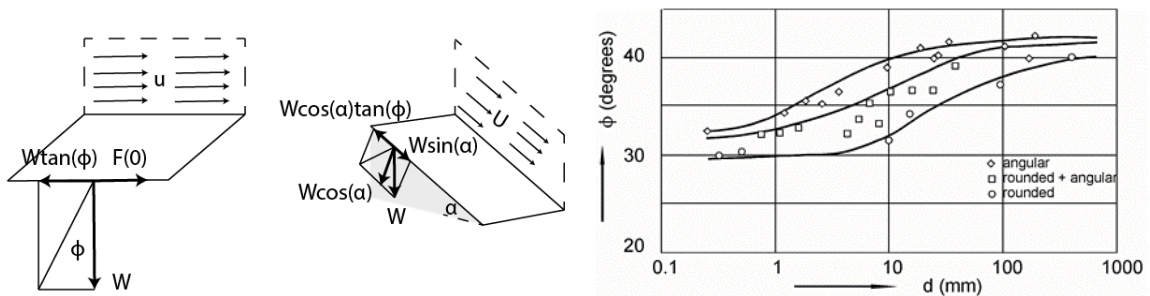


Figure 14: Left; Effect of gravitational force; Right; Angle of repose per stone size G. J. SCHIERECK & VERHAGEN, [2012].

$$\text{slope effect} = \frac{W \cos(\alpha) \tan(\varphi) - W \sin(\alpha)}{\sin(\varphi)} = \cos \beta \left(1 \pm \frac{\tan \beta}{\tan \varphi} \right) \quad \text{Equation 3-10}$$

$\varphi = \text{internal angle of repose}$
 $\beta = \text{Angle of the bed.}$

The effect of a slope is obviously bigger for steeper slopes than for mild slopes. The outcome of this slope effect for three common angles of repose is shown in Table 5. For a 1:25 slope there is hardly any influence of the slope correction factor. For the area between the 1:6 and 1:10 slopes, which is the scope of this research, the slope effect is between 0.70 and 0.88. It should be realised that when erosion is taking place this slope effect also occurs on a more local scale inside the erosion hole, where it can have more effect.

Table 5: Influence slope angle and internal angle of repose on the slope effect.

Slope	Slope effect $\phi = 30^\circ$	Slope effect $\phi = 35^\circ$	Slope effect $\phi = 40^\circ$
1:2	0.12	0.26	0.36
1:4	0.55	0.62	0.68
1:6	0.70	0.75	0.79
1:8	0.78	0.82	0.84
1:10	0.82	0.85	0.88
1:12	0.85	0.88	0.90
1:25	0.93	0.94	0.95

The right part in the formulation for the slope effect describes an avalanching principle. This avalanching principle is also included in XBeach-G and described with Equation 3–11. If the angle of the bed is bigger than the internal angle of repose the bed will slide downwards because it cannot hold such a steep slope. For an bed slope angle lower than the angle of repose, the bed will react normal to the shear stresses.

$$\begin{aligned} \text{if } \phi > \beta \text{ than } \frac{\tan \beta}{\tan \phi} < 1 &\rightarrow \text{Normal} \\ \text{if } \phi < \beta \text{ than } \frac{\tan \beta}{\tan \phi} > 1 &\rightarrow \text{Sliding} \end{aligned} \quad \text{Equation 3–11}$$

Effective Shields

The effective Shields parameter is the Shields parameter with the slope correction factor. The implementation of the slope effect in the shields parameter is a quite rough method to take the slope into account and other effects such as the breaking of waves are not taken into account. Currently, there are no better alternatives to take the slope effect into account.

$$\theta' = \theta \cdot \underbrace{\cos \beta \left(1 \pm \frac{\tan \beta}{\tan \phi} \right)}_{\text{Slope effect}} \quad \text{Equation 3–12}$$

3.4.3 Sediment transport due to Acceleration

Both NIELSEN, [2006] as VAN RIJN, [2007] tried to include the sediment transport due to acceleration in their sediment transport formulation. As is described in the Hydrodynamics the wave shape changes when approaching the shore. The occurring wave asymmetry influence the sediment transport, and this is described in the acceleration term of the transport equations.

The cross-shore sediment transport is described by BOSBOOM & STIVE, [2015] with Equation 3–13 as the velocity times the third power. This formula shows that the sediment transport is caused due to three components, the mean current, the skewness and the bound long waves. These three components are explained in the Appendix B: Hydrodynamics..

$$\langle \bar{U} |U|^2 \rangle = \underbrace{3 \langle \bar{U} |U_{hi}|^2 \rangle}_{\text{Mean Current/Undertow}} + \underbrace{\langle U_{hi} |U_{hi}|^2 \rangle}_{\text{Skewness}} + \underbrace{3 \langle U_{lo} |U_{hi}|^2 \rangle}_{\text{Long Waves}} \quad \text{Equation 3–13}$$

For asymmetric waves (vertical asymmetric) the onshore velocity is as big as the offshore velocity and no net sediment transport is expected. ($\overline{u_\infty^3} = 0$). This is however not the case as a net sediment transport can be generated even if $\overline{u_\infty^3} = 0$. This can be explained with the help of Figure 15.

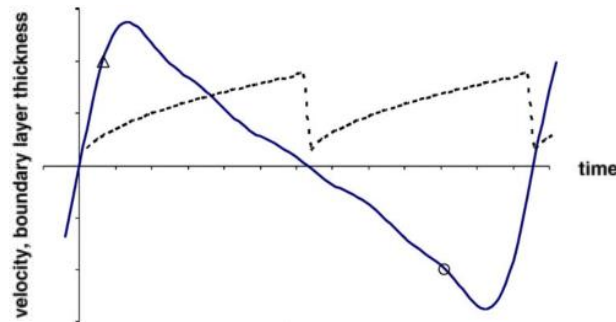


Figure 15: velocity and boundary layer in time. NIELSEN, [2006]

The graph shows an asymmetric wave with on the vertical axis the free stream velocity (blue line) and boundary layer thickness (dotted line) and on the horizontal axis the time. The steepness of the blue line gives the acceleration $\frac{du}{dt}$. At the point indicated with a triangle the acceleration is higher than at the round indicator. The velocities in the graph are the same so there is no velocity skewness but considerable acceleration skewness. The sediment transport that is occurring for asymmetric waves is caused by this difference in acceleration.

In addition the boundary layer is thinner at the point indicated with a triangle than it is at the point with the round dot. The shear stress as function of the boundary layer thickness and the velocity is determined with Equation 3–14. NIELSEN, [2002]. In this formula the velocity is in the nominator and the boundary layer thickness in the denominator. The velocity is the same at both points but the boundary layer at the round point is bigger. This gives according to the formula lower shear stresses for the round point and thus less sediment transport. The same mechanism occurs in the swash zone with plunging breakers, already explained in the chapter Hydrodynamics.

$$\tau_b(t) = \rho v_t \frac{u_\infty(t)}{\delta(t)} \quad \text{Equation 3–14}$$

3.4.4 Bed Shear stress

As described in the Shields formulation the main destabilizing force is the bed shear stress created due to waves and currents. The bed shear stress describes the friction force from the water on the bed. This is expressed with the unit $[N/m^2]$. Both the NIELSEN, [2006] and VAN RIJN, [2007] method distinguish the bed shear stress created due to waves and due to currents. The bed shear stress due to currents is the drag component and the bed shear stress due to waves is the inertia component.

$$\tau_b = \tau_{bd} + \tau_{bi} \quad \text{Equation 3–15}$$

This method processes the acceleration effects, due to wave asymmetry, directly in the bed shear stress. Other methods are based on a modification of the effective Shields parameter to include the asymmetry effects but these are not included in this thesis. MCCALL, [2015].

Drag component

The drag component of the bed shear stress describes forces on the bed created by friction of the currents. This can be determined with Equation 3–16, as a friction coefficient times the density and the velocity squared.

$$\tau_{bd} = c_f \rho u |u| \quad \text{O'BRIEN \& MORISON, [1952]} \quad \text{Equation 3–16}$$

The friction factor can be explained with the theory of Kobayashi who describes the shear stresses due to run-up and implements the friction factor, $c_{f,0}$. (KOBAYASHI, OTTA, & ROY, [1987]) This bed friction factor is described with $c_{f,0} = \frac{g}{(18 \log(\frac{12h}{k}))^2}$. With a characteristic roughness of $k = 3D_{90}$ for flat beds.

This dimensionless friction coefficient ($c_{f,0}$) is later adjusted by CONLEY & INMAN, [1994] who implemented the boundary ventilation effects $(\frac{\Phi}{e^{\Phi}-1})$. The ventilation effects are used to reproduce the infiltration and exfiltration, of porous beaches, explained in the chapter Hydrodynamics. These effects are especially important for more coarse beaches, such as the VAN DER MEER [1988] experiments. In XBeach-G the ventilation effects are included and are limited with a minimum of 0.1 and maximum of 3.0. (MCCALL, [2015])

$$\begin{aligned} c_f &= c_{f,0} \left(\frac{\Phi}{e^{\Phi}-1} \right) & \text{CONLEY \& INMAN, [1994]} & \text{Equation 3–17} \\ \Phi &= -\frac{1}{2} \frac{0.9}{c_{f,0}} \frac{S}{|u|} \\ c_{f,0} &= \frac{g}{(18 \log(\frac{12h}{k}))^2} \end{aligned}$$

Inertia component

The inertia component describes the bed shear stress created by asymmetric waves. The inertia term tries to reproduce the sediment transport due to acceleration, described before.

In Equation 3–18 the method, described by VAN GENT, [1995] is used to calculate the inertia effects. The shear stresses due to inertia are created due to the acceleration times the stone weight and a couple of calibration coefficients. The calibration coefficients are for the stone shape (c_v), the inertia component with the added mass ($c_m = 1 + c_a$) and the number of grains on the surface (c_n).

$$\tau_{bi} = \rho c_m c_v c_n D_{50} \frac{\partial u}{\partial t} \quad \text{Equation 3–18}$$

3.4.5 VAN RIJN, [2007] transport formula

The VAN RIJN, [2007] transport formula starts with a description for the transport due to currents only. (VAN RIJN, [1984]). The influence of waves is later added to this description in the paper VAN RIJN, [2007].

VAN RIJN, [1984] – Currents only

Forces acting on a particle.

To understand the physics behind the transport of sediment particles VAN RIJN, [1984] started in 1984 with a model based on the forces working on a single particle, when bed load transport is taking place. The forces for a horizontal bed and for a situation with currents only were taken into account so the wave orbital movement is not taken into account. The forces can be divided into the stabilizing drag and weight component and the destabilizing lift and relative velocity force. The forces acting on a particle is schematised in Figure 16. In 1984 VAN RIJN, [1984] solved the equations of motion for a single particle and computed characteristics of saltation transport, like the saltation height, length and concentration. This is further explained in Appendix C: Morphodynamics.

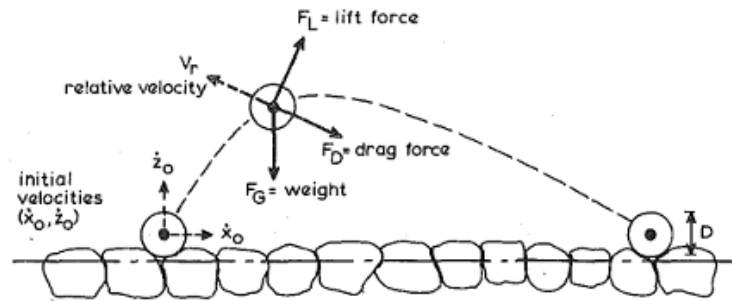


Figure 16: Forces acting on a particle.

Calculation particle parameter and transport stage parameter

The VAN RIJN, [1984] method assumes that the transport of a particle can be described with two dimensionless parameters, the particle parameter (D_*) and the transport stage parameter (T). The transport stage parameter describes the mobility of the parameter in percentage of the critical shear stress. The dimensionless particle parameter is the mobility parameter rewritten in a form without shear stresses. This is done by implementing the Reynolds number in the mobility parameter. The parameter 's' in the particle parameter describes the specific density formulated as $s = \frac{\rho_s}{\rho}$ and the parameter ν is the kinematic viscosity. The particle parameter and the transport stage parameter is given in Equation 3–19 and Equation 3–20.

$$D_* = D_{50} \left[\frac{(s-1)g}{\nu^2} \right]^{\frac{1}{3}} = \text{particle par.} \quad \begin{cases} \frac{u_*^2}{(s-1)gD} = \text{mobility par.} \\ \frac{u_* D}{\nu} = \text{part. Reynolds numb.} \end{cases} \quad \text{Equation 3–19}$$

$$T = \frac{(u_*')^2 - (u_{*,cr})^2}{(u_{*,cr})^2} = \text{Transport stage parameter} \quad \text{Equation 3–20}$$

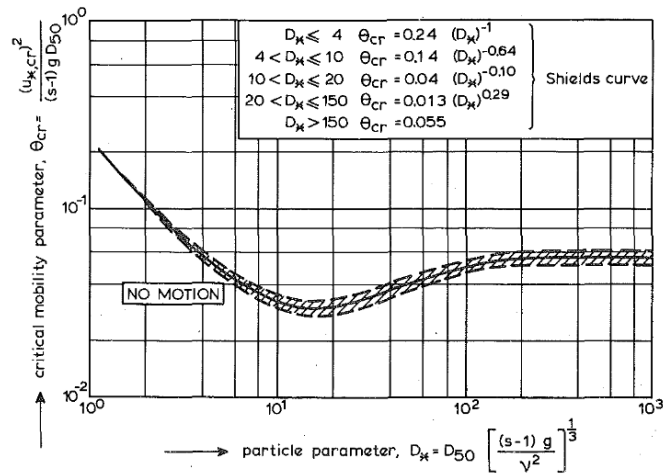


Figure 17: Shields parameter adjusted by VAN RIJN, [1984].

The adjusted shields diagram by VAN RIJN, [1984] gives the particle parameter vs. the mobility parameter as can be seen in Figure 17. The particle parameter can be determined with Equation 3–19 and from the shields curve the mobility parameter can be read. With the mobility parameter the critical shear velocity ($u_{*,cr}$) is determined, which is needed for the transport stage parameter.

The other unknown variable in the transport stage parameter is the shear velocity (u'_*) which is determined with Equation 3–21. In this formula the mean flow velocity (\bar{u}) is used and the Chezy number. (VAN RIJN, [1984])

$$u'_* = \frac{g^{0.5} \bar{u}}{C'}$$

Equation 3–21

$$u'_* \max = u_*$$

$$C' = 18 \log \left(\frac{12 R_b}{3D_{90}} \right)$$

With the equations above the transport stage parameter is determined and next the bed load transport for currents only is calculated.

Calculation Bed-load transport

The bed load transport is defined as the product of the bed load concentration, the particle velocity and the bed saltation height. Combination of these three equations give a description for the bed-load transport as is described with Equation 3–23

The saltation height indicates the end of the bed load transport and the start of the suspended load transport. This is difficult to determine as due to suspension of the particles it is difficult to observe in wave flume tests. The opinion about the saltation height varies. VAN RIJN, [1984] assumed that it can be described with $\frac{\delta_b}{D} = 0.3D_*^{0.7}T^{0.5}$ with an inaccuracy of about 10%. The particle velocity is determined with experiments of Francis and can be approximated with 20% inaccuracy according to the following formula: $\frac{U_b}{[(s-1)gD]^{0.5}} = 1.5 T^{0.6}$ and the bed load concentration is determined with:

$$\frac{C_b}{C_0} = 0.18 \frac{T}{D_*}$$

$$\text{Van Rijn (Currents)} \quad \frac{q_b}{[(s-1)g]^{0.5} D_{50}^{1.5}} = 0.053 \frac{T^{2.1}}{D_*^{0.3}} \quad \text{Equation 3-22}$$

VAN RIJN, [2007] Currents + Waves

In 2007 VAN RIJN, [2007] implemented the effect of waves in his formula. Experimental studies show that near bed streaming is depended on both bed roughness as wave asymmetry. These asymmetry effects (phase lag effect between shear stress and sediment concentration) are especially important in the swash and inner surf zone. VAN RIJN, [2007]. This quasi steady approach of VAN RIJN, [2007] is achieved by time averaging over the wave period. For gravel situations the parameters become $f_{silt} = 1$ and $\eta = 1$ and $\gamma = 0.5$.

$$\text{Van Rijn (Currents + waves)} \quad q_b = \gamma \rho_s f_{silt} D_{50} D_*^{-0.3} \left(\frac{\tau'_{b,cw}}{\rho} \right)^{0.5} \left[\frac{(\tau'_{b,cw} - \tau_{b,cr})}{\tau_{b,cr}} \right]^\eta \quad \text{Equation 3-23}$$

The shear stress due to currents and waves is calculated with Equation 3-24 where the coefficient α determines the relative strength of the wave and current motion and the coefficient β the vertical structure of the velocity profile. The parameter $\tau_{b,cr}$ is determined with the shields diagram.

$$\tau'_{b,cw} = 0.5 \rho_w f'_{cw} (U_{\delta,cw})^2 \quad \text{Equation 3-24}$$

$U_{\delta,cw}$ = velocity at edge of bound. layer

$$f'_{cw} = \alpha \beta f'_c + (1 - \alpha) f'_w$$

$$f'_c = \frac{8g}{\left\{ \left[18 \log \left(\frac{12h}{k_{s,grain}} \right) \right]^2 \right\}}$$

$$f'_w = e^{-6+5.2 \left(\frac{A_w}{k_{s,grain}} \right)^{-0.19}}$$

$$\alpha = \left(\frac{u_c}{u_c + U_w} \right)$$

$$k_{s,grain} = 1 D_{90}$$

When rewriting the shear stress to the shields parameter the formula becomes as Equation 3-25.

$$q_b = \gamma D_{50} D_*^{-0.3} \sqrt{\frac{\tau_b}{\rho} \frac{(\theta' - \theta_{cr})}{\theta_{cr}} \frac{\tau_b}{[\tau_b]}} \quad \text{Equation 3-25}$$

Approximation of bed load transport

The bed shear stress can also be approximated with a simplified formula which is implemented in XBeach-G under the name TR2004.

$$q_b = 0.015 \rho_s u h \left(\frac{d_{50}}{h} \right)^{1.2} M_e^{1.5} \quad \text{Equation 3-26}$$

$$M_e = \frac{(u_e - u_{cr})}{[(s-1)g d_{50}]^{0.5}} = \text{mobility parameter}$$

$$u_e = u + \gamma U_w$$

$$\gamma = 0.4 \text{ (Irregular waves)}$$

$$U_w = \frac{\pi H_s}{[T_p \sinh(kh)]} = \text{peak orbital velocity}$$

$$u_{cr} = \beta u_{cr,c} + (1 - \beta)u_{cr,w}$$

$$\left. \begin{aligned} u_{cr,c} &= 0.19 D_{50}^{0.1} \log\left(\frac{12h}{3d_{90}}\right) \\ u_{cr,w} &= 0.24 [(s-1)g]^{0.66} D_{50}^{0.33} T_p^{0.33} \end{aligned} \right\} \text{ for } 5 \cdot 10^{-5} < d_{50} < 5 \cdot 10^{-4} \text{ m}$$

$$\left. \begin{aligned} u_{cr,c} &= 8.5 D_{50}^{0.6} \log\left(\frac{12h}{3d_{90}}\right) \\ u_{cr,w} &= 0.95 [(s-1)g]^{0.57} D_{50}^{0.43} T_p^{0.14} \end{aligned} \right\} \text{ for } 5 \cdot 10^{-4} < d_{50} < 2 \cdot 10^{-3} \text{ m}$$

3.4.6 NIELSEN, [2006] transport formula

Critical Shear velocity NIELSEN, [2002]

NIELSEN, [2002] focused on a method to easily include saw-tooth waves in a sediment transport formulation. To do so a wave friction factor (f_s) and a phase lag angle (φ_τ) is implemented. The phase lag angle describes the difference in phase between the bed shear stress and the free stream velocity that is used. With these new parameters the amount of shear $\tau(t)$ that is created due to acceleration effects for a certain velocity $u_\infty(t)$ can be determined.

Research by NIELSEN, [2002] about transport rates in the swash zone and to the vertical sediment transport corresponding to sheet flow, show both an optimal phase lag angle of around $\varphi_\tau \approx 40$. NIELSEN, [2002], NIELSEN & CALLAGHAN, [2003]. The grain roughness wave friction factor f_s can be calculated from the standard wave friction factor $f_s = \exp\left[5.5 \left(\frac{2.5d_{50}}{A}\right)^{0.2} - 6.3\right]$ with $A = \frac{\sqrt{2}}{\omega_p} \sqrt{\text{Var}\{u_\infty(t)\}}$. In the model XBeach-G this friction factor is assumed to be constant with $f_s = 0.025$. With this friction factor the friction velocity is determined with Equation 3–27.

$$u_* = \sqrt{\frac{f_s}{2} \left(\cos(\varphi) \cdot u + \frac{T_{m-1.0}}{2\pi} \sin(\varphi) \frac{\partial u}{\partial t} \right)} \quad \text{Equation 3–27}$$

$u_* = \text{Friction velocity}$
 $f_s = \text{Sediment friction factor [-]}$
 $\varphi = \text{phase lag angle [-]}$
 $T_{m-1.0} = \text{Offshore spectral mean period [s]}$

The Shields parameter, the critical value for which sediment transport on flat beds takes place, can be rewritten in the form with the shear velocity as is shown in Equation 3–28.

$$\theta = \frac{u_*^2}{\Delta g D_{50}} \quad \left\{ \begin{aligned} \theta &= \frac{\tau}{\rho \Delta g D_{50}} \\ \tau &= u_*^2 \rho \end{aligned} \right. \quad \text{Equation 3–28}$$

The research of WIT [2015] was conducted with the transport formula of NIELSEN, [2002]. It appeared that the phase difference and friction coefficient which are used in this method have quite a

significant influence on the formed erosion. Per beach type (geometry, gravel size) the corresponding correction factors should be used.

Phase lag angle (φ)

The phase lag angle describes the difference in phase between the free stream velocity and the occurring shear stresses.

This phase lag angle is investigated by WATANABE AND SATO [2004]. This study describes several experiments in a U-tube. The goal of this study is to find the optimal phase lag angle for different hydraulic parameters. Eight of these experiments are used by NIELSEN, [2006] which are given in Table 6.

Table 6: Experimental test results WATANABE AND SATO [2004] used by NIELSEN, [2006]

	d_{50} (mm)	T (s)	U_0 (m/s)	β (-)	Optimal φ_τ (°)
1	0.2	5	0	0.547-0.68	40±18
2	0.2	3	0	0.547-0.68	62±15
3	0.2	3	-0.1	0.547-0.68	55±4
4	0.2	3	-0.2	0.547-0.68	50±7
5	0.74	3	0	0.547-0.68	44±16
6	0.2-0.74	3-5	-0.2-0	0.547	55±20
7	0.2-0.74	3-5	-0.2-0	0.60	53±12
8	0.2-0.74	3-5	-0.2-0	0.68	51±6
Overall:					51±16

Four conclusions are made on this data by NIELSEN, [2006]

1. Bigger periods correspond to smaller optimal phase angles (compare row 1 and 2)
2. Coarser sand gives smaller optimal phase angles (compare row 5 with row 2)
3. A stronger offshore current gives smaller optimal phase angles. (Compare row 2,3 and 4)
4. There seems to be no correlation between β and the optimal phase angle.

These results give the impression that the phase lag angle is a function of the period; the stone diameter and the mean current. $\varphi_\tau = f(d_{50}, T, U_0)$. This is verified in this thesis by changing the phase lag angle for tests with the same stone size but different wave period. This is described in the chapter Model test stages.

Sediment transport

A phase lag angle of $\varphi_\tau = 0$ gives total drag dominated transport and a phase lag angle of $\varphi_\tau = 90$ degree gives pressure gradient dominated transport. NIELSEN, [2006] found a corresponding transport rate in the form of Meyer-Peter and Müller transport equations as is shown in Equation 3–29. (MCCALL, [2015])

$$q_b = 12(\theta' - 0.05)\sqrt{\theta'} \sqrt{\frac{\rho_s - \rho}{\rho} g D_{50}^3}$$

Equation 3–29

3.5 Damage quantification methods

There are several existing methods to quantify the amount of damage on a structure, usually depending on type of structure (statically stable or dynamically stable). These methods can be divided in the following subcategories

1. Counting the amount of stones displaced (damage level, N_{od} , or damage percentage)
2. Eroded area (damage level, S)
3. Erosion profile

3.5.1 Eroded Area

The most used method to quantify the amount of damage is the method of BRODERICK [1983]. This method is also used by VAN DER MEER [1988] to compare its tests.

None of the above mentioned methods describe the formed erosion with the erosion depth, while the erosion depth is the most used design criteria. Research by WIT [2015], already showed the importance of the erosion depth as a damage formulation. She developed an alternative description, which is given in Equation 3–30.

$$S_{new}(\alpha) = S_{start} * \frac{\sin(\alpha_{start})}{\sin(\alpha)} \quad \text{Equation 3–30}$$

It is based on a start slope with a corresponding design damage level. With this criteria the accepted damage level for more mild slopes is given. This methods is optimised with another description of the eroded area. Both results are given in Figure 18. An extensive analysis of the different methods and the method used by Wit [2015] is added in Appendix D: Damage quantification methods.

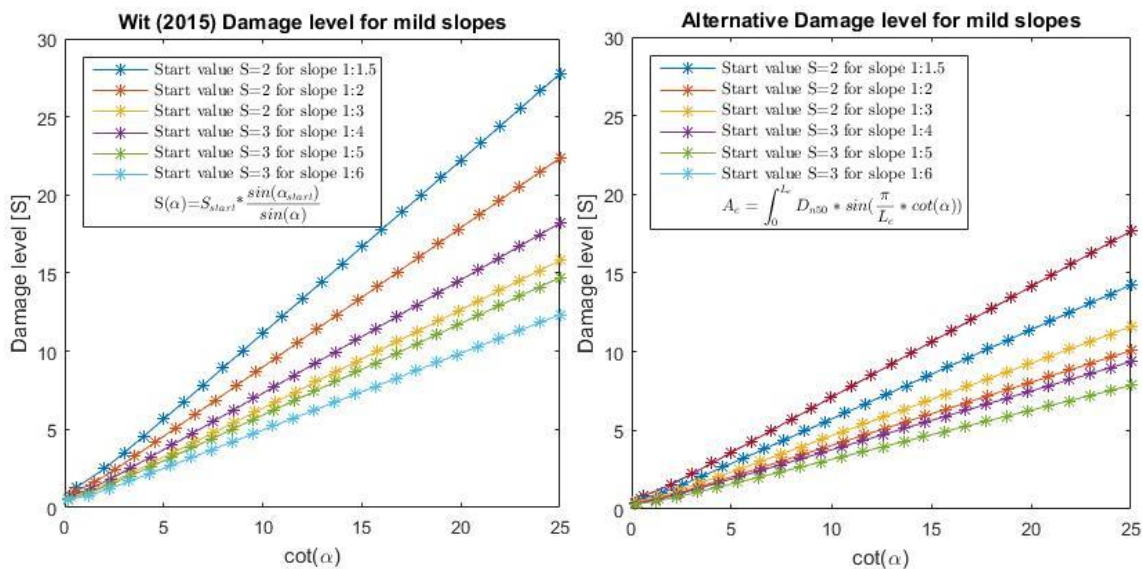


Figure 18: Damage level; Left: Method of Wit; Right: Alternative method

For this thesis the formula developed by WIT [2015], is not used as it cannot give a comparison with the experiments of VAN DER MEER [1988]. The VAN DER MEER [1988] damage description and the erosion depth is used to quantify the damage. To make the eroded depth dimensionless, the relative erosion depth is used. This is the erosion depth divided by the nominal grain size.

$$\text{Damage level: } S = \frac{A_e}{D_{n50}^2} \quad \text{Equation 3-31}$$

$$\text{Rel. Erosion depth} = \frac{d_e}{D_{n50}} \quad \text{Equation 3-32}$$

3.5.2 Erosion profile

For big damage levels the erosion is described with the profile and not with the number. The research of WIT [2015] and VAN DER MEER [1988] clearly indicates that the profiles shape can change. A distinction is made between a bar profile and a crest profile. The theory is that the profile adapts to the ratio between the forcing and stabilizing parameters. The forcing parameters are the wave height and period and the stabilizing parameters are the stone weight and the slope angle.

VAN DER MEER [1988] described the influence of the initial slope. He changed the initial slope and kept the rest of the parameters the same. The profile tends to go to a standard profile marked with black as can be seen in Figure 19. When the initial profile is steeper (case 1:1.5 initial slope) the standard profile erosion becomes more and it forms a crest profile. When the initial slope becomes smaller (case 1:5 slope) the profile becomes a bar profile.

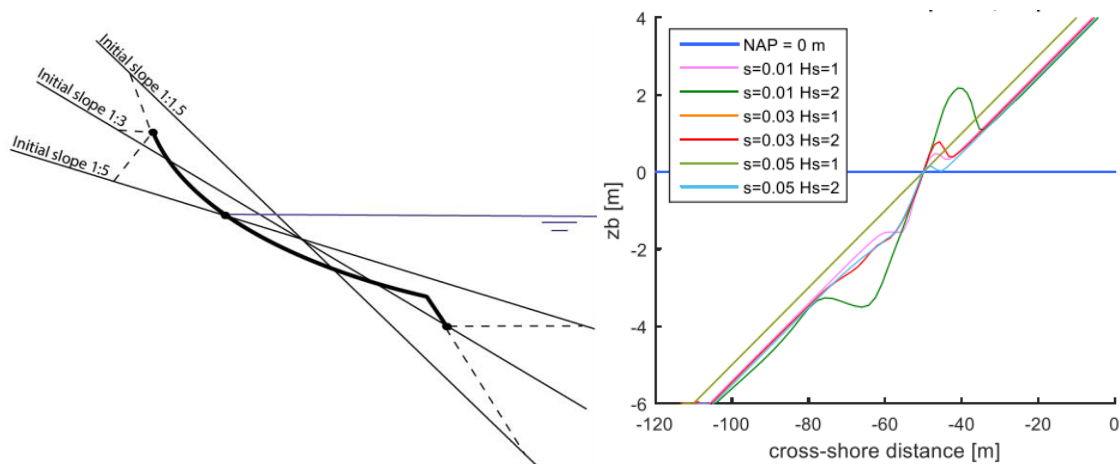


Figure 19: Left: Influence initial profile VAN DER MEER [1988]; Right: Influence hydr. Forcing WIT [2015]

Wit (2015) confirmed these results by redoing the tests in Xbeach-G. She investigated it by keeping the stabilizing parameters the same and changed the hydrodynamic forcing. It is clear from her results that the equilibrium profile tends to go to the angle of repose of the gravel material, as all the profile shapes cross the initial slope under the same angle. See Figure 19.



4

SELECTED NUMERICAL MODEL

- Why XBeach-G
- Alternatives
- How does XBeach-G work?
- Model Validation
- Model limitations

The used numerical model is XBeach-G. This model is chosen because it is one of the few that describes the more coarse sediments during a storm attack. This chapter focuses on the tool XBeach-G that is used. It treats the alternative models, how it is working and its limitations.

4.1 Why XBeach-G

For this research the tool XBeach-G is used, which is developed to predict the profile development of gravel beaches under wave attack. It is a numerical, process based, model that describes the depth-averaged morphodynamics for a cross shore profile. For the bed load transport both the VAN RIJN, [2007] as the NIELSEN, [2006] transport formula are included. The hydrodynamics are calculated with the non-linear shallow water equations with non-hydrostatic extensions to include the surface water elevation due to waves and bound long waves.

Because this model is specially designed for gravel beaches, the groundwater surface water interaction is taken into account because that plays an important role in the sediment transport. As a lot of research is conducted to sandy beaches, not so much research is done for gravel. This model is one of the few models which look at more coarse material.

4.2 Alternatives

There are some alternative less detailed models beside XBeach-G which are developed in the past. Distinction is made between the type of models, there are conceptual models; empirical; parametric and process-based models. Conceptual models describe qualitatively the situation and its processes. Empirical and parametric models use datasets to quantitatively describe the result without or with limited underlying physics. The process based models focuses on the physics and model the situation numerically over time and space. Only alternatives for the process-based models are elaborated.

The current process based models can be divided in wave-resolving and wave-averaged models. Wave-resolving models are original made for situations with man-made structures. Wave-averaged models are based on pre-existing formulae for sandy beaches. Wave resolving models are made for structures which are not made to deform. That is why the main attention in these models was given to the hydrodynamics and not to the morphodynamic response. (MCCALL, [2015])

The first process based model for gravel beaches is made by van Gent in 2002. The model describes besides the surface water also the groundwater in the cross-shore. The model is depth-averaged and describes also the infra-gravity waves with the Non-linear shallow water equations (NLSWE) for

porous media. The morphodynamics are rather rough as it describes one particle per grid, if the destabilising force exceeds the threshold of motion it moves to the next grid.

The other process based model is called Coulwave and is designed in 2007 on the Boussinesq wave model and an adjustment of the Meyer-Peter and Müller transport equation. This model did not include groundwater processes but nevertheless shows good results when adjusting the friction factor for uprush and backwash. (MCCALL, [2015])

The last wave-resolving model is the model BeachWin which is also depth-averaged and describes the water motion with the Non Linear Shallow Water Equations (NLSWE) and the groundwater with a 2D model and the Darcy law. The sediment transport is described with the model of BAGNOLD, [1966] and the occurring transport by HARDISTY [1984]. This model is unable to predict changes which occur lower on the beach. Wave averaged models are for example Cshore, CrosMore, modifications of XBeach.

4.3 How does XBeach-G work?

4.3.1 Model Overview

XBeach-G is a 1D process based model which starts with the input parameters such as the bathymetry. When the program is running the model is divided in vertical grids. (This is called depth-averaged). For every grid the bottom depth is determined and the corresponding hydrodynamic parameters are calculated such as the surface water, the waves and the corresponding currents. The waves and currents interact with the groundwater as infiltration and exfiltration effects occur due to the pressure differences.

The hydrodynamics with, the calculated velocities and accelerations are used as input parameter for the sediment transport formula's (morphodynamics). These formulas determine the amount of shear and the corresponding mass/volume that should move per grid. The groundwater also has an influence on the morphodynamics in the form of infiltration/exfiltration effects and the hydraulic conductivity.

With the amount of sediment transport, the bed level is updated and the loop starts back again with the new input parameters for a new time step. In the next chapters the hydrodynamics and the morphodynamics are elaborated on the specific formulas that are used.

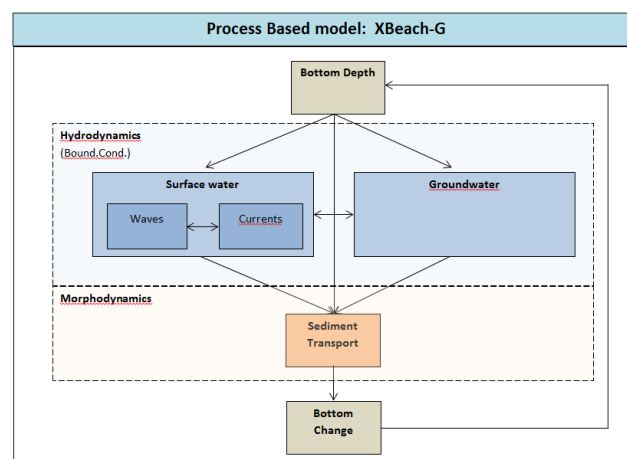


Figure 20: Overview of the process based model XBeach-G.

4.3.2 Model Hydrodynamics

The hydrodynamics in the model can be divided in the surface water, the groundwater and their interaction as is schematised in Figure 21.

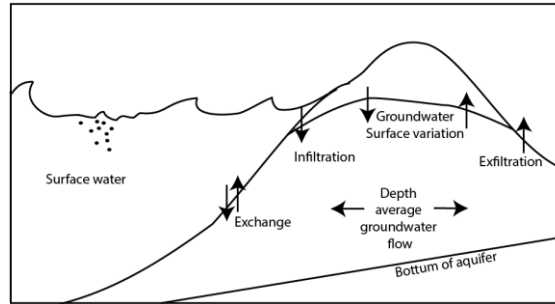


Figure 21: groundwater; surface water and their interaction.

Surface water

The surface water is described with the non-linear shallow water equations which are based two laws. The continuity of momentum and the continuity of mass. Added to this linear shallow water equations are the non-hydrostatic pressure term and the groundwater exchange. The non-linear shallow water equations with the non-hydrostatic pressure term is described in Appendix B: Hydrodynamics.

Ground water

The groundwater is based on the conservation of mass; equations of motion and a parameterisation for the non-hydrostatic groundwater pressure. For the conservation of mass the continuity equation is used and an incompressible flow is assumed. (MCCALL, [2015])

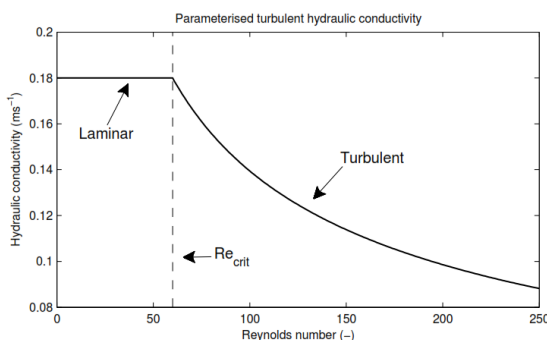
Law of Darcy

The law of Darcy [1856] describes a laminar flow through a homogeneous structure. This law is based on the hydraulic conductivity (K) and the hydraulic head (H).

$$u_{gw} = -K \frac{\partial \bar{H}}{\partial x} \quad \text{Darcy (1856)} \quad \text{Equation 4-1}$$

Hydraulic conductivity

The hydraulic conductivity is estimated based on the laminar hydraulic conductivity and the Reynolds number. $\left(Re = \frac{|u_{gw}| D_{50}}{nv} \right)$ This transition between laminar and turbulent flow is around a Reynolds number of 60. (MCCALL, [2015]).



$$K = \begin{cases} K_{lam} \sqrt{\frac{Re_{crit}}{Re}} & Re > Re_{crit} \\ K_{lam} & Re \leq Re_{crit} \end{cases}$$

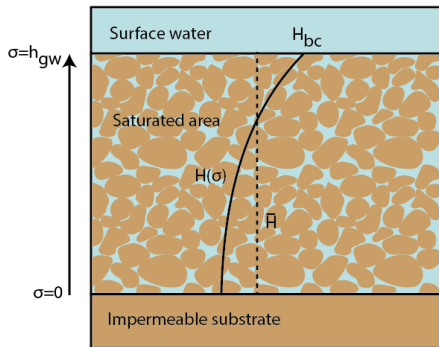
$n = \text{porosity}$
 $v = \text{hydraulic viscosity}$

Groundwater head

The groundwater head cannot be schematised correctly in the model as the model is depth averaged. To implement the groundwater head in the model an approximation is used. Three conditions are set for this approximation

- 1 No exchange of water between aquifer and aquitard (impermeable layer)
- 2 The groundwater head ($\sigma = h_{gw}^2$) is the same as the head at the surface (H_{bc}).
- 3 Linear increase or decrease for the velocity profile from the bottom to the surface

These three conditions are fulfilled with the following approximation for the vertical groundwater hydraulic head.



$$H(\sigma) = \beta(\sigma^2 - h_{gw}^2) + H_{bc}$$

β = parabolic curvature coefficient
 σ = vert. coordinate above the bottom of the aquifer
 H_{bc} = head imposed at the groundwater surface

The depth averaged hydraulic head is obtained by integrating the formula above over the vertical.

$$\bar{H} = \frac{1}{h_{gw}} \int_0^{h_{gw}} H(\sigma) d\sigma = \bar{H} = H_{bc} - \frac{2}{3} \beta h_{gw}^2 \quad \text{Equation 4-2}$$

Exchange with surface water

The groundwater and surface water have exchange in three different ways, submarine exchange; infiltration and exfiltration. The rate of exchange is processed in the parameter (S).

- 1 Submarine exchange

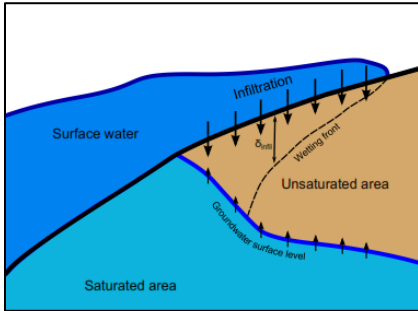
The submarine exchange is only possible when the groundwater and the surface water are connected. This formula is derived from the groundwater head approximation (MCCALL, [2015])

$$S_s = -w(h_{gw}) = K \left. \frac{\delta H}{\delta \sigma} \right|_{\sigma=h_{gw}} = 2\beta h_{gw} K \quad \text{Equation 4-3}$$

- 2 Infiltration

Infiltration and exfiltration happens where the groundwater and surface water are not connected. This is more in the swash zone and not underwater. When the surface water is lower than the groundwater; exfiltration occurs and when the groundwater is lower the water infiltrates into the pores.

PACKWOOD, [1983] designed an approach to calculate the infiltration which is a function of among other the wetting front (δ_{wf}) and the pressure at the bed of the water pressure ($p|^{z=\zeta}$). This method is shown in Equation 4-4.

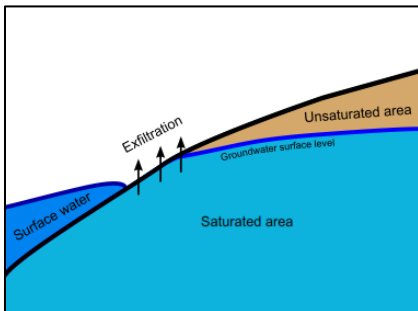


3 Exfiltration

$$S_i = -K \left(\frac{1}{\rho g} \frac{p|^{z-\zeta}}{\delta_{wf}} + 1 \right) \quad \text{PACKWOOD, [1983]}$$

Equation 4-4

$$\delta_{wf}(t) = \int \frac{S_i}{n_p} dt$$



$$S_e = n_p \frac{\partial(\zeta - \zeta_{gw})}{\partial t}$$

Equation 4-5

The last phenome is exfiltration and is described with Equation 4-5.

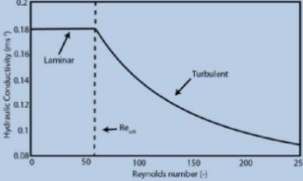
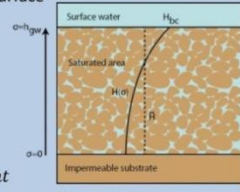
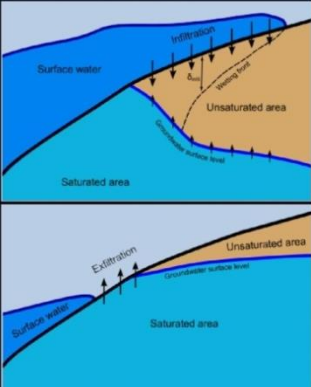
For every vertical grid the sum of these submarine exchange; infiltration and exfiltration is taken and this is the groundwater effect. These effects are implemented in the ventilation factor for the morphology, reducing the friction factor to the dimensionless friction factor. (see chapter morphology).

Groundwater and surface water level.

The groundwater and surface water exchange is determined with the equations shown below. (MCCALL, [2015])

Submarine exchange	Groundwater	$n_p \frac{\partial \zeta_{gw}}{\partial t} = w + S_s = 0$
	Surface water	$\frac{\partial \zeta}{\partial t} = -S_s$
Infiltration/Exfiltration	Groundwater	$n_p \frac{\partial \zeta_{gw}}{\partial t} = w + S_i + S_e$
	Surface water	$\frac{\partial \zeta}{\partial t} = -S_i - S_e$

INTERMEZZO: MODEL HYDRODYNAMICS OVERVIEW

Surface water (waves and currents)	Groundwater
<p>NLSW equations, including non-hydrostatic pressure term and a source term for groundwater exchange.</p> <p>1: Conservation of mass:</p> $\frac{\partial \zeta}{\partial t} + \frac{\partial hu}{\partial x} + S = 0$ <ul style="list-style-type: none"> Waterlevel change Gradient influx Exchange with GW <p>S = rate of exchange between surface water and GW</p> <p>2: Conservation of Momentum:</p> $\frac{\partial u}{\partial t} + u \frac{\partial u}{\partial x} - \frac{\partial}{\partial x} \left(v_h \frac{\partial u}{\partial x} \right) = - \frac{1}{\rho} \frac{\partial (\rho \bar{q} + \rho g \zeta)}{\partial x} - c_f u u $ <p style="text-align: center;">Acceleration advection Pressure gradient bed friction</p> <p>2a: Acceleration advection</p> $v_h = 2(c_s \cdot \Delta x)^2 \sqrt{2 \left(\frac{\partial u}{\partial x} \right)^2} = \text{horizontal viscosity}$ <p>$c_s = 0.1$ = smagorinsky constant Δx = computational grid</p> <p>2b: Pressure gradient</p> <p>\bar{q} = Depth average dynamic pressure (normalised)</p> <p>Vertical momentum balance, whitout adv. & diff terms:</p> $\frac{\partial w}{\partial t} + \frac{\partial q}{\partial z} = 0$ <p>w = vertical velocity z = vertical coordinate</p> $w_b = u \frac{\partial \xi}{\partial x} = u \frac{\partial (\zeta - h)}{\partial x} = \text{Vertical vel. at bed (bound. cond.)}$ <p>Dynamic pressure at bed:</p> $q_b = - \frac{h}{2} \left(\frac{\partial q}{\partial z} \right)_s + \frac{\partial q}{\partial z} \Big _b = 0$ <p>Vertical momentum balance at surface:</p> $\frac{\partial w_s}{\partial t} = 2 \frac{q_b}{h} - \frac{\partial w_b}{\partial t}$ $\frac{\partial u}{\partial x} + \frac{w_s - w_b}{h} = 0$ <p>2c: bed friction</p> $c_f = \frac{g}{C^2} = \frac{g}{(18 \log \left(\frac{12h}{k} \right))^2} = \text{Chézy for turbulent flow}$ <p>$k = 3D90$ = characteristic roughness</p>	<p>law of Darcy (Incompressible flow)</p> $u_{gw} = -K \frac{\partial \bar{H}}{\partial x}$ <p>u_{gw} = Depth – averaged horizontal groundwater velocity K = hydraulic conductivity \bar{H} = Depth – averaged hydraulic head</p> <p>1: Hydraulic conductivity</p> $K = \begin{cases} K_{lam} \sqrt{\frac{Re_{crit}}{Re}} & Re > Re_{crit} \\ K_{lam} & Re \leq Re_{crit} \end{cases}$ $Re = \frac{ u_{gw} D_{50}}{nv}$ <p>n = porosity v = hydraulic visosity</p>  <p>2: Vert. groundwater head</p> <p>Assumptions:</p> <p>a: No groundwater exchange between aquifer and imp. Underlayer. $w_b = 0$ therefore $\frac{\partial H}{\partial \sigma} \Big _{\sigma=0} = 0$</p> <p>b: Groundwater head at surface is continuous with head at the surface: $H(h_{gw}) = H_{bc}$</p> <p>c: Vert. vel. is linear from bottom of aquifer to the surface $w(\sigma) = \alpha \sigma$ therefore $\frac{\partial^2 H}{\partial \sigma^2} = \alpha$</p>  $\bar{H} = \frac{1}{h_{gw}} \int_0^{h_{gw}} H(\sigma) d\sigma$ $H(\sigma) = \beta (\sigma^2 - h_{gw}^2) + H_{bc}$ <p>β = parabolic curvature coefficient σ = vert. coordinate above the bottom of the aquifer</p> $\bar{H} = H_{bc} - \frac{2}{3} \beta h_{gw}^2$ <p>H_{bc} = head imposed at the groundwater surface</p> <p>3: Waterlevels</p> <p>Groundwaterlevel: $n_p \frac{\partial \zeta_{gw}}{\partial t} = w_{gw,s} + S$</p> $w_{gw,s} = \frac{\partial h_{gw} u_{gw}}{\partial x}$ <p>Surfacewater level: $\frac{\partial \zeta_{sw}}{\partial t} = -S$</p>
Groundwater- surface water exchange	
<p>1: Submarine Exchange:</p> $S = -w_{gw,s} = 2\beta h_{gw} K$ <p>S = rate of exchange between surface water and groundwater</p> <p>2: Infiltration:</p> $S = K \left(\frac{1}{\rho g} \frac{P_b}{d_i} + 1 \right)$ <p>P_b = total surface water pressure at the bed $P_b = \rho(q_b + gh)$ d_i = thickness of wetting front $d_i(t) = \int \frac{S}{n} dt$</p> <p>3: Exfiltration:</p> $S = n_p \frac{\delta(\xi - \zeta_{gw})}{\delta t}$ <p>ξ = bed level ζ_{gw} = groundwater level n_p = porosity</p> 	

4.3.3 Model Morphodynamics

Bed shear stress

The model calculates the bed shear stress depended on the type of transport formula that is chosen. The most common formula's that are implemented in the model are the NIELSEN, [2006] and the VAN RIJN, [2007] transport formula. Both formulas have a part of the shear created due to drag and due to inertia.

The drag part of VAN RIJN, [2007] is determined in the same way as is done for the hydrodynamics. So the same shear stress used for the dampening of the waves is used as drag shear on the bottom. For NIELSEN, [2006] this works a bit different as in this case the shear stress for the hydrodynamics is not used for the morphodynamics. This shear stress is calculated separately according to Equation 4–7.

Because the ventilation effects due to infiltration and exfiltration are included in the friction factor, (c_f) these effect do not play a role in the sediment transport when using the NIELSEN, [2006] transport formula.

$$\text{van Rijn: } \tau_b = \underbrace{c_f \rho u |u|}_{\text{Drag}} + \underbrace{c_i \rho D_{50} \frac{\partial u}{\partial t}}_{\text{Inertia}} \quad \text{Equation 4-6}$$

$$\text{Nielsen: } u_* = \sqrt{\frac{f_s}{2} \left(\cos(\theta) \cdot u + \frac{T_{m-1.0}}{2\pi} \sin(\varphi) \frac{\partial u}{\partial t} \right)} \quad \text{Equation 4-7}$$

$$u_* = \underbrace{\sqrt{\frac{f_s}{2} \cos(\theta) \cdot u}}_{\text{Drag}} + \underbrace{\sqrt{\frac{f_s}{2} \frac{T_{m-1.0}}{2\pi} \sin(\varphi) \frac{\partial u}{\partial t}}}_{\text{Inertia}}$$

The main input for the bed shear stress out the hydrodynamics is the velocity and the acceleration. The internal calculation time of the model is around $dt \approx 0.006 \text{ sec.}$ which means that every 0.006 seconds the velocity is calculated per grid point. From this velocity the acceleration is calculated, but to filter out the errors a high frequency filter is implemented. The filter is implemented on the local "uu", which means that it is implemented on the velocity at point u. Point u is the point between the grid cells. The filter that is used (Equation 4–3) is to filter out the extreme differences that happen within a really small time period.

$$u_{local} = (1 - factime)u_{local \text{ old}} + factime \cdot uu \quad \text{Equation 4-8}$$

$$factime = \frac{dt}{\frac{T_{rep}}{20}}$$

The output given in the model is however the unfiltered velocity, so it is difficult to guess how much influence this filter has on the results.

Shields

The shields parameter for incipient motion is calculated the same way. The only difference is that the shear velocity, used in the NIELSEN, [2006] transport formula, is converted to the shear stress according to the following formula: $\tau = u_*^2 \cdot \rho$

Sediment transport

The actual sediment transport is calculated different according to the formula's explained in the chapter Morphodynamics.

INTERMEZZO MODEL MORPHODYNAMICS OVERVIEW

ed shear stress - Van Rijn- Mc Call	Bed shear stress - Nielsen
$\tau_b = \tau_{bd} + \tau_{bi}$ $\tau_b = c_f \rho u u + c_i \rho D_{50} \frac{\partial u}{\partial t}$ <p>drag part inertia part</p> $\tau_b = \text{bed friction}$ $c_f = c_{f_0} \left(\frac{\phi}{e^{\phi} - 1} \right) = \text{dim. frict. fact.}$ <ul style="list-style-type: none"> • Min = 0.1 • Max = 0.3 $\phi = -\frac{1}{2} \cdot \frac{0.9}{c_{f_0}} \cdot \frac{S}{ u } = \text{Ventilation parameter}$ $c_{f_0} = \frac{g}{\left(18 \log \left(\frac{12h}{3D_{90}} \right) \right)^2}$ $c_i = c_m c_v c_n = \text{inertia callibration coefficient}$ $c_m = 1 + c_a = 1.5 = \text{mass of grain}$ $c_v = \frac{1}{6} \pi (\text{spheres}) = \text{volume of grain}$ $c_n = \text{number of grains}$	$u_* = \sqrt{\frac{f_s}{2}} \left(\cos(\varphi) \cdot u + \frac{T_{m-1.0}}{2\pi} \sin(\varphi) \frac{\partial u}{\partial t} \right)$ <p>$u_* = \text{Friction velocity}$</p> <p>$f_s = \text{Sediment friction factor [-]} = 0.025$</p> <p>$\varphi = \text{phase lag angle [-]} = 25$</p> <p>$T_{m-1.0} = \text{Offshore spectral mean period [s]}$</p>
Shields - Van Rijn- Mc Call	Shields - Nielsen
$\theta' = \theta \cdot \cos\beta \left(1 \pm \frac{\tan\beta}{\tan\phi} \right)$ <p>$\theta' = \text{effective shields parameter [-]}$</p> <p>$\beta = \text{local angle of bed}$</p> <p>$\phi = 35 - 45 = \text{angle of repose}$</p> $\theta = \frac{\tau_b}{\rho g \Delta_i D_{50}}$ <p>$\theta = \text{shields parameter [-]}$</p> $\Delta_i = \frac{\rho_s - \rho}{\rho} + \alpha \frac{S}{K} = \text{relative effective weight}$ <p>$\alpha = \text{seepage} = 0.5$</p> <p>$K = \text{Hydraulic Conductivity}$</p>	$\theta' = \theta \cdot \cos\beta \left(1 \pm \frac{\tan\beta}{\tan\phi} \right)$ <p>$\theta' = \text{effective shields parameter}$</p> <p>$\beta = \text{local angle of bed}$</p> <p>$\phi = 35 - 45 = \text{angle of repose}$</p> $\theta = \frac{u_*^2}{\Delta_i g D_{50}} \rightarrow (\tau_b = \rho \cdot u_*^2)$ <p>$\theta = \text{shields parameter [-]}$</p> $\Delta_i = \frac{\rho_s - \rho}{\rho} + \alpha \frac{S}{K} = \text{relative effective weight}$ <p>$\alpha = \text{seepage} = 0.5$</p> <p>$K = \text{Hydraulic Conductivity}$</p>
Sediment transport Van Rijn- Mc Call	Sediment Transport Nielsen
$q_{bs} = \gamma D_{50} D_*^{-0.3} \sqrt{\frac{\tau_b}{\rho} \cdot \frac{\theta' - \theta_{cr}}{\theta_{cr}} \frac{\tau_b}{ \tau_b }}$ <p>$q_{bs} = \text{Sediment transport} \left[\frac{m^2}{s} \right]$</p> <p>$\gamma = \text{callibration coefficient} = 0.5$</p> $D_* = D_{50} \left(\frac{\Delta g}{\nu^2} \right)^{\frac{1}{3}}$ <p>$\nu = \text{kinematic viscosity}$</p> $\theta_{cr} = \frac{0.3}{1 + 1.2D_*} + 0.055(1 - e^{-0.020D_*})$	$q_{bs} = 12(\theta' - 0.05) \sqrt{\theta'} \sqrt{\frac{\rho_s - \rho}{\rho} g D_{50}^3}$ <p>$q_{bs} = \text{Sediment transport} \left[\frac{m^2}{s} \right]$</p> <p>$\theta = \text{adjusted shields parameter [-]}$</p>

Bed level change

$$\frac{\partial \xi_b}{\partial t} + \frac{1}{(1-n)} \frac{\partial q_{bs}}{\partial x} = 0$$

4.4 Model Validation

4.4.1 Validation Locations

The model XBeach-G is validated on five different beaches along the coast of the UK. The beaches form a homogeneous structure, so XBeach-G is not validated for impermeable structures. As mentioned earlier, these beaches have little or no net longshore sediment transport and thus only the cross shore transport is important. The validation is done by comparison between the model and the measurements on the beach after a storm attack. The accuracy is expressed with the BSS which is the Brier Skill Score. The Brier Skill Score (BSS) shows the accuracy of the model results relative to the measured data. A BSS of 1 is completely accurate, and a score of 0 has zero accuracy.

The validation locations have slopes ranging from 1:5 till 1:9 and grain sizes ranging from 0.2cm till 8 cm. The VAN DER MEER [1988] experiments fit within the validation range of XBeach-G. So XBeach-G should be able to reproduce the experiments correct.

Table 7: : Validation location and characteristics. (MCCALL, [2015])

Location		Duration [days]	H_{mo} [m]	T_p [s]	$s = \frac{H_{mo}}{L_0}$ [-]	D_{50} [m]	K [mms ⁻¹]	$\tan(\beta)$ [-]
BARDEX	BAB3	1.7	0.8	4.3	0.029	11	155	0.19
	BABR	0.1	1.0	10.0	0.005			
	BAE9	1.2	0.8	7.7	0.007			
	BAE10	1.2	0.8	7.7	0.007			
Chesil Beach	CB1	25.0	2.9	8.6	0.027	40	(200-600)	0.20
	CB2	21.5	7.6	13.9	0.025			
Loe Bar	LB5	122.8	8.-	14.5	0.024	2	(3-30)	0.12
Slaption Sands	SS2	9.8	2.0	6.9	0.029	6	19-150)	0.15
	SS3	36.0	4.6	9.5	0.035			
Sillion de Talbert	ST1	74.0	9.5	16.0	0.024	80	(200-600)	0.11

4.4.2 Morphological validation

Berm formation

One of the characteristics of gravel is the formation of berms due to steps. Due to the breaking of the waves on the steps, a mild slope is getting steepened forming a berm. This process is not yet completely covered with the current hydrodynamics and morphodynamics in the model. The berms are made but are in general under predicted by the model. Because the berm is morphological related to the step, accurate modelling of the step can solve the problem. (MCCALL, [2015]).

This difference in results is explained with the lack of knowledge and complexity of complex hydrodynamics under breaking waves. (turbulence). For lower energetic conditions the model will probably give more accurate results than under high energetic conditions. (MCCALL, [2015])

Beach erosion

The global trend of the gravel beach erosion seems to be quite accurately described in the model as can be seen in Figure 22. However, quantitatively the differences in damage values and erosion depths between the measured and calculated values are significant. For global trends after a storm it is quite accurate but for design purpose of statically stable structures this could be different. This is an important aspect to consider when the model is used for a design purpose.

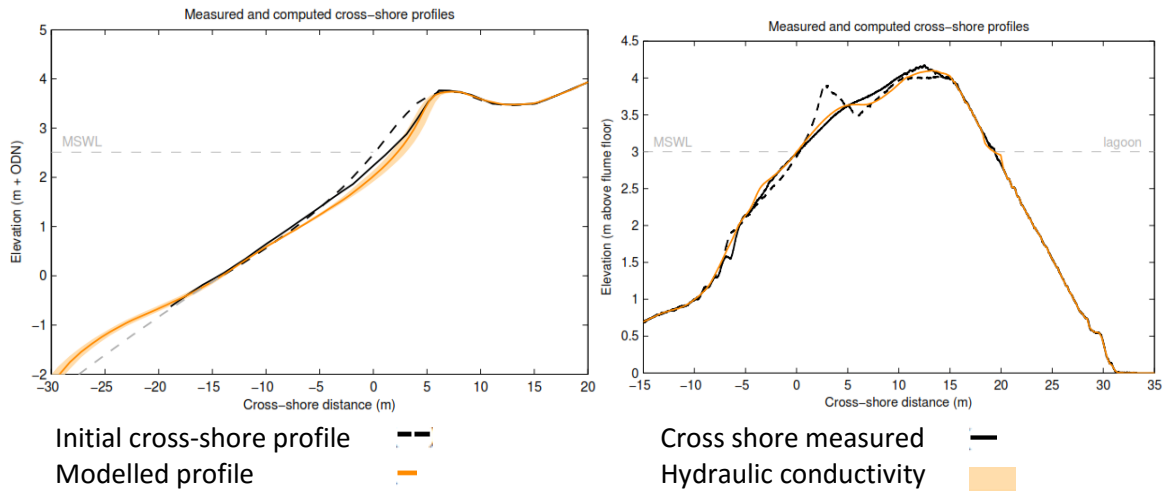


Figure 22: Beach erosion validation tests

4.4.3 Hydrodynamic validation

Wave transformation

Spectrum

The validation of the wave spectrum along the shore is shown in the figure below. Only for the higher and lower frequencies the energy is sometime under-predicted. Overall the spectral significant wave height is well described with a maximum relative bias of 5.7%.

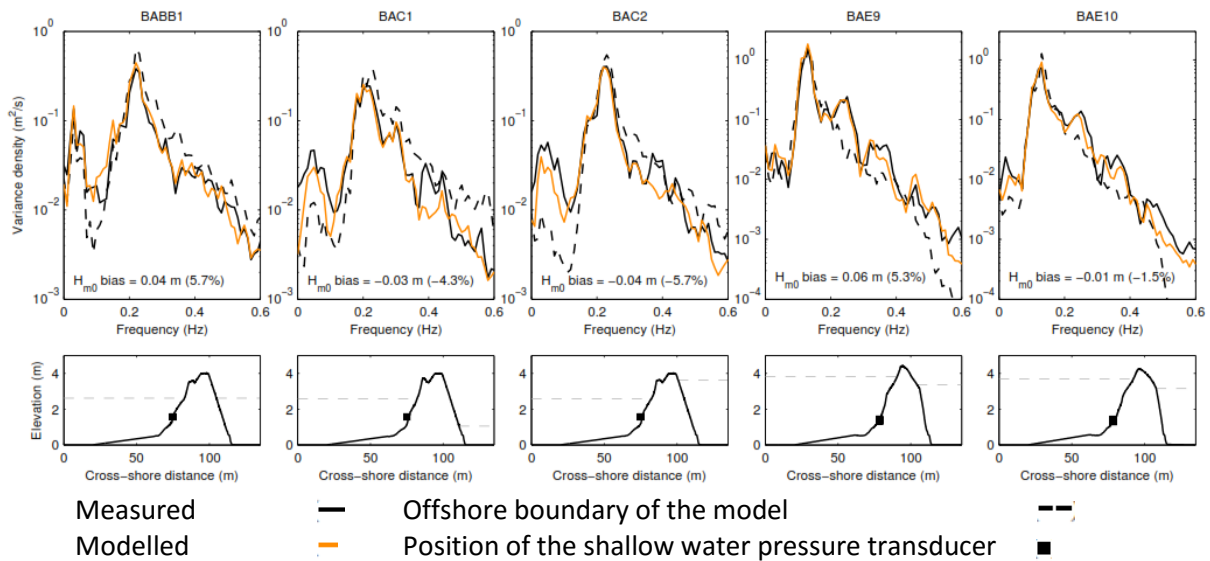


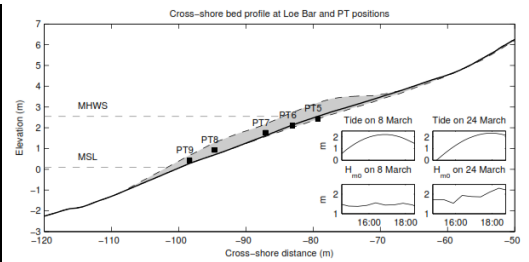
Figure 23: Spectrum at different locations along the slope.

Wave height

The wave transformation from offshore to nearshore is described by placing five pressure meters along the shore, measuring the wave height at that location. The results are presented in the table underneath for two test locations. (LB1 and LB2) A positive Bias indicates an over-prediction of the wave height and a negative BIAS an under-prediction. Most tests give an over-prediction of the significant wave height.

Table 8: Wave height transformation from offshore to nearshore (MCCALL, [2015])

	LB1			LB2		
	RMSE [m]	SCI [-]	Bias [m]	RMSE [m]	SCI [-]	Bias [m]
PT9	0.08	0.05	-0.03	0.28	0.17	0.21
PT8	0.11	0.07	0.03	0.16	0.11	0.13
PT7	0.27	0.27	0.27	0.34	0.40	0.32
PT6	0.17	0.21	0.16	0.31	0.32	0.29
PT5	N/A	N/A	N/A	0.25	0.27	0.23
Combined	0.11	0.14	0.11	0.28	0.21	0.23



Wave shape

The skewness and asymmetry are also measured along the five measuring points along the coast. The results show that the offshore situation is quite well described at point 8 and 9. For the measuring points closer to the shore, the asymmetry is over predicted. (MCCALL, [2015]). The root-mean squared error for wave skewness is 0.27 and for asymmetry it is 0.33. The over-prediction of the wave asymmetry could be due to the simplified method of modelling the hydrodynamics of breaking waves and excluding effects as turbulence and vertical vorticities.

Wave set-up

The wave set-up is achieved by subtracting the surge level and the tide from the measured water level. The wave set-up increases in shoreward direction and is predicted reasonably well. The errors which are still there are addressed to a lack of morphological updating. The RMS of the wave set-up is smaller than 0.10m for test LB1 and smaller than 0.25 for test LB2. This higher error for beach LB2 is due to the errors in the most shoreward measuring points (PT5 and 6) where the set-up is under estimated.

4.4.4 Groundwater validation

The groundwater is calibrated with the BARDEX physical model experiments. The groundwater is coupled to the surface water with infiltration and exfiltration effects.

The groundwater run-up is tested with three different experiments from which the hydrodynamics were modelled well. The groundwater head is measured at 4 different locations in the dike. The results show quite good agreement, as the median RMSE is between 0.04 and 0.05, which is twice to five times the accuracy of the measurements. .

Table 9: Run-up validation results.

	BABB1			BAC1			BAC2		
	RMSE [m]	Bias [m]	BSS [-]	RMSE [m]	Bias [m]	BSS [-]	RMSE [m]	Bias [m]	BSS [-]
Maximum	0.09	0.08	0.97	0.08	0.07	0.98	0.08	-0.08	0.88
Median	0,05	<0.01	0.78	0.04	<-0.01	0.89	0.05	-0.02	0.71
Minimum	0.02	<0.01	0.23	0.02	<-0.01	-0.63	<0.01	<-0.01	0.32

4.5 Model limitations

There are a couple of things to consider when modelling with XBeach-G. There are overall limitations of the model and model input limitations. The overall limitations do not form a problem as this research is limited for 1D situation and no mixed sand compositions. Also the storm conditions are part of the scope so this forms no problem. The input limitations are considered with the model input.

Overall limitation

- 1D model so longshore uniformity
- No mixed sand/gravel options
- Only (energetic) storm conditions

Model Input limitation

- Maximum grid distance: $\Delta x_{max} = \frac{L_0}{50}$
- Offshore water depth must be at least twice the offshore significant wave height.
- Wave period must be in relation to the offshore water depth as Figure 24

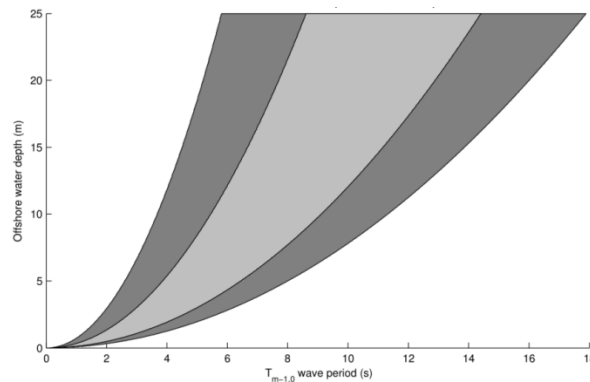


Figure 24: Input limitations wave period vs. offshore water depth.

Figure 24 shows the offshore water depth relative to the wave period. These are the recommended values. The dark lower bound is to make sure bound long waves are modelled well. The dark upper bound is to make sure the water depth does not exceed the limits of the non-hydrostatic pressure solver. (MCCALL, [2015])

5

DATA ANALYSIS

- Available data
- Used experimental data

The numerical model XBeach-G is validated from a 1:5 slope till a 1:9 slope, as is described in the chapter Model Validation. In this analysis the VAN DER MEER [1988] data is compared with the validation range of XBeach-G. This is used to choose the VAN DER MEER [1988] experiments that are reproduced with the numerical model.

5.1 Available data

Most of the experiments are executed for steep slopes and the data for mild slopes is scarce. Three sources of data were found, the VAN DER MEER [1988] experiments, the GWK-Gravel data (LÓPEZ DE SAN ROMÁN-BLANCO ET AL., [2006]) and the data used by SCHIERECK & FONTIJN [1996].

The available data is almost all in the range between 1:2 and 1:6 slopes. Most data is achieved from the VAN DER MEER [1988] experiments with the damage level. In the report of LÓPEZ DE SAN ROMÁN-BLANCO ET AL., [2006] also experiments on a 1:8 gravel slope are described. These experiments are executed on a thick layer of gravel, so a homogeneous situation can be assumed. The experiments for the GWK-Gravel had a nominal stone diameter of 0.021 meter. It was however not possible to extract the data and use this experiment.

The numerical model XBeach-G is only validated for several beaches. So only a homogeneous situation is validated. The range of the experiments is between a 1:5 and 1:9 slope but the model should be valid till a 1:10 slope according to MCCALL, [2015].

Table 10: Overview current available data and model validation area.

		1:2	1:3	1:4	1:5	1:6	1:7	1:8	1:9	1:10	1:25	
VAN DER MEER [1988]	Imp.	■										
	Hom.	■			■							
SCHIERECK & FONTIJN [1996],	Imp.										■	
	Hom.											
GWK – Gravel (LÓPEZ DE SAN ROMÁN-BLANCO ET AL., [2006])	Imp.											
	Hom.								■			
Xbeach-G	Imp.											
	Hom.					■		■		■		

- Within validity range and tested
- Within validity range but not tested

5.2 Used experimental data

Most of the VAN DER MEER [1988] experiments are executed on steep slopes. For this thesis only the mild slopes with low iribarren numbers are interesting. ($\xi_m < 2.5$). The VAN DER MEER [1988] experiments for 1:6 slopes are only executed for impermeable structures as is described above. For these impermeable structures, not a lot of experiments are performed so also some 1:4 slope experiments are used. The used experiments are all impermeable experiments from VAN DER MEER [1988] and categorised in test series A, test series B and test series C.

Test series A consist out of four experiments on a 1:6 slope and five experiments with a 1:4 slope. These tests are determined with a damage curve as is explained in the chapter Design formula of . This implements that these tests are not really executed but determined from curve fitting with other tests. The stone size of test series A range from 1,64cm stones till 3,6 cm stones and the wave height ranges from 4,2cm till 9,7cm with wave steepness's of respectively 0,4% and 3.6%. Test 1 and 4 have the most extreme variables for the 1:4 slope tests and test 5 and 9 for the 1:6 slope tests.

Test series B consist out of five tests which are executed in the wave flume. It is decided to use tests with damage levels around $S \approx 2$ after 3000 waves. These tests area all executed on a 1:6 slope with the same stone diameter (3,6cm). The wave steepness is changing from 0.8% till 5.2%. In test series B the stabilizing parameters are the same and only the hydraulic forcing is changed.

Test series C consists out of two tests and is used for their profile description. VAN DER MEER [1988] only describes the profile for dynamic tests. This are tests where significant damage occurs. In these cases the profile is more important than the formed damage level. The tests have an initial slope of 1:3 and 1:5. The wave conditions and the stability parameters are almost the same for both tests.

Table 11: Overview used experimental test series.

		Test	slope	Δ	D_{n50}	T_m	$L_{0,m}$	H_s	S_m	t_{model}	ζ_m	$\frac{H_s}{\Delta D_{n50}}$	$S = \frac{A_e}{D_{n50}^2}$
			[]	[-]	[m]	[s]	[m]	[m]	[-]	[s]	[-]	[-]	[-]
Impermeable	Test series A	1	6	1.7	0.0164	1.15	2.065	0.058	0.028	3450	1	2.07	2.0
		2	6	1.7	0.0164	1.31	2.679	0.042	0.016	3930	1.33	1.52	2.0
		3	6	1.63	0.036	2.63	10.80	0.089	0.008	7890	1.81	1.52	2.0
		4	6	1.63	0.036	3.15	15.50	0.062	0.004	9450	2.64	1.05	2.0
		5	4	1.7	0.0164	0.99	1.530	0.056	0.036	2970	1.31	2	2.0
		6	4	1.7	0.0246	1.15	2.065	0.067	0.032	3450	1.39	1.6	2.0
		7	4	1.7	0.0246	1.31	2.679	0.075	0.028	3930	1.5	1.79	2.0
		8	4	1.7	0.0328	1.31	2.679	0.097	0.036	3940	1.31	1.74	2.0
		9	4	1.61	0.036	1.76	4.836	0.085	0.018	5280	1.88	1.47	2.0
	Test series B	10	6	1.63	0.036	2.15	7.217	0.114	0.016	6450	1.33	1.94	2.81
		11	6	1.63	0.036	2.66	11.05	0.084	0.008	7980	1.91	1.43	1.25
		12	6	1.63	0.036	3.23	16.29	0.069	0.004	9690	2.57	1.17	2.53
		13	6	1.63	0.036	1.81	5.115	0.121	0.024	5430	1.09	2.06	2.61
		14	6	1.63	0.036	1.37	2.930	0.152	0.052	4110	0.73	2.59	1.74
Serie C	15/Dyn.1	5	1.59	0.011	1.75	4.78	0.19	0.040	5250	1.01	10.8		
	16/Dyn.2	3	1.59	0.011	1.75	4.78	0.19	0.040	5250	1.73	10.67		

6

TEST SETUP

- Input model
- Model test stages

The model is explained and the available data is analysed. The next step is to reproduce these conditions in the model and reproduce the experiments. In this chapter the input in the model is discussed.

6.1 Input Model

6.1.1 Parameter conversion

For the input in the model the standard General User Interface (GUI) is used and the data is extrapolated to change specific parameters in the core of the model. Some of the data of VAN DER MEER [1988] is described with a D_{n50} (nominal stone diameter) instead of a D_{50} (sieve diameter) which is used in the Xbeach-G model. This sieve diameter, D_{50} , was converted using an empirical ratio of $D_{50} = \frac{1}{0.84} D_{n50}$ as proposed by LAAN [1980]. For the test of VAN DER MEER [1988] with the fixed damage levels (test series A) only the mean period was given. A ratio of $T_p = 1.15 T_m$ is used to convert this parameter such that it can be used in XBeach-G.

6.1.2 Hydrodynamics

The wave spectrum used in this research is a Pierson Moskowitz spectrum, just like VAN DER MEER [1988] did for most of his experiments. In the paper of VAN DER MEER [1988] is already described that the type of spectrum does not have a significant effect on the results. This thesis uses fixed storm duration of 3000 waves (approximately 5-6 hours storm) with a constant water level. For every test the variable "order=1" is added which excludes the Bound Long Waves in the model. VAN DER MEER [1988] did not model the bound long waves as this was not possible in the wave flume at that time.

6.1.3 Model bathymetry

VAN DER MEER [1988] uses for all the experiments a water depth of -0.8m and a crest height of +0.4m. The wave height and period are measured with two wave gauges at the toe of the structure. The conditions at the wave board are unknown.

In the model the same water depth and crest height is used. It was not possible to model the whole wave flume due to dampening of the waves. Therefore the slope is only modelled and not the rest of the flume. In the test method description some model shape variations are executed to investigate the effect.

For the impermeable layers a layer thickness of 0.08m is used, just like the VAN DER MEER [1988] experiments. The layer thickness is implemented in the numerical model with a technique in which

the aquifer layer is modelled with the code: “aquiferbotfile=zandlaag.dep”. A text file is made with the right y-coordinates named zandlaag.dep that figures as impermeable layer.

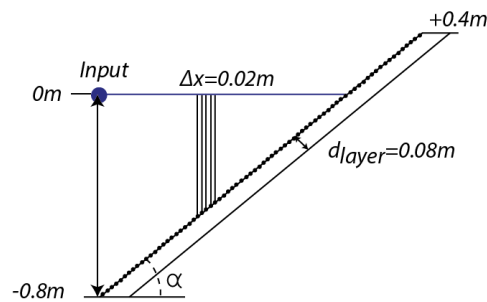


Figure 25: Modelled profile

6.1.4 Grid distance

To model the hydrodynamics well, a maximum grid distance of $\Delta x_{max} = L_0/50$ is needed. For the used tests a minimal grid distance of $\Delta x = 0.02m$ is necessary. The accuracy of the measuring rod used by VAN DER MEER [1988] to measure the erosion is $\Delta x = 0.04m$. The minimal grid distance for the hydrodynamics is leading so for all tests a grid distance of $\Delta x = 0.02m$ is used.

6.1.5 Overview Model input

An overview of the previously described input parameters is given in Table 12.

Table 12: Overview Model input.

Profile		Parameters	
Grid size	2cm	Duration	3000 waves
Top	+0.4m	Groundwater level	+0m
Bottom	-0.8m	Bottom aquifer	0 (Homo.)
Slope	Test depended		Aquiferbotfile (Imp.)
		Stone size (D50)	Test depended
		Hydraulic conductivity	0.01 m/s
Hydrodynamics		Morphology	
Number of waves	3000	Transp. Method	VAN RIJN, [2007]
Period (Tp)	Test depended		NIELSEN, [2006]
Wave Height Hs	Test depended	Sed. friction factor	0.025
Spectrum	Pierson Moskowitz	Phase lag angle	25°
		Angle of repose	35°
		Tide	
		No tide	-

6.2 Model test stages

The final objective is to investigate if XBeach-G can function as a design tool for rocks on mild slopes. To achieve this goal the XBeach-G tests are executed in different stages. These stages are numbered from 1 till 4 and describe the approach used to find the working of XBeach-G for mild slopes.

6.2.1 Stage 1: Model size

Initially, the model setup has been evaluated to verify the influence from the model domain on the results. The effect on the hydrodynamics between a model domain with the full wave flume or with a domain starting at the start of the slope needs to be incorporated.

6.2.2 Stage 2: NIELSEN, [2006] vs. VAN RIJN, [2007]

Following, test series A and B are modelled exactly according to the experiments performed by VAN DER MEER [1988]. Because the model XBeach-G is not able to implement layers the experimental tests are numerical reproduced without an under layer. The chosen VAN DER MEER [1988] experiments are executed with an impermeable under layer. With a numerical manoeuvre it is possible to bypass this problem and implement an underlayer in XBeach-G. The effect of this method is not known and therefore is decided to reproduce the experimental tests with a homogeneous structure. For test series A and B the calculated damage with Xbeach-G is compared with the damage measured by VAN DER MEER [1988]. For test series C the profile is compared.

6.2.3 Stage 3: Variation parameters

In the third stage several parameters are varied to systematically verify the physical processes in Xbeach-G and to explain the differences in modelled and measured results. The first parameter that is changed is the slope angle. This is done for test series A and B with as goal to investigate the influence of the slope on the formed damage. In the stability vs. iribarren graph the tests are shifting more to the left as can be seen in Figure 26. Also the stone diameter is changed, which causes the test to shift upward (more stable) for bigger stones and lower (less stable) for smaller stones.

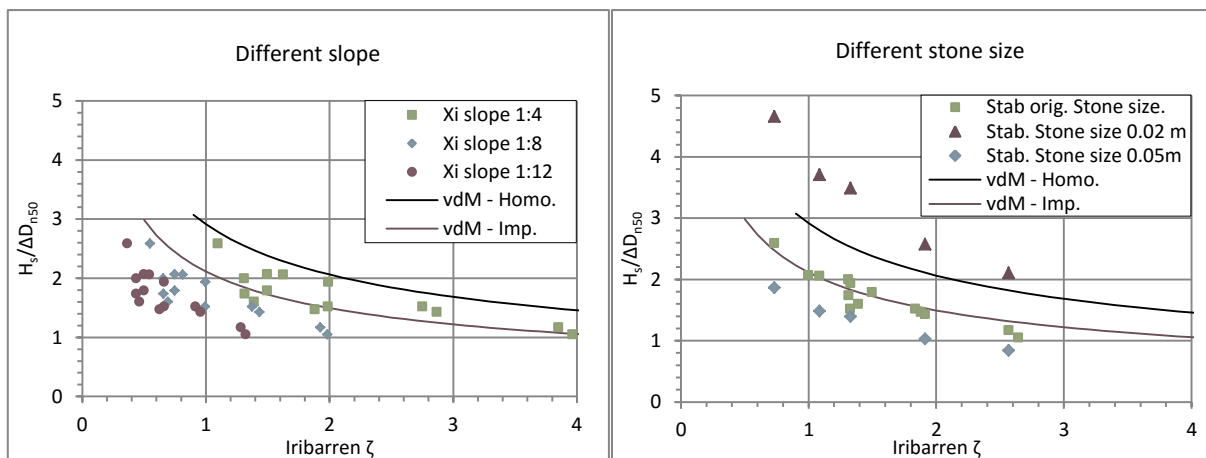


Figure 26: Executed tests with variation in slope and stone diameter visualised in the stability vs. iribarren graph.

Other parameters that are varied are, the layer thickness, phase lag angle and hydraulic conductivity for the NIELSEN, [2006] transport formula. An overview of the executed tests is shown in Table 13. For the tests with implementation of a layer the stability should decrease according to the VAN DER MEER [1988] formula.

Table 13: Stage B Tests executed for different parameters.

	VAN RIJN, [2007] & NIELSEN, [2006]			NIELSEN, [2006]	
	Slope [-]	D_{n50} [cm]	t_{layer} [cm]	φ [°]	K [ms ⁻¹]
Test series A	1:4 1:6		$t_{layer} = 8$		
Test series B	1:8 1:10 1:12	$D_{n50}=2$ $D_{n50}=5$	$t_{layer} = 8$ $t_{layer} = 4$	$\varphi=35$	K=0.4
Test series C	1:3 1:5 1:8 1:10 1:12		$t_{layer} = 8$		

- Layered
- Homogeneous
- Both layered as homogeneous

6.2.4 Stage 4: Hydrodynamics and Morphodynamics

The fourth stage consists of investigating the detailed model output in Xbeach-G concerning several hydrodynamic and morphological parameters. With a detailed understanding of the working of the hydrodynamics and morphodynamics the trends in stage 3 are explained. For the hydrodynamics the velocity, acceleration and infiltration is analysed. For the morphology the shear stress/ velocity the shields parameter and the occurring sediment transport rates are analysed.

Both the morphodynamics as the hydrodynamics is compared with a case without morphological updating. The goal is to find out which of the above parameters play a general role in the sediment transport and how can this be linked to the observed damage.

7

RESULTS

- Stage 1: Model size
- Stage 2: NIELSEN, [2006] vs. VAN RIJN, [2007]
- Stage 3: Variation parameters
- Stage 4: Hydrodynamics vs. Morphodynamics.

The results of the executed tests are described in the following chapter. The results are described per stage as is explained in the previous chapter Model test Stage. Per stage a recap gives the interim conclusions.

7.1 Stage 1: Model size

To investigate the model size, several alternatives have been investigated. The wave conditions in the VAN DER MEER [1988] experiments were measured at the toe of the slope. From this perspective three alternatives have been investigated as presented in Figure 27. From left to right the first alternative is the model with a two meter long horizontal foreshore in front of toe (Model a). When the foreshore is made too long significant dampening effects occurred. The second model (Model b) includes only the slope, which has an advantage reducing the calculation times. Model c starts at the toe of the structure, but has a 2 meter long horizontal segment placed on top to investigate if no groundwater problems occur at the landward boundary of the model.

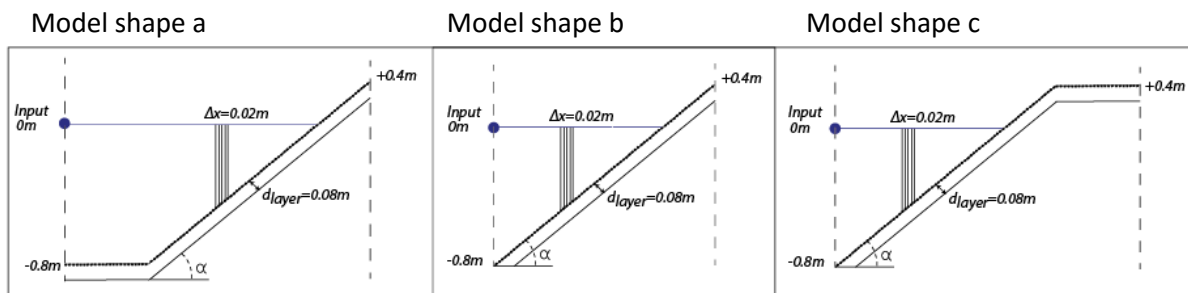


Figure 27: From left to right model size a, b and c respectively.

Xbeach-G was run for these three alternatives and compared with the experimental data from test series B. The damage created for test series B for the original 1:6 slope are presented in Table 14. All the tests show more or less the same amount of damage. The model size has only minor influence on the results and therefore is chosen to use Model b because it has the least grid points and thus the fastest calculation time.

Table 14: Calculated damage for Model a, Model b and Model c.

		Test series B			
		$S = \frac{A_e}{D_{n50}}$			
		NIELSEN, [2006]			VAN DER MEER [1988]
		Model a	Model b	Model c	Exp. Damage
1:6 slope	Test 10	5.2	5.7	5.4	2.8
	Test 11	4.9	4.9	5.0	1.3
	Test 12	4.9	4.6	4.5	2.5
	Test 13	1.8	2.7	2.3	2.6
	Test 14	0	0.0	0.0	1.7

7.2 Stage 2: NIELSEN, [2006] vs. VAN RIJN, [2007]

Stage two contains the comparison between the Nielsen, [2006] and Van Rijn, [2007] transport method. Both sediment transport methods are compared with the original experiments executed by VAN DER MEER [1988]. The experiments are compared on the created damage after a storm of 3000 waves.

7.2.1 Damage level

The Van der Meer experiments for Test series A and Test series B were recalculated with Xbeach-G using Model b as described in the previous section. In Table 15 are the measured damage levels for both test series A as B. The NIELSEN, [2006] transport formula seems to give answers which are closer to the expected damage level than the VAN RIJN, [2007] method does. When the damage level is near the expected result, this is visualised with green and when it is under- or overestimated this is marked with red. All the VAN RIJN, [2007] tests show a higher results than the expected damage. In the case with the NIELSEN, [2006] transport formula, some results are overestimated and some underestimated.

For the tests which are originally executed by VAN DER MEER [1988] on a 1:6 slope the VAN RIJN, [2007] method gives very high and unrealistic damage levels. This is for tests 1-4 and 10-14. The NIELSEN, [2006] method seems for these tests more applicable. However for tests 1,2 and 14 the NIELSEN, [2006] method underestimates the damage. Tests 1 and 2 and 14 have compared to the other tests a lower wave period. This lower wave period has two effects. The first effect is the model time, as only 3000 waves are tested the model models a shorter time period. The second effect is in the calculation of the shear velocity. In the NIELSEN, [2006] transport formula, the wave period is implemented directly in the inertia term. (See Equation 7-1). This results in a lower inertia term for these tests, which might explain the underestimation of the damage. It also indicates that the inertia term might have a significant influence in the sediment transport.

$$Nielsen: \quad u_* = \underbrace{\sqrt{\frac{f_s}{2}} \cos(\theta) \cdot u}_{Drag} + \underbrace{\sqrt{\frac{f_s}{2}} \frac{T_{m-1.0}}{2\pi} \sin(\varphi) \frac{\partial u}{\partial t}}_{Inertia} \quad \text{Equation 7-1}$$

Table 15: Measured damage levels for tests series A and B.

		Test series A		Test series B		
		$S = \frac{A_e}{D_{n50}^2}$		$S = \frac{A_e}{D_{n50}^2}$		
		NIELSEN, [2006]	VAN RIJN, [2007]	NIELSEN, [2006]	VAN RIJN, [2007]	Exp. damage
1:6 slope	Test 1	0	31.1			
	Test 2	0	27.1			
	Test 3	5.3	47.2			
	Test 4	2.4	31.0			
1:4 slope	Test 5	0	4.6			
	Test 6	0	5.2			
	Test 7	0	8.9			
	Test 8	0	7.5			
	Test 9	0	7.2			
1:6 slope	Test 10	5.7	55.2			2.8
	Test 11	4.9	44.7			1.3
	Test 12	4.6	35.1			2.5
	Test 13	2.7	49.7			2.6
	Test 14	0.0	43.8			1.7

For the 1:4 slope tests (tests 5-9) the VAN RIJN, [2007] method seems more accurate as it is closer to $S=2$. The results however still give more damage than expected. It is notable that the tests on a 1:6 slope are modelled worse than the test on a 1:4 slope with the VAN RIJN, [2007] formula. This cannot be explained directly, except for inaccuracies in the damage curve method for the 1:4 or 1:6 tests of test series A.

The NIELSEN, [2006] method gives for the 1:4 slope tests an underestimation with a damage of 0 for all the tests. This underestimation can be due to two reasons. The first is the same arguments as for test 1,2 and 14 where the wave period was higher than the rest. Also for test 5--9 the wave period is lower than test 3 and 4 who gave a good answer with the NIELSEN, [2006] method. The second option could be due to inaccuracies in the damage curve method. In case of the last argument the 1:4 tests or the 1:6 tests should be determined wrong with the damage curve.

In general the NIELSEN, [2006] formula is always lower than the VAN RIJN, [2007] is. The NIELSEN, [2006] formula gives answers more close to the expected value but in a lot of cases it gives an underestimation which is more dangerous for a design formula than an over prediction.

7.2.2 Erosion depth

The research of WIT [2015] already stresses out the importance of a damage description depended on the erosion depth for mild slopes. That is why for all tests the erosion depth is also taken into account. The relative erosion depth is divided with the stone diameter to compare the erosion depth correct and make it dimensionless. This dimensionless erosion depth is called the relative erosion depth. Table 16 shows the measured relative erosion depth for test series A and B. The relative erosion depth is the erosion depth (d_e) divided by the median nominal stone diameter (D_{n50}), so when this value is larger than two, the filter layer is visible. (Assuming a top layer of $2D_{n50}$).

The start-of-damage criterion of $S=2$, as proposed by VAN DER MEER [1988] is determined such that for this amount of damage the filter layer is always protected after a storm attack. In this formulation for the damage level, the erosion depth is not taken into account. So it could be possible that high erosion rates have not such big erosion depths and vice versa low damage levels with big erosion depths.

Interesting about measured erosion depths are the low erosion depths for the high damage levels that were found. This is especially clear for the VAN RIJN, [2007] tests with high damage levels. For example for test 10 with VAN RIJN, [2007], a damage level of 55, creates a relative erosion depth of 1.74. None of the tests show erosion holes deeper than the $2D_{n50}$ -design criteria, which is often used. This indicates that the erosion holes are long and not so deep. The formed erosion profile is added in Appendix E: Results

Table 16: Relative erosion depth for tests series A and B.

		Test Series A		Test series B			
		$\frac{d_e}{D_{n50}}$		$\frac{d_e}{D_{n50}}$			
		NIELSEN, [2006]	VAN RIJN, [2007]	NIELSEN, [2006]	VAN RIJN, [2007]		
1:6 slope	Test 1	0	1.4	1:6 slope	Test 10	0.8	1.7
	Test 2	0	1.4		Test 11	0.7	1.9
	Test 3	0.7	1.9		Test 12	0.6	1.7
	Test 4	0.5	1.6		Test 13	0.4	1.6
1:4 slope	Test 5	0	0.5	1:6 slope	Test 14	0	1.4
	Test 6	0	0.5				
	Test 7	0	0.6				
	Test 8	0	0.6				
	Test 9	0	0.5				

7.2.3 Damage level vs. Relative erosion depth

To indicate the effect of the relative erosion depth the damage level is compared with the relative erosion depth. This is done for both the NIELSEN, [2006] as the VAN RIJN, [2007] data for test series B. The expectation is an increasing damage for an increasing erosion depth. Points in the top left corner show high damage levels for limited erosion depth and thus long stretched erosion profiles. There are no points in which the erosion depth deflects significantly from the damage level.

The VAN RIJN, [2007] method increases linear for higher damage levels till a point where the relative erosion depth is not increasing anymore. In Figure 28 can be seen that the damage level is still increasing but the relative erosion depth is not. This is clarified with the three trend lines that are going through test 10, 11 and 13. For test 14 the amount of erosion and also the amount of erosion depth does not decrease much in time.

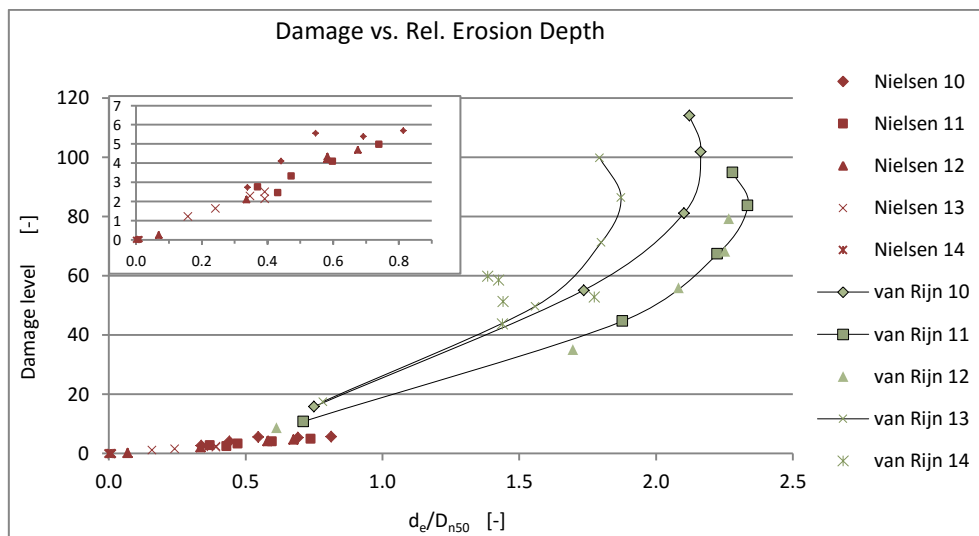


Figure 28: Calculated damage vs. relative erosion depth for both NIELSEN, [2006] as VAN RIJN, [2007] transport formula.

The NIELSEN, [2006] results are the red points and these show less erosion and are more positioned at the bottom. The bigger illustration of the NIELSEN, [2006] values in the top left corner also gives a linear line for an increase in relative erosion depth. Compared to the VAN RIJN, [2007] results the linear line is less steep. The erosion depth seems to increase faster for higher damage levels compared with the VAN RIJN, [2007] results. This implies deeper erosion holes with the NIELSEN, [2006] method for the same amount of damage. As the damage levels are significantly lower than the VAN RIJN, [2007] results, no conclusions can be drawn about the relative erosion depth for bigger damage levels.

It can be concluded that for the used test cases, no extreme long stretching profiles occurred. In the VAN RIJN, [2007] method the relative erosion depth clearly stabilizes for higher damage levels. In the NIELSEN, [2006] method the linear line is less steep than the VAN RIJN, [2007] method which gives bigger relative erosion depths for the same damage level.

7.2.4 Erosion profile shape

The damage level versus relative erosion depth already indicate the importance of the erosion profile. Long stretched profiles are much less harmful than deep short erosion holes. VAN DER MEER [1988] describes the erosion profiles for his dynamic tests. To compare the formed erosion profile with his experiments, two dynamic experiments called series C are reproduced.

The first test of test series C is executed on a 1:3 profile and shows a profile with a bar above MSL, followed by erosion and a second bar below MSL. This is the right picture in Figure 29 which is reproduced from VAN DER MEER [1988]. The bar above MSL is a typical gravel beaches. Both the NIELSEN, [2006] as the VAN RIJN, [2007] method do not model this bar. With a visual observation it can be seen that the NIELSEN, [2006] method seem to reproduce the profile better than the VAN RIJN, [2007] method does. The profile which is formed is highly depended on the groundwater processes and the hydraulic conductivity because this influences the amount of sediment transported up and downwards.

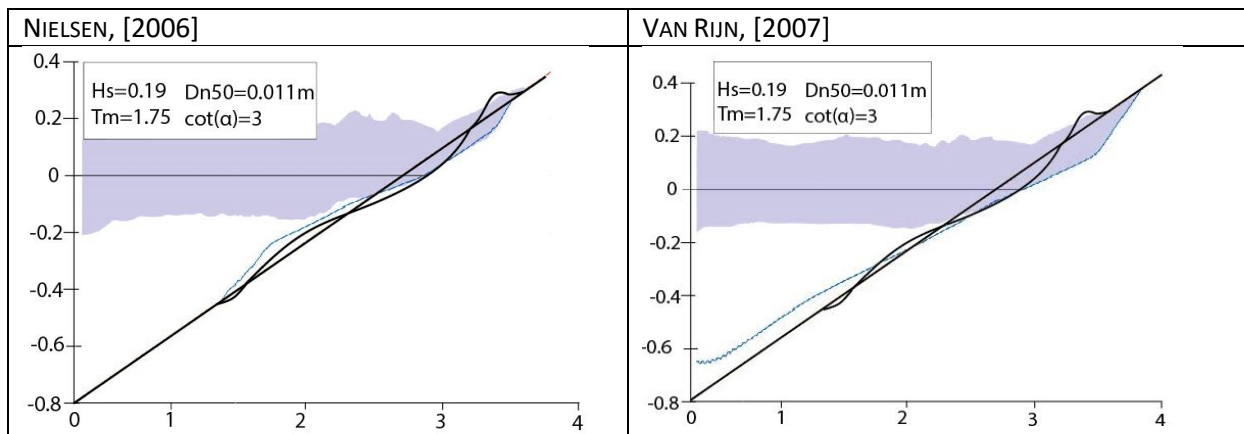


Figure 29: Test series C with test 1 for both the NIELSEN, [2006] as the VAN RIJN, [2007] method.

The second test of test series C is executed on a 1:5 slope and shows quite a big bar on the beach, so a lot of upslope sediment transport. The results of XBeach-G show quite different profiles than that of the VAN DER MEER [1988] experiments. The NIELSEN, [2006] transport formula shows a crest profile instead of a bar profile. The VAN RIJN, [2007] method shows the expected bar profile but does still not create the big bar as in the VAN DER MEER [1988] experiments. This is already explained in the chapter Model Validation where is shown that the model has difficulties modelling the second bar created by the uprush in the swash zone.

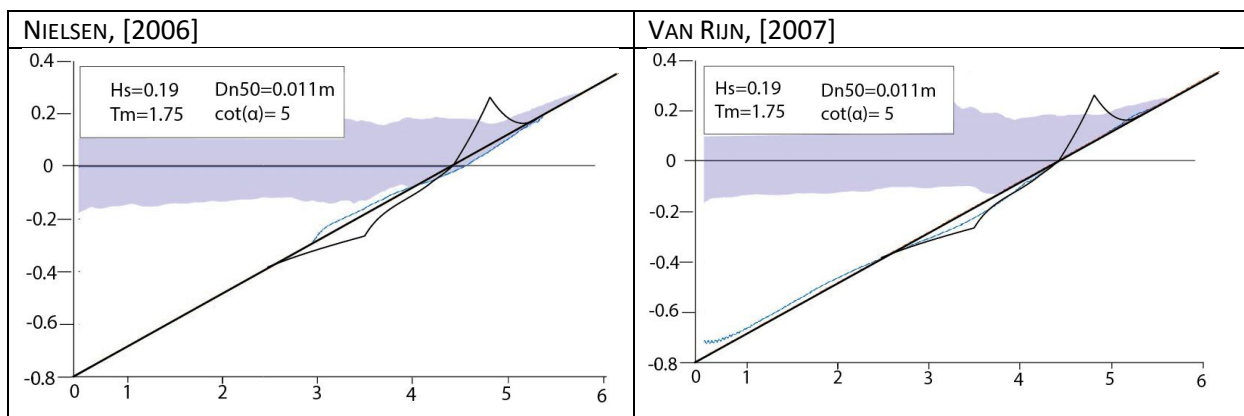


Figure 30: Test series C with test 2 for both the NIELSEN, [2006] as the VAN RIJN, [2007] method.

7.2.5 Recap stage 2

- The damage level shows big differences in the created erosion between the NIELSEN, [2006] and the VAN RIJN, [2007] transport formulae.
- The VAN RIJN, [2007] method overestimates the damage for all tests. The big damage levels do not lead to high relative erosion depths as the relative erosion depth seems to stabilise for bigger damage levels.
- The NIELSEN, [2006] method is highly dependent on the wave period for the formed damage. Smaller wave periods lead to an underestimation and bigger wave periods to a realistic estimation.
- The NIELSEN, [2006] method gives bigger erosion depths for the same damage level as the VAN RIJN, [2007] method. This implies shorter and deeper profiles for the NIELSEN, [2006] method compared to the VAN RIJN, [2007] method.
- Both methods have difficulties modelling the typical gravel profile with a bar on the beach. The results of XBeach-G differ too much from the measured experimental profile.

7.3 Stage 3: Variation Parameters

In stage three several parameters are systematically verified by varying parameters and comparing it with the original experiments of VAN DER MEER [1988]. The parameters are varied to verify the underlying physical processes in XBeach-G.

7.3.1 Slope effect

The first parameter that is varied is the slope angle. The original VAN DER MEER [1988] experiments are executed on a 1:4 or 1:6 slope. The goal of this thesis is to find out if XBeach-G is suitable as design tool for more gentle slopes. The slope is changed to investigate the formed damage level for milder slope.

VAN RIJN, [2007] transport formula

The created damage with the VAN RIJN, [2007] method overestimated the damage levels for the original VAN DER MEER [1988] experiments. The result for the created damage level for different slopes is illustrated in Figure 31.

For the VAN RIJN, [2007] transport formula there is a clear trend of an increase in damage for milder slopes. This is observed for both test series A as B. The only exception is test 14 on a 1:4 slope where there is an increase in damage compared to the 1:6 slope. Test 14 has of all test series (both A and B) the steepest waves of 5%, and the biggest wave period with $T_m=3.23s$. This also gives the lowest irribarren number of 0.73. This trend in the damage level is the same for the erosion depth and the relative erosion depth. See appendix E: Results.

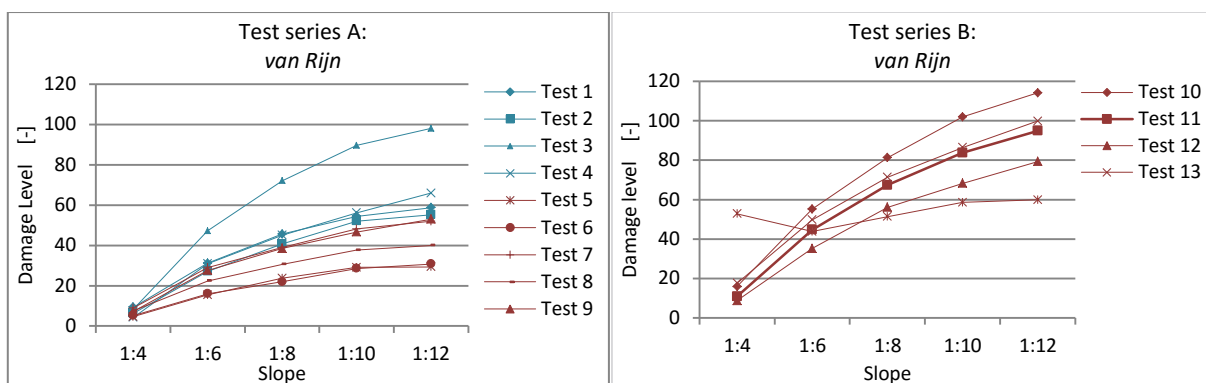


Figure 31: Slope effect with the VAN RIJN, [2007] transport formula for both tests series A as B.

NIELSEN, [2006] transport formula

The NIELSEN, [2006] transport formula shows another trend than the VAN RIJN, [2007] method does. With the NIELSEN, [2006] transport formula there seems to be a maximum erosion around the 1:6 or 1:8 slope. For both steeper as milder slopes the erosion decreases as can be seen in Figure 32. Also for the eroded depth the same pattern as the damage level is observed, which can be seen in the Appendix E: Results. The amount of erosion is significantly lower than is observed with the Van Rijn, [2007] method. In the Van Rijn, [2007] method damage levels are found of $S=\pm 120$ and with the NIELSEN, [2006] method a maximum erosion of $S=\pm 7$ is found. The 1:4 results in this case cannot be explained. The results from the 1:6 slope and lower show a correct trend for decreasing damage level (erosion) and increasing stability for more mild slopes.

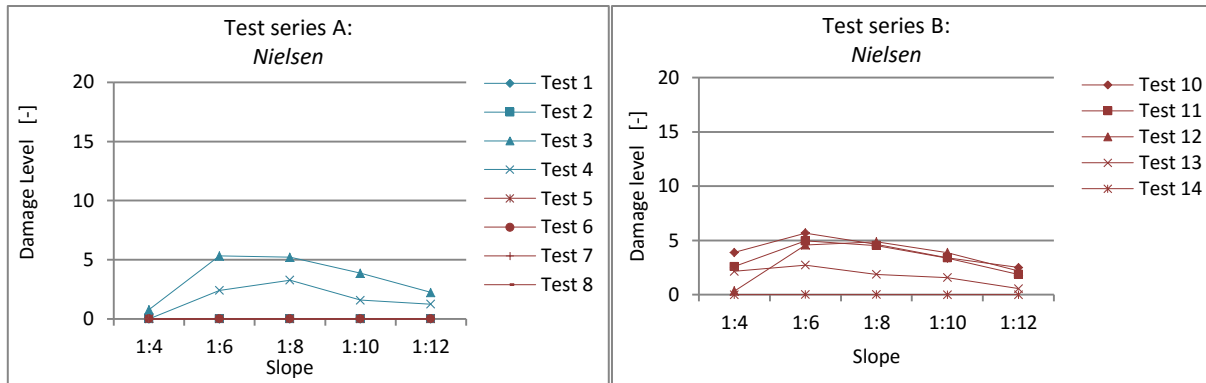


Figure 32: Slope effect with the NIELSEN, [2006] transport formula for both tests series A as B.

Expected trend

Both methods show a trend which is unexpected. There are two type of trends that can be explained by logical reasoning.

The first trend is the least of damage for the mildest slopes and an increase in damage for the steeper slopes. The milder the slope the more stability the grain particles gain and the more the hydrodynamic energy is spread along the bed.

The second trend is based on the principle of an optimal slope corresponding to the hydrodynamic forcing. In this case the minimum erosion is occurring for the optimal slope. Initial slopes deflecting from this slope give more damage. This principle is also explained in the chapter Damage quantification methods.

The NIELSEN, [2006] method seem to show a comparison with trend one. Only the 1:4 results deflect from this theory. In the VAN RIJN, [2007] approach the unexpected 1:4 result for test 14 might indicate an optimal for the 1:6 slope and thereby confirming trend two.

Iribarren number

Because the changing slope influences the breaking of the waves, a possible explanation for the results could be a change in type of wave breaking. The type of breaker is described with the iribarren number. When the iribarren number is plot against the damage level the same pattern occurs as when the slope is used. This is illustrated for test series B in Figure 33. The changes in breaking type do not explain the trends observed for the changing slope. Attention in this comparison should be given on the axis in the graph as the VAN RIJN, [2007] method shows much more erosion than the NIELSEN, [2006] method does.

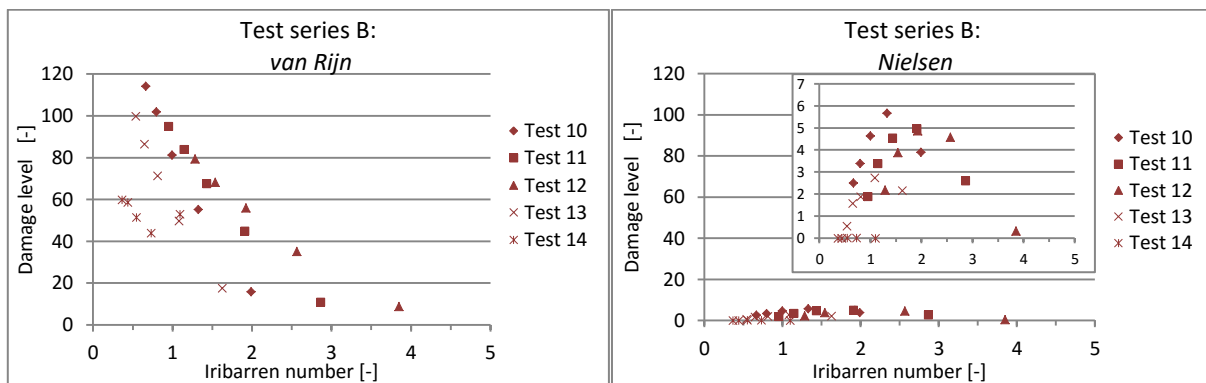


Figure 33: Test series B; Calculated Damage level vs. Iribarren number.

Erosion in time

The model run time of the tests is determined such that 3000 waves are generated. This gives different model run times per test. The erosion is modelled in time to observe the effect of the model run time on the results.

The VAN RIJN, [2007] method shows a trend which is also described by VAN DER MEER [1988], in which most of the erosion occurs in the first 1000 waves. Especially for the 1:4 slope tests all the erosion takes place in the first 100 waves and after this there is hardly an increase in erosion. This strengthens the theory that the least erosion occurs for the slope closest to the optimal slope for the hydraulic forcing. In that case is the 1:4 slope the closest to the initial slope and with minimal erosion the profile can be reshaped to the optimal profile.

The same tests with the NIELSEN, [2006] method show more fluctuations in time. Especially the 1:4 slope and 1:10 slope tests are fluctuating in damage level. The overall damage level in time seems to increase more linear than the VAN RIJN, [2007] method does.

The erosion in time for test 10 is visualised for both transport formulae in Figure 34; the other tests are in Appendix E: Results.

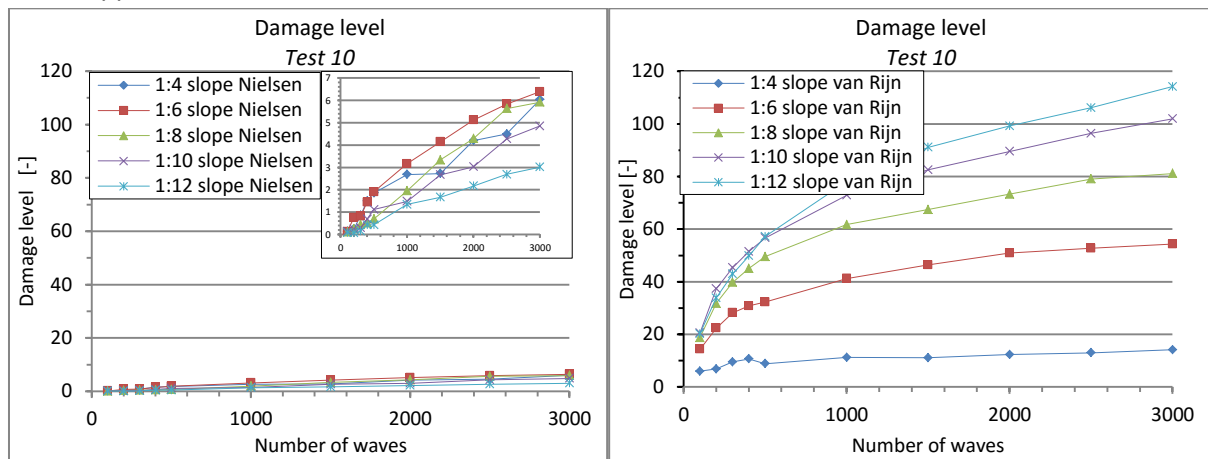


Figure 34: Damage in time for test 10.

When the slope angle is changed the damage levels show unexpected results. The VAN RIJN, [2007] method shows increase in erosion for more mild slopes. The NIELSEN, [2006] method show a decrease in erosion for more mild slopes and a decrease in erosion for the 1:4 tests. Almost all the erosion for the 1:4 slope with the VAN RIJN, [2007] method occurs in the first 100 waves. This indicates that the amount of damage is depended on an optimal slope corresponding to the hydrodynamic forcing.

7.3.2 Layer thickness

The chosen VAN DER MEER [1988] experiments are executed with an impermeable underlayer. Because the model is not validated with an impermeable layer the homogeneous situation is modelled. The layer is implemented in the model to simulate the real VAN DER MEER [1988] experiments and to observe the effect of an impermeable underlayer

An impermeable layer causes the wave to penetrate less in the structure, creating a pressure that can destabilise the stone stability. The used layer thickness is 8 cm and the stones used in the experiments are for test series B 3.6 cm and for test series A between 1.6 and 3.6cm. This gives a layer thickness which is slightly bigger than the $2D_{n50}$ design criteria which is often used.

VAN RIJN, [2007] transport formula

The VAN RIJN, [2007] transport formula show hardly any differences with a layer thickness compared with the homogeneous situation. Therefore the layer thickness is decreased from 8cm to 4cm. Also for these tests no difference is observed as can be seen in Figure 35. Interesting is the continuity in the model results. Even the deviating result for the 1:4 slope of test 14 is constantly modelled.

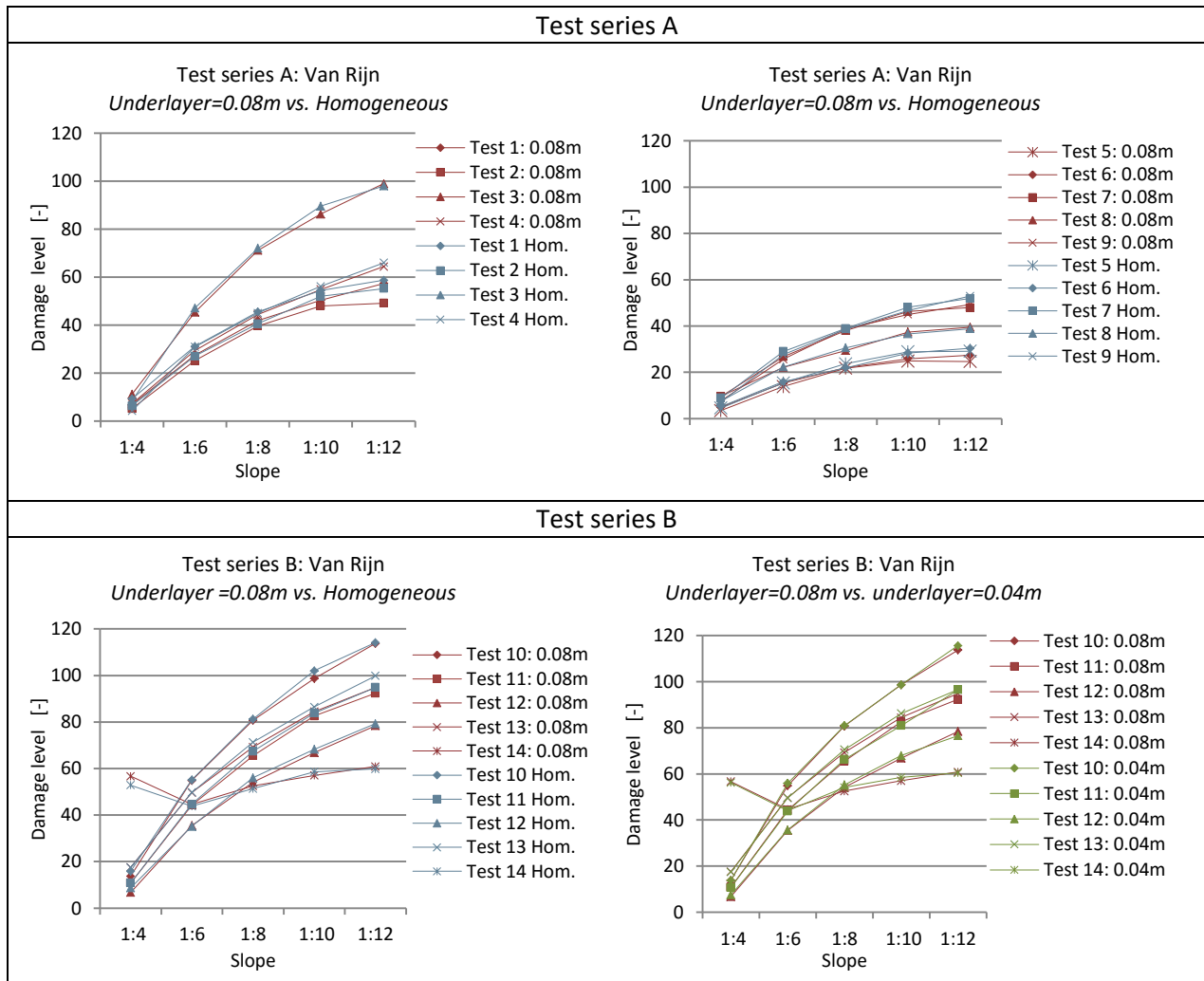
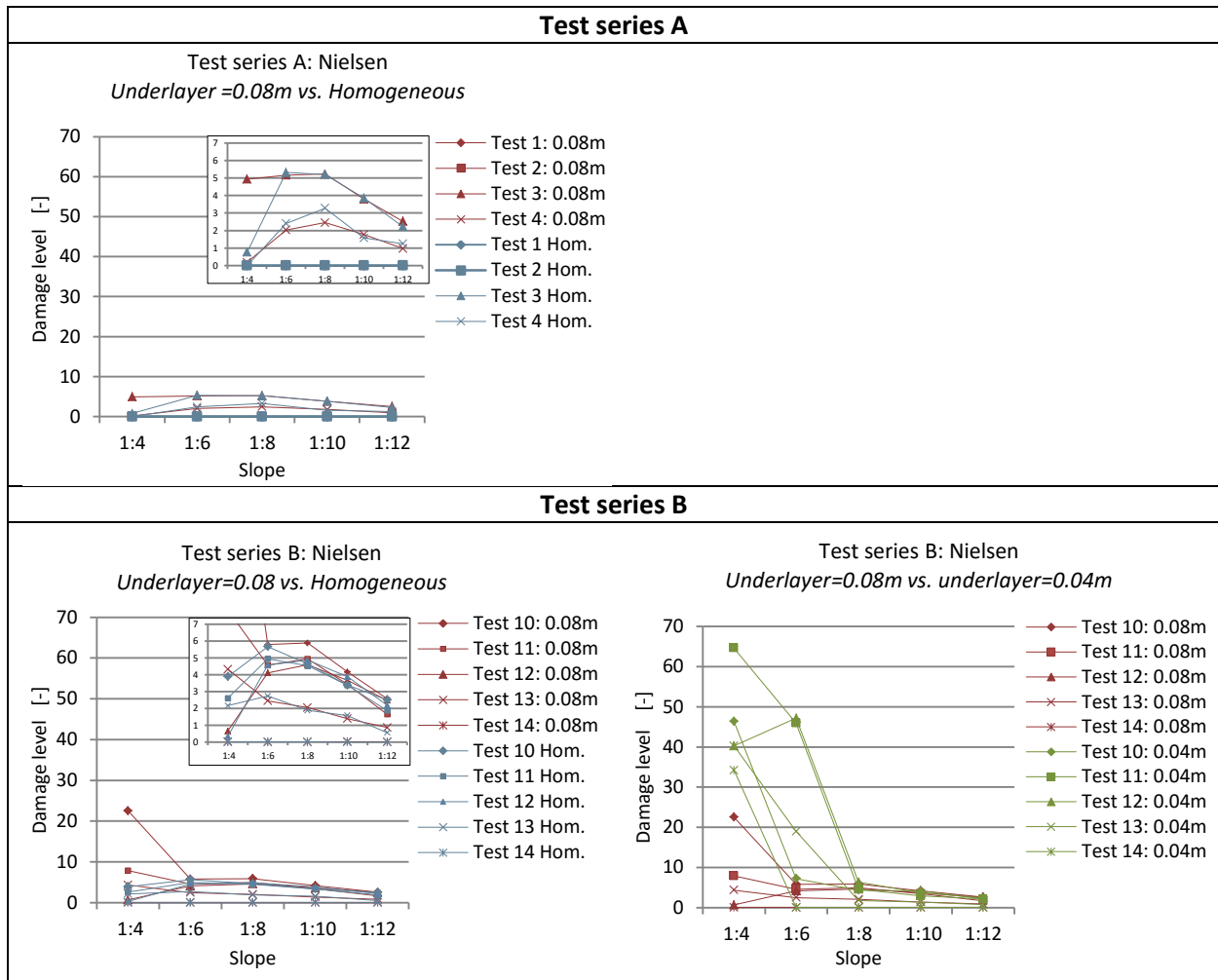


Figure 35: Test series A and B with different layer thickness for the VAN RIJN, [2007] transport formula

NIELSEN, [2006] transport formula

For the NIELSEN, [2006] transport formula the layer thickness do have effect on the sediment transport. Especially for milder slopes the created damage increases. Test 3, 10,11 and 13 show an increase in transport for the 1:4 slope with an underlayer of eight centimetre. With a layer thickness of 4 centimetres the increase in erosion happens also for the milder 1:6 slope. The slopes milder than 1:6 hardly show any effect of the implementation of a layer.

Table 17: Test series A and B with different layer thickness for the NIELSEN, [2006] transport formula



The VAN RIJN, [2007]. Method does not show any influence of the impermeable underlayer. The NIELSEN, [2006] method only show differences for the steeper 1:4 and 1:6 slopes.

7.3.3 Stone size

The period seems to have an important aspect in the erosion of NIELSEN, [2006] as is observed with the variation of the slope. This arouses the suspicion that the advection term of the sediment transport formula has a serious influence in the sediment transport. The stone size is varied because the VAN RIJN, [2007] formula has the stone size in the advection part of the shear stress. This advection part might become dominant situations with big stones on milder slopes. When this is the case the model should give less erosion for the smaller stones as the model will function normally again with a normal advection term. More erosion should occur for the bigger stones as the advection part becomes even more dominant.

VAN RIJN, [2007] transport formula

The stone sizes are only changed for test series B. All the tests in test series B are executed with a stone diameter of 3.6cm. The tests are in this variation also modelled for 2cm stones and 5cm stones which gives as expected more damage for the smaller stones and less damage for the bigger stones. Also the deviating trend for test 14 with the 1:4 slope stays the same.

Because the big damage levels still occur for the small stones and do not get worse for the big stones it is not expected that the acceleration term is dominant in the sediment transport term of VAN RIJN, [2007].

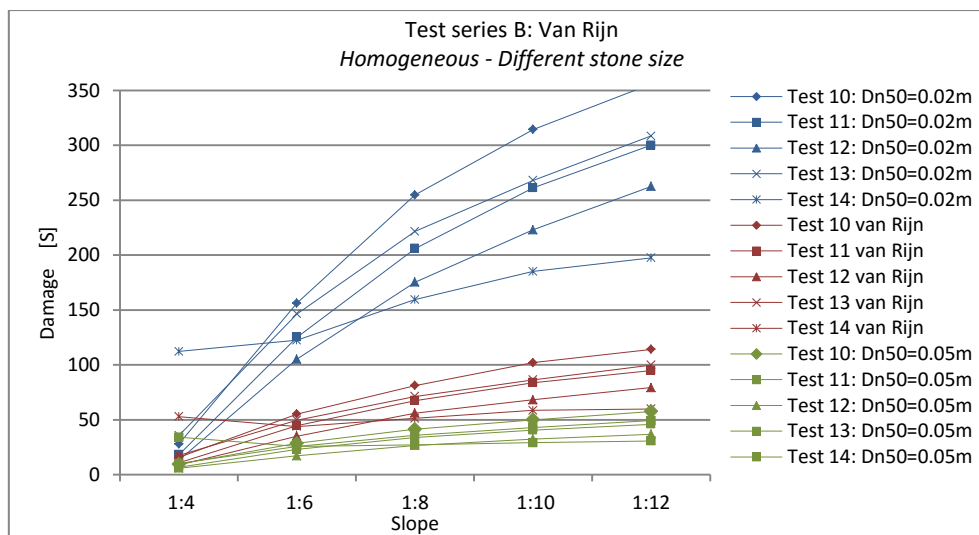


Figure 36: Test series B with changing slope and the VAN RIJN, [2007] transport formula

NIELSEN, [2006] transport formula

In the NIELSEN, [2006] transport formula the stone size is only implemented in the shields parameter. Also for the NIELSEN, [2006] transport formula the same trend is found as with VAN RIJN, [2007]. More erosion is occurring for smaller stones than for bigger stones, as expected. There is not a specific trend visible for less erosion for milder slopes. With the 3.6cm stones this is happening for slope milder than 1:6 and for the 2cm stones the erosion stays more or less the same for the more mild slopes.

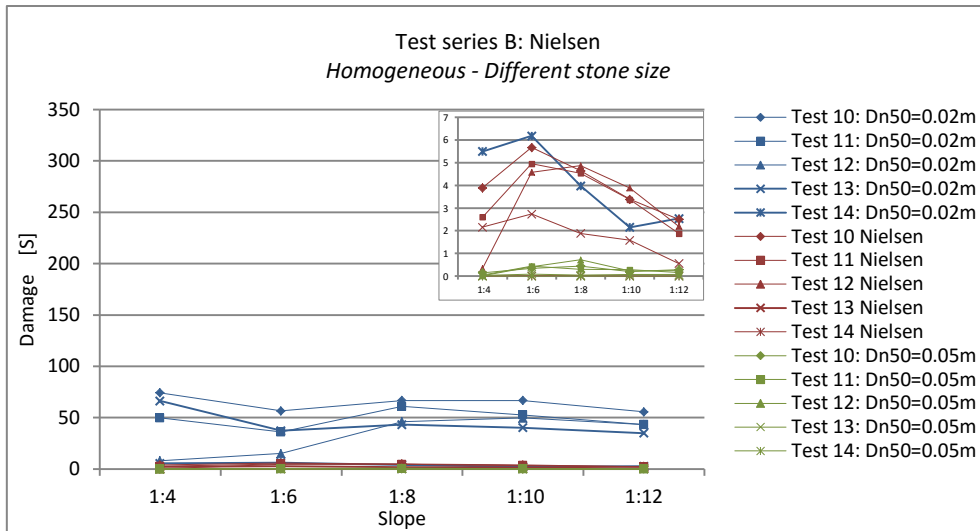


Figure 37: Test series B with changing slope and the NIELSEN, [2006] transport formula

Both the VAN RIJN, [2007] as the NIELSEN, [2006] method show more erosion for smaller stones. The change in stone size does not indicate a dominance of the advection term.

7.3.4 Phase lag angle φ

The phase lag angle is a constant, included in the NIELSEN, [2006] transport formulation. It describes the phase difference between the mean stream velocity and the bed shear stresses. This is created due to asymmetric waves. In the previous tests the phase lag angle was kept constant on the advised value of 25 degree.

In the paper of NIELSEN, [2006] already some connections between the phase lag angle and other parameters are observed:

1. Smaller phase lag for bigger periods.
2. Smaller phase lag for coarser sand

In the tests observed by NIELSEN, [2006] a phase lag angle of $40^\circ \pm 18^\circ$ was found for waves with a period of $T=5$ seconds. For a smaller wave period of 3 seconds phase lag angles of $62^\circ \pm 15^\circ$ is found. (NIELSEN, [2006]). In this variation the phase lag angle is changed from 25 degree to 35 degree. In test series B the stone size is the same so only the effect of the wave period is investigated.

The tests are modelled twice to make sure no model errors occurred. The first run is shown in light blue and the second run in dark blue. The red line is the result with a phase lag angle of 25 degree.

The results are presented in Figure 38 and show more damage than the original modelling with a phase lag angle of 25 degree. Especially for the 1:4 and 1:6 slope the measured damage differ a lot for both runs. Two trends can be observed. The trend of test 14 which shows consistently less erosion. The other tests (10,11 and 13) show an increase in erosion, especially for the steep slopes.

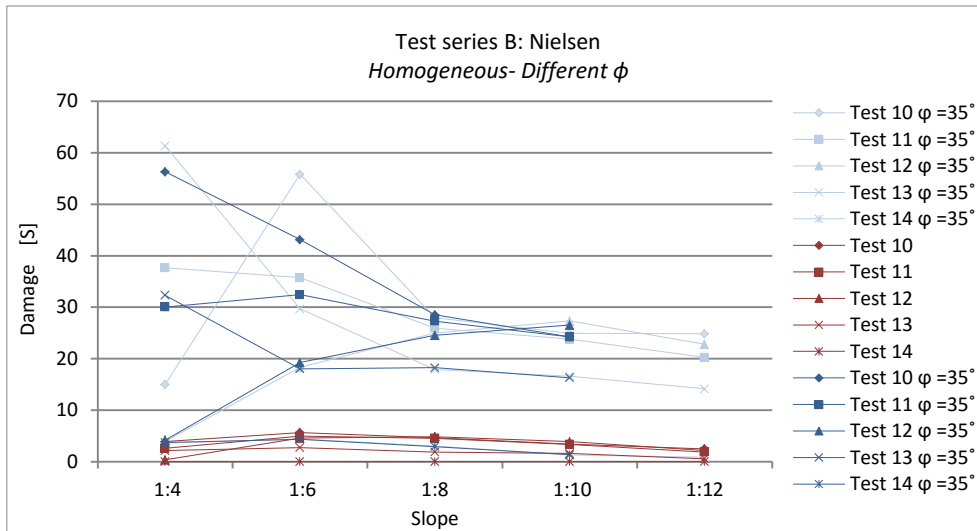


Figure 38: Test series B with changing phase lag angle.

Test 14 has with a wave period of 1.23 seconds the lowest wave period of all tests in test series B. That is probably causing the lower damage levels. In the reproduction of the original experiments, all tests were reproduced well except for test 12. When the phase lag angle is changed to 35 degree all the other tests show an overestimation except for test 14 which is quite correct in this case. (Table 18)

Table 18: Damage level of 1:6 slope tests with two different phase lag angles.

	1:6 $\phi=25^\circ$	1:6 $\phi=35^\circ$
Test 10	5.673	55.814
Test 11	4.953	35.726
Test 12	4.582	18.319
Test 13	2.736	29.686
Test 14	0.009	4.434

It indicates that the phase lag angle is a coefficient with a lot of influence in the sediment transport. It is necessary to calibrate this coefficient for the right period and stones before the NIELSEN, [2006] methods gives the right answers.

The phase lag angle is a strong calibration tool for the NIELSEN, [2006] transport formula. It is implemented as a constant so calibration is necessary before the NIELSEN, [2006] formulation gives correct answers.

7.3.5 Hydraulic conductivity

The hydraulic conductivity influences the water flowing through the particles and is included in the groundwater effects of the model. The parameter is one of the calibration factors of the model. In the other tests a hydraulic conductivity of 1cm/s. The test validation locations of XBeach-G(MCCALL, [2015]) show hydraulic conductivities changing from 1cm/s to 40cm/s.

Hydraulic conductivities of 40cm/s are found on beaches with a stone size of two centimetre. This resembles the VAN DER MEER [1988] experiments the best. The results are presented in Figure 39 and show no significant differences in damage level. The difference in damage level are displayed in the right top corner, which shows that there is no bigger difference than $S=1$ between the results. There is however also no connection for more influence of the hydraulic conductivity per slope.

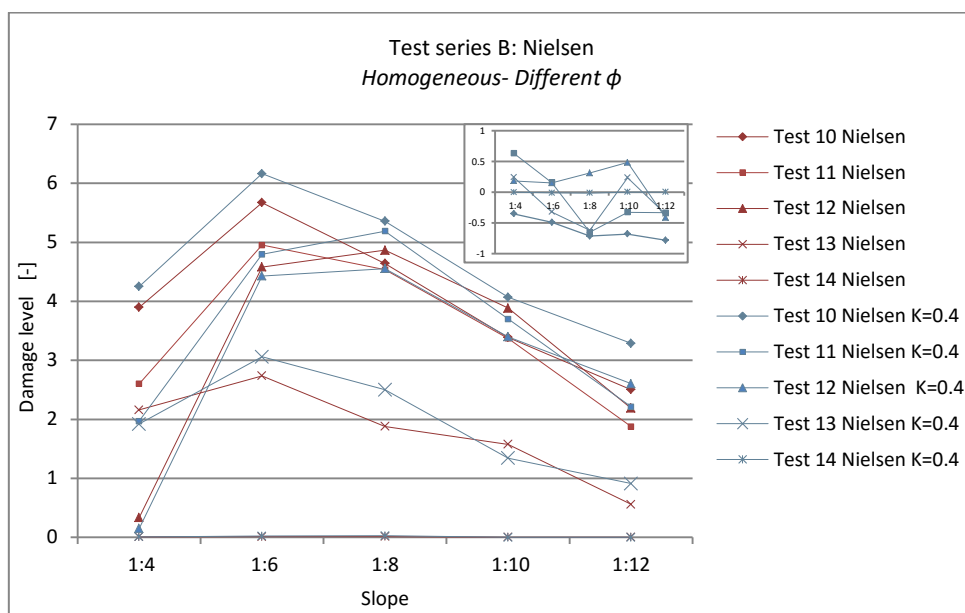


Figure 39: Slope effect with a bigger hydraulic conductivity.

7.3.6 Recap stage 3

A lot of parameters are varied and a lot of results are analysed, so what are the basic conclusions so far.

VAN RIJN, [2007].

- Conservative approach with high damage levels
- Less erosion depth for high damage levels.
- Shows no influence for an impermeable layer

NIELSEN, [2006]

- Erosion highly depended on the wave period
- Shows expected trend with decreasing erosion for mild slopes. Except for the 1:4 results.
- Difficult to calibrate with the phase lag angle to the right stone size and wave period.
- The hydraulic conductivity has only minor influence on the amount of erosion

7.4 Stage 4: Hydro- and Morphodynamics

In stage 4 the hydro and morphodynamic parameters are investigated on their behaviour for mild slopes with as goal to understand the physics in the model better and to find answers for the observed trends. All parameters are tested for three cases e.g. the VAN RIJN, [2007] method; the NIELSEN, [2006] and a case without morphological updating. Test 10 is used as example for the trends. The other tests are added in Appendix G: Results.

7.4.1 Hydrodynamics

The main parameters for the hydrodynamics are the velocity and the acceleration as these are the input for the shear stresses, used in the sediment transport formulas. For mild slopes both the velocity as the acceleration should decrease, when no morphological bed updating is executed. It is essential to have no morphological bed updating as in erosion holes steeper or gentler slopes can occur. The third parameter is the infiltration effect as that is a typical effect for gravel beaches which is implemented in Xbeach-G.

Velocity

The maximum and minimum of the occurred velocities is plot for tests 10, the other tests are added in Appendix G: Results. The velocity is presented for three different cases with the NIELSEN, [2006] transport formula, the VAN RIJN, [2007] and the case with no morphological updating.

In Figure 40, both the overall velocity as the output velocity is shown in the graph. The overall velocity (red line) shows the outer contour lines as it gives the maximum and minimum velocity that occurs between every output step. The output velocity (black line) shows the velocity at the time of every output. The frequency of every output determines if the output velocity gives an accurate description. The VAN RIJN, [2007] is modelled with an output step of every 1 second and the NIELSEN, [2006] case is modelled with an output of every 0.1 second. The NIELSEN, [2006] case shows a good description of the velocity profile while the VAN RIJN, [2007] has a lower accuracy.

The difference between the three velocity profiles is caused by changes in the bed level. As in general the NIELSEN, [2006] transport formula show less erosion than the VAN RIJN, [2007], a more deflecting shape is expected for the VAN RIJN, [2007] method.

For the case with no morphological updating the 1:12 slope results show lower velocities than on a 1:4 slope. This is the expected trend which indicates that the basic hydrodynamics is well implemented in the model.

In the NIELSEN, [2006] case the total velocities are higher than with the case with no morphological updating and VAN RIJN, [2007]. This higher velocities are the results of the erosion hole. The damage levels of NIELSEN, [2006] are lower than VAN RIJN, [2007] so this is an unexpected result. As is concluded in stage 2, the relative erosion depth for the NIELSEN, [2006] method is higher than for the VAN RIJN, [2007] method. This implies shorter and deeper erosion holes. This shape can explain the higher velocities for the NIELSEN, [2006] case.

The VAN RIJN, [2007] case show velocities in the same range as the case without morphological updating. The profile deflects more for mild slopes than it is for the steep slopes. The most erosion for the VAN RIJN, [2007] case took place for the mildest slopes. This difference in velocity profile is

caused by the increase in erosion. Interesting is the small range on the x-axis for which the velocities increase.

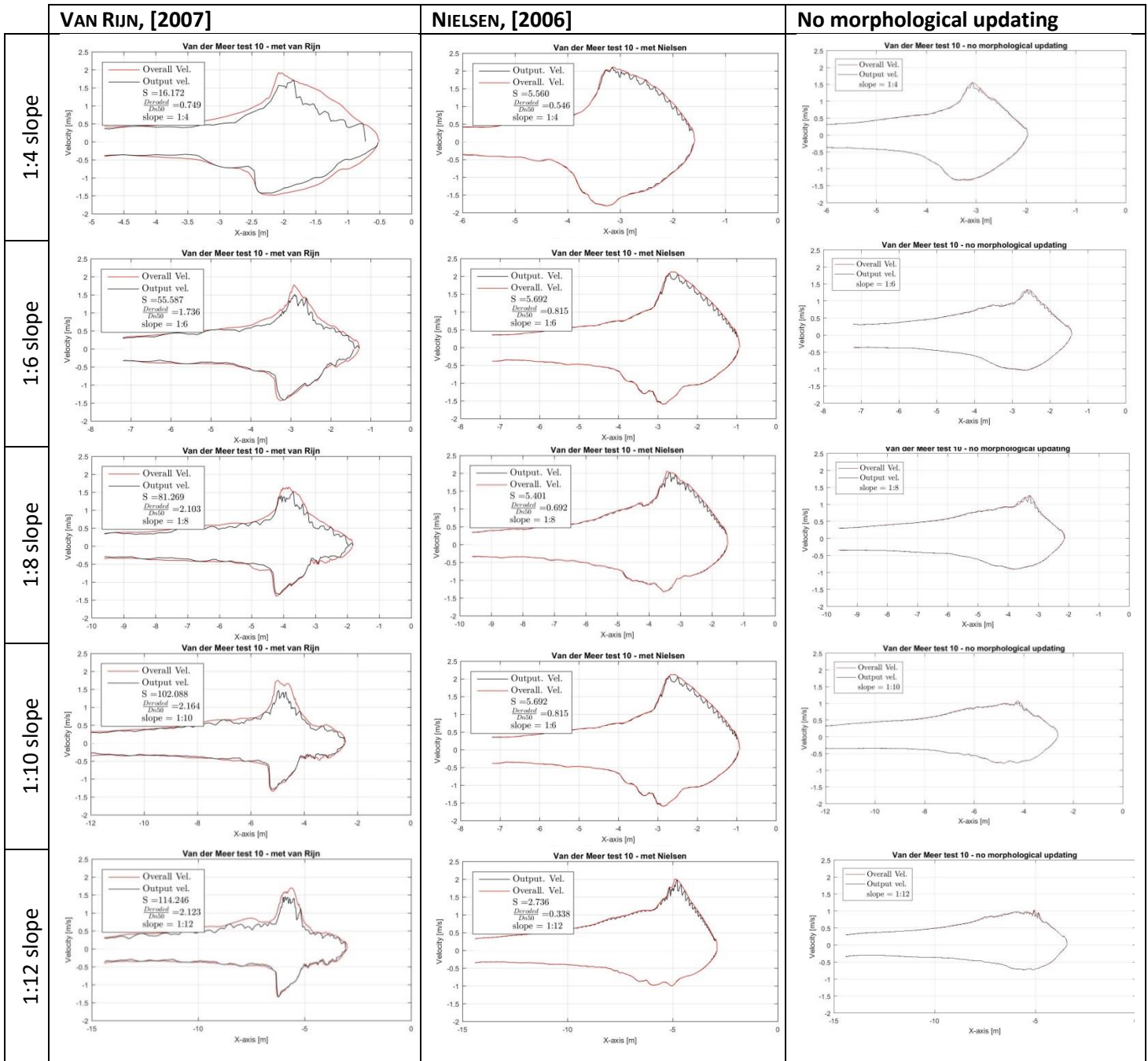


Figure 40: velocity for test 10 with Van Rijn, [2007]; Nielsen, [2006] and no morphological updating

The minimum and maximum velocity of all the other test are plot in a graph in the Appendix G: Results. The trend is the same for all the situations. For the case without morphological updating the velocities decrease for mild slopes. For the cases with the transport formula this is less visible due to the peaks caused by the erosion holes.

Acceleration

The second parameter which is important for the morphology is the acceleration. The acceleration is responsible for the inertia effects in the shear stresses. In the chapter

Model Morphodynamics, already the principle of a filter on the acceleration is explained. The velocity of two different grid points is used to calculate the acceleration. Unrealistic values are filtered out with this method. The acceleration given as output is not the filtered acceleration and the influence of the filter is unknown.

Also for the acceleration term the three scenarios are visualised for test 10 and the other tests are added in the Appendix G: Results. The output accelerations show with 250 [m/s^2] very high accelerations, especially compared to the velocity term previously discussed. The acceleration happens on a very short time scale as it cannot be reproduced well with an output time step of 0.1 seconds.

In all the cases the acceleration decreases for mild slopes; which is the expected trend. The NIELSEN, [2006] case show just like with the velocity term higher acceleration than the other two cases. To observe the effect of the filter, the acceleration term is reproduced. Because the model runs with an internal time step of 0.006 seconds the output velocity cannot reproduce the velocity this accurate. That is why it is not possible to calculate the filtered acceleration from the given output velocity. The filtered acceleration term is achieved from other parameters. As not the same output is available for all the cases, the reproduced filtered acceleration is done differently per case.

1. VAN RIJN, [2007] case & no morphological updating

In the VAN RIJN, [2007] case the inertia part is described with the variable "taubx_add". This inertia part has the acceleration term included. When the equation is rewritten in the form of Equation 7–2 this parameters can be used to reproduce the filtered accelerations.

$$\frac{\partial u}{\partial t} = \frac{"taubx_add"}{c_i \rho D_{50}}. \quad \text{Equation 7-2}$$

2. NIELSEN, [2006] case

In the NIELSEN, [2006] shear velocity formula also a drag and inertia part can be distinguished as is shown in Equation 7–3. The total shear velocity is reproduced with the variable name "ustar" and the drag part can be calculated with the velocity. The assumption is made that the filtered velocity can be reproduced well enough to calculate with. This assumption is verified by recalculating the shear stress due to drag, in the VAN RIJN, [2007] formulation. It was possible to reproduce this shear stress very accurately, so this can also be done for the drag part in the NIELSEN, [2006] formulation. The reproduced acceleration becomes as Equation 7–4. In this long equation the only variable is the velocity. The other parameters are constants.

$$\text{Nielsen: } u_* = \underbrace{\sqrt{\frac{f_s}{2}} \cos(\theta) \cdot u}_{\text{Drag}} + \underbrace{\sqrt{\frac{f_s}{2}} \frac{T_{m-1.0}}{2\pi} \sin(\varphi) \frac{\partial u}{\partial t}}_{\text{Inertia}} \quad \text{Equation 7-3}$$

$$\frac{\partial u}{\partial t} = \frac{"ustar" - \sqrt{\frac{f_s}{2}} \cos(\theta) \cdot u}{\frac{T_m - 1.0}{2\pi} \sin(\varphi)}$$

Equation 7-4

The recalculated acceleration is indicated with the red line in Figure 41. The resulting calculated accelerations differ a factor ten from the given output. This factor ten must be caused due to the filter on the acceleration as the other terms, used are constants.

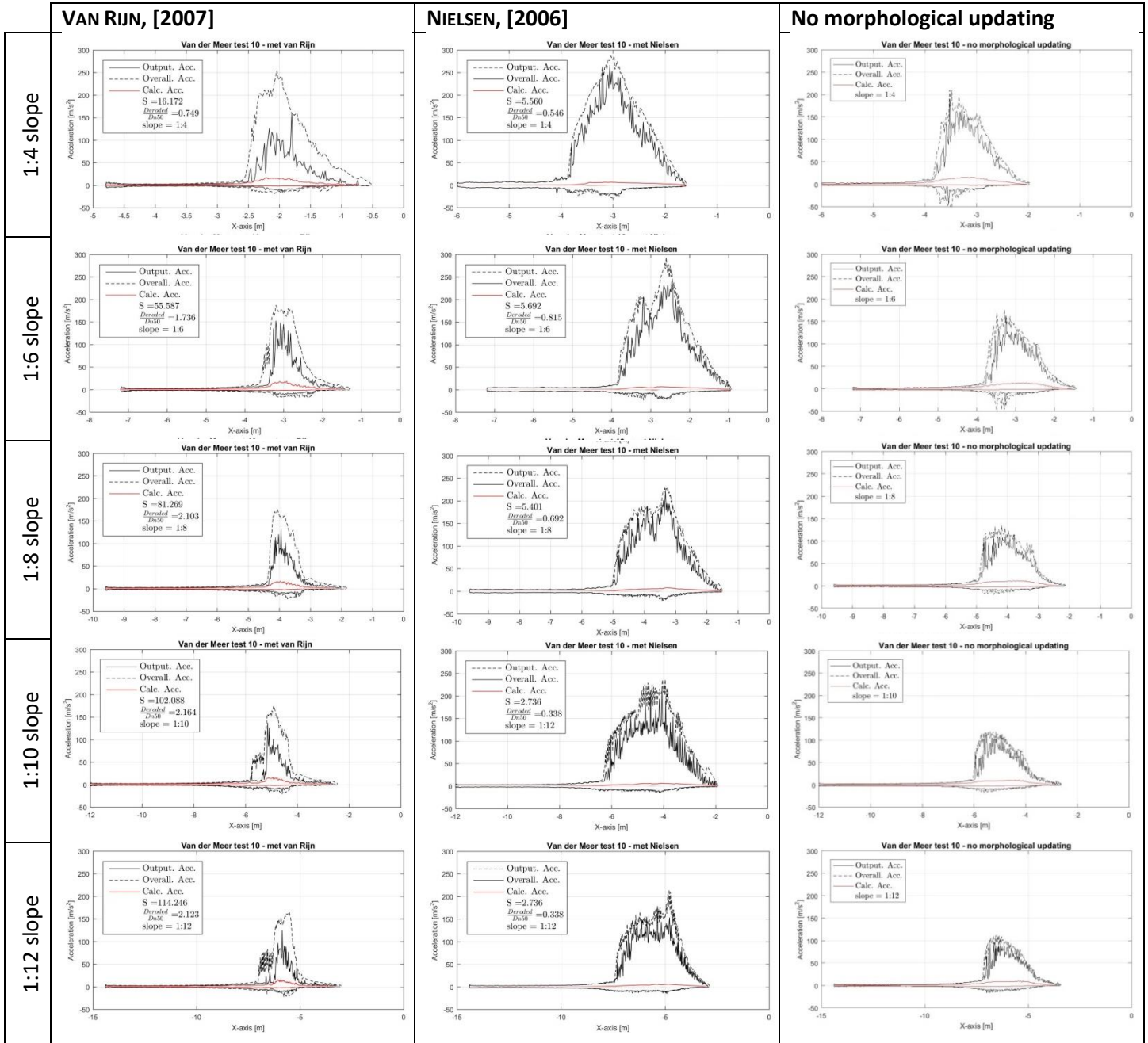


Figure 41: Acceleration for test 10 with the Van Rijn; NIELSEN, [2006] and the case without morphological updating.

Infiltration/ exfiltration effects

The infiltration and exfiltration effect play a role in the swash zone (so around MSL) and is especially important for gravel beaches. The infiltration effect is the parameter S described in the chapter Model Hydrodynamics. The infiltration effects are determined due to three effects; submarine exchange; infiltration and exfiltration. These are described in the chapter Model Hydrodynamics. The main parameters influencing the groundwater – surface water exchange are:

- Hydraulic conductivity
- Porosity
- Pressure at the bed
- Wetting front
- Bed level compared to groundwater level

As the hydraulic conductivity and porosity are constant, the difference should be created by one of the other three factors.

The infiltration results for the three scenarios for test 10 is given in Figure 42 and the rest is added in the Appendix G: Results. The infiltration results are quite different for all the three scenarios. The axes of all the tests are kept the same with an maximum infiltration of 0.4 and a minimum infiltration of -0.1.

The scenario with no morphological updating show really low and compact infiltration effects compared with NIELSEN, [2006] and VAN RIJN, [2007] case. The infiltration effects for no morphological updating are $\pm 0.04 [m/s]$.

The VAN RIJN, [2007] case shows the biggest infiltration effects. The maximum infiltration is about $+ 0.4 [m/s]$, which is a factor 10 higher than for the case without morphological updating. The exfiltration is a lot lower with $- 0.01 [m/s]$.

The NIELSEN, [2006] formula shows infiltration effects which are quite the same as the case without morphological updating. Only the 1:4 slope test show huge down rush exfiltration's. The minimum is too large for the fixed model axis but is $- 1.0 [m/s]$. It is interesting that the big exfiltration effects occur for the 1:4 slope as the NIELSEN, [2006] method already showed difficulties modelling the 1:4 slopes.

The difference in scale between the three tests is difficult to explain. The most obvious reason would be that the high infiltration effects for VAN RIJN, [2007] are caused by the big erosion holes. This cannot be verified however. The infiltration effect is included in the ventilation parameter for the dimensionless friction coefficient (c_f) and in the relative effective weight for the shields formula (Equation 7-2).

$$\theta_{cr} = \frac{1}{\left(\Delta + \alpha \frac{S}{K}\right) \rho g D_{50}} \cdot \tau_{cr} \quad \text{Equation 7-5}$$

The Shields formula can be seen as the marked part times the critical shear stress. The marked part consists only about constants and the only variable is the infiltration effect. For the constants $K = 0.01 [m/s]$, $D_{50} = 0.04 [m]$ and $\Delta = 1.63$ the marked part and shields parameter is given in Table 19. The results show that the shields parameter is influenced a lot by the infiltration

parameter. Higher infiltration effects give lower shield parameters, and thus more easily transport of sediment. The VAN RIJN, [2007] and NIELSEN, [2006] method give maximum shear stresses of $\tau = 1000 [m/m^2]$ and $\tau = 100 [m/m^2]$. For these shear stresses the shields parameter ranges between 0.00048 and 0.12. This are extreme differences from the expected value of 0.05 for the Shields parameter.

Table 19: Influence of the infiltration term

	S=1.0	S=0.4	S=0.01
Factor (marked part)	$4.8 \cdot 10^{-6}$	$1.15 \cdot 10^{-5}$	$1.2 \cdot 10^{-4}$
Shields ($\tau = 1000$)	0.0048	0.011	0.12
Shields ($\tau = 100$)	0.00048	0.0011	0.012

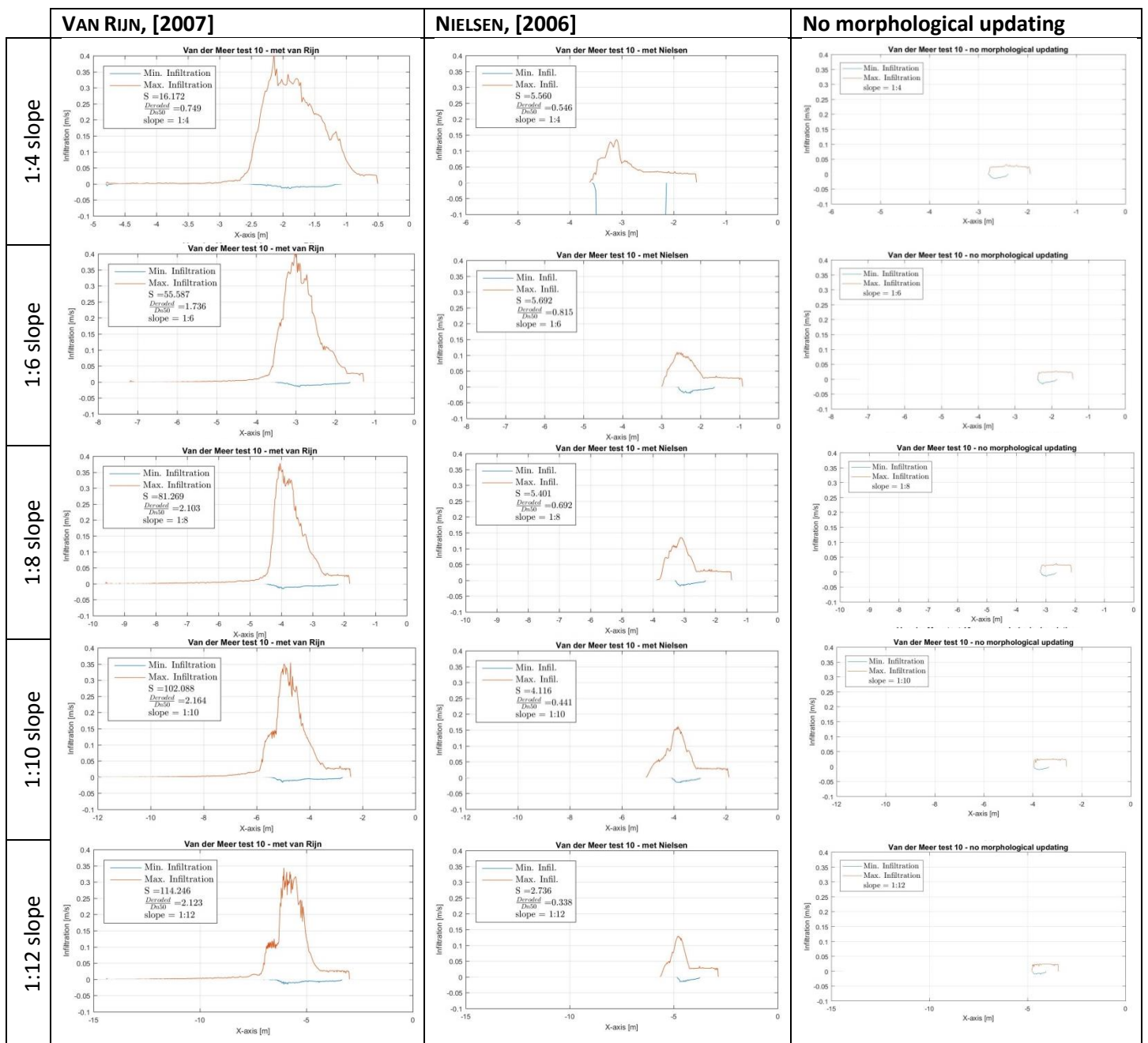


Figure 42: Infiltration effects for test 10 for the three cases: NIELSEN, [2006]; VAN RIJN, [2007] and no morph. updating

7.4.2 Morphodynamics

The morphodynamics follow from the hydrodynamics as the parameters described before are the input in the sediment transport formulations. The hydrodynamics seem to be modelled well except for the infiltration effects which show high fluctuations and big impacts on the shields parameter. The sediment transport description consists of three parts. The shear stress/velocity definition; the shields parameter and the actual sediment transport. These three aspects are considered in this chapter.

Shear stress

The shear stresses for test 10 is again visualised for the VAN RIJN, [2007], the NIELSEN, [2006] and the no morphological updating scenario. Because the NIELSEN, [2006] method works with a shear velocity, the shear stresses are achieved with a different method.

In the scenario of VAN RIJN, [2007] the total shear stress and the shear stress due to advection are reproduced with the variables: “taubx” and “taubx_add”, the difference is then caused by the drag part, shown in the right top corner of every plot.

For the NIELSEN, [2006] transport formula the total shear velocity is obtained with the variable: “ustar”. The drag part can be reproduced with the output velocity. The difference between the drag part and the total shear velocity is caused by the inertia part. The total shear velocity is converted to the shear stress according to, $\tau = u_*^2 \cdot \rho$.

For the last case without morphological updating the shear stresses by VAN RIJN, [2007] are reproduced. The shear stresses of NIELSEN, [2006] could not be reproduced as the variable “ustar” is not determined by the model as the sediment transport is not activated.

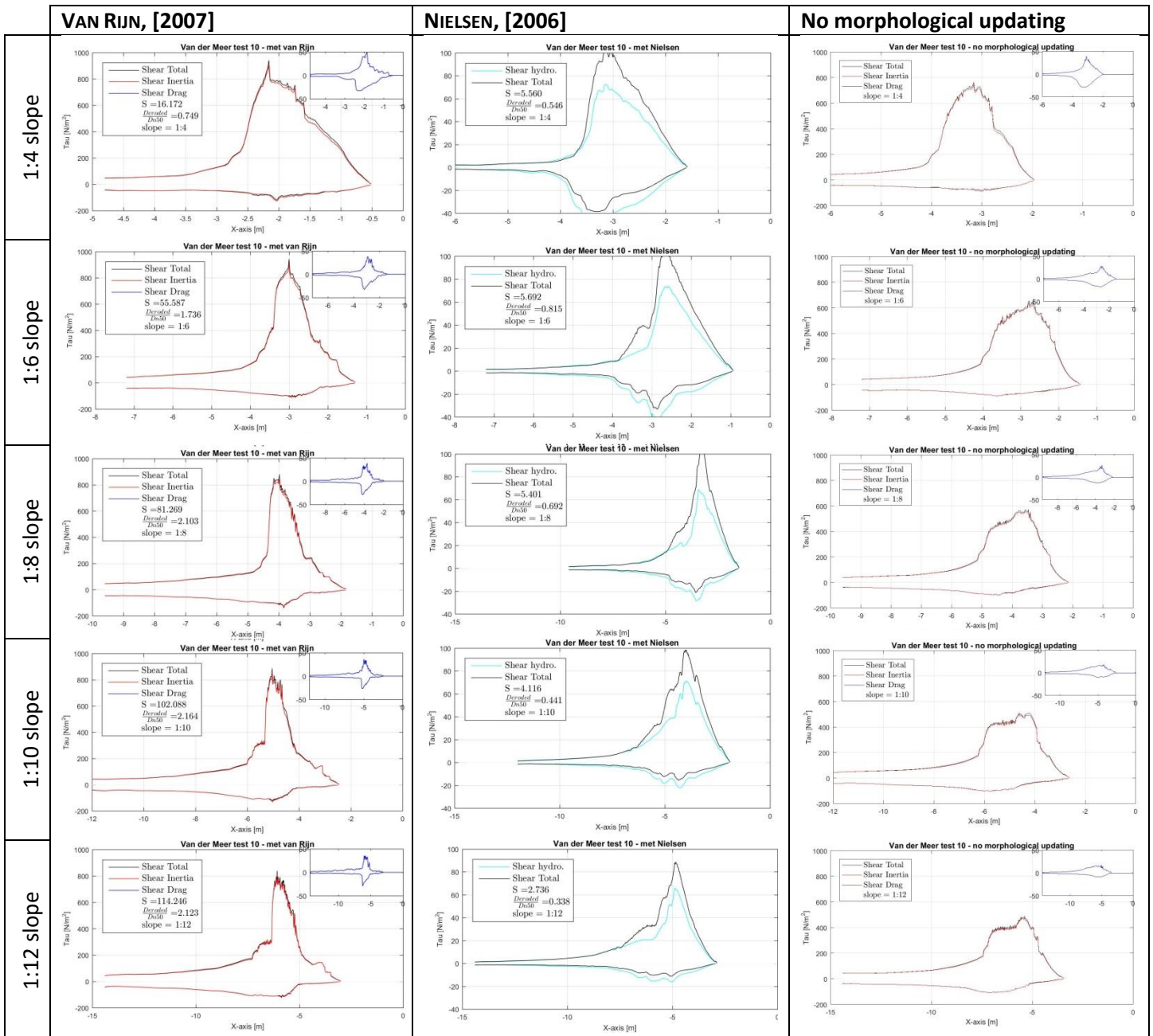


Figure 43: shear stresses for test 10 with the VAN RIJN, [2007], the NIELSEN, [2006] and the VAN RIJN, [2007] with no morphological updating.

The VAN RIJN, [2007] method shows for the 1:12 slope a steep peak near MSL, which is not present in the scenario without morphological updating. For this case quite a severe erosion occurred which probably gives this peak. The peak was also visible in the acceleration and velocity term previously discussed. In all the VAN RIJN, [2007] tests the inertia part is very dominant compared to the drag part. The drag part is therefore displayed in the right top corner of every plot.

The NIELSEN, [2006] method shows overall much lower shear stresses than the VAN RIJN, [2007]. The difference in shear stresses is a factor 10 with shear stresses of 100 N/m² for NIELSEN, [2006] and 1000 N/m² for VAN RIJN, [2007]. The light blue line in the NIELSEN, [2006] method indicates the shear stress used for the hydrodynamics.

Shear velocity

The shear velocity is used in the NIELSEN, [2006] transport method. The ratio between the drag and inertia part can be seen with the blue and the red line in Figure 44. Contrary to the VAN RIJN, [2007] method the drag part is dominant for the NIELSEN, [2006] case. The ratio between the drag term and the inertia term seems better for the NIELSEN, [2006] case.

In the case without morphological updating the output velocity and calculated acceleration terms are used to calculate the shear velocities. This shows shear velocities in the same order of size. Especially the inertia part (red line) seems to decrease for the milder slopes. This is less the case for the NIELSEN, [2006] method.

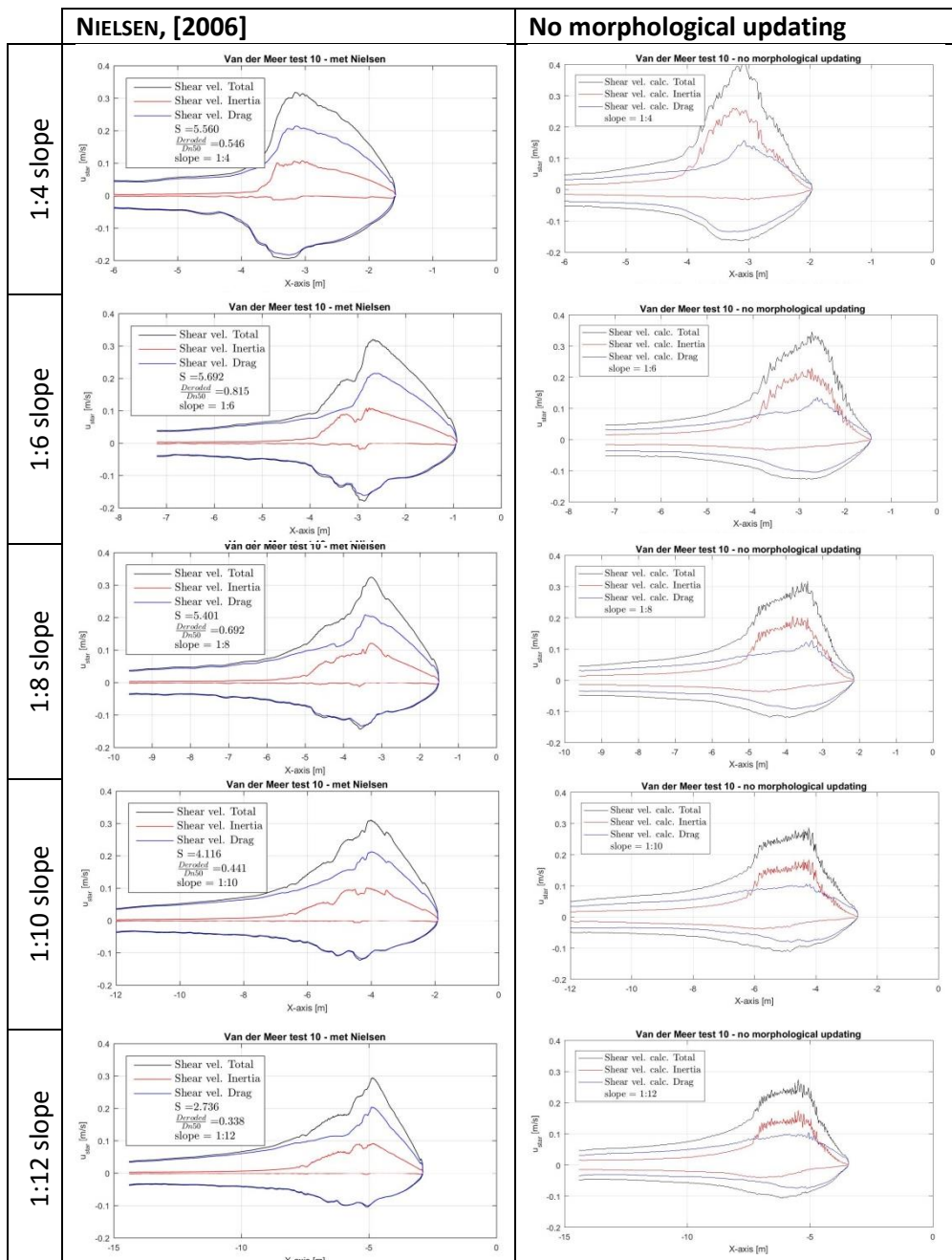


Figure 44: Shear velocity for test 10 with the Nielsen and the case without no morphological updating

Shields parameter

The Shear stresses are the input for the shields parameter. Both parameters can be determined with the in Equation 7–6.

$$\theta = \frac{\tau_b}{\rho g \Delta_i D_{50}} \text{ (van Rijn)} \quad | \quad \theta = \frac{u_*^2}{g \Delta_i D_{50}} \text{ (Nielsen)} \quad \text{Equation 7-6}$$

$$\Delta_i = \frac{(\rho_s - \rho)}{\rho} + \alpha \frac{S}{K}$$

The shields parameter consists of two variables, the shear stress/velocity and the infiltration. The other parameters are constants. The shields parameter is reproduced for test 10 for the tree scenarios. The shields parameter seems to deviate quite a lot. For the VAN RIJN, [2007] shield values of 0.9 are found which are unrealistic high. NIELSEN, [2006] seems to give results which are more in the range of expectations with values of 0.14. This is still higher than the expected value of 0.05,

$$\theta_{cr} = \frac{0.3}{1 + 1.2D_*} + 0.055(1 - e^{-0.020D_*}) \quad \text{Equation 7-7}$$

$$D_* = D_{50} \left(\frac{\Delta g}{\nu^2} \right)^{\frac{1}{3}}$$

The VAN RIJN, [2007] transport formula uses a specific description for the critical shear stress (Equation 7–7) while the NIELSEN, [2006] transport formula uses the value 0.05. For test series B this critical shear stress becomes with a kinematic viscosity of $\nu = 1 * 10^{-6}$ as Table 20, which is for test series B: $\theta_{cr} = 0.05528$. The given shield values found for VAN RIJN, [2007] are so high that a lot of erosion is expected. The situation with no morphological updating is calculated also with the VAN RIJN, [2007] method and shows also unrealistic high shield values.

Table 20: critical shear stress according to VAN RIJN, [2007].

	Test	D^* [-]	θ_{cr} [-]
Test series A	1	419	0.05558
	2	419	0.05558
	3	907	0.05528
	4	907	0.05528
	5	419.	0.05558
	6	628	0.05540
	7	628	0.05540
	8	838	0.05530
	9	904	0.05528

	Test	D^* [-]	θ_{cr} [-]
Test series B	10	907	0.05528
	11	907	0.05528
	12	907	0.05528
	13	907	0.05528
	14	907	0.05528

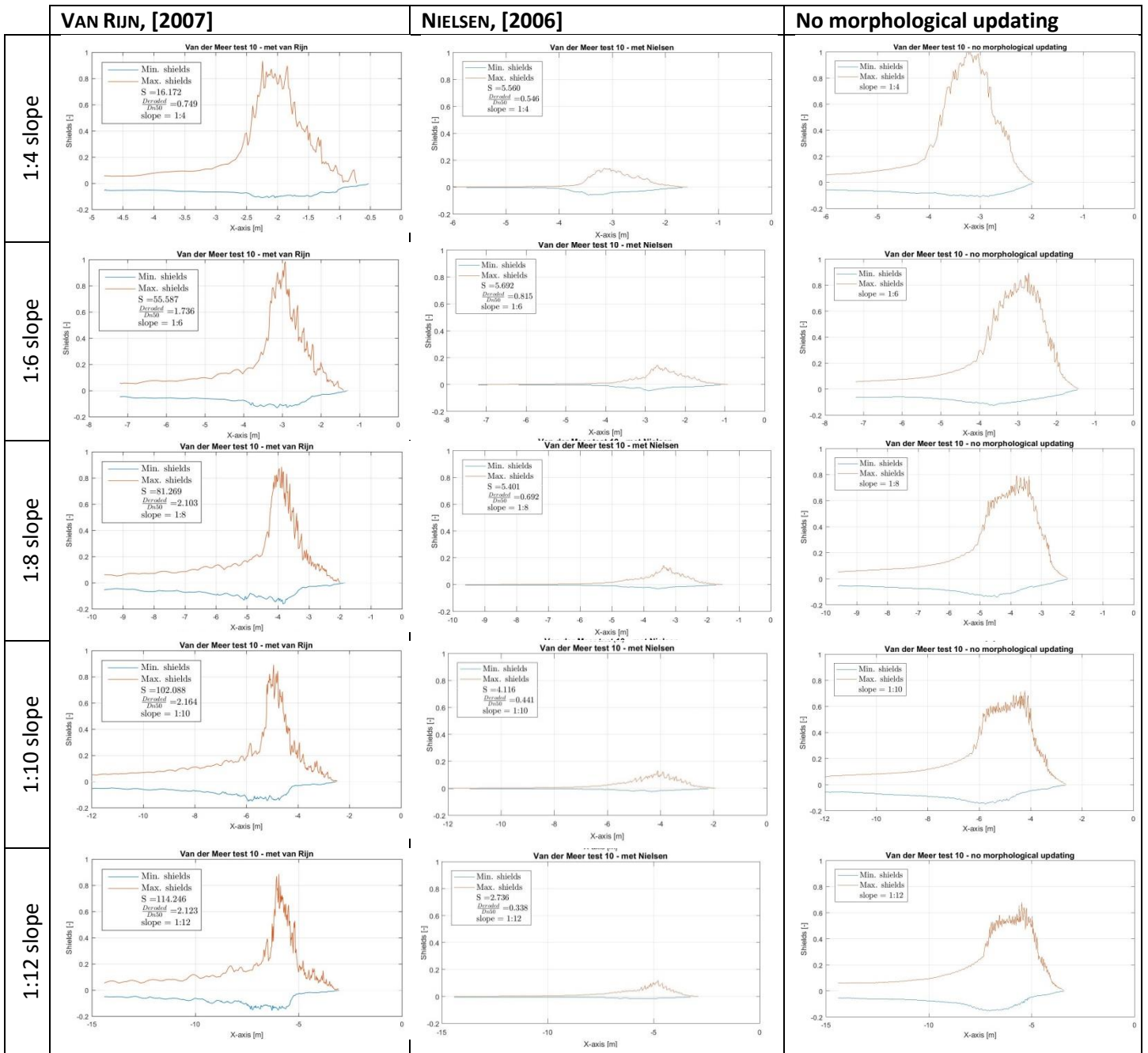


Figure 45: Shields parameter for test 10 with the VAN RIJN, [2007], the NIELSEN, [2006] and the case with no morphological updating.

Sediment transport

The shields parameter is used in the sediment transport equations. Both methods use another sediment transport formula as is explained in the chapter Morphodynamics of the theoretical framework. Both formulas are repeated below in Equation 7–8 and Equation 7–9.

$$\begin{aligned} \text{VAN RIJN, [2007]} \quad q_{bs} &= \gamma D_{50} D_*^{-0.3} \sqrt{\frac{\tau_b}{\rho}} \cdot \frac{\theta' - \theta_{cr}}{\theta_{cr}} \frac{\tau_b}{|\tau_b|} \\ \theta_{cr} &= \frac{0.3}{1 + 1.2D_*} + 0.055(1 - e^{-0.020D_*}) \\ D_* &= D_{50} \left(\frac{\Delta g}{\nu^2} \right)^{\frac{1}{3}} \end{aligned} \quad \text{Equation 7-8}$$

$$\text{NIELSEN, [2006]:} \quad q_{bs} = 12(\theta' - 0.05) \sqrt{\theta'} \sqrt{\frac{\rho_s - \rho}{\rho}} g D_{50}^3 \quad \text{Equation 7-9}$$

The high shear stresses at VAN RIJN, [2007] also gives unrealistic high shield parameters. Both the shear stresses as the shields parameter is used in the transport formula. The NIELSEN, [2006] transport rates are a factor 2 lower than the VAN RIJN, [2007] method. (Figure 46). The increase in erosion that is observed for milder slopes is not clear in the sediment transport rates.

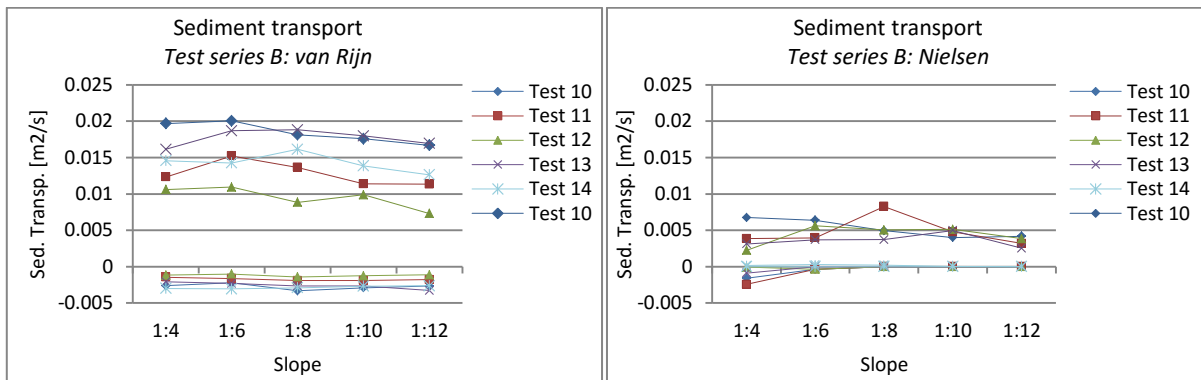


Figure 46: Sediment transport rates for the VAN RIJN, [2007] and NIELSEN, [2006] transport method.

For test 10 the results of the sediment transport are given in Figure 47. The sediment transport range is much wider for the VAN RIJN, [2007] method than for the NIELSEN, [2006] method. Both cases show more transported offshore than down shore.

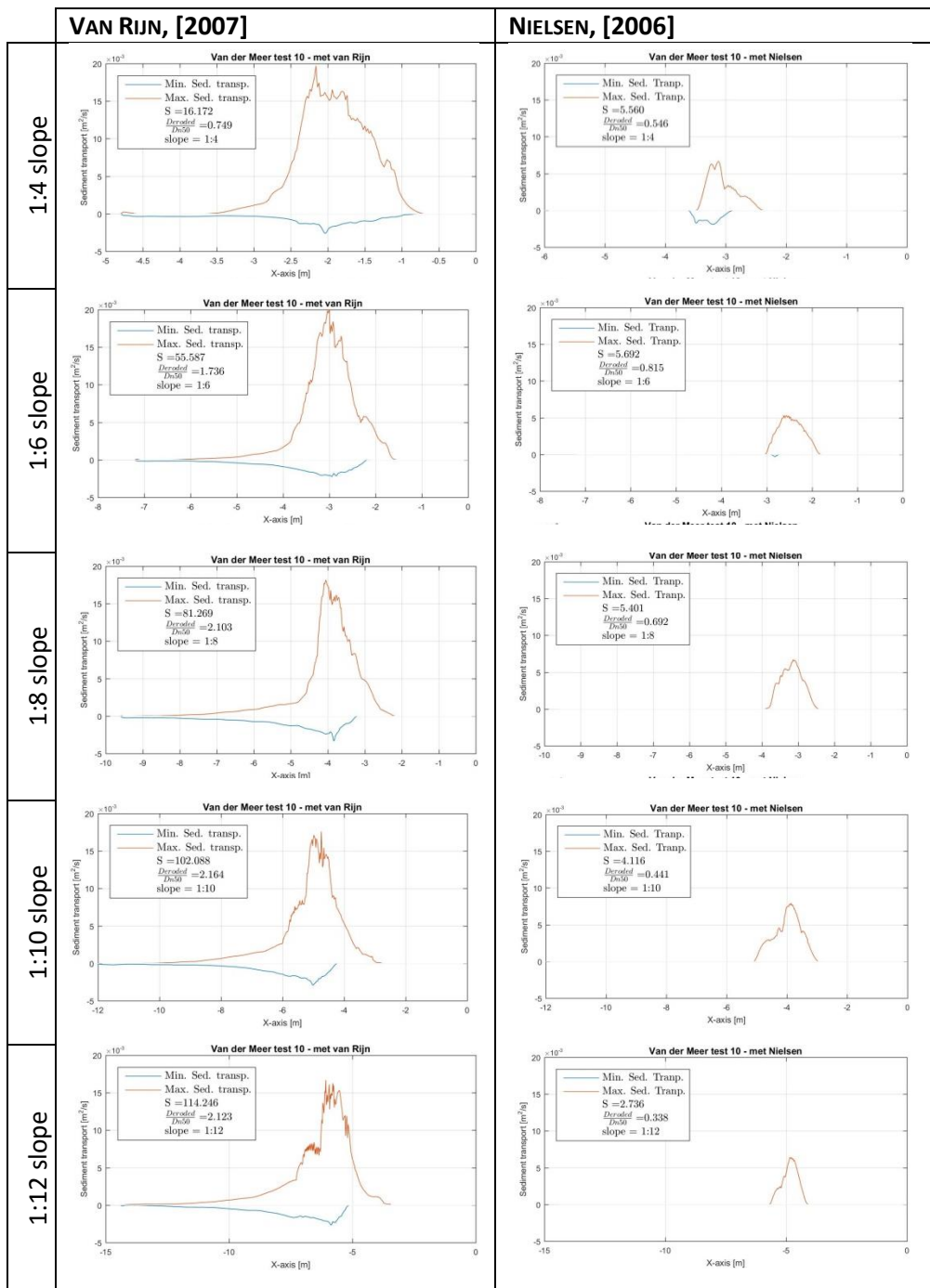


Figure 47: Sediment transport rates for test 10 with the VAN RIJN, [2007], the NIELSEN, [2006] transport formula

7.4.3 Recap stage 4

Hydrodynamics

- The velocity and acceleration in the hydrodynamics are modelled well.
- Assumption is made that the velocity is reproduced well enough to calculate with for an output time step of $dt=0.01s$.
- The filter influences the acceleration significantly.
- The infiltration effects have a substantial effect on the sediment transport.

Morphodynamics

- Shear stresses differ significantly with 10 times lower shear stresses for the NIELSEN, [2006] formula
- The NIELSEN, [2006] method has a better ratio between the inertia and drag shear stresses. For the VAN RIJN, [2007] tests the advection part is dominant.
- The shields parameter for both methods is higher than the expected value. For the VAN RIJN, [2007] tests the values are unrealistic high.

8

CONCLUSIONS & RECOMMENDATIONS

- Conclusions
- Recommendations

A summary of the already described conclusions is presented in this chapter. The resulting recommendations are also listed, which can be used for further research.

8.1 Conclusions

The objective of this master thesis was to find out if XBeach-G can be used as a design tool for rock armour protection under wave loading on mild slopes. Several research questions are formulated to answer this question. These questions are answered below.

How well does the numerical model XBeach-G reproduce the experiments, executed by VAN DER MEER [1988] with the transport formulas of NIELSEN, [2006] and VAN RIJN, [2007]. Which of the two transport formulas reproduces the experiments the best?

Xbeach-G is not able to accurately model the damage of rock on mild slopes. At first it seems that the reshaping profile shows some similarities. However, quantification of the damage using damage level (S), or the erosion depth, shows large deviations between the experiments. This counts for both transport formulae currently available for Xbeach-G.

The NIELSEN, [2006] method is more accurate and consistent for slopes milder than 1:6. Although attentions should be given to the right calibration factors as the wave period has a substantial effect on the result.

The VAN RIJN, [2007] method is more appropriate for the steep slopes and gives more conservative damage levels. The start of damage seems to be modelled better than the big erosion profiles. Problems might occur with the VAN RIJN, [2007] method when large rocks are modelled on mild slopes.

How well are the hydrodynamics modelled, and is this correctly translated to the morphodynamics?

The general trend for the velocity and acceleration is incorporated well in the model as they both decrease for mild slopes. The filter incorporated for the acceleration has a significant influence on the results. The fluctuations in the infiltration, observed for the steep slopes and deeply eroded profiles, have a substantial influence on the sediment transport and the eventually formed erosion profile.

Both shear stress formulations distinguish a drag and inertia part in their formulation. The resulting shear stresses are however completely different for both formula. The VAN RIJN, [2007] formulation gives a factor ten higher shear stresses and the inertia component is dominant for all the VAN RIJN,

[2007] tests. The NIELSEN, [2006] method gives lower and more realistic values for the shear stress and a better ratio between the drag and inertia component. The lack of feedback to the hydrodynamics in the NIELSEN, [2006] method is however a big disadvantage.

The Shields parameter is for both cases higher than the expected value ($\theta = 0.05$). Especially the VAN RIJN, [2007] method gives unrealistic high maximum shields values ($\theta = 0.4$). This results in significantly more erosion for the VAN RIJN, [2007] formulation.

The slope correction factor on the shields parameter just changes the influence of the gravity component on a slope. This is a quite rough method to include the slope effect on the stones. For sandy beaches it is proven to be reasonably accurate, but for more coarse material it is not. This is because also other processes play a role, such as the turbulence, the type of wave breaking and the wave penetration for low wave periods. Optimisation of the slope correction factor is necessary and needs further research.

The overall conclusion is that the translation from the morphodynamics to the hydrodynamics is incorrect for both methods. The NIELSEN, [2006] method gives more realistic results for the mild slopes and the VAN RIJN, [2007] for the steeper slopes

How can the amount of erosion best be quantified, for mild slopes, such that the safety requirements are still assured?

The erosion quantification method depends on the type of slope as for mild slopes, more erosion can be tolerated than for steep slopes. For mild slopes the erosion depth is the leading parameter to quantify the damage. For steep slopes, the damage level used by VAN DER MEER [1988] is sufficient.

For a dynamic situation with high damage levels, the relative erosion depth stabilises and proportionally to the damage level, less deep erosion depths occur. This means that for high damage levels, the erosion hole become longer but not deeper.

The results with the model XBeach-G show deeper and more compact erosion profiles for the NIELSEN, [2006] transport equation and more long stretched profiles for the VAN RIJN, [2007] formulation. The same damage level gives deeper erosion holes for the NIELSEN, [2006] transport formulation than for the VAN RIJN, [2007] transport formula.

Future research on erosion on mild slopes should focus on the formed erosion profile, mainly quantified by the erosion depth. The main priority for the XBeach-G model is the correct modelling of the point of incipient motion. This should be done before improving the formation of erosion profiles in time.

8.2 Recommendations

The items listed below are still unexplained results and data gaps than can form possible subjects for further research.

- a) The model seems to describe the point of incipient motion better than the big erosion profiles. More research should be done to optimise the start of damage point in the model. A comparison of wave flume experiments, focussed on the point of incipient motion with the XBeach-G results would be interesting.
- b) The formula of van der VAN DER MEER [1988] is valid up to a 1:6 slope. Experimental tests with more mild slopes could improve the formula for the more spilling breaker type of waves with lower iribarren numbers.
- c) The NIELSEN, [2006] method shows better transport rates but has some disadvantages. The calibration factors such as the phase lag angle and the friction coefficient affect the results significantly. A physical description for the phase lag angle and friction factor is necessary to improve the model.
- d) The effect of the filter on the velocity is not known. The first indications show that it dampens the accelerations significantly. Research on the effect of the filter on the acceleration term is necessary to verify these findings.
- e) The current description of the infiltration effects show fluctuations, which affect the sediment transport substantially. A research focused on the optimisation of the infiltration effect can improve the numerical model.
- f) As most sediment transport formulas are developed for horizontal beds the bed slope effect is added in the shields parameter. An optimisation of the bed slope parameter could give more insight in the behaviour of stones on mild slopes.
- g) In the VAN RIJN, [2007] approach the unexpected 1:4 result for test 14 might indicate an optimum in damage level for the 1:6 slope. It would thereby confirm the expected trend of minimal damage for the optimal slope corresponding the hydrodynamic forcing. Steeper slopes should be modelled with the VAN RIJN, [2007] method to observe if this optimal slope is present.

9

DISCUSSION

The chapter discussion treats the weak points in this research. It describes the assumptions made, the way the data is used and the conclusions which might have been drawn too quickly.

The first discussable point of this research is the amount of numerical tests which have been used to verify the observed trends. A larger number of numerical tests should strengthen the theories made in this report. Also the recalculation of the acceleration term should be verified with more research, such as experimental tests.

The second point is the hydrodynamic and morphodynamic parameters, which are only compared on the maximum and minimum values that occurred during the whole run. For parameters with a large fluctuation, minimum and maximum values can give a wrong impression as they visualise the peaks. The average value with the standard deviation can give a different impression.

The use of the damage level gives only limited information about the formed damage. The comparison with the VAN DER MEER [1988] experimental tests is therefore limited. The numerical parameters are studied on the formed trends, because of the lack of experimental data. More detailed experimental data is necessary for a better validation of the hydrodynamic and morphodynamic parameters and to strengthen the observed results.

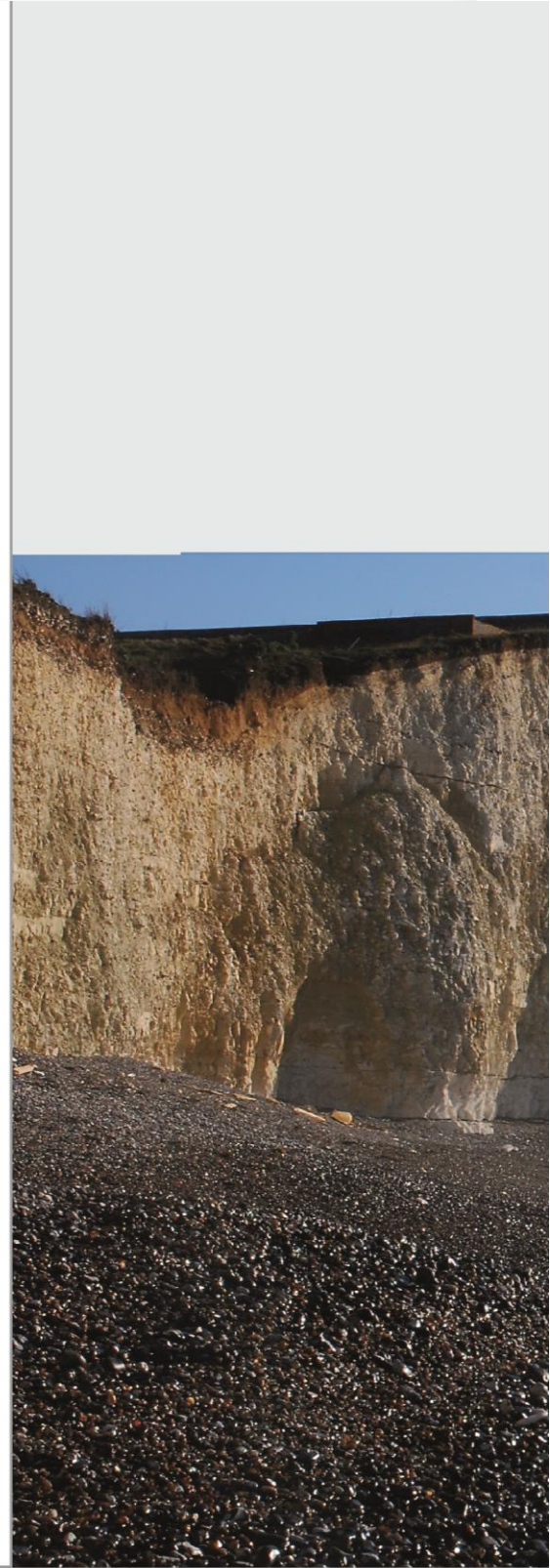
The motive for this research were the unexpected results of Wit [2015], with a different behaviour of the damage level compared to the erosion depth. This unexpected trend is still not explained and new unexpected trends occurred.

10

REFERENCES

- Bagnold, R. A. (1966). An approach to the sediment transport problem. *General Physics Geological Survey, Prof. Paper*.
- Bosboom, J., & Stive, M. J. F. (2015). *Coastal Dynamics I* (version 0.). Delft Academic Press.
- Butt, T., Russell, P., & Turner, I. (2001). The influence of swash infiltration-exfiltration on beach face sediment transport: Onshore or offshore? *Coastal Engineering*, 42(1), 35–52. [http://doi.org/10.1016/S0378-3839\(00\)00046-6](http://doi.org/10.1016/S0378-3839(00)00046-6)
- Chadwick, A. J. (n.d.). Coastal wiki. Retrieved from http://www.coastalwiki.org/wiki/Gravel_Beaches
- Conley, D. C., & Inman, D. L. (1994). Ventilated oscillatory boundary layers. *Journal of Fluid Mechanics*, 273, 261–284.
- Gent, M. R. A. Van. (1995). Wave Interaction With Berm Breakwaters, 121(October), 229–238.
- Grote, W. (1994). *Protection of outfall structures*. TU Delft.
- Hudson, R. Y. (1959). laboratory investigation of rubble-mound breakwaters.
- Kobayashi, N., Otta, A. K., & Roy, I. (1987). Wave Reflection and Run Up on Rough Slopes. *Journal of Waterway, Port, Coastal, and Ocean Engineering*, 113(3), 282–298. [http://doi.org/10.1061/\(ASCE\)0733-950X\(1987\)113:3\(282\)](http://doi.org/10.1061/(ASCE)0733-950X(1987)113:3(282))
- López de San Román-Blanco, B., Coates, T. T., Holmes, P., Chadwick, A. J., Bradbury, A., Baldock, T. E., ... Grüne, J. (2006). Large scale experiments on gravel and mixed beaches: Experimental procedure, data documentation and initial results. *Coastal Engineering*, 53(4), 349–362. <http://doi.org/10.1016/j.coastaleng.2005.10.021>
- Mccall, R. T. (2015). Process-based modelling of storm impacts on gravel coasts, (October).
- McCall, R. T. (2015). Process-based modelling of storm impacts on gravel coasts. Retrieved from <https://pearl.plymouth.ac.uk//handle/10026.1/3929>
- Nielsen, P. (2002). Shear stress and sediment transport calculations for swash zone modelling. *Coastal Engineering*, 45(1), 53–60. [http://doi.org/10.1016/S0378-3839\(01\)00036-9](http://doi.org/10.1016/S0378-3839(01)00036-9)
- Nielsen, P. (2006). Sheet flow sediment transport under waves with acceleration skewness and boundary layer streaming. *Coastal Engineering*, 53(9), 749–758. <http://doi.org/10.1016/j.coastaleng.2006.03.006>
- Nielsen, P., & Callaghan, D. P. (2003). Shear stress and sediment transport calculations for sheet flow under waves. *Coastal Engineering*, 47(3), 347–354. [http://doi.org/10.1016/S0378-3839\(02\)00141-2](http://doi.org/10.1016/S0378-3839(02)00141-2)
- O'Brien, M. P., & Morison, J. R. (1952). The forces exerted by waves on objects. *Eos, Transactions American Geophysical Union*, 33(1), 32–38.

- Packwood, A. R. (1983). The influence of beach porosity on wave uprush and backwash. *Coastal Engineering*, 7(1), 29–40.
- Pedrozo-Acuña, A., Simmonds, D. J., Chadwick, A. J., & Silva, R. (2007). A numerical-empirical approach for evaluating morphodynamic processes on gravel and mixed sand-gravel beaches. *Marine Geology*, 241(1-4), 1–18. <http://doi.org/10.1016/j.margeo.2007.02.013>
- Pedrozo-Acuña, A., Simmonds, D. J., Otta, A. K., & Chadwick, A. J. (2006). On the cross-shore profile change of gravel beaches. *Coastal Engineering*, 53(4), 335–347. <http://doi.org/10.1016/j.coastaleng.2005.10.019>
- Pedrozo-Acuña, A., Simmonds, D. J., & Reeve, D. E. (2008). Wave-impact characteristics of plunging breakers acting on gravel beaches. *Marine Geology*, 253(1-2), 26–35. <http://doi.org/10.1016/j.margeo.2008.04.013>
- Research, C. I., Association, I., (Netherlands), C. C. U. R. en R., & (France), C. d'études maritimes et fluviales. (2007). *The Rock Manual: The use of rock in hydraulic engineering* (Vol. 683). Ciria.
- Rijn, L. C. van. (1984). Sediment transport, part I: bed load transport. *Journal of Hydraulic Engineering*, 110(10), 1431–1456. [http://doi.org/10.1061/\(ASCE\)0733-9429\(1987\)113:9\(1187\)](http://doi.org/10.1061/(ASCE)0733-9429(1987)113:9(1187))
- Rijn, L. C. Van. (2007). Unified View of Sediment Transport by Currents and Waves . I : Initiation of Motion , Bed Roughness , and Bed-Load Transport, 133(June), 649–667.
- Schiereck, G. . J., & Verhagen, H. J. (2012). Bed, bank and shore protection.
- Schiereck, G., Fontijn, H. L., Grote, W. V., & Sisternans, P. G. J. (1994). Stability of Rock on Beaches, 1553–1567.
- Schiereck, G. J., & Fontijn, H. L. (1996). Pipeline protection in the surf zone, 4228–4241.
- Sisternans, P. G. J. (1993). *Stability of rock on beaches*. TU Delft.
- Van Der Meer, J. W. (1988). Rock Slopes and Gravel Beaches under Wave Attack, 214.
- Wit, M. (2015). Stability of Gravel on Mild Slopes in Breaking Waves, (November).
- Ye, L. (1996). *Stability of Rock on Beaches*. TU Delft.



Master of Science Thesis

Title: XBeach-G as a Design Tool for Rock on mild slopes under wave loading.

University: TU Delft - Faculty Civil Engineering and Geoscience

Author: Dhr. M.G. Postma

Year: 1 July 2016

Publisher: TU Delft Repository

APPENDIX

XBeach-G as a Design Tool for Rock on mild slopes under wave loading.



TABLE OF CONTENTS

APPENDIX A: DESIGN FORMULA'S	95
1.1 Horizontal bed	95
1.2 Sloping bed	96
APPENDIX B.- HYDRODYNAMICS.....	99
2.1 Offshore to nearshore wave transformation	99
2.2 Non-Linear Shallow Water Equations (NLSWE)	103
APPENDIX C.- MORPHODYNAMICS	107
3.1 Van Rijn – Bed Load	107
3.2 Van Rijn - Suspended load	108
3.3 Sediment transport due to Acceleration	111
APPENDIX D: DAMAGE QUANTIFICATION METHODS	115
4.1 Overview.....	115
4.2 Amount of stones displaced	115
4.3 Eroded Area	116
4.4 Erosion profile	118
APPENDIX E: REPRODUCED VAN DER MEER, [1988] EXPERIMENTS +SLOPE EFFECT.....	121
5.1 Damage number	121
5.2 Relative Erosion Depth	124
5.3 Formed erosion profile	127
5.4 Test series B; Erosion in time.....	145
APPENDIX F: RESULTS OF THE VARIED PARAMETERS – TEST SERIES B.....	151
6.1 Different Layer thickness (0.04m)	151
6.2 Different Stone size	157
6.3 Different Phase lag angle.....	170
6.4 Different Phase lag angle run 2	174
6.5 Different Hydraulic Conductivity	175
APPENDIX G.1: RESULTS HYDRODYNAMICS – TEST SERIES B.....	179
7.1 Velocity	179
7.2 Acceleration.....	185
7.3 Infiltration.....	191
APPENDIX G.2: RESULTS MORPHODYNAMICS – TEST SERIES B	198
8.1 Shear stress.....	199
8.2 Shear velocity	205
8.3 Shields.....	208
8.4 Sediment transport.....	214

Appendix A

Design formula's

APPENDIX A: DESIGN FORMULA'S

1.1 Horizontal bed

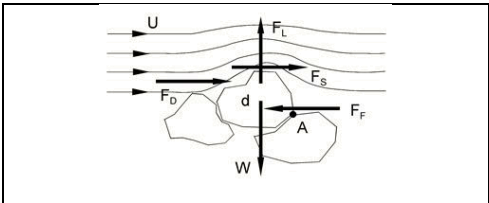
For horizontal beds there are two main approaches possible. The IZBASH [1930] , who considered for an individual grain the forces that work on it. Or the SHIELDS [1938] approach who considered the shear stress on a particle as driving force for movement.

1.1.1 IZBASH [1930] – Turbulent flow

IZBASH [1930] considered several forces that work on a particle on a horizontal bed and searched for the critical value for which the forces are not in equilibrium anymore. The following forces were determined:

Table 1: forces on a particle according to IZBASH [1930]

De-stabilizing forces	Stabilizing forces
Drag force	Momentum around A
Shear force	Friction force
Lift force	Submerged weight



When the de-stabilizing forces are bigger than the stabilising forces the particle starts to move. This is described in the IZBASH [1930] formula(Equation 1–1). The factor K in the formula is a constant which has to be determined experimentally.

$$\frac{u_c^2}{Load} = \frac{K\Delta gd}{Strength} \quad (IZBASH [1930]) \quad \text{Equation 1-1}$$

1.1.2 SHIELDS [1938] – Uniform Flow

Most sediment transport formula's work with the concept of a critical shear stress that is created by a current that flows over the sediment particles. If the force on the particle exceeds a certain threshold, the particle starts to move. The basis for this theory is created by shields who realised that the velocities create a shear stress on the particle. The shear stress is the driving force that causes the particle to move. The particle gets it's stabilizing strength due to the underwater weight and the corresponding gravitational component. When the shear stress is bigger than the strength, movement will take place. This is formulated in the Shields parameter shown in Equation 1–2 where the nominator is the shear stress and the denominator the stabilizing weight component.

$$\Psi_{cr} = \frac{\tau_{cr}}{(\rho_s - \rho_w)gD} = \frac{u_{*cr}^2}{\Delta gD} = \frac{load}{strength} \quad (SHIELDS [1938]) \quad \text{Equation 1-2}$$

This approach is valid for horizontal beds without a slope and for a uniform flow, laminar flow with no waves. The Shields criteria is assumed to be 0.05 but laboratory studies from BREUSERS AND SCHUKKING [1971] and from PAINTAL[1971] show that for situations with an high Reynolds numbers (turbulent flow) the shields criteria can range from $0.03 \leq \Psi_{cr} \leq 0.07$. (RESEARCH, ASSOCIATION, (NETHERLANDS), & (FRANCE), [2007]). According to the Rock Manual for rock fill the following should be assumed:

$\Psi_{cr} = 0.03 - 0.035$	First stones start to move
$\Psi_{cr} = 0.05 - 0.055$	Limited movement

1.1.3 SLEATH [1978] – Oscillating flow (Non-Breaking waves)

SLEATH [1978] investigated the influence of non-breaking waves, and the occurring oscillating flow in 1978. In this research the same dimensionless shear stress is used as SHIELDS [1938] did. The results are summarized by (GERRIT J. SCHIERECK, FONTIJN, GROTE, & SISTERMANS, [1996]) and are shown in Equation 1–3.

$$d_{n50} = \frac{2.15 \hat{u}_b^{2.5}}{\sqrt{T}(\Delta g)^{1.5}} \quad \text{Equation 1–3}$$

When comparing the results with Shields, it can be observed in Figure 1 that the formula of SLEATH [1978] also goes to $\Psi_{cr} = 0.055$ for high Reynolds numbers.

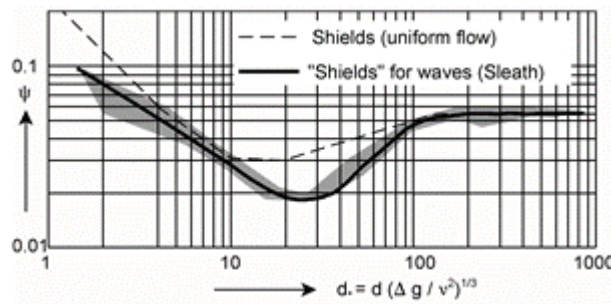


Figure 1: Shields diagram and Adjusted Shields for waves SLEATH [1978]

1.2 Sloping bed

Several researches have been conducted to describe the movement of stones on slopes. In this chapter an overview will be given about their attempts and when possible a comparison will be made.

1.2.1 IRIBARREN [1938]

In 1938 IRIBARREN [1938] did research on the stability of stones on breakwaters. Breakwaters differ from dikes with rock protection in the porosity as the breakwater are more porous structures than dikes. IRIBARREN [1938] started with the formula's for stability in flow on a horizontal bed and tried implementing a slope correction factor and the influence of breaking waves. The resulting IRIBARREN [1938] formula, shown in Equation 1–4, consist of a drag part, a resisting force part and a slope correction part. The formula can also be written in another form because the mass is proportional to the density times the volume so $M \propto \rho_s d^3$, the formula became as Equation 1–5.

$$\begin{array}{l} \rho_w g H d^2 \quad \propto \quad (\rho_s - \rho_w) g d^3 * (\tan(\phi) \cos(\alpha) \pm \sin(\alpha)) \\ \text{Drag force} \quad \quad \quad \text{Resisting force} \quad \quad \text{Slope correction} \end{array} \quad \text{Equation 1–4}$$

$$M \propto \frac{\rho_s H^3}{\Delta^3 (\tan(\phi) \cos(\alpha) \pm \sin(\alpha))^3} \quad (\text{Iribarren [1938]}) \quad \text{Equation 1–5}$$

1.2.2 HUDSON [1953]

HUDSON [1953] went further with investigating the stability of stones on a slope. This was done with a lot of experiments at the US Army Corps of Engineers. The result was another, rather simple, but more practical formula for different type of armour layers, shown in Equation 1–6. The K_D factor is the rest factor where the effects which were not well described in the formula of IRIBARREN [1938] were processed. This factor is determined with the help of the dataset created with the experiments.

In 1977 CERC published guidelines for the K_D factor for different type of armour layers and type of structures and in 1984 these guidelines were updated. In the guidelines of 1984, it was advised to use $H_{1/10}$ instead of H_s , ($H_{1/10}=1.27 H_s$), which changed the formula and gave about 200% bigger stone sizes, see Equation 1–7. This is the version as we know it today. For this version of the formula other K_D factors were determined and this led to considerable higher stone sizes of about 3.5 times as big.

$$\left. \begin{aligned} M &= \frac{\rho_s H_s^3}{K_D \Delta^3 \cot(\alpha)} \\ \frac{H_s}{\Delta D_{n50}} &= (K_D \cot(\alpha))^{\frac{1}{3}} \end{aligned} \right\} \quad \text{(HUDSON [1953] ; CERC [1977])} \quad \text{Equation 1-6}$$

$$\frac{H_s}{\Delta D_{n50}} = \frac{(K_D \cot(\alpha))^{\frac{1}{3}}}{1.27} \quad \text{(HUDSON [1953]; CERC [1984])} \quad \text{Equation 1-7}$$

K_D factor (-)

The K_D factor used by HUDSON [1953] is a dustbin factor, which has different values for all the adjusted formula’s and for different situations. This dustbin factor mainly depends on three elements:

1. The used version of the HUDSON [1953] formula
2. If the waves are breaking or non-breaking
3. The material that is used as armour layer.

For the most common situations the corresponding factors are shown in Table 2

Table 2: CERC advise for K_D values (*Rock Manual, n.d.*)

CERC advice	K_D	Situation
CERC [1977]	3.5	Waves breaking on foreshore
	4	Non-breaking waves on the foreshore
CERC [1984]	2	Breaking waves
	4	Non-breaking waves

Limitations

The HUDSON [1953] formula has some disadvantages and limitations, which are described in the Rock manual. The tests are executed with only regular waves on permeable structures with no overtopping. The amount of parameters in the formula is limited and there are for example no wave period; storm duration or damage level included such as in the VAN DER MEER, [1988]. Also the slope range is only valid for slopes within $1.5 < \cot(\alpha) < 4$, which is quite limited and a lot lower than (VAN DER MEER, [1988]) which is applicable for $1.5 < \cot(\alpha) < 6$. (G .J. SCHIERECK & VERHAGEN, [2012]).

Table 3: Overview test limitations

Test limitations:	Formula limitations
<ul style="list-style-type: none"> • Regular waves only • Permeable structures • Non-overtopped structures 	<ul style="list-style-type: none"> • No wave period or storm duration included • No damage level included • Only valid for steep slopes $1.5 < \cot(\alpha) < 4$

Appendix B

Hydrodynamics

APPENDIX B.- HYDRODYNAMICS

2.1 Offshore to nearshore wave transformation

The nearshore zone can be divided in several regions. Terminology used to describe the process of waves and currents in the surfzone is illustrated in Figure 2 ("PILE BUCK," [n.d.]). The nearshore zone reaches from the offshore point to the end of the swash zone. The breaker zone is the zone where the waves feel the bottom and become unstable. The surf zone is where the waves break and where also bores can occur and the swash zone is where the run up and run down due to waves occur.

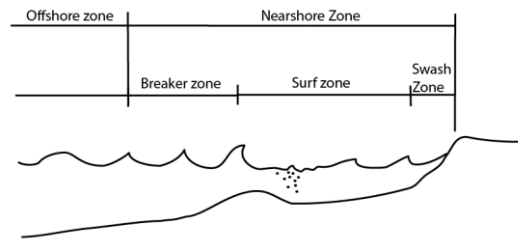


Figure 2: different region in the cross shore. ("PILE BUCK," [n.d.])

2.1.1 Offshore

The offshore waves are generated by shear stresses of the wind on the water surface. During a storm on sea, several waves with different phase speeds are generated and spread out in the direction of the wind. The wave with a high phase speed will travel fast over the sea and form a group and the waves with a lower phase speed as well. This phenomena is called frequency dispersion.

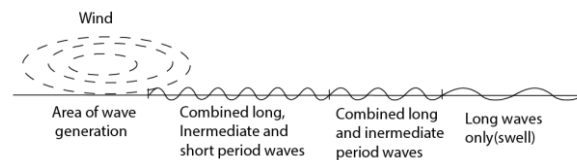


Figure 3: frequency dispersion of waves after a storm. (HOLTHUIJSEN, [n.d.])

2.1.2 Breaker zone

Shoaling/ skewness

When the waves becomes in a more shallow area, the wave starts to feel the bottom and is therefore reducing speed. ($c = \sqrt{gh}$). Because of continuity in energy, this reduction in speed causes an increase in energy density with as consequence that the wave shape changes. The wave grows in height and changes from a sinusoidal wave to a wave with a high crest and flat trough. This shape of the wave where the wave crest is getting higher and the trough is getting lower is called skewness.(asymmetric around horizontal axis, shown in Figure 5). This is modelled as the sum of two higher harmonics (sines), which amplifies at the crest and dampens at the trough.

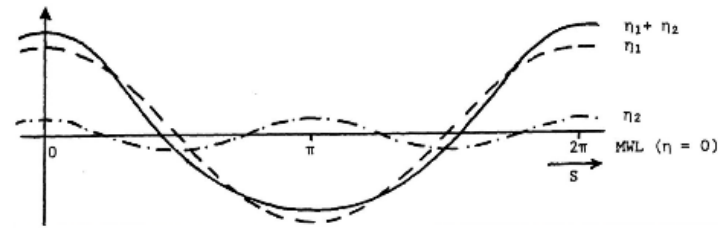


Figure 4: Skewness (JUDITH BOSBOOM & STIVE, [2015])

Asymmetry

The speed of the wave is determined by $c = \sqrt{g(h \pm \eta)}$, which states that the velocity at the crest of the wave is higher than at the trough. This difference in speed causes the wave to pitch forward, asymmetric about the vertical axis. This phenomena is modelled with a phase shift between the first and the second harmonic. When shoaling the wave gets slowly more asymmetric until the point of breaking.

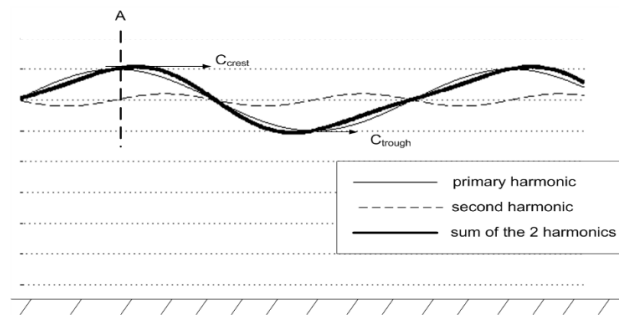


Figure 5: Asymmetry (JUDITH BOSBOOM & STIVE, [2015])

Breaking point - Plunging Breaker

There are different forms of breaking which are described by IRIBARREN [1938]. In this case the focus is on plunging breakers, so only this type of breaker is considered.

Plunging breakers occur on relative mild slopes where the upper part of the wave breaks over the lower part. Most energy is released in just one big splash. The influence of the impact of the plunging wave is often discussed as possible effect for sediment movement. This effect is investigated by (ADRIAN PEDROZO-ACUÑA, SIMMONDS, & REEVE, [2008]), who clearly shows a link between the impact of waves and the pressure on the bed. The research of ADRIAN PEDROZO-ACUÑA, SIMMONDS, & REEVE, [2008] divides the plunging breaker in three situation, which are shown in Figure 6.

At the most left picture the wave is shown just before breaking. The infiltration and exfiltration effects due to up and down rush can be seen in the pressure diagram in the right top corner.

The picture in the middle shows the situation when the wave is just on the moment of breaking on the shore. The impact of this wave is clearly visible in the pressure diagram (top corner) and are in the range of 15-30kPa, which is big enough to influence the sediment transport. The peaked sudden pressure on the bed has as effect that the pore pressure between the grains increases, which reduces the intergranular stresses and thus reducing the strength of the stones. It is even found out that liquefaction for gravel beaches is possible. (ADRIAN PEDROZO-ACUÑA ET AL., [2008])

While the stones are still weakened by the pressure, the wave is rushing over the bed, as a kind of bore, taking all the particles to the upper part of the profile. This is shown in the most right picture.

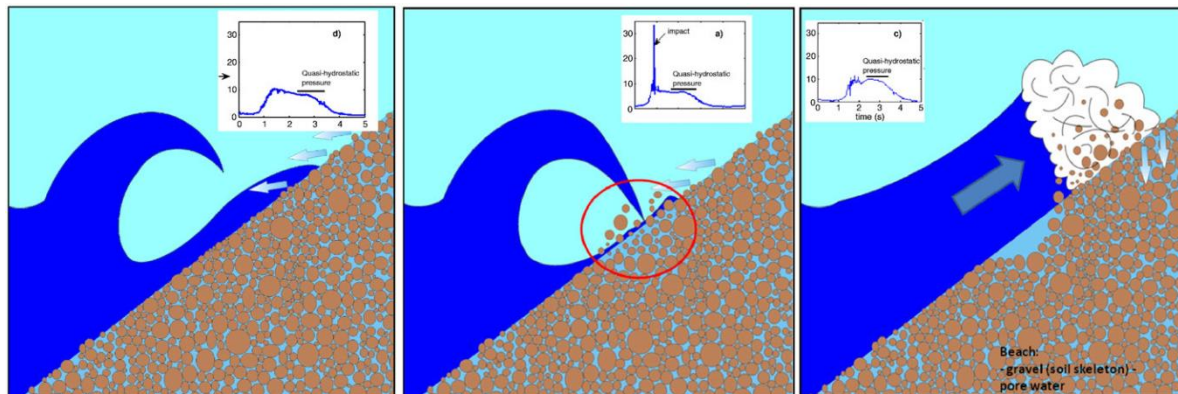


Figure 6: Concept of the effect of breaking of a plunging breaker. (ADRIAN PEDROZO-ACUÑA ET AL., [2008])

Swash zone

During the run up and run down the water is flowing over the stones and between the stones due to the higher permeability of coarse beaches. Three main mechanisms are important during this process. (ADRIÁN PEDROZO-ACUÑA, SIMMONDS, CHADWICK, & SILVA,[2007]).

1. Reduction of backwash volume
2. Change in effective weight of particles (vertical pressure differences)
3. Change in shear force (boundary layer)

The investigation of BUTT, RUSSELL, & TURNER, [2001] is aimed at understanding the contrary processes that happen in the swash zone. In the swash zone there is a high interaction between the groundwater and the surface water and as consequence other processes happen during uprush than during backwash.

During uprush the infiltration has a stabilizing effect on the sediment transport as the water is causing a force directed downward on the stones. This has as consequence that the turbulent boundary layer is getting pressed towards the shore, giving a thinner boundary layer thickness during uprush. A thinner boundary layer gives higher bed shear stresses and thus more transport.

During downrush, exfiltration of the water particles is taking place with as consequence an upward directed destabilizing force. This effect has also as results a thickening of the boundary layer and thus a reduction of the bed shear stresses.

A secondary effect of the infiltration is the reduction of the backwash volume which creates less erosion. This process is especially important for situations with a hydraulic conductivity higher than $1 \cdot 10^{-1} \text{ ms}^{-1}$. The swash zone is found to be unsaturated for mild beaches and long wave periods and also for steep slopes the swash zone is also most of the time unsaturated. (Figure 7). This indicates the effect and importance of the infiltration and exfiltration that is taking place on gravel beaches.

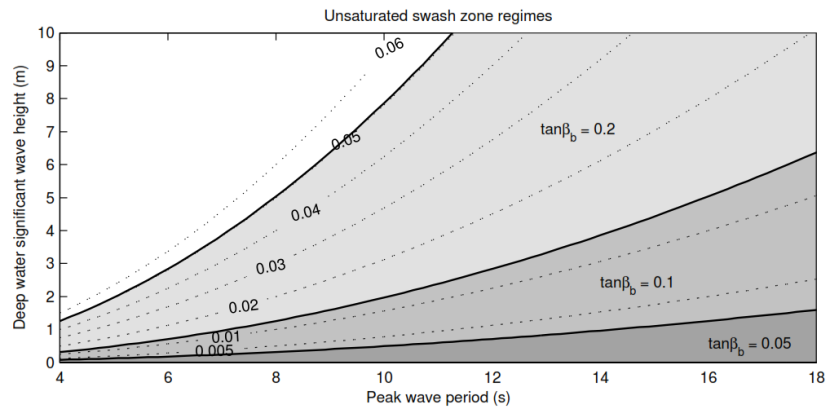


Figure 7: Unsaturated swash zone regimes. Shaded area: Unsaturated area for 1:20; 1:10 and 1:5 slope. (McCALL, [2015])

These processes which are explained above are summarized in Figure 8. The ratio between these stabilizing and destabilizing processes is important to give an approximation for the amount of sediment transport in the swash zone and the direction. The research of BUTT ET AL., [2001] to the infiltration and exfiltration effects show a decrease in uprush transport of 10.5% and an increase in backwash transport of 4.5% which implements more backwash transport than uprush transport. This effect due to infiltration and exfiltration can change in direction for different stone sizes. This research claims that there is a critical stone sizes for which the sediment transport changes from onshore to offshore. (BUTT ET AL., [2001]).

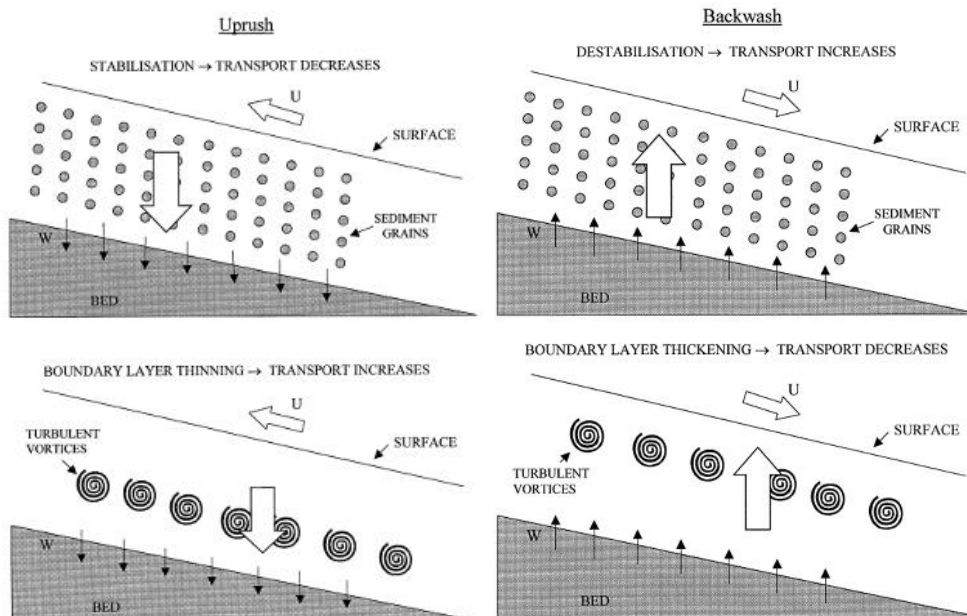


Figure 8: Left: Uprush effects; Right: Downrush effects (BUTT ET AL., [2001])

2.2 Non-Linear Shallow Water Equations (NLSWE)

2.2.1 Mass and continuity equation

This process from offshore to nearshore is often described in models with the Non-Linear Shallow Water Equation (NLSWE) with extra terms such as non-hydrostatic pressure and groundwater exchanges. The non-hydrostatic pressure term is included to model the short waves. The groundwater exchange term has mainly an effect in the swash zone. The NLSWE are based on two laws; the conservation of mass and the conservation of momentum. These two laws in combination with the non-hydrostatic pressure and the groundwater exchange are described below in Equation 2-1 and Equation 2-2.

$$\begin{aligned} \text{conservation of mass} \quad \frac{\partial \zeta}{\partial t} + u \frac{\partial h}{\partial x} + S = 0 \end{aligned} \quad \text{Equation 2-1}$$

$\zeta = \text{free surface elevation}$
 $u = \text{depth - averaged cross - shore velocity}$
 $h = \text{total waterdepth}$
 $S = \text{groundwater - surface water exchange}$

$$\begin{aligned} \text{conservation of momentum} \quad \frac{\partial u}{\partial t} + \underbrace{u \frac{\partial u}{\partial x}}_{\text{Acceleration advection}} - \frac{\partial}{\partial x} \left(v_h \frac{\partial u}{\partial x} \right) = \underbrace{- \frac{1}{\rho} \frac{\partial (\bar{q} + \rho g \zeta)}{\partial x}}_{\text{Pressure gradient}} - \underbrace{\frac{\tau_b}{\rho h}}_{\text{Bed friction}} \end{aligned} \quad \text{Equation 2-2}$$

$\bar{q} = \text{depth - averaged dynamic pressure}$

$v_h = \text{horizontal viscosity}$

$$v_h = 2(0.1 \Delta x)^2 \sqrt{2 \left(\frac{\partial u}{\partial x} \right)^2} \quad \text{Smagorinsky [1963]}$$

$$\tau_b = c_f \rho u |u| \quad \text{Morison [1952]}$$

The parameter v_h is the horizontal viscosity, which can be described with the Smagorinsky formula as is shown above. The bed shear stress (τ_b) due to currents can be described as above.

2.2.2 Depth-Averaged dynamic pressure

The averaged dynamic pressure (q), which describes the pressure due to waves is difficult to describe for depth-averaged models, such as XBeach-G. A common method is by taking the mean of the dynamic pressure at the surface and at the bed and assuming that the pressure at the surface is zero.

The pressure gradient in the vertical can be described by the Keller-Box method of Zijlema. (MCCALL, [2015]). With this method the dynamic pressure at the bed can be described with the following formula:

$$q_b = -\frac{h}{2} \left(\frac{\partial q}{\partial z} \Big|_s + \frac{\partial q}{\partial z} \Big|_b \right) \quad \text{Equation 2-3}$$

The vertical momentum balance is described with $\left(\frac{\partial q}{\partial z} = -\frac{\partial w}{\partial t} \right)$, when neglecting the advection and diffusion terms. Implementing the vertical momentum balance in the dynamic pressure at the bed gives a new vertical momentum balance which can be solved with the local continuity equation. $\left(\frac{\partial u}{\partial x} + \frac{w_s - w_b}{h} = 0 \right)$ ((MCCALL, [2015]))

$$\frac{\partial w_s}{\partial t} = 2 \frac{q_b}{h} - \frac{\partial w_b}{\partial t} \quad (\text{vertical momentum balance}) \quad \text{Equation 2-4}$$

Appendix C

Morphodynamics

APPENDIX C.- MORPHODYNAMICS

3.1 Van Rijn – Bed Load

3.1.1 Forces acting on a particle.

The parameter needed for the transport stage parameter and the particle parameter are achieved by first evaluating the forces working on a single particle on a horizontal bed. The forces acting on a particle are shown in Figure 9.

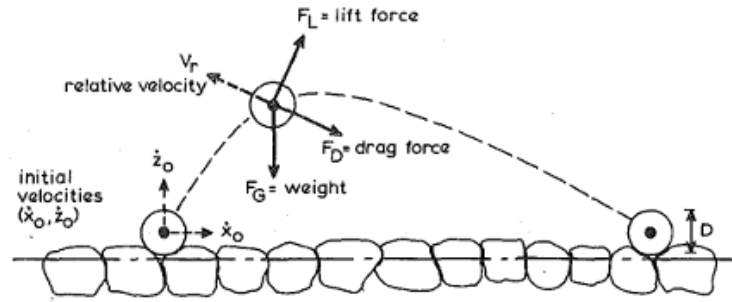


Figure 9: Forces acting on a particle.

Lift force

The lift force can be divided in a part due to shear and a part due to the spinning motion. The shear part of the lift force is described for a viscous flow by Equation 3–1 and is only valid for small Reynolds numbers. It is assumed that the lift force is mainly caused by the shear effect and the spinning motion is neglected.

$$F_{L(Shear)} = \alpha_L \rho v^{0.5} D^2 v_r \left(\frac{\partial u}{\partial z} \right)^{0.5} \quad \text{Equation 3-1}$$

$\alpha_L = \text{lift coefficient} = 1.6 \text{ (viscous flow)}$
 $\left(\frac{\partial u}{\partial z} \right) = \text{velocity gradient}$

Drag force

The second force is the drag force which describes the viscous skin friction and the pressure on the particle. The direction of the drag force depends on if the particle is going up or down. The lift force is always directed in upward direction, so sometimes the forces are in the same direction and sometimes in opposite direction.

$$F_D = \frac{1}{2} C_D \rho A v_r^2 = \text{drag force} \quad \text{Equation 3-2}$$

$C_D = \text{drag coefficient}$
 $A = \frac{1}{4} \pi D^2 = \text{cross sectional area of the sphere}$

Gravitational weight

The weight of the particle is assumed to be a spherical cube with equally spread density.

$$F_G = \frac{1}{6} \pi D^3 (\rho_s - \rho) g \quad \text{Equation 3-3}$$

Relative velocity

The relative particle velocity is opposite of the drag force and relative to the flow.

$$v_r = [(u - \dot{x})^2 + (\dot{z})^2]^{0.5} = \text{part. vel. rel. to the flow} \quad \text{Equation 3-4}$$

$u = \text{local flow velocity}$

Total balance

These four forces form a balance and this is described in the equations of motion. (Equation 3-5). These equations of motion are transformed to first order differential equations such that it can be solved numerically. The equations are described in the next chapter about the computation of the bed load transport.

$$\text{Equations of Motion} \quad \begin{cases} m\ddot{x} - F_L \left(\frac{\dot{z}}{v_r} \right) - F_D \left(\frac{u - \dot{x}}{v_r} \right) = 0 \\ m\ddot{z} - F_L \left(\frac{u - \dot{x}}{v_r} \right) + F_D \left(\frac{\dot{z}}{v_r} \right) + F_G = 0 \end{cases} \quad \text{Equation 3-5}$$

$m = \frac{1}{6}(\rho_s + \alpha_m \rho) \pi D^3 = \text{particle mass and added fluid mass}$
 $\alpha_m = 0.5 = \text{added mass coefficient}$
 $\dot{x} \ \& \ \dot{z} = \text{longitudinal and vertical particle velocity}$
 $\ddot{x} \ \& \ \ddot{z} = \text{longitudinal and vertical particle accelerations}$

3.2 Van Rijn - Suspended load**3.2.1 Computation of Suspended - load transport****Step 1: Particle Diameter; Step 2: Critical bed shear velocity; Step 3: Transport stage**

Step 1-3 are the same for suspended load transport as it is for the bed-load transport, explained above. In the first 3 steps, the particle diameter, critical bed shear velocity and transport stage are determined.

Step 4: Compute reference level

The reference level is introduced to calculate the reference concentration. This reference level is shown in Figure 10.

$$a = 0.5 \Delta \quad \text{or} \quad a = k_s, \quad \text{with } a_{\text{min}} = 0.01d \quad \text{Equation 3-6}$$

Step 5: Compute reference concentration

With the reference level the reference concentration can be calculated according to Equation 3-7. The factor a_2 is determined by assuming the reference level a is the same as the roughness height of Nikuradse. With the experiments it was obtained that an a_2 of 2.3 gives the best agreement.

$$c_a = \frac{0.035}{a_2} \frac{D_{50} T^{1.5}}{a D_*^{0.3}} = 0.015 \frac{D_{50} T^{1.5}}{a D_*^{0.3}} \quad \text{Equation 3-7}$$

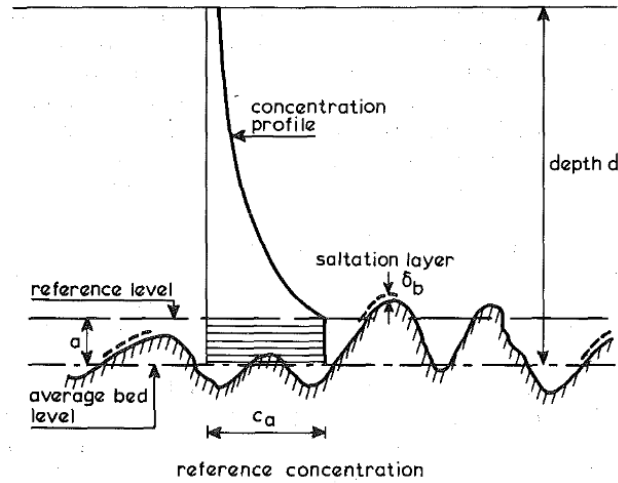


Figure 10: Reference level for suspended transport (VAN RIJN, [1985b]).

Step 6: Compute particle size

This parameter determines the particle size of the suspended sediment, D_s , in ratio with the D_{50} of all the sediment. The D_s is expected to be lower than the D_{50} as lighter sediment will be earlier in suspension. For $T=25$ the suspended sediment size is the same as the D_{50} .

$$\frac{D_s}{D_{50}} = 1 + 0.011(\sigma_s - 1)(T - 25) \quad \text{Equation 3-8}$$

$$\sigma_s = 0.5 \left(\frac{D_{84}}{D_{50}} + \frac{D_{60}}{D_{50}} \right)$$

Step 7: Compute fall velocity

The particle fall velocity can be calculated for different stone sizes. For a clear still fluid, particles will settle at other velocities than in a turbulent flow. The first equation describes the fall velocity for a clear, still fluid and stones smaller than $100 \mu m$. For bigger stones, the formula is formulated by Zanke as Equation 3-10. (VAN RIJN, [1985a]). The last formula describes the velocity for the biggest stones. In this formula the D_s is used as a parameter, which describes the suspended particle diameter which is smaller than the D_{50} .

$$\omega_s = \frac{1}{18} \frac{(s - 1)gD_s^2}{v} \quad D < 100 \mu m \quad \text{Equation 3-9}$$

$$\omega_s = 10 \frac{v}{D_s} \left\{ \left[1 + \frac{0.01(s - 1)gD_s^3}{v^2} \right]^{0.5} - 1 \right\} \quad 100 < D < 1000 \mu m \quad \text{Equation 3-10}$$

$$\omega_s \approx 1.1[(s - 1)gD_s]^{0.5} \quad D > 1000 \mu m \quad \text{Equation 3-11}$$

The falling velocity is influenced by other surrounding particles. This is called hindered settlement and can be calculated with the formula underneath.

$$\omega_{s,m} = (1 - c_s)^4 \omega_s \quad \text{Equation 3-12}$$

Step 8: compute β factor

The β parameter is the parameter related to the diffusion of the sediment particle. It is difficult to give a good prediction about the β parameter which gives it a rather poor accuracy. Some

investigations claim that the factor should be less than 1, because the influence of the turbulence should be dampened, while other investigations claim it should be bigger than 1. The formula shown in Equation 3–13 is derived from Coleman and gives values bigger than 1. (VAN RIJN, [1985a]).

$$\beta = 1 + 2 \left[\frac{\omega_s}{u_*} \right]^2 \quad \text{for } 0.1 < \frac{\omega_s}{u_*} < 1 \quad \text{Equation 3–13}$$

Step 9: compute overall bed-shear velocity

$$u_* = (gdS)^{0.5} \quad \text{Equation 3–14}$$

Step 10 compute φ factor

The overall correction factor is derived with trial and error and is therefore not so accurate ,about 25%. The main parameters, where the factor is dependent on are: . $\varphi = f\{\omega_s; u_*; c_a; c_0\}$.and the formula shown in Equation 3–15 is determined.

$$\varphi = 2.5 \left[\frac{\omega_s}{u_*} \right]^{0.8} \left[\frac{c_a}{c_0} \right]^{0.4} \quad \text{for } 0.01 \leq \frac{\omega_s}{u_*} \leq 1 \quad \text{Equation 3–15}$$

Step 11: Compute suspension parameter

The suspension parameter is a balance between the upward turbulent forces and the downward gravity forces. If the falling velocity is smaller than the upward turbulent forces, the suspension parameter will be smaller than 1 and the particle will be in suspension.

$$Z = \frac{\omega_s}{\beta \kappa u_*} = \text{suspension parameter.} \quad \text{Equation 3–16}$$

$\beta = \text{coefficient related to diffusion of sediment particles.}$

The modified suspension number, Z' , is introduced to make it possible to calculate the sediment transport without numerical integration. The overall correction factor is added to the suspension parameter to create the modified version. The overall correction factor is determined in step 10 and is dependent on the main hydraulic parameters.

$$Z' = Z + \varphi \quad \text{Equation 3–17}$$

Step 12: Compute F-factor

The F-factor can be determined with Equation 3–18, and helps simplifying the function for the suspended load parameter. For the conditions where this formula is valid it has an inaccuracy of about 25%.

$$F = \frac{\left[\frac{a}{d} \right]^{Z'} - \left[\frac{a}{d} \right]^{1.2}}{\left[1 - \frac{a}{d} \right]^{Z'} [1.2 - Z']} \quad \text{for } \begin{matrix} 0.3 \leq Z' \leq 3 \\ 0.01 \leq \frac{a}{d} \leq 0.1 \end{matrix} \quad \text{Equation 3–18}$$

Step 13: Compute suspended load parameter.

The results of this 13 step approach is the suspended load and is visualised with Equation 3–19.

$$q_s = F \bar{u} d c_a$$

$$q_s = \frac{u_* c_a}{\kappa} \left[\frac{a}{d-a} \right]^{z'} \left[\int_a^{0.5d} \left[\frac{d-z}{z} \right]^{z'} \ln \left(\frac{z}{z_0} \right) + \int_{0.5d}^d \left[e^{-4z' \left(\frac{z}{d} - 0.5 \right)} \ln \left(\frac{z}{z_0} \right) dz \right. \right. \quad \text{Equation 3-19}$$

3.3 Sediment transport due to Acceleration

As is described in the Equation 3-20 the wave shape changes when approaching the shore. The wave energy is compressed and the crest is getting higher and eventually breaks on the slope. These asymmetry and skewness phenomena also influence the sediment transport.

The cross-shore sediment transport is described by JUDITH BOSBOOM & STIVE, [2015]) with Equation 3-20 as the velocity times the third power. This formula shows that the sediment transport is caused due to three components, the mean current, the skewness and the bound long waves. For a perfect sinusoidal wave, the sediment transport is zero as the sediment transported onshore is also transported back offshore. (velocity at the trough is the same as at the crest).

$$\langle \bar{U} |U|^2 \rangle = \underbrace{3 \langle \bar{U} |U_{hi}|^2 \rangle}_{\text{Mean Current/Undertow}} + \underbrace{\langle U_{hi} |U_{hi}|^2 \rangle}_{\text{Skewness}} + \underbrace{3 \langle U_{lo} |U_{hi}|^2 \rangle}_{\text{Long Waves}} \quad \text{Equation 3-20}$$

Experiments executed by Stive show the ratio of these three components along the shore for a specific storm situation. (J. Bosboom & Stive, 2015). This is visualised in Figure 11, where also the main cross-shore hydraulic mechanisms are shown.

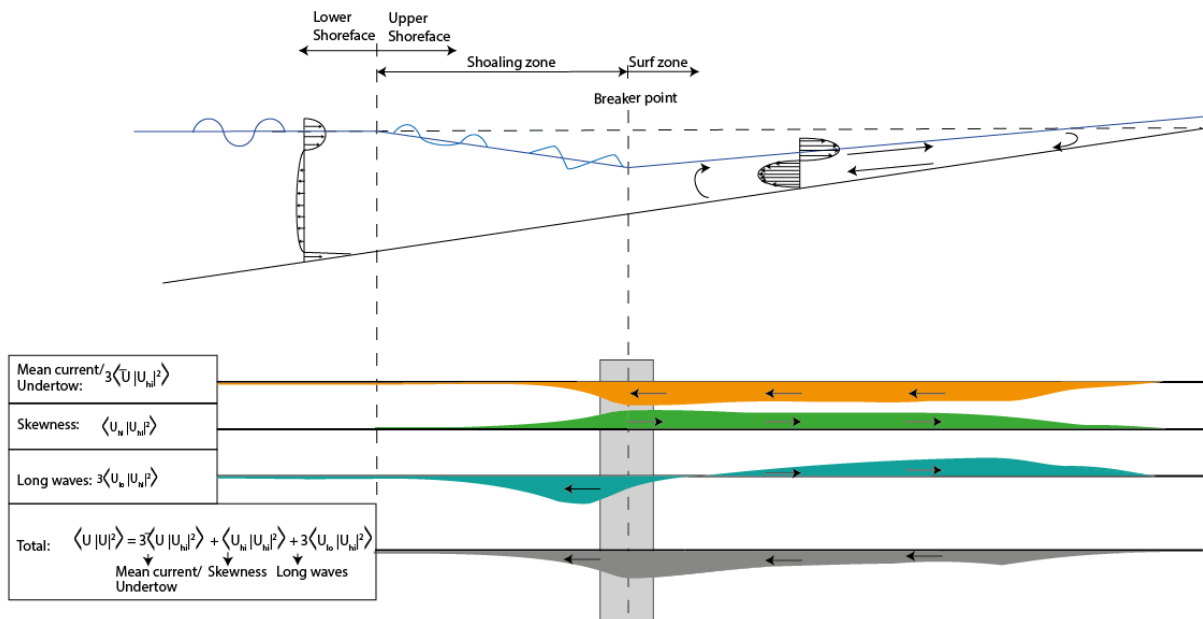


Figure 11: Visualisation three mechanisms along the shore.

3.3.1 Mean current

The mass of water that is transported onshore with the waves is according to the mass balance also flowing back. This is happening with a return current flowing over the bottom, described as Mean current/ Undertow.

3.3.2 Skewness

In the case of skewness (horizontal asymmetric) the offshore velocities (trough) are lower than the onshore velocities (crest) and thus a net onshore sediment transport is occurring.

3.3.3 asymmetry

For asymmetric waves (vertical asymmetric) the onshore velocity is as big as the offshore velocity and no net sediment transport is expected. ($\overline{u_{\infty}^3} = 0$). This is however not the cases as a net sediment transport can be generated even if $\overline{u_{\infty}^3} = 0$. This can be explained with the help of Figure 12.

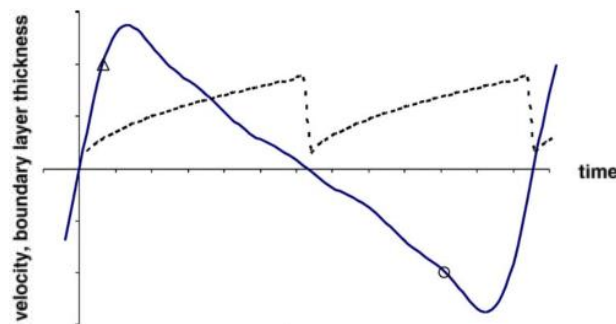


Figure 12: velocity and boundary layer in time. (Nielsen, 2006)

The graph shows an asymmetric wave with on the vertical axis the velocity (blue line) and boundary layer thickness (dotted line) and on the horizontal axis the time. The steepness of the blue line gives the acceleration $\frac{du}{dt}$. At the point indicated with a triangle the acceleration is higher than at the round indicator. The velocities, however, are the same at both points. The sediment transport that is occurring for asymmetric waves is caused by this difference in acceleration. So there is no velocity skewness but there is acceleration skewness in this case.

In addition the boundary layer thickness (Nielsen, 2002) investigated the thickness of the boundary layer. The boundary layer is thinner at the point indicated with a triangle than it is at the point with the round dot. The shear stress as function of the boundary layer thickness and the velocity is shown in Equation 3–21. (Nielsen, 2002). The velocity at both points is the same but the boundary layer at the round point is bigger, which gives according to the formula lower shear stresses for the round point and thus less sediment transport. The same mechanism occurs in the swash zone with plunging breakers, already explained in the chapter hydrodynamics.

$$\tau_b(t) = \rho v_t \frac{u_{\infty}(t)}{\delta(t)}$$

Equation 3–21

3.3.4 Bound long waves

The last term is generated by the bound long waves, which is less important for plunging waves. This is because the waves break close to shore so there is no time to develop the bound long waves. The boundary waves are created due wave height differences within a wave group. In Figure 13 both the bound as the free long wave are schematised. Offshore, the waves travel in a wave group which creates a water level difference between the highest waves and the lowest waves. To compensate this pressure difference a bound long wave is generated to compensate. The bound long wave is called bound because it is trapped within the wave group. The sediment stirred up with the high waves in the wave group corresponds with the offshore (trough) velocity of the bound long wave. The sediment stirred up with the lower waves corresponds with the onshore (crest) directed velocity of the bound long wave. Because less sediment is stirred up with the lower waves than with the higher waves a net sediment transport direction occurs. When the waves break the wave does not travel in a group anymore and the bound long wave becomes a free long wave. This changes the direction of the sediment transport as can be seen in Figure 13.

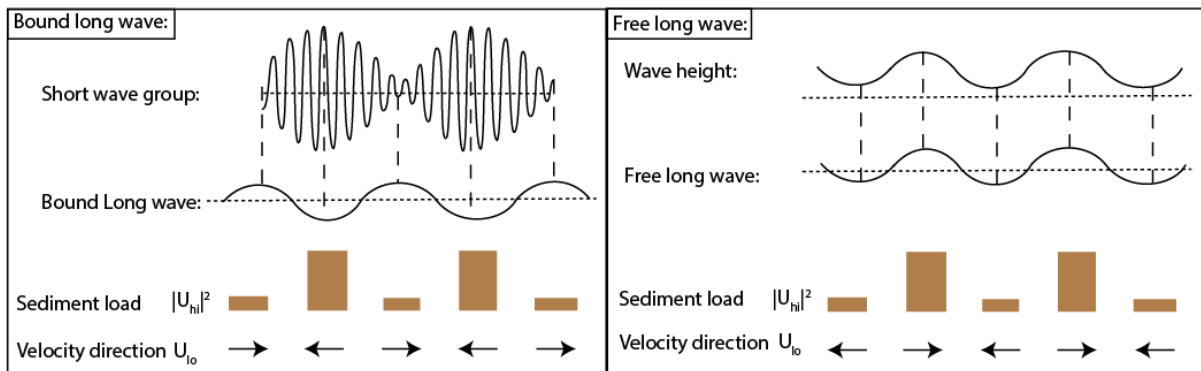


Figure 13: Bound long wave schematisation.

Appendix D

Damage Quantification Methods

APPENDIX D: DAMAGE QUANTIFICATION METHODS

4.1 Overview

There are several existing methods to quantify the amount of damage on a structure, usually depending on type of structure (statically stable or dynamically stable). These methods can be divided in the following subcategories

1. Counting the amount of stones displaced (damage level, N_{od} , or damage percentage)
2. Eroded area (damage level, S)
3. Erosion profile

There are currently no quantification methods which take the eroded depth into account. Most design methods use a double armour layer in which not many erosion is tolerated. The filter layer should always be protected with the top layer to ensure structure integrity.

4.2 Amount of stones displaced

HUDSON [1953] started counting the amount of stones that were displaced and compared it with the total amount of stones on the slope. When less than 1% of the stones were displaced, the no damage criterion was still valid.

Thompson and Shuttler went further and looked at strips with a width $9D_{50}$ along the slope. The amount of stones that were displaced in such area gives an indication of the damage according to Equation 4–1.

$$N_{\Delta} = \frac{A\rho_b 9D_{50}}{\rho_a D_{50}^3 \left(\frac{\pi}{6}\right)} \quad \text{Equation 4-1}$$

N_{Δ} = damage parameter
 A = erosion area in a cross section
 ρ_b = bulk denksity of material as laid on the slope
 ρ_a = mass density of stone

The damage level, N_{od} , is usually used to quantify the damage for concrete elements and for rock in a structure toe, The damage level is defined as the number of displaced units within a strip with a width of 1 unit diameter.

The damage classification with the amount of displaced stones is usually applied for statically stable structures and is therefore not further used in this thesis.

4.3 Eroded Area

4.3.1 Broderick 1983

Broderick went further with the equation of Thompson and Shuttler and tried to extract the bulk density out of the formula. He came with a dimensionless formula depending on the damage area divided by the stone diameter squared.

It has as advantage that it is only dependent on the D_{n50} and independent of the slope angle, length and height of the structure. The eroded area is defined as the amount of erosion around Mean Sea Level (MSL) divided by the stone size. This approach is adopted by VAN DER MEER, [1988].

$$S = \frac{A_e}{D_{n50}^2} \quad \text{Equation 4-2}$$

4.3.2 S factor WIT [2015]

WIT [2015] recognized in her thesis that the definition of S_d as given in the previous section gave very high damage values although the erosion depth was limited. The damage extended over a wide area along the slope, but the erosion depth was very limited. The erosion depth was lower than $1D_{n50}$. The gravel diameters were small because the mild slope resulted in stable structures. The large erosion area in combination with small gravel size resulted in the high damage levels. She concluded that S_d may not be the best way to classify damage on mild slopes. Therefore she proposed an alternative damage description for milder slopes. In the report of WIT [2015] an equation is formulated that describes the start of damage for mild slopes (Equation 4-3), which includes the effect of the erosion width (l_e) and erosion depth. Main reason for doing so was to achieve to get a better comparison of the Xbeach-G results with experiments from VAN DER MEER, [1988].

The damage description by WIT, [2015] is based on two assumptions.

1. The height over which the damage occurs is independent on the slope angle.
2. The threshold for damage is $1D_{n50}$.

In the left part of Table 4 the equilibrium wave height is determined. This is done by assuming a start slope and corresponding damage level that gives a statically stable structure. The tests of VAN DER MEER, [1988] gives an indication for these start values of the damage per slope, see chapter Design formula's. With the old damage formulation of VAN DER MEER, [1988] the eroded area, eroded length and eroded height is determined.

With the assumed threshold for the erosion depth (H_e), the new damage level is calculated for other slopes as is done in the right part of Table 4. The final formula is Equation 4-3 which gives for the chosen start slope and start damage level the extrapolation for the damage that occurs for milder slopes than these start values.

Table 4: Determining constant He and the new corresponding damage level.

Determining H_e		Determining S_{new}	
Damage	$S_{start} = \frac{A_{e\ start}}{D_{n50}^2}$	Eroded height	$H_e = \text{threshold of } 1D_{n50} \text{ (assumption)}$
Eroded area	$A_{e\ start} = S_{start} * D_{n50}^2$	Eroded length	$L_{e\ new} = \frac{H_e}{\sin(\alpha_{new})}$
Eroded length	$L_{e\ start} = \frac{A_{e\ start}}{D_{n50}}$	Eroded area	$A_{e\ new} = L_{e\ new} * D_{n50}$
Eroded height	$H_e = \sin(\alpha_{start}) * L_{e\ start}$		$A_{e\ new\ alt} = \int_0^\pi 2D_{n50} * \sin\left(\frac{\pi}{L_e} * \cot(\alpha)\right)$
		Damage	$S_{new} = \frac{A_{e\ new}}{D_{n50}^2}$

$$S_{new}(\alpha) = S_{start} * \frac{\sin(\alpha_{start})}{\sin(\alpha)} \quad \text{Equation 4-3}$$

The eroded area is marked because in the report of Wit [2015] the eroded area is calculated as a rectangle with an erosion depth of $1 D_{n50}$. More accurate would be to use a parabola to calculate the eroded area as is done in the optimised eroded area, marked with red in the table above. Figure 14 shows the eroded area of both methods.

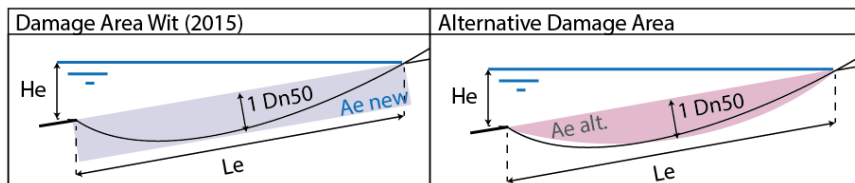


Figure 14: Damage levels for milder slopes; 2 approaches.

When the parabolic method is used to calculate the eroded area, the allowable damage levels are as expected lower than when a square is used. (Figure 14) In the right image the eroded area is calculated with the area under a sine curve and in the left image the eroded area is calculated as a square.

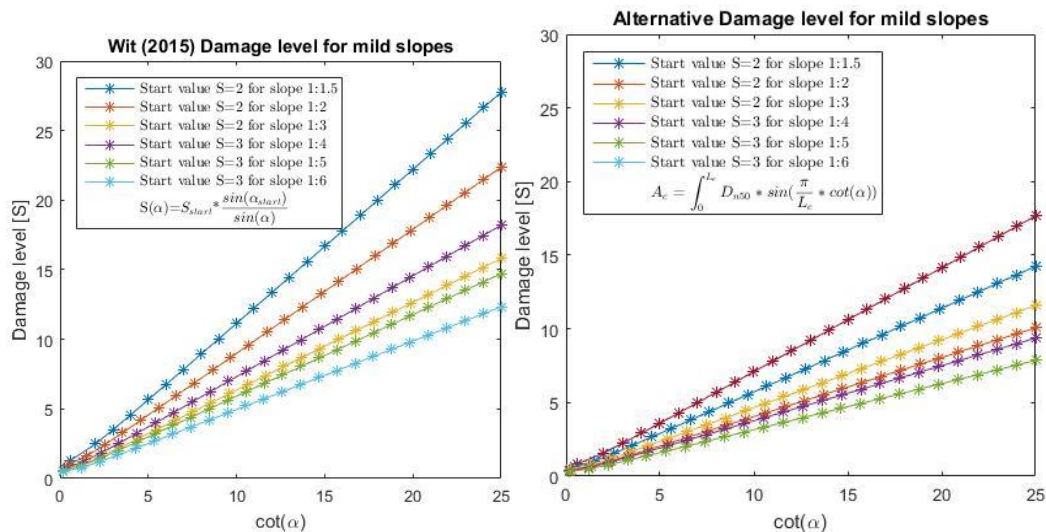


Figure 15: Damage level; Left: Method of Wit; Right: Alternative method

In this thesis is decided to not use the alternative damage description of Wit, [2015] but to use the eroded area and the damage level of VAN DER MEER, [1988]. This is done for better comparison between the XBeach-G results with the VAN DER MEER, [1988] experiments.

4.4 Erosion profile

4.4.1 Previous works

Dynamically stable structures usually consider a profile description rather than a damage approach. Especially for mild slopes, an approach with an erosion profile is interesting to consider. For sandy beaches this is often used but for rock protection this is not.

HIJUM AND PILARCZYK [1982] made a schematisation of the profile depending on the length, height and angle of the slope in combination with the angle of repose. The results were obtained with experimental tests on a 1:5 and 1:10 slope. Because the tests were also executed on a mild 1:10 slopes, the difference in profile between steep and mild slopes could be distinguished. For the mild slopes the formation of a step was introduced by HIJUM AND PILARCZYK [1982].

POWEL [1986] did research on shingle (type of gravel) beaches with a 1:5.5 slope and described the results with two power curves that describe the profile shape. Because the tests were only executed with monochromatic waves (waves with a single frequency) the data is often assumed not be sufficiently to use in practical situations with irregular waves.

4.4.2 VAN DER MEER, [1988]

This background information was the start point of VAN DER MEER, [1988] who also described the profile development for the experiments he executed. VAN DER MEER, [1988] clearly indicates the influence of the initial slope on the profile development. This is described with the stability parameter. For larger stability parameters, the initial profile has no influence and for lower stability numbers it has big influence. The used VAN DER MEER, [1988] experimental tests have an stability number of 1-2.5 for the statically tests and 10 for the dynamic tests.

$\frac{H_s}{\Delta D_{n50}} < 10$ The initial profile has a large influence on the profile.

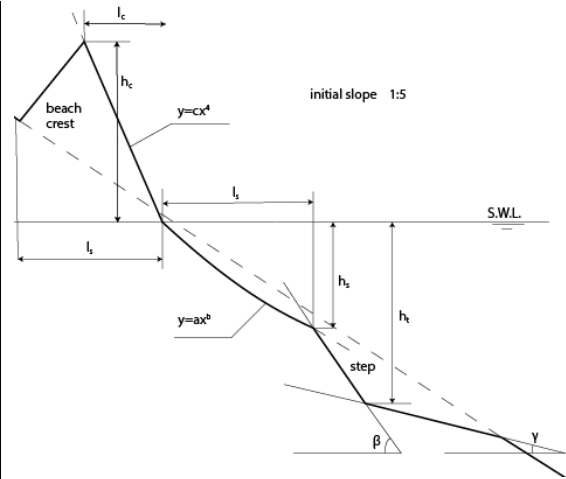
$\frac{H_s}{\Delta D_{n50}} = 10 - 15$ The initial profile has some influence on the profile.

$\frac{H_s}{\Delta D_{n50}} > 15$ The initial profile has no influence on the profile.

The dynamic profile he defined depends on the following parameters and relationships, as can be seen in Table 5.

Table 5: Relationships between parameters according to VAN DER MEER, [1988].

Run-up Length	$l_r = \left(\frac{H_0 T_0}{2.9}\right)^{\frac{1}{1.3}} D_{n50} N^{0.05}$
Crest height	$h_c = 0.089 s_m^{-0.5} H_s N^{0.15}$
Crest Length	$l_c = \left(\frac{H_0 T_0}{21}\right)^{\frac{1}{1.2}} D_{n50} N^{0.12}$
Step height	$h_s = 0.22 s_m^{-0.3} H_s N^{0.07}$
Step Length	$l_s = \left(\frac{H_0 T_0}{3.8}\right)^{\frac{1}{1.3}} D_{n50} N^{0.07}$
Transition height	$h_t = 0.73 s_m^{-0.2} H_s N^{0.04}$
Angles (β & γ)	$\tan(\beta) = 1.1 \tan(\alpha)^{1-0.45} e^{-\frac{500}{N}}$ $\tan(\gamma) = 0.5 \tan(\alpha)$
Power function between h_c and h_s	$y = a4 x^{0.83}$ Below SWL $y = a5 (-x)^{1.15}$ Above SWL * The constants A4 and A5 are determined with the values of $h_c, l_c, h_s,$ and l_s .



4.4.3 Type of profiles

The research of WIT [2015] and VAN DER MEER, [1988] clearly indicates that the profiles shape can change. A distinction is made between a bar profile and a crest profile. The theory is that the profile adapts to the ratio between the forcing and stabilizing parameters. The forcing parameters are the wave height and period and the stabilizing parameters are the stone weight and the slope angle.

VAN DER MEER, [1988] described the influence of the initial slope. He changed the initial slope and kept the rest of the parameters the same. The profile tends to go to a standard profile marked with black as can be seen in Figure 16. When the initial profile is steeper (case 1:1.5 initial slope) than the standard profile erosion becomes more and it forms a crest profile. When the initial slope becomes smaller (case 1:5 slope) the profile becomes a bar profile.

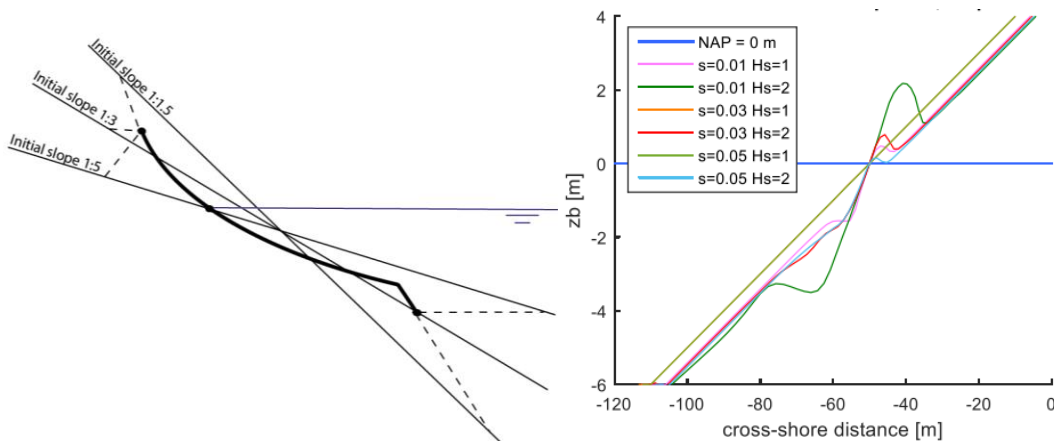


Figure 16: Left: Influence initial profile VAN DER MEER, [1988]; Right: Influence hydr. Forcing WIT [2015]

WIT [2015]) confirmed these results by redoing the tests in Xbeach-G. She investigated it by keeping the stabilizing parameters the same and changed the hydrodynamic forcing. It is clear from her results that the equilibrium profile tends to go to the angle of repose of the gravel material, as all the profile shapes cross the initial slope under the same angle. See Figure 16.

Appendix E

*Reproduced VAN DER MEER, [1988]
Experiments + Slope Effect*

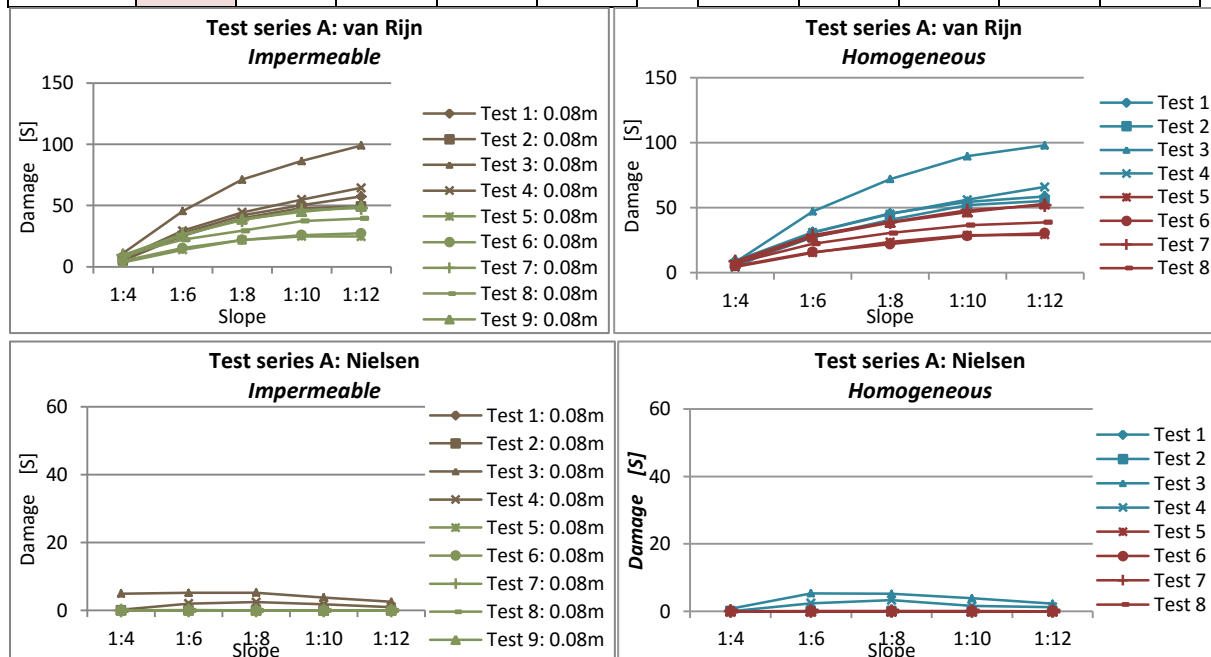
APPENDIX E: REPRODUCED VAN DER MEER, [1988] EXPERIMENTS +SLOPE EFFECT

5.1 Damage number

5.1.1 Test series A

Damage										
VAN RIJN [2007]	Impermeable $t_{layer} = 0.08\text{ m}$					Homogeneous				
	1:4	1:6	1:8	1:10	1:12	1:4	1:6	1:8	1:10	1:12
Test 1	8.78	27.47	42.00	50.36	57.40	9.32	31.14	45.60	54.44	58.72
Test 2	5.22	25.21	39.66	48.07	49.18	6.35	27.10	40.67	52.06	55.24
Test 3	11.19	45.42	71.22	86.37	99.00	8.34	47.19	72.09	89.66	98.03
Test 4	7.31	29.43	44.46	54.90	64.41	4.25	30.97	45.05	56.21	65.99
Test 5	3.51	13.85	21.83	24.87	24.70	4.62	15.46	23.69	28.89	29.16
Test 6	4.94	15.30	22.02	25.89	27.39	5.23	15.97	21.95	28.35	30.43
Test 7	9.57	26.69	37.97	46.29	47.95	8.92	28.99	38.93	48.09	51.92
Test 8	9.64	22.15	29.41	37.42	39.51	7.54	22.34	30.59	36.60	38.87
Test 9	7.70	25.70	38.76	45.00	49.36	7.19	27.61	38.50	46.65	52.97

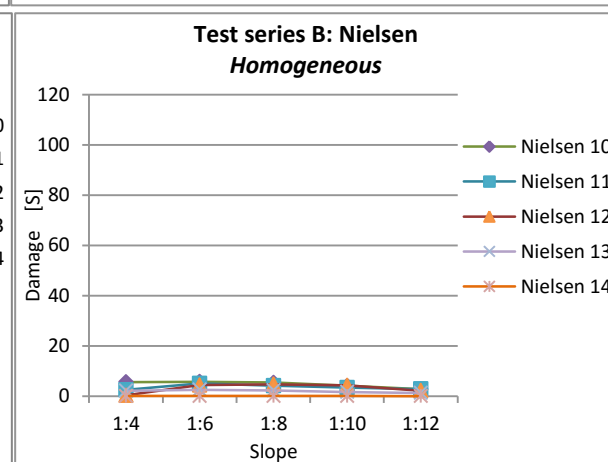
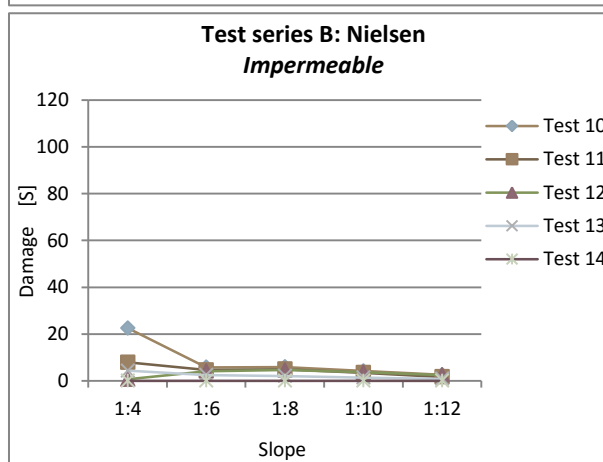
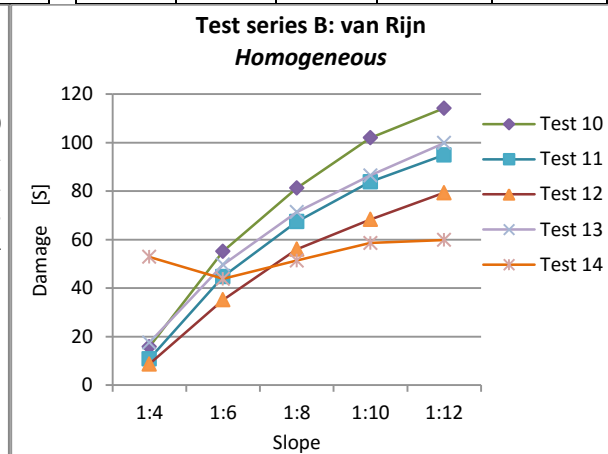
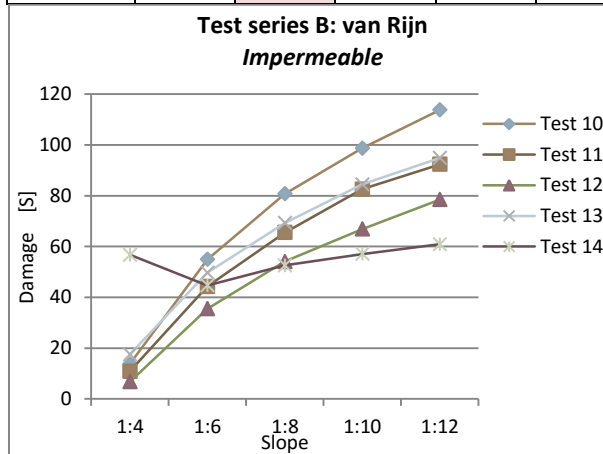
NIELSEN [2006]	Impermeable $t_{layer} = 0.08\text{ m}$					Homogeneous				
	1:4	1:6	1:8	1:10	1:12	1:4	1:6	1:8	1:10	1:12
Test 1	0	0	0	0	0	0	0	0	0	0
Test 2	0	0	0	0	0	0	0	0	0	0
Test 3	4.94	5.17	5.23	3.81	2.53	0.77	5.32	5.21	3.86	2.23
Test 4	0.19	2.03	2.45	1.78	0.98	0.004	2.40	3.28	1.58	1.25
Test 5	0	0	0	0	0	0	0	0	0	0
Test 6	0	0	0	0	0	0	0	0	0	0
Test 7	0.01	0	0	0	0	0	0	0	0	0
Test 8	0	0	0	0	0	0	0	0	0	0
Test 9	0.05	0.07	0.06	0.01	0.03	0	0.08	0.06	0.05	0.02



5.1.2 Test series B

Damage										
VAN RIJN [2007]	Impermeable $t_{layer} = 0.08 m$					Homogeneous				
	1:4	1:6	1:8	1:10	1:12	1:4	1:6	1:8	1:10	1:12
Test 10	13.77	54.88	80.76	98.69	113.76	15.85	55.17	81.22	101.99	114.17
Test 11	10.85	44.27	65.50	82.57	92.34	10.83	44.71	67.40	83.81	94.90
Test 12	6.78	35.50	54.10	66.85	78.46	8.72	35.14	56.03	68.27	79.32
Test 13	17.54	49.66	69.26	84.43	94.86	17.56	49.70	71.32	86.45	99.84
Test 14	56.72	44.66	52.54	57.03	60.85	52.84	43.82	51.33	58.59	59.85

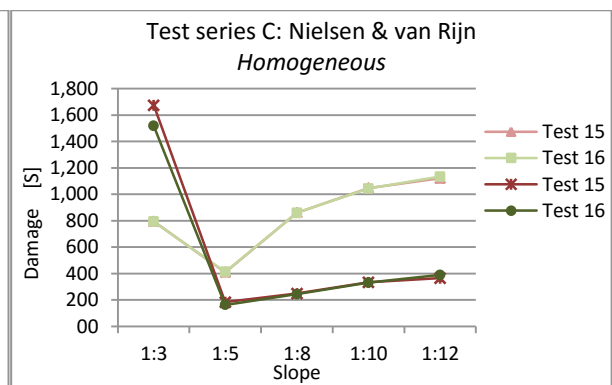
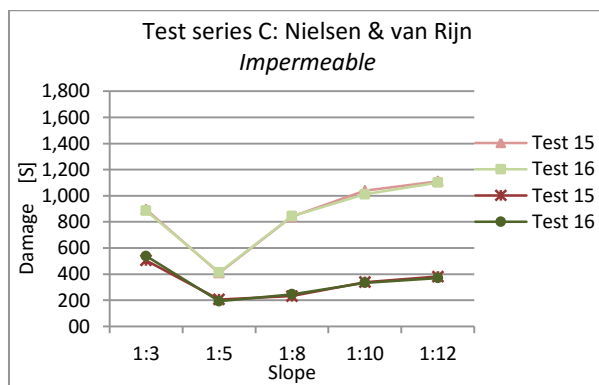
NIELSEN [2006]	Impermeable $t_{layer} = 0.08 m$					Homogeneous				
	1:4	1:6	1:8	1:10	1:12	1:4	1:6	1:8	1:10	1:12
Test 10	22.52	5.80	5.89	4.17	2.58	5.56	5.69	5.40	4.12	2.74
Test 11	7.86	4.57	4.94	3.43	1.65	2.47	5.00	4.12	3.34	2.78
Test 12	0.66	4.12	4.60	3.66	2.49	0.26	4.34	4.70	4.21	2.11
Test 13	4.33	2.45	2.05	1.39	0.87	2.14	2.52	2.29	1.64	1.23
Test 14	0.02	0.01	0.01	0.02	0.01	0.02	0.03	0.01	0.015	0.001



5.1.3 Test series C

Damage										
VAN RIJN [2007]	Impermeable $t_{layer} = 0.08 m$					Homogeneous				
	1:3	1:5	1:8	1:10	1:12	1:3	1:5	1:8	1:10	1:12
Test 15	894.7	410.3	839.9	1037.9	1110.3	794.8	410.1	860.1	1047.3	1121.6
Test 16	884.7	412.8	843.9	1011.6	1101.0	792.8	412.3	859.7	1043.4	1133.8

NIELSEN [2006]	Impermeable $t_{layer} = 0.08 m$					Homogeneous				
	1:3	1:5	1:8	1:10	1:12	1:3	1:5	1:8	1:10	1:12
Test 15	505.0	205.8	231.8	338.5	381.2	1673.9	183.6	248.8	333.9	365.1
Test 16	538.0	192.3	245.4	333.8	370.6	1517.6	163.1	244.2	331.1	389.9

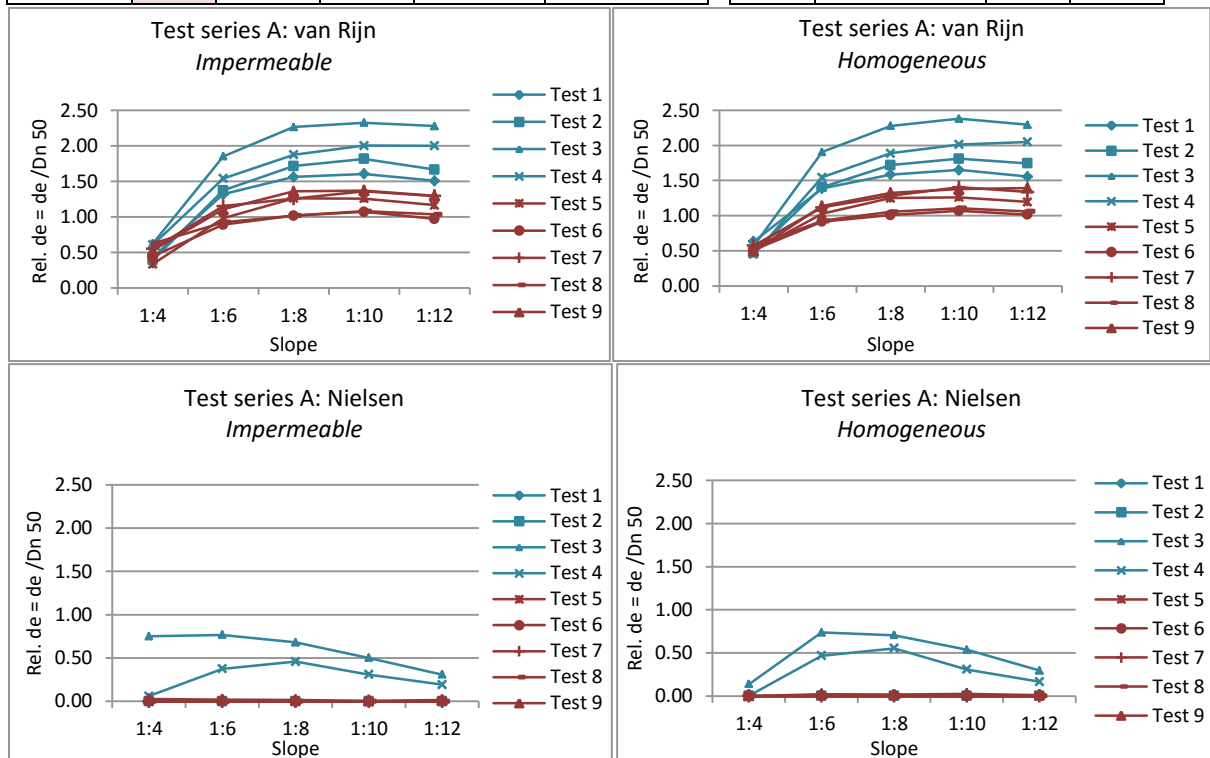


5.2 Relative Erosion Depth

5.2.1 Test series A

Rel. erosion depth $\frac{d_e}{D_{n50}}$										
VAN RIJN [2007]	Impermeable $t_{layer} = 0.08 m$					homogeneous				
	1:4	1:6	1:8	1:10	1:12	1:4	1:6	1:8	1:10	1:12
Test 1	0.43	1.32	1.56	1.60	1.51	0.63	1.39	1.59	1.65	1.55
Test 2	0.39	1.37	1.71	1.82	1.66	0.48	1.41	1.72	1.81	1.74
Test 3	0.63	1.85	2.26	2.33	2.28	0.57	1.91	2.28	2.38	2.29
Test 4	0.61	1.54	1.88	2.00	2.00	0.45	1.55	1.89	2.01	2.05
Test 5	0.34	0.98	1.26	1.26	1.16	0.50	1.03	1.25	1.26	1.20
Test 6	0.44	0.89	1.02	1.07	0.97	0.51	0.91	1.01	1.07	1.02
Test 7	0.55	1.15	1.26	1.36	1.29	0.57	1.12	1.28	1.41	1.34
Test 8	0.63	0.92	1.02	1.08	1.03	0.57	0.93	1.05	1.11	1.06
Test 9	0.53	1.11	1.36	1.37	1.30	0.50	1.14	1.33	1.38	1.39

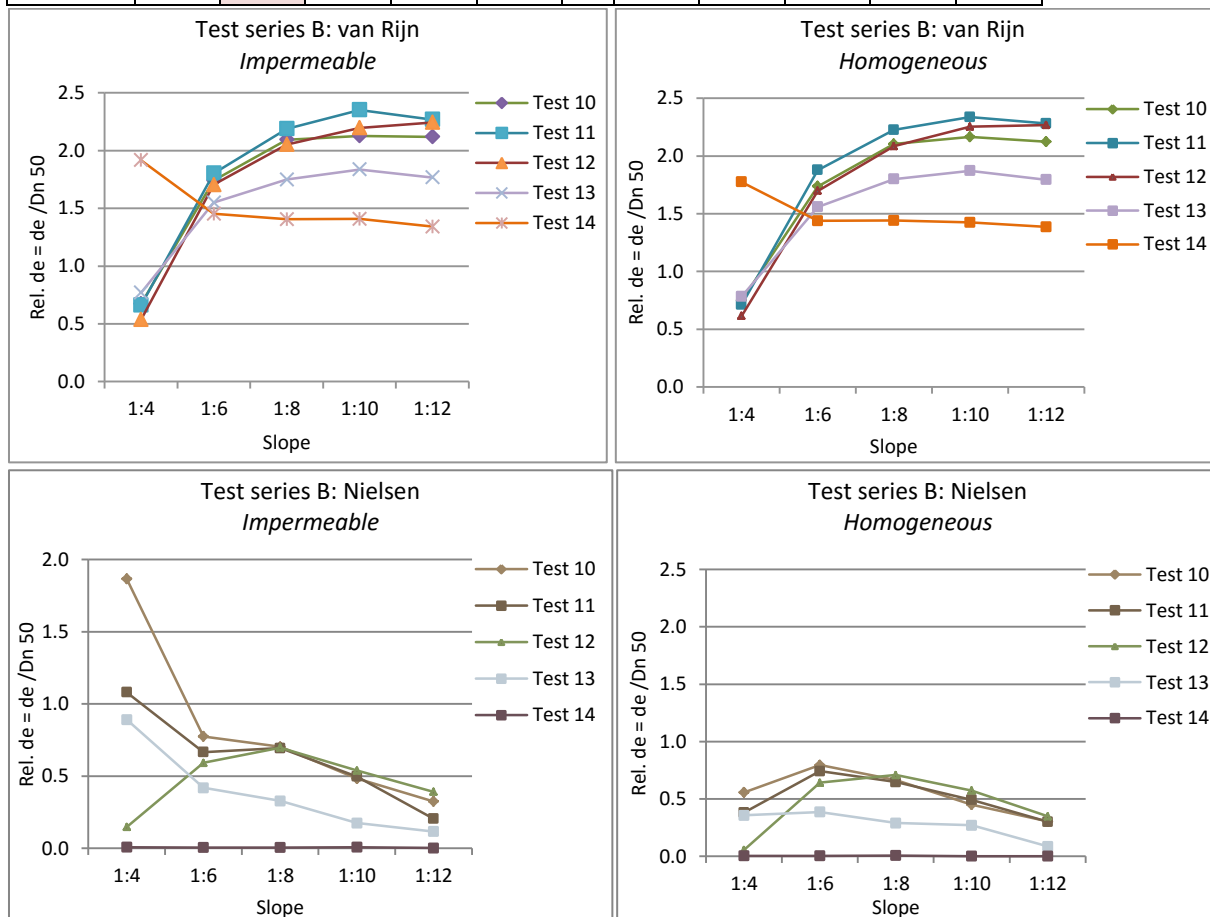
NIELSEN [2006]	Impermeable $t_{layer} = 0.08 m$					homogeneous				
	1:4	1:6	1:8	1:10	1:12	1:4	1:6	1:8	1:10	1:12
Test 1	0	0	0	0	0	0	0	0	0	0
Test 2	0	0	0	0	0	0	0	0	0	0
Test 3	0.75	0.77	0.68	0.50	0.31	0.14	0.74	0.71	0.54	0.29
Test 4	0.06	0.38	0.46	0.31	0.19	0.00	0.47	0.55	0.31	0.16
Test 5	0	0	0	0	0	0	0	0	0	0
Test 6	0	0	0	0	0	0	0	0	0	0
Test 7	0	0	0	0	0	0	0	0	0	0
Test 8	0	0	0	0	0	0	0	0	0	0
Test 9	0.03	0.02	0.01	0.00	0.01	0.00	0.02	0.02	0.03	0.01



5.2.2 Test series B

Rel. erosion depth $\frac{d_e}{D_{n50}}$										
VAN RIJN [2007]	Impermeable $t_{layer} = 0.08 m$					homogeneous				
	1:4	1:6	1:8	1:10	1:12	1:4	1:6	1:8	1:10	1:12
Test 10	0.67	1.74	2.09	2.13	2.12	0.75	1.74	2.10	2.16	2.12
Test 11	0.66	1.80	2.19	2.35	2.27	0.71	1.88	2.23	2.34	2.28
Test 12	0.54	1.71	2.05	2.20	2.24	0.61	1.70	2.08	2.25	2.27
Test 13	0.77	1.55	1.75	1.84	1.77	0.78	1.56	1.80	1.87	1.79
Test 14	1.92	1.45	1.41	1.41	1.34	1.78	1.44	1.44	1.43	1.39

NIELSEN [2006]	Impermeable $t_{layer} = 0.08 m$					homogeneous				
	1:4	1:6	1:8	1:10	1:12	1:4	1:6	1:8	1:10	1:12
Test 10	1.87	0.78	0.70	0.48	0.33	0.56	0.79	0.66	0.45	0.30
Test 11	1.08	0.67	0.69	0.50	0.21	0.38	0.74	0.65	0.49	0.30
Test 12	0.15	0.59	0.70	0.54	0.39	0.05	0.64	0.71	0.57	0.35
Test 13	0.89	0.42	0.33	0.18	0.12	0.36	0.39	0.29	0.27	0.09
Test 14	0.01	0.01	0.01	0.01	0.00	0.00	0.00	0.01	0.00	0.00



5.2.3 Test series C

Relative Erosion depth $\frac{d_e}{D_{n50}}$										
VAN RIJN [2007]	Impermeable $t_{layer} = 0.08 m$					Homogeneous				
	1:3	1:5	1:8	1:10	1:12	1:3	1:5	1:8	1:10	1:12
Test 15	11.43	3.97	5.95	6.35	5.91	10.89	4.17	6.19	6.38	6.19
Test 16	11.09	4.03	5.99	6.26	5.94	10.69	4.28	6.16	6.46	6.12

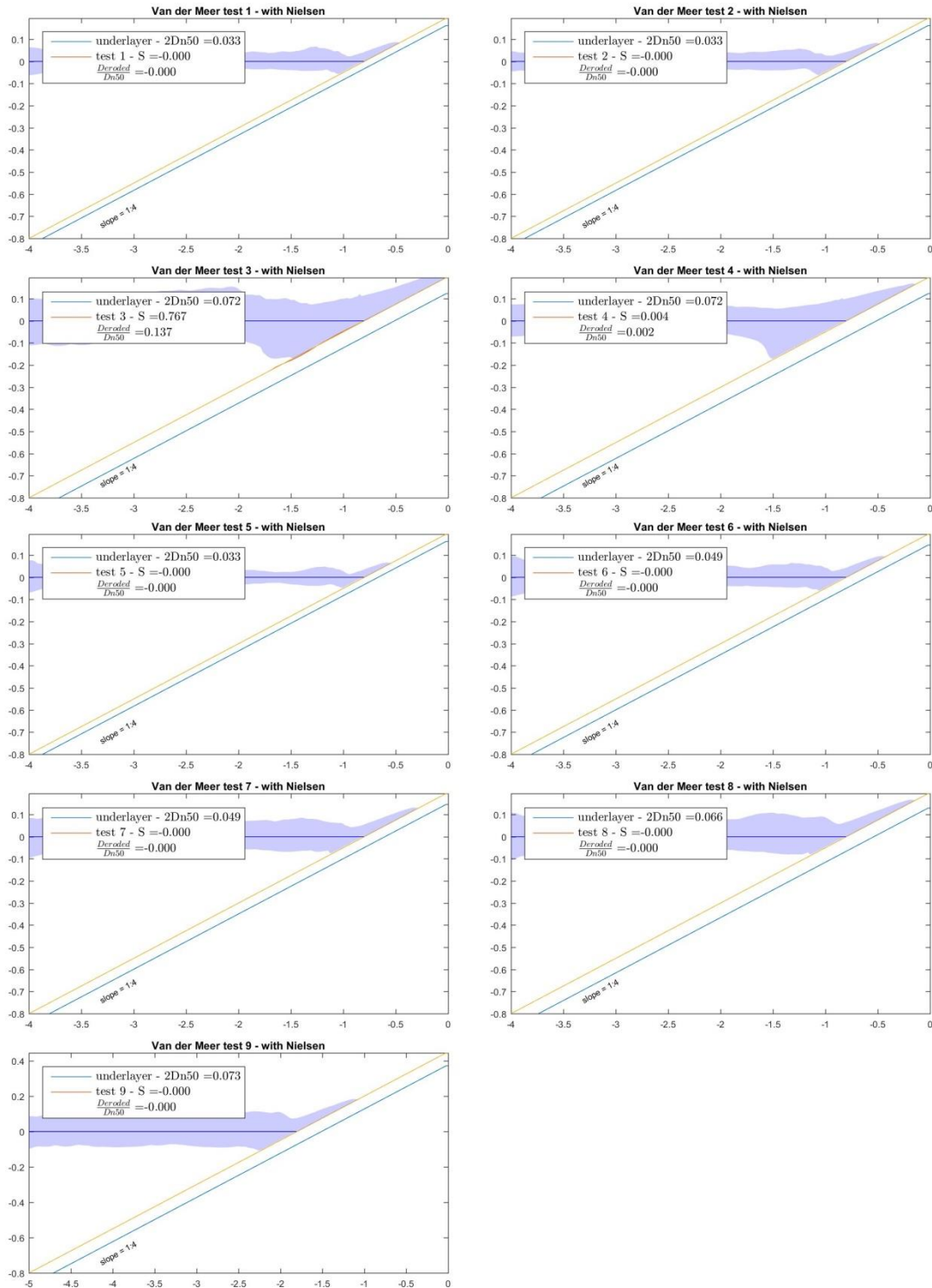
NIELSEN [2006]	Impermeable $t_{layer} = 0.08 m$					Homogeneous				
	1:3	1:5	1:8	1:10	1:12	1:3	1:5	1:8	1:10	1:12
Test 15	5.76	2.49	2.51	3.55	4.25	19.18	2.40	2.18	3.47	4.01
Test 16	6.49	2.56	2.77	3.85	4.38	16.41	2.40	2.61	3.45	4.38



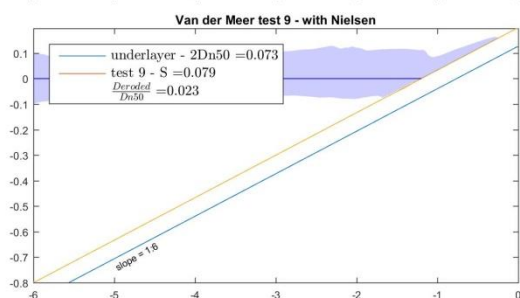
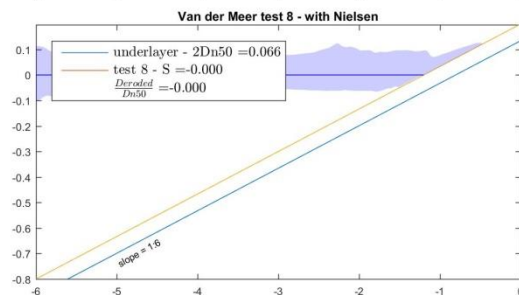
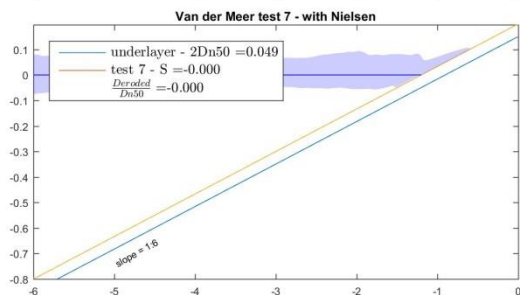
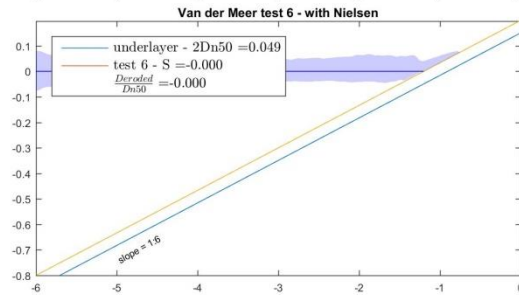
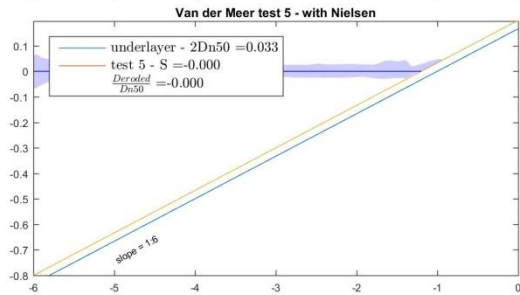
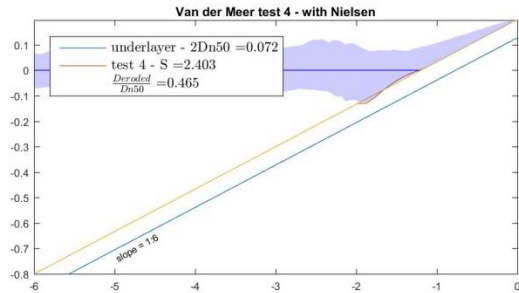
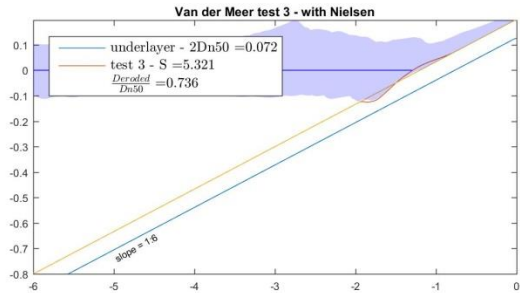
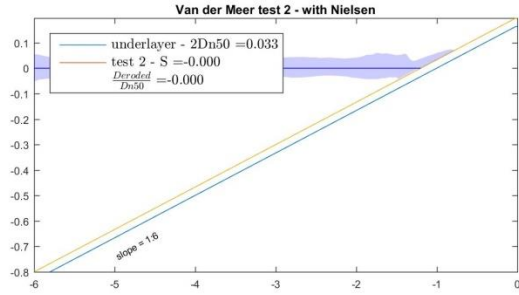
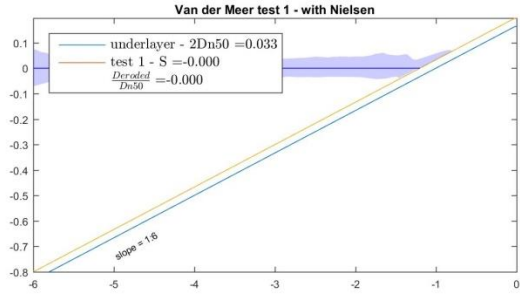
5.3 Formed erosion profile

5.3.1 Test series A

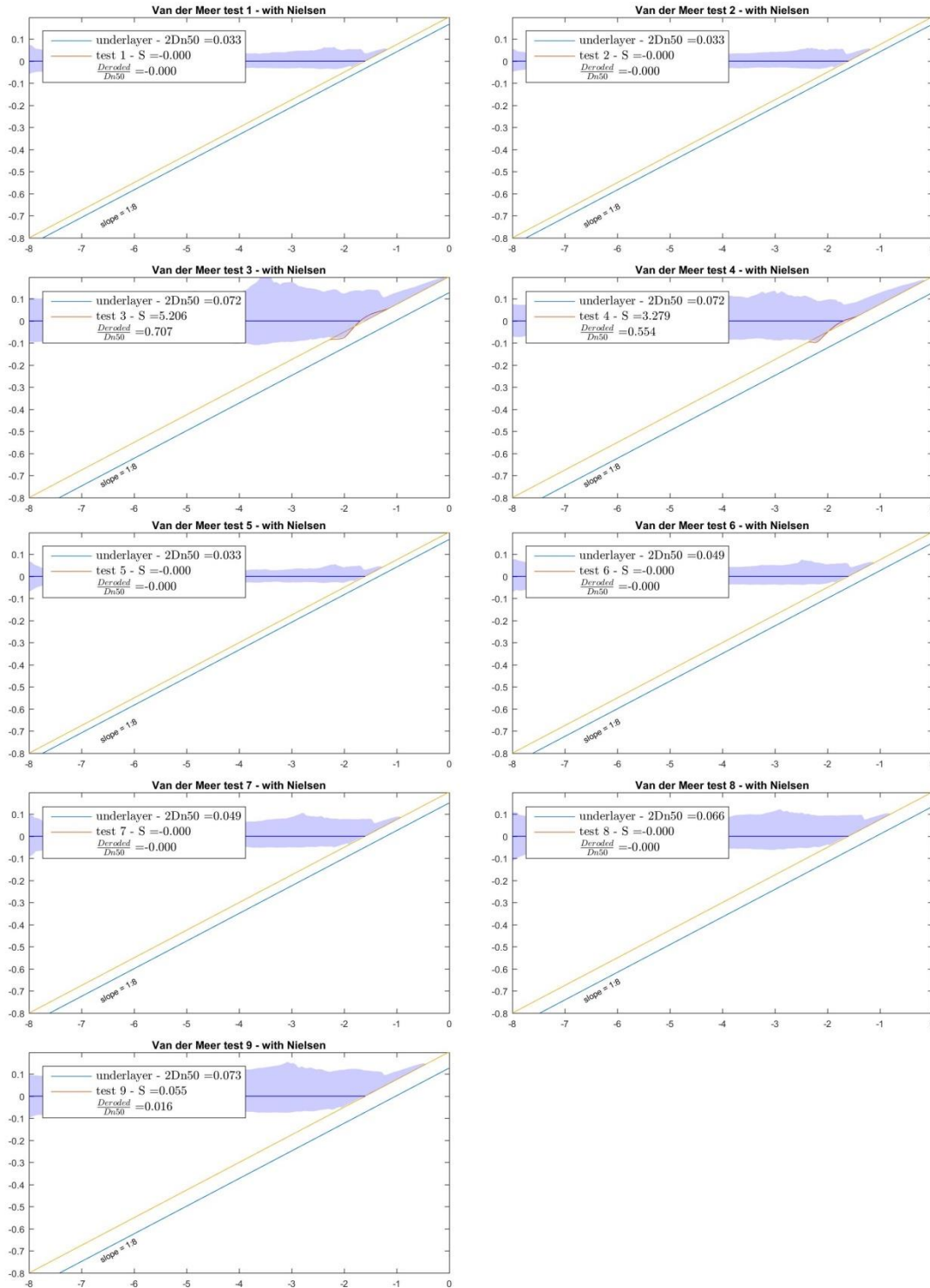
NIELSEN [2006] 1:4 slope



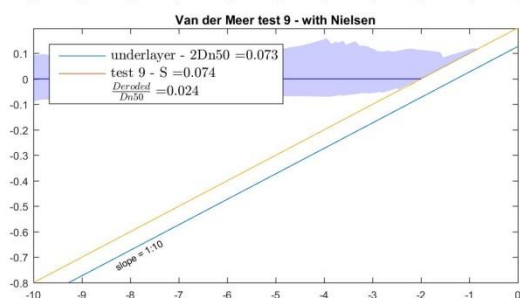
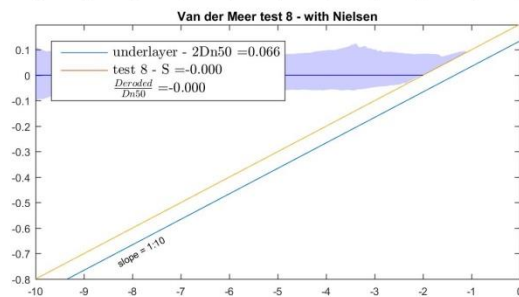
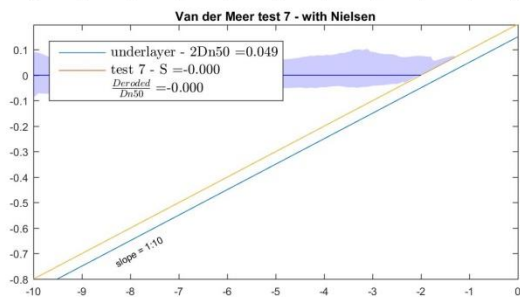
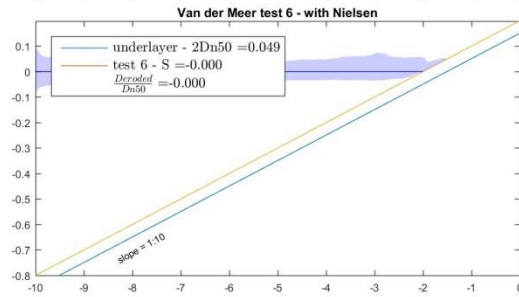
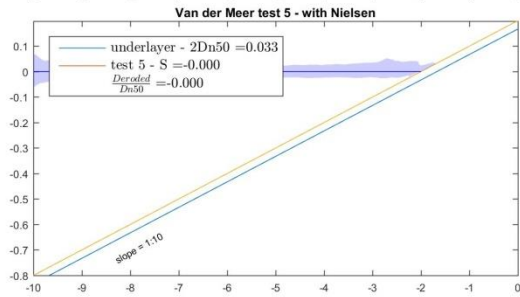
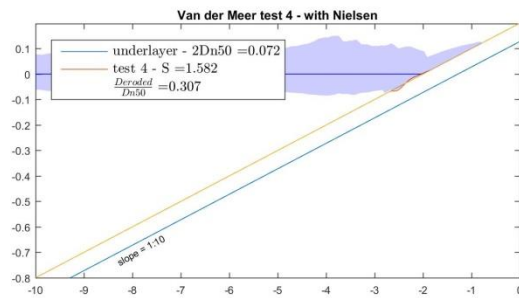
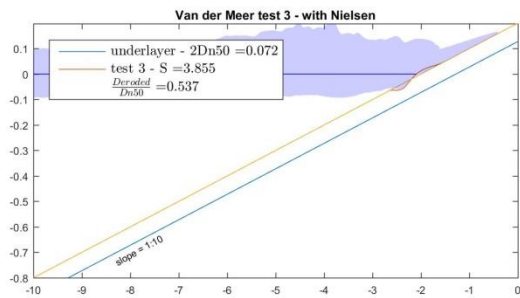
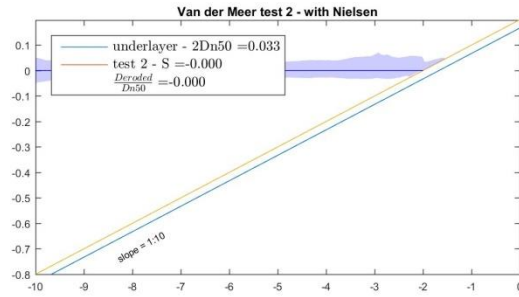
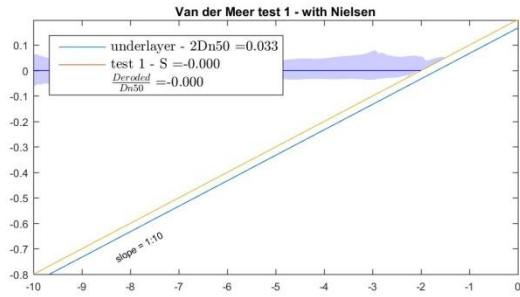
NIELSEN [2006] 1:6 slope



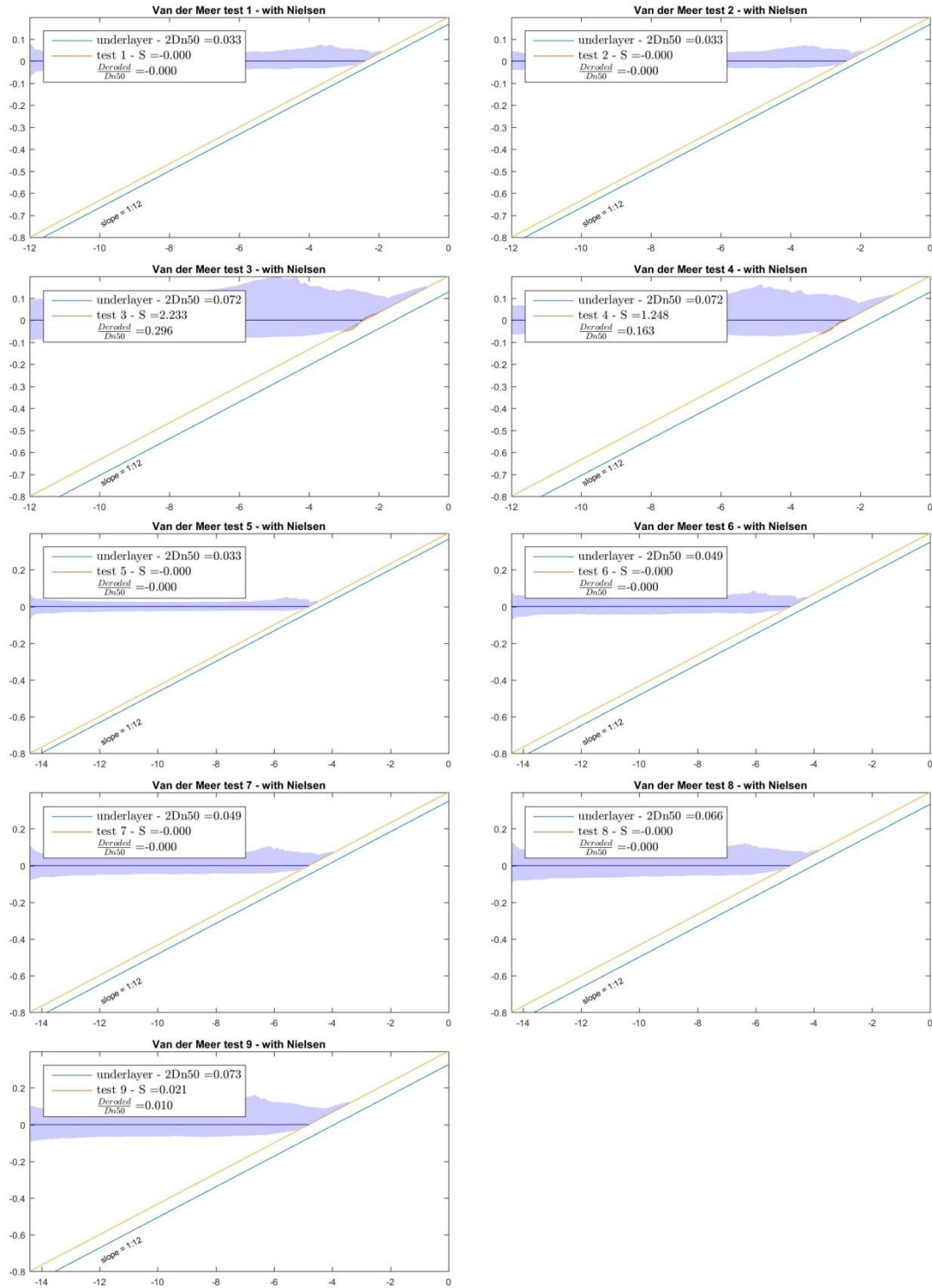
NIELSEN [2006] 1:8 slope



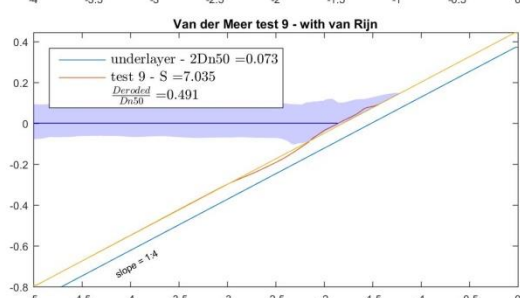
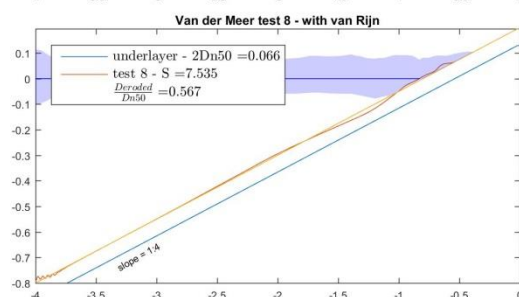
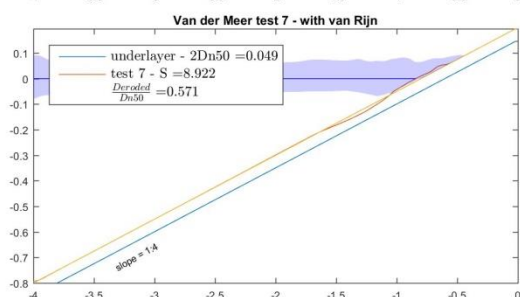
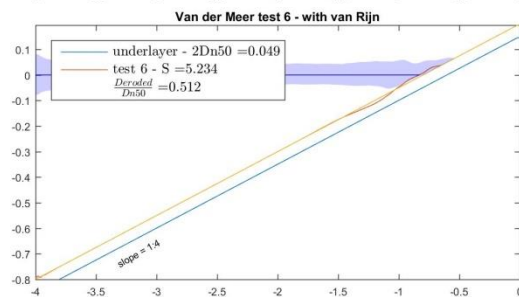
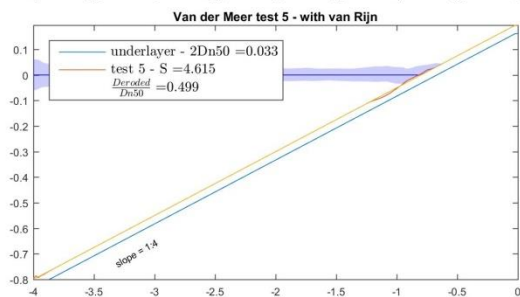
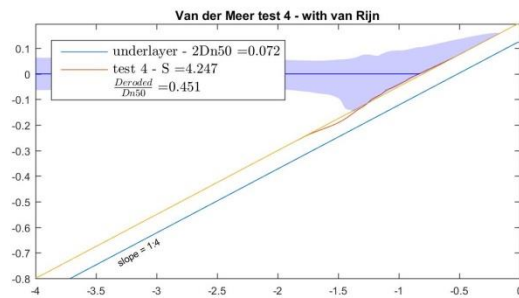
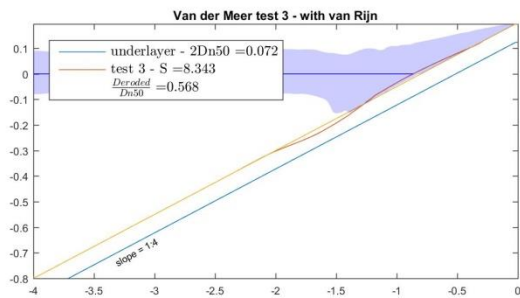
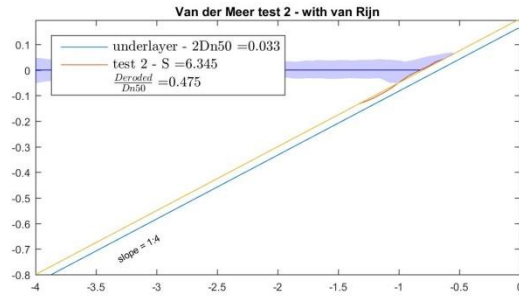
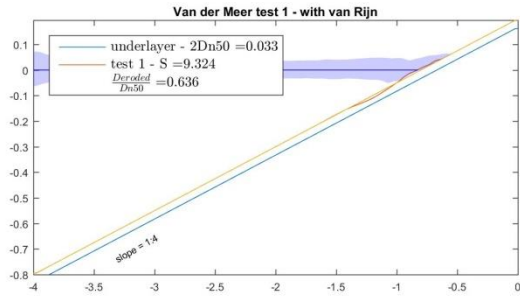
NIELSEN [2006] 1:10 slope



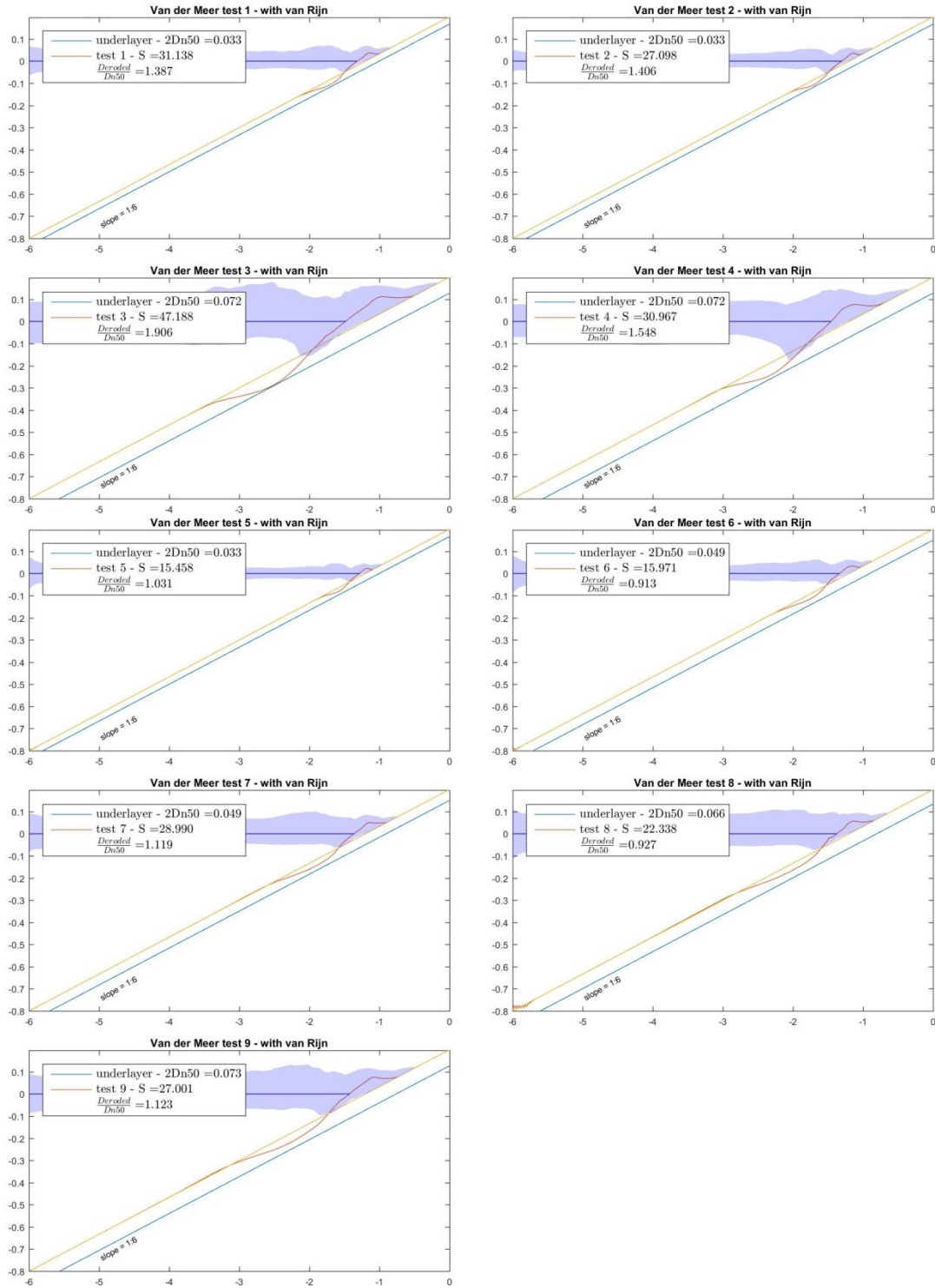
NIELSEN [2006] 1:12 slope



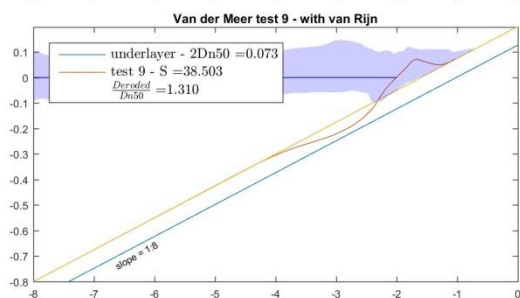
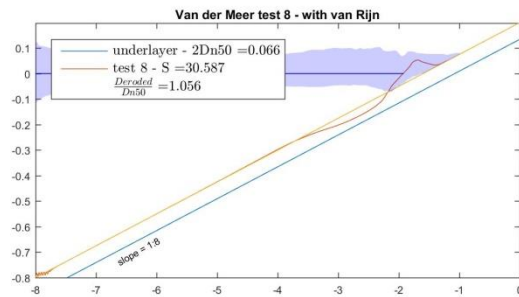
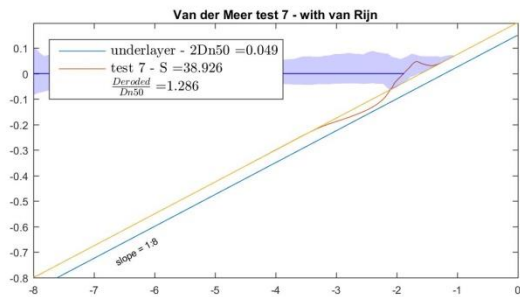
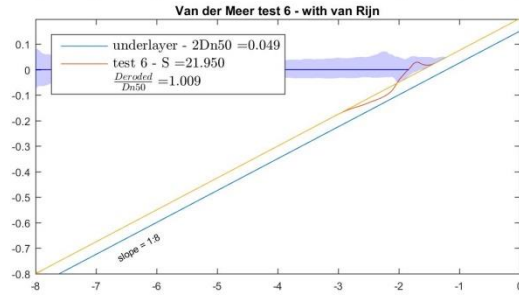
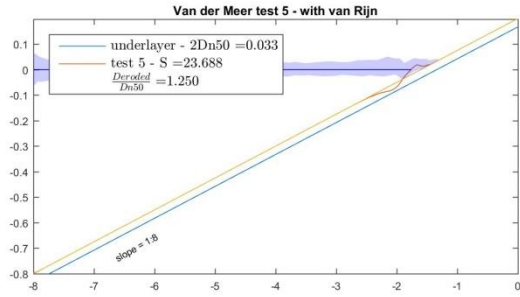
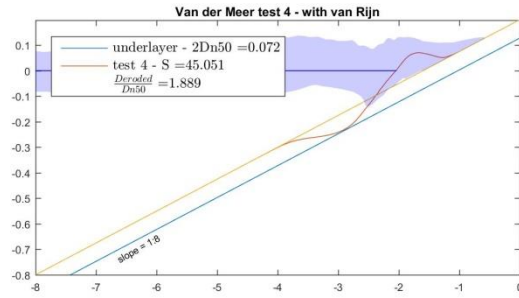
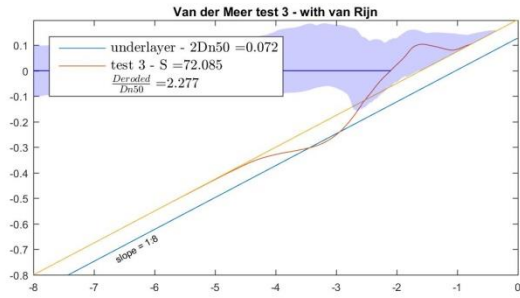
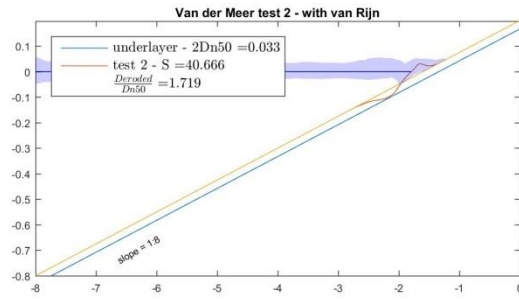
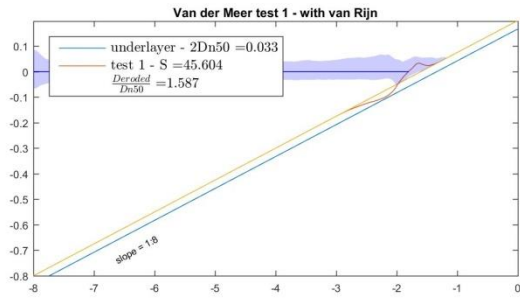
VAN RIJN [2007] 1:4 slope



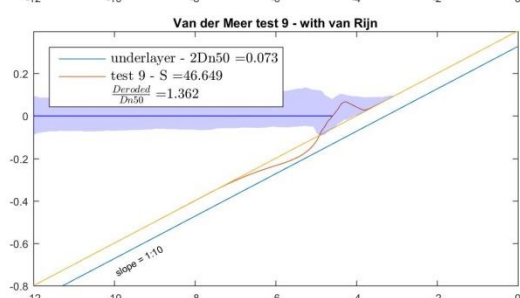
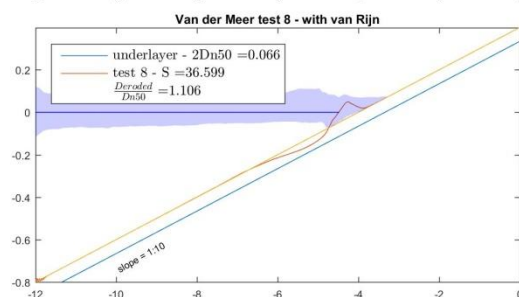
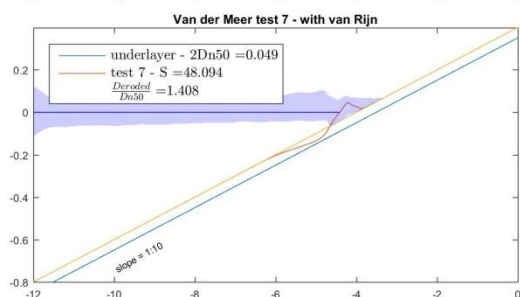
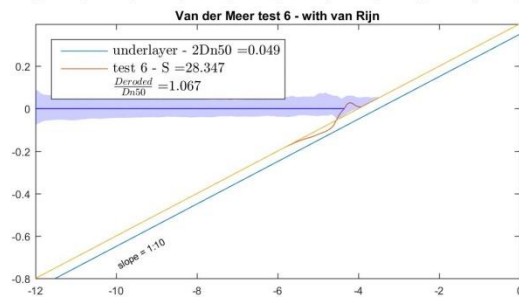
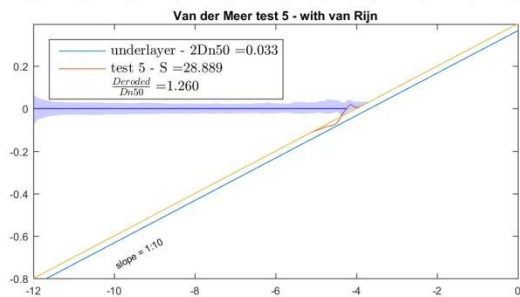
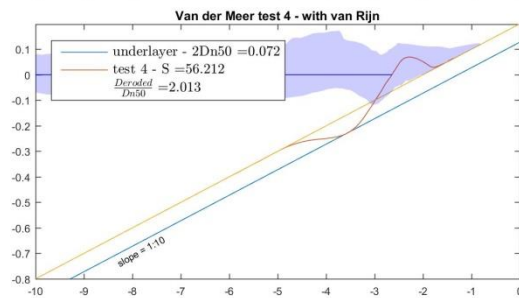
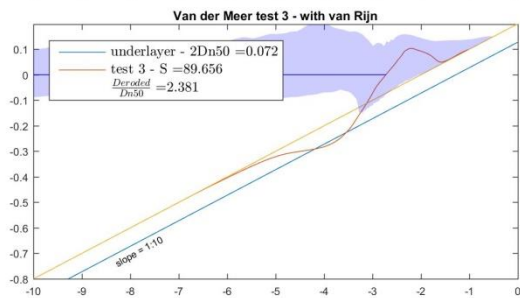
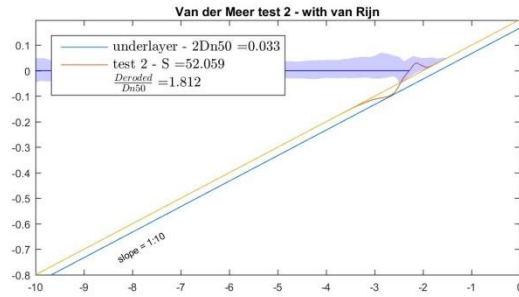
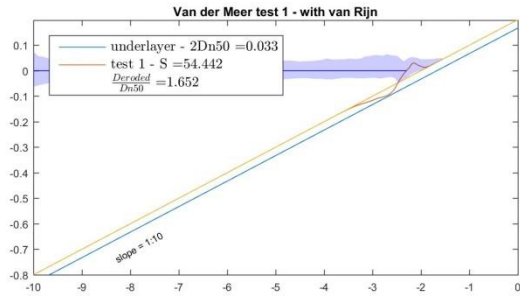
VAN RIJN [2007] 1:6 slope



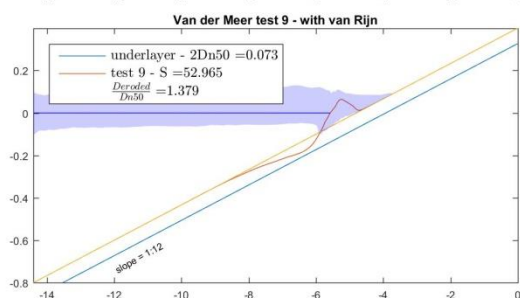
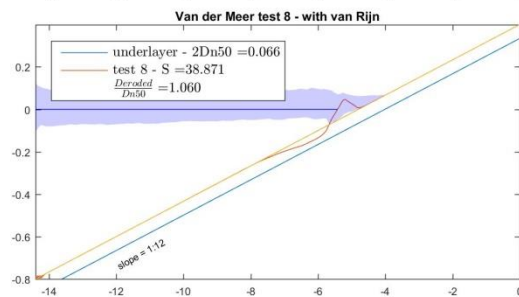
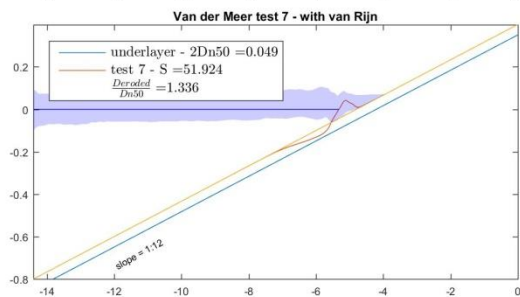
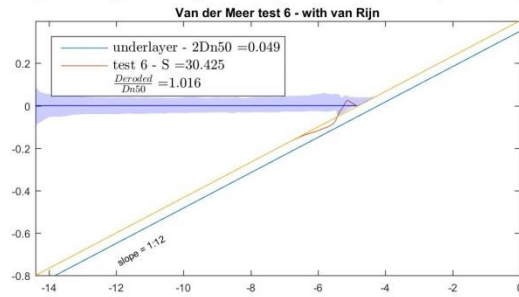
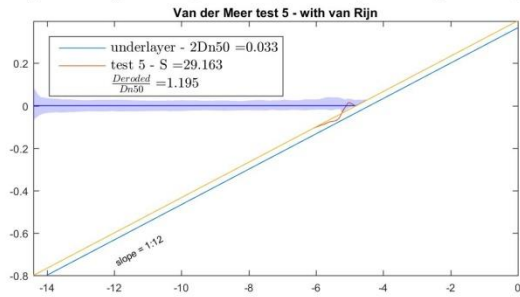
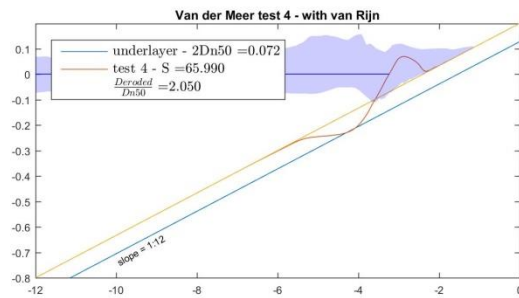
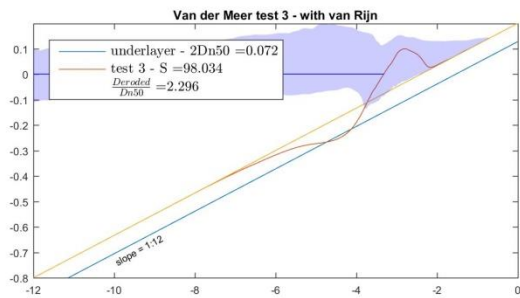
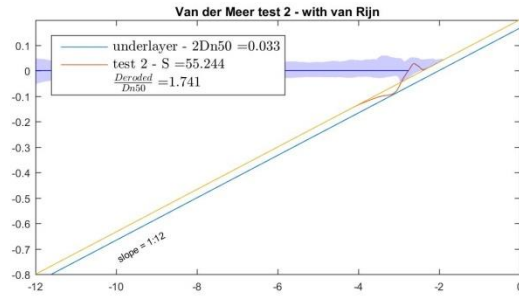
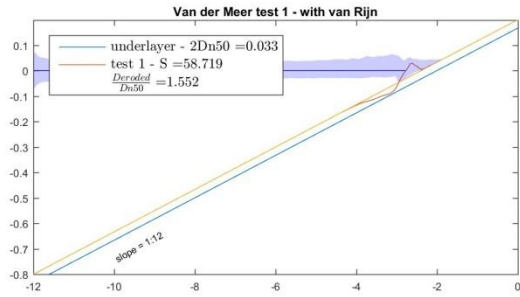
VAN RIJN [2007] 1:8 slope



VAN RIJN [2007] 1:10 slope

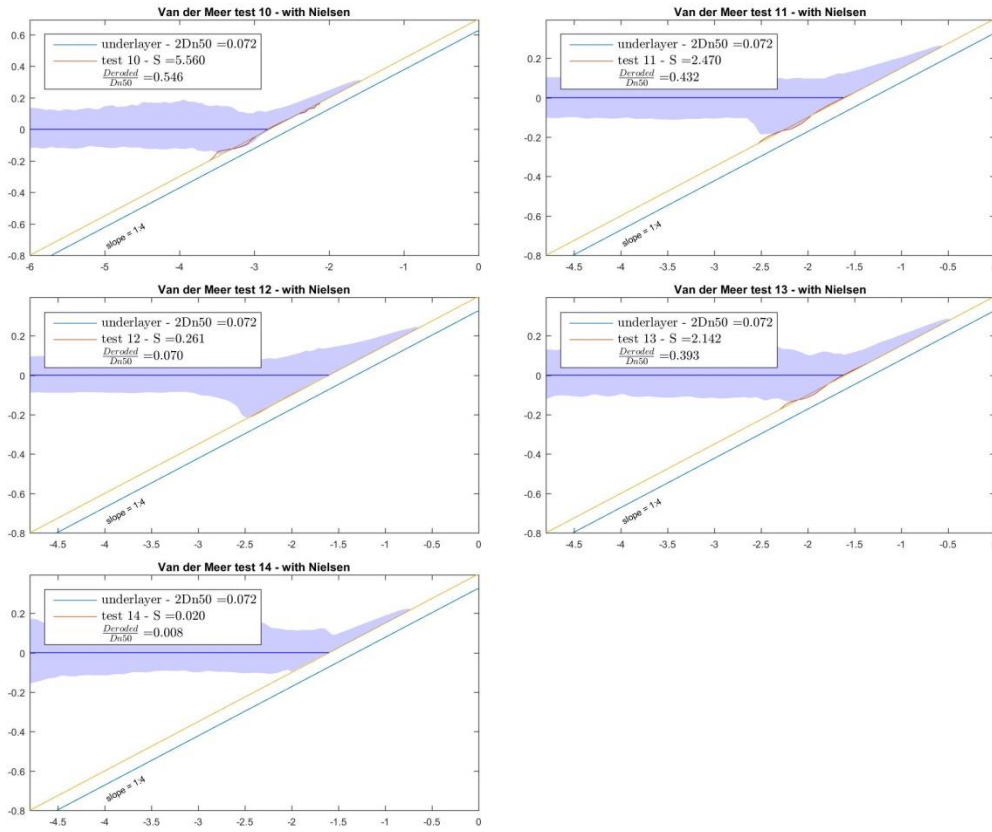


VAN RIJN [2007] 1:12 slope

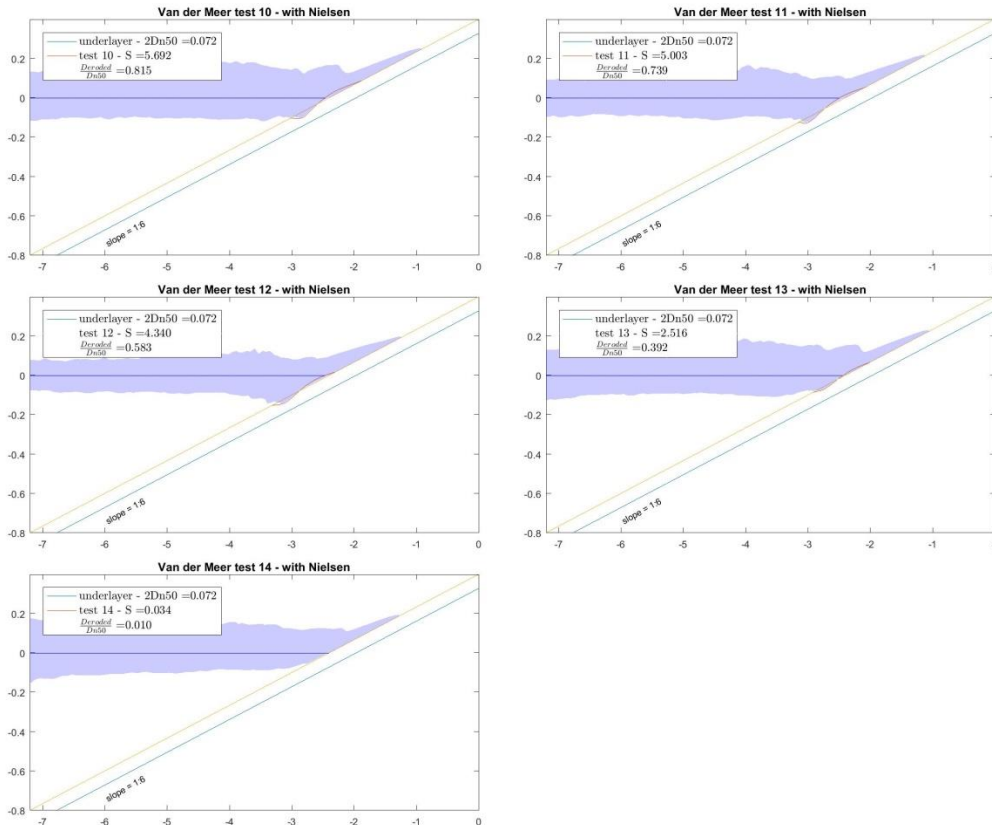


5.3.2 Test series B

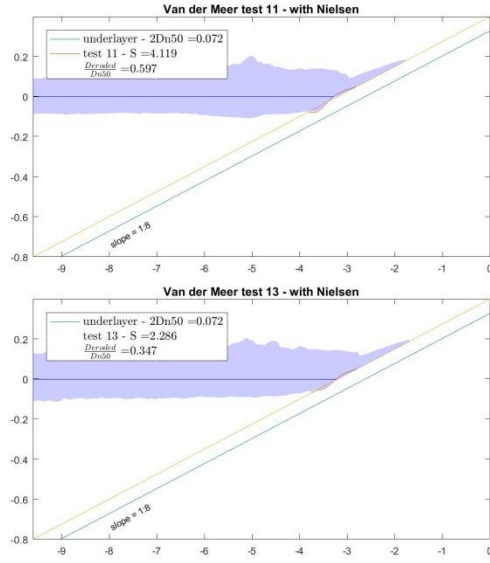
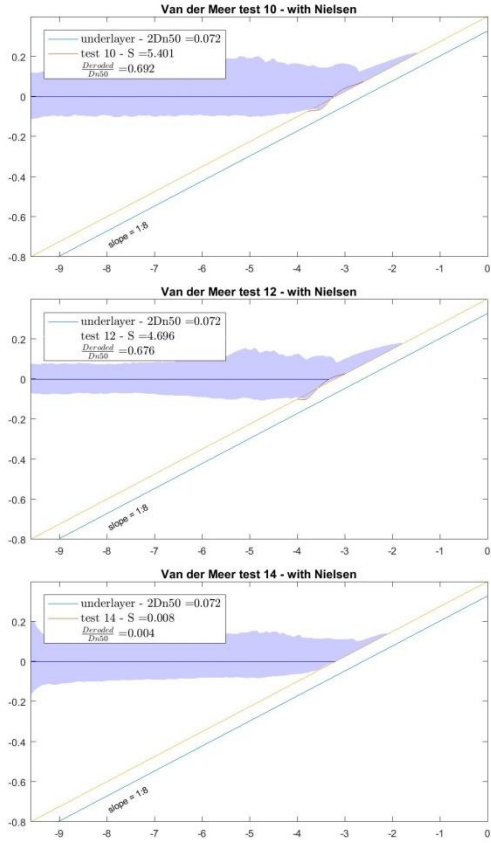
NIELSEN [2006] - 1:4 slope



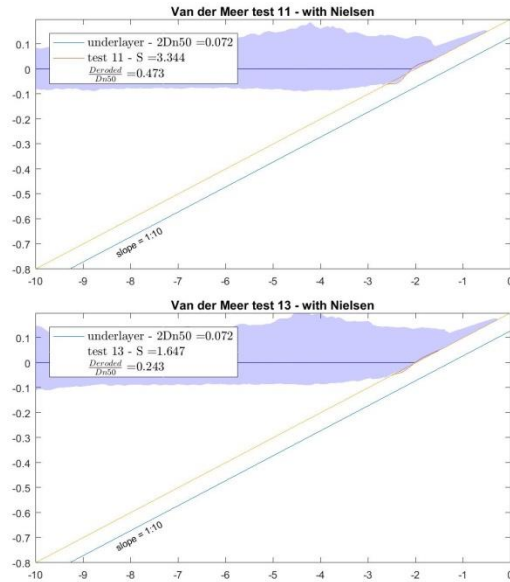
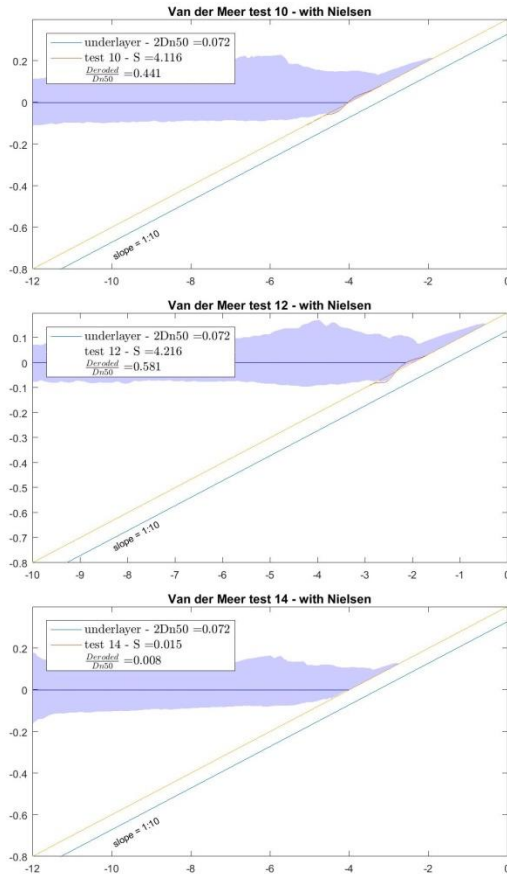
NIELSEN [2006] - 1:6 slope



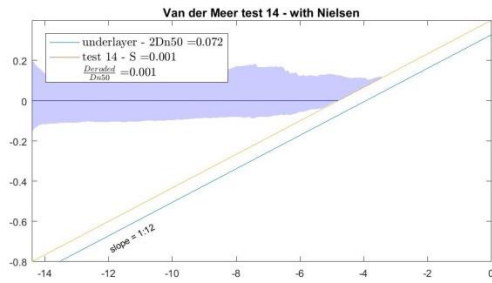
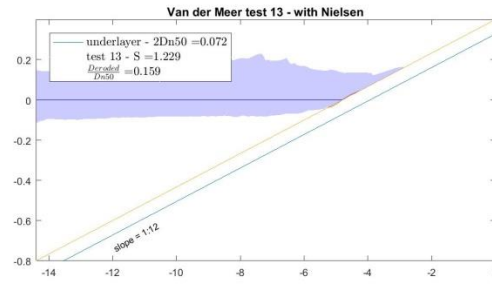
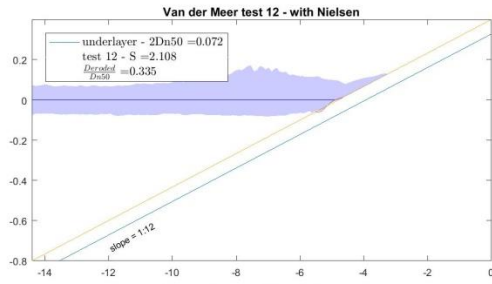
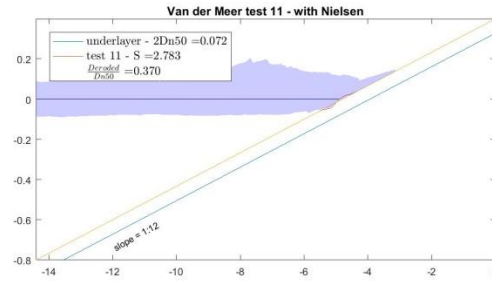
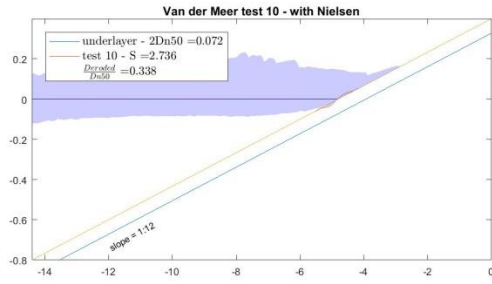
NIELSEN [2006] - 1:8 slope



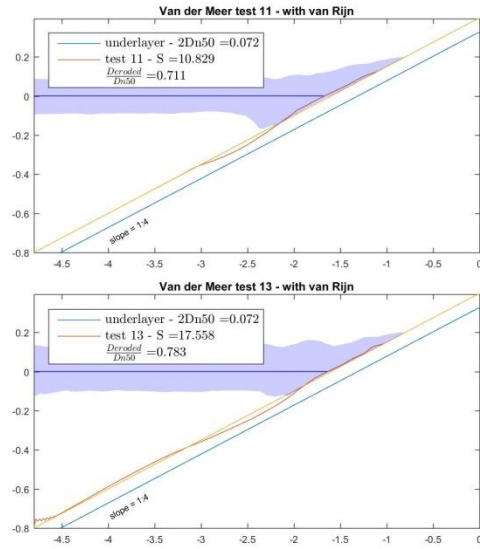
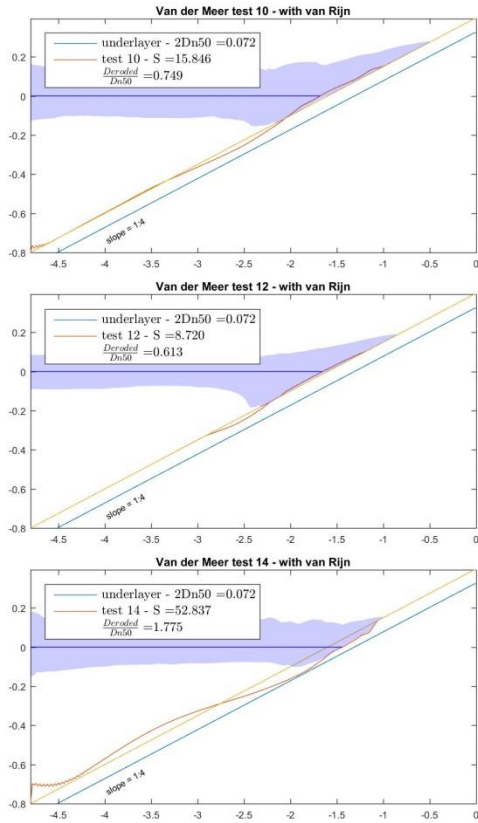
NIELSEN [2006] - 1:10 slope



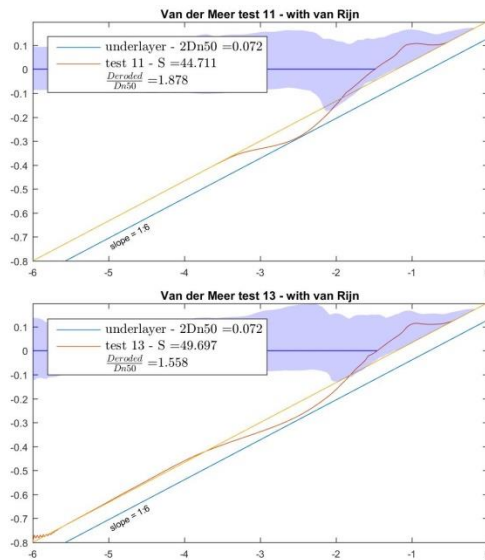
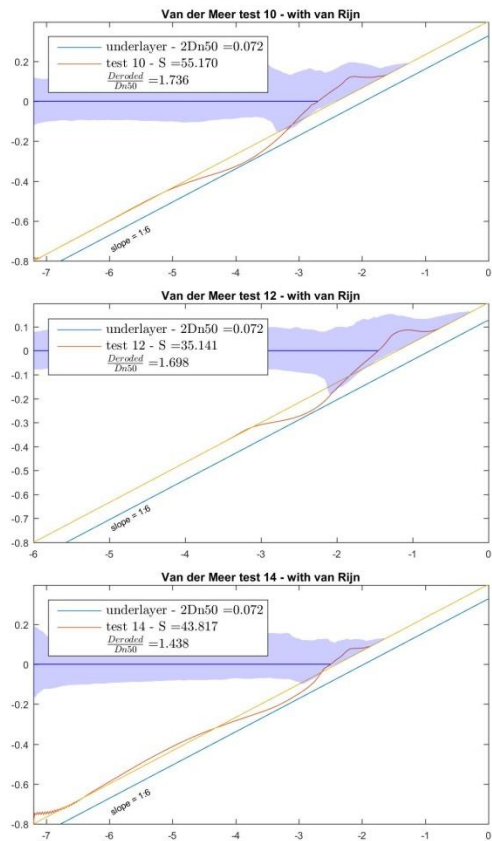
NIELSEN [2006] - 1:12 slope



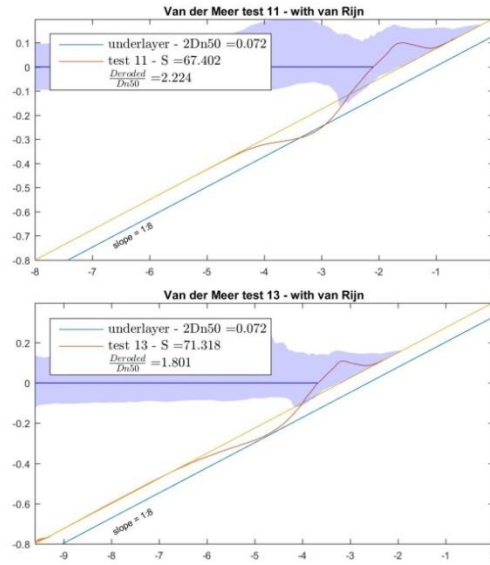
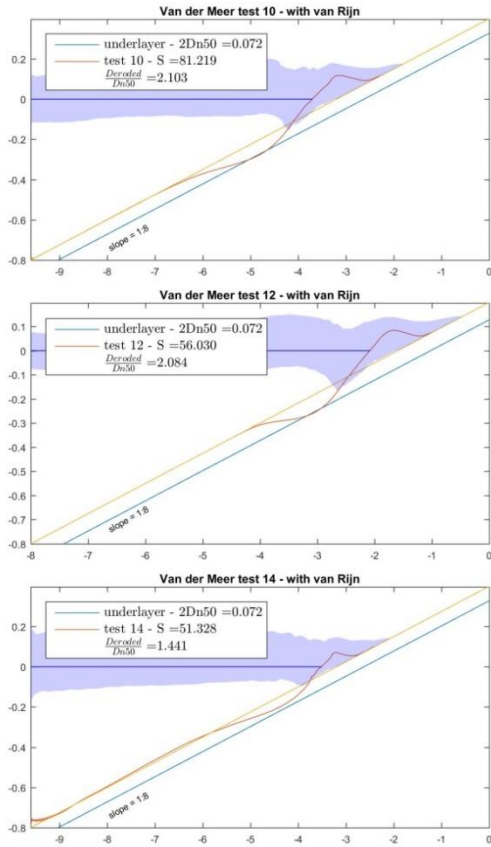
VAN RIJN [2007] - 1:4 slope



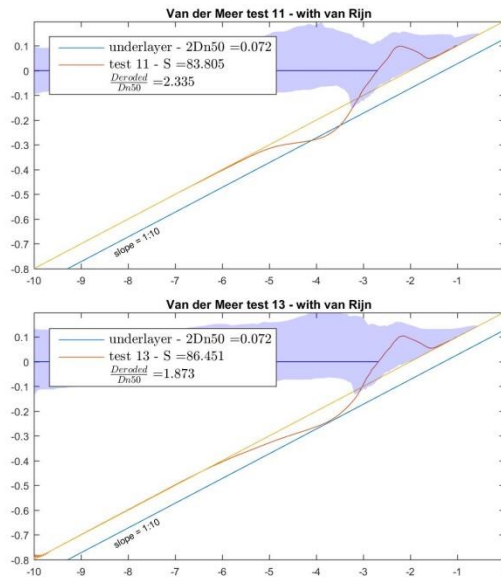
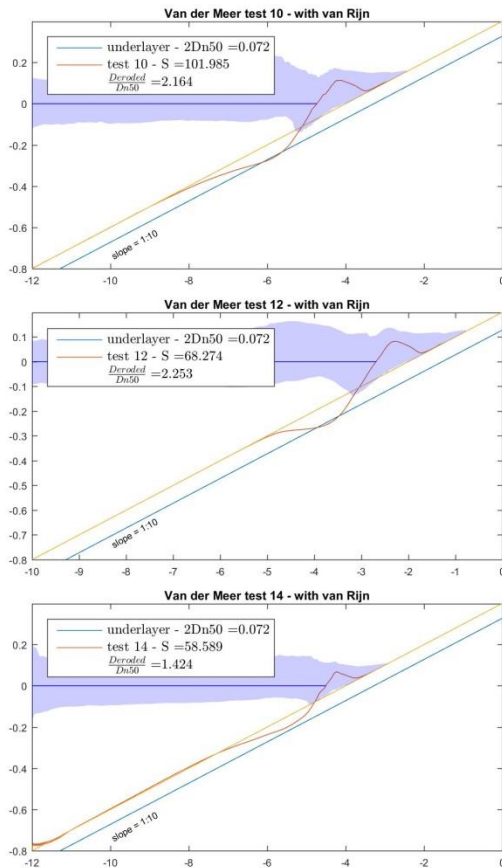
VAN RIJN [2007] - 1:6 slope



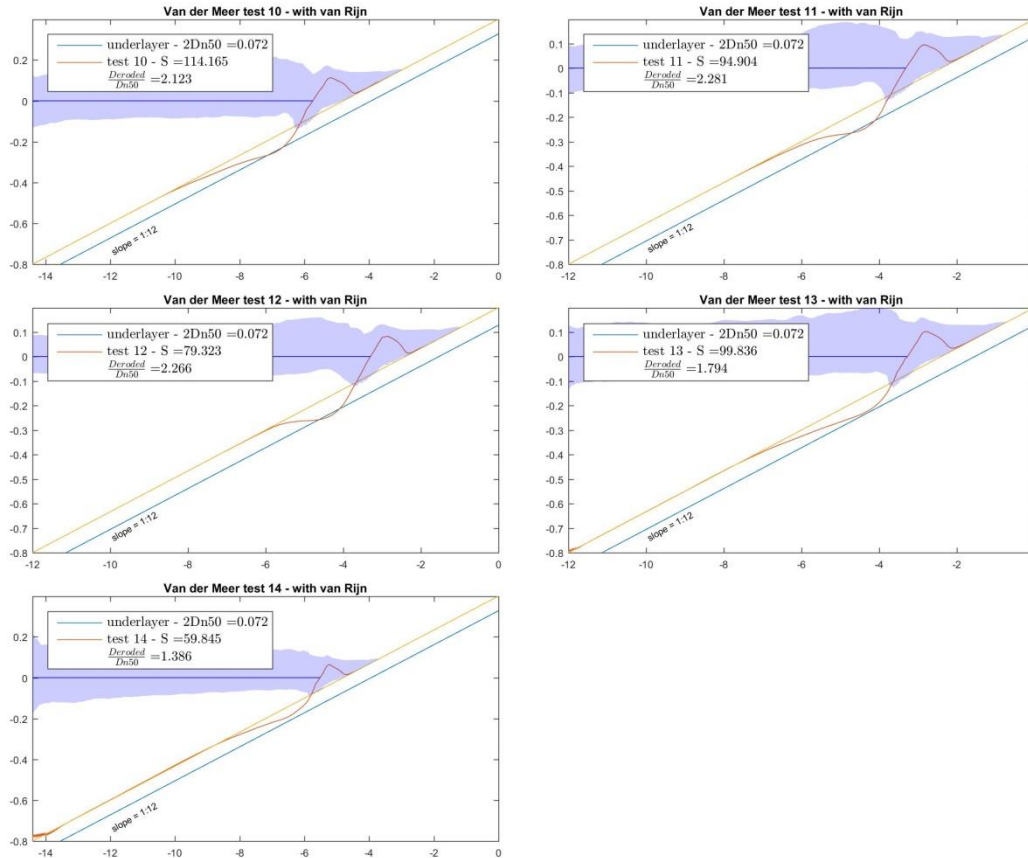
VAN RIJN [2007] - 1:8 slope



VAN RIJN [2007] - 1:10 slope

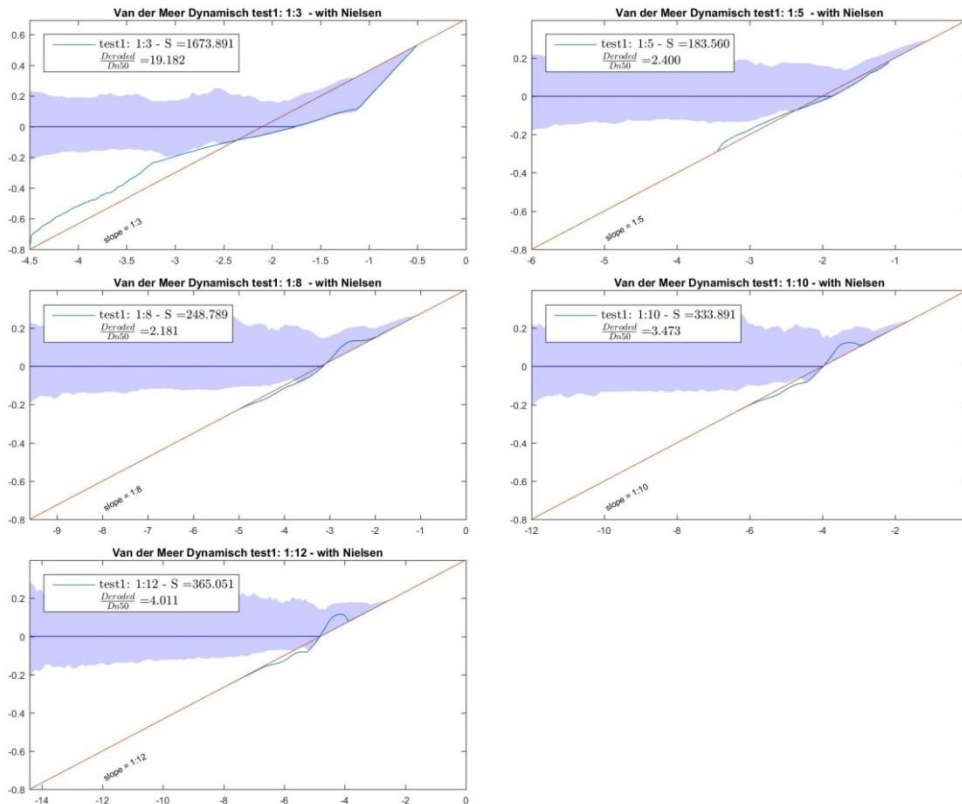


VAN RIJN [2007] - 1:12 slope

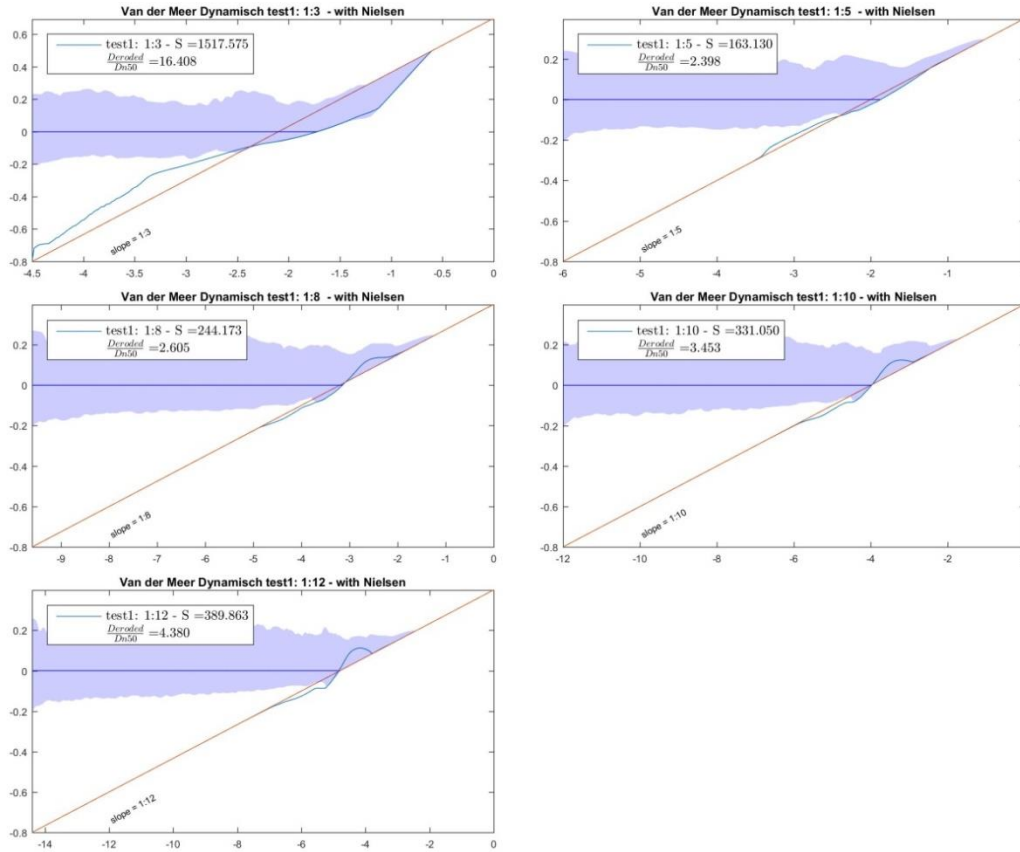


5.3.3 Test series C

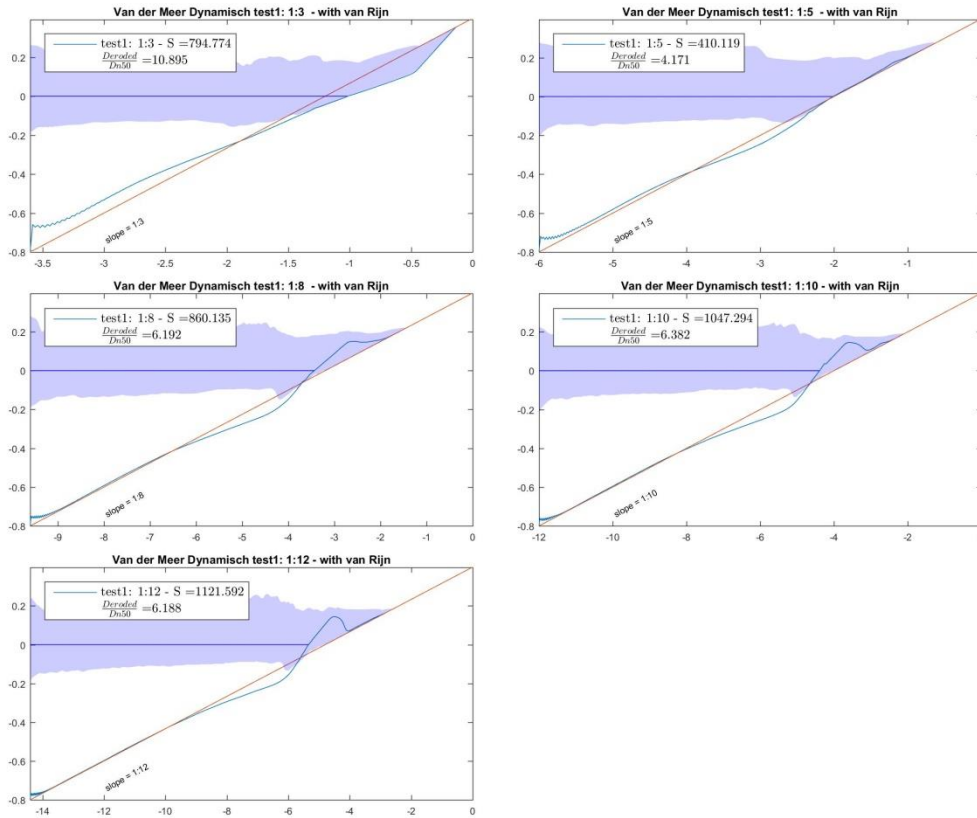
NIELSEN [2006] test 1



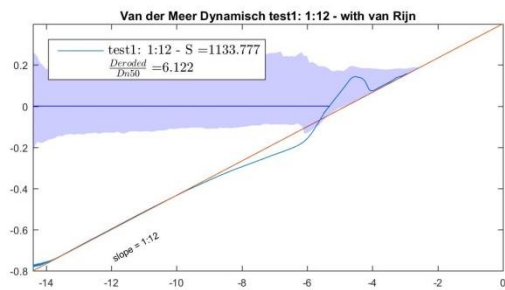
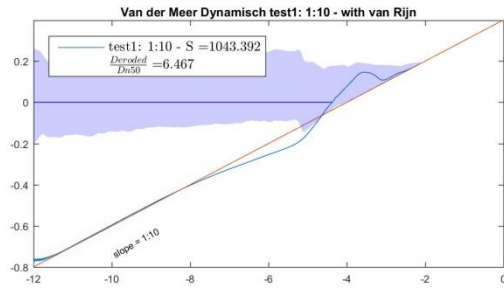
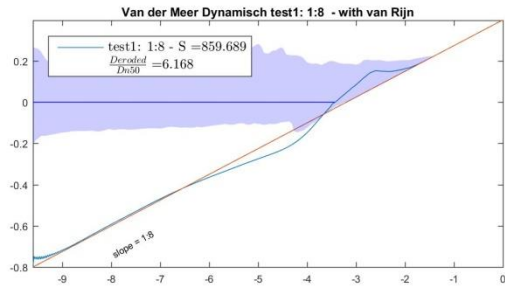
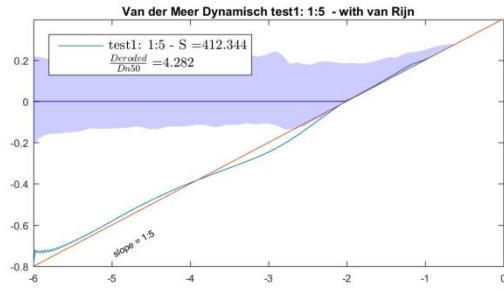
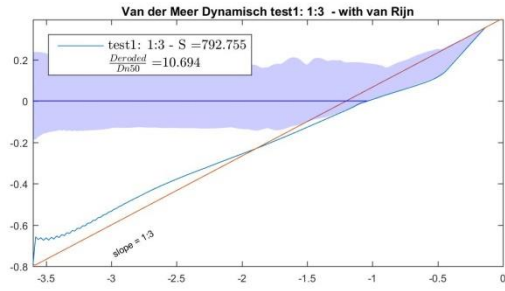
NIELSEN [2006] test 2



VAN RIJN [2007] test 1



VAN RIJN [2007] test 2

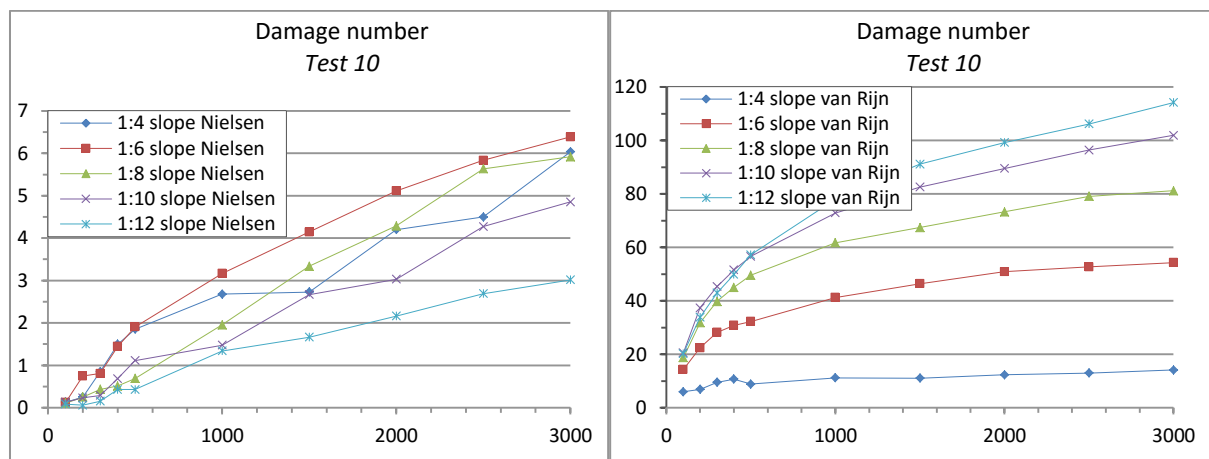


5.4 Test series B; Erosion in time

5.4.1 Test 10

Test 10	NIELSEN [2006]				
	1:4 slope	1:6 slope	1:8 slope	1:10 slope	1:12 slope
100	0.13	0.12	0.11	0.13	0.08
200	0.25	0.75	0.25	0.23	0.06
300	0.85	0.81	0.43	0.29	0.15
400	1.50	1.45	0.51	0.68	0.43
500	1.85	1.90	0.69	1.11	0.43
1000	2.68	3.17	1.95	1.48	1.34
1500	2.73	4.14	3.34	2.67	1.66
2000	4.20	5.12	4.29	3.03	2.16
2500	4.50	5.84	5.64	4.27	2.69
3000	6.03	6.39	5.92	4.85	3.01

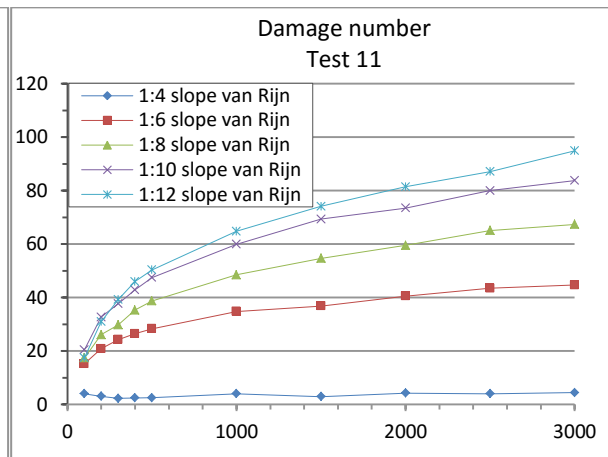
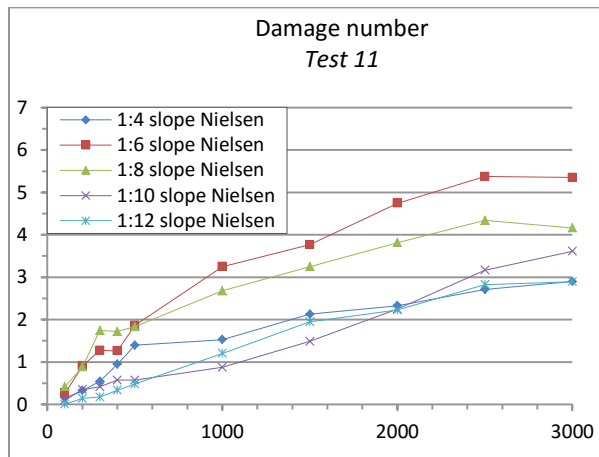
Test 10	VAN RIJN [2007]				
	1:4 slope	1:6 slope	1:8 slope	1:10 slope	1:12 slope
100	5.98	14.30	18.74	20.55	20.25
200	6.86	22.37	31.78	37.35	33.84
300	9.50	28.17	39.73	45.34	42.89
400	10.67	30.83	45.05	51.52	49.88
500	8.85	32.27	49.56	56.66	57.24
1000	11.20	41.24	61.75	72.84	78.03
1500	11.08	46.41	67.42	82.56	91.11
2000	12.32	50.91	73.31	89.54	99.19
2500	12.98	52.70	79.10	96.39	106.15
3000	14.13	54.32	81.17	101.92	114.16



5.4.2 Test 11

Test 11	NIELSEN [2006]				
	1:4 slope	1:6 slope	1:8 slope	1:10 slope	1:12 slope
100	0.15	0.26	0.42	0.10	0.00
200	0.33	0.91	0.89	0.35	0.14
300	0.54	1.27	1.74	0.41	0.17
400	0.95	1.26	1.72	0.57	0.34
500	1.40	1.86	1.83	0.57	0.48
1000	1.53	3.25	2.68	0.88	1.20
1500	2.13	3.76	3.25	1.49	1.95
2000	2.33	4.74	3.82	2.25	2.23
2500	2.71	5.37	4.34	3.17	2.83
3000	2.90	5.35	4.16	3.61	2.89

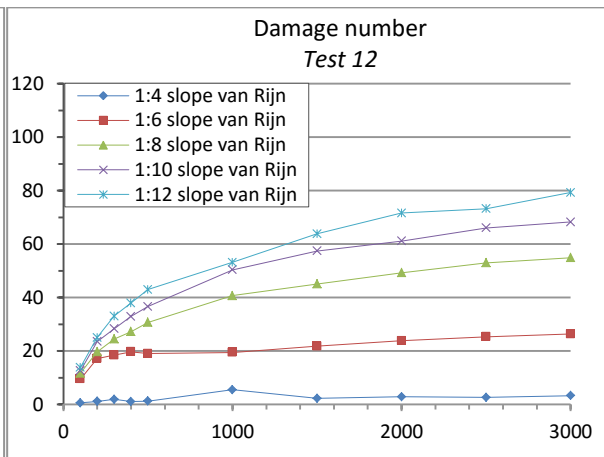
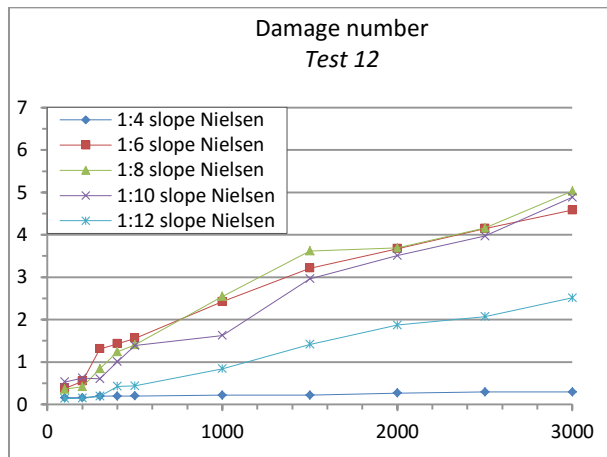
Test 11	VAN RIJN [2007]				
	1:4 slope	1:6 slope	1:8 slope	1:10 slope	1:12 slope
100	3.97	15.22	17.40	20.46	17.45
200	3.05	20.82	26.10	32.67	30.95
300	2.26	24.27	29.75	37.66	39.23
400	2.41	26.46	35.29	42.89	45.98
500	2.50	28.29	38.71	47.47	50.34
1000	3.97	34.77	48.47	59.91	64.81
1500	2.89	36.83	54.65	69.32	74.13
2000	4.24	40.50	59.48	73.44	81.41
2500	3.99	43.45	65.11	79.96	87.10
3000	4.42	44.64	67.38	83.77	94.89



5.4.3 Test 12

Test 12	NIELSEN [2006]				
	1:4 slope	1:6 slope	1:8 slope	1:10 slope	1:12 slope
100	0.16	0.38	0.36	0.53	0.14
200	0.16	0.54	0.42	0.62	0.14
300	0.20	1.31	0.84	0.60	0.19
400	0.20	1.43	1.24	1.01	0.42
500	0.20	1.56	1.41	1.39	0.44
1000	0.22	2.42	2.55	1.63	0.84
1500	0.22	3.21	3.62	2.96	1.41
2000	0.27	3.67	3.69	3.51	1.87
2500	0.29	4.15	4.16	3.97	2.07
3000	0.29	4.58	5.03	4.88	2.51

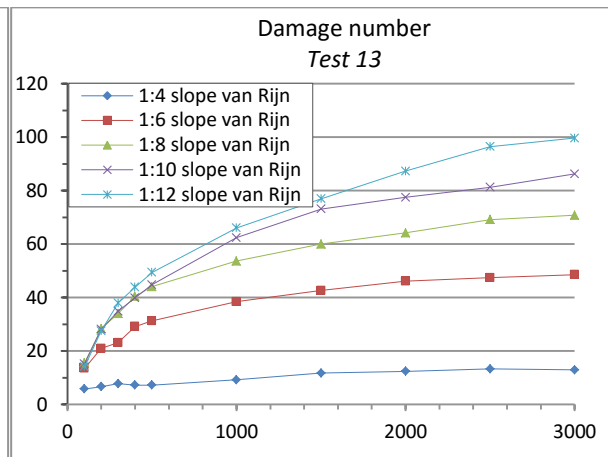
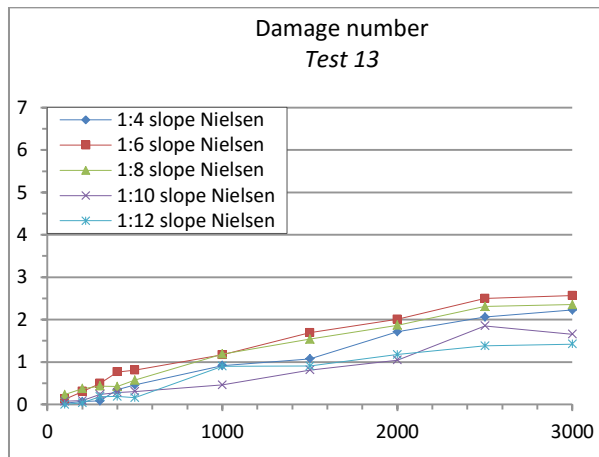
Test 12	VAN RIJN [2007]				
	1:4 slope	1:6 slope	1:8 slope	1:10 slope	1:12 slope
100	0.56	9.49	11.74	12.63	13.91
200	1.14	17.14	19.67	23.54	25.03
300	1.91	18.43	24.46	28.33	33.05
400	1.04	19.66	27.24	32.95	37.92
500	1.23	19.03	30.71	36.62	43.01
1000	5.49	19.47	40.69	50.34	53.16
1500	2.26	21.77	45.06	57.42	63.82
2000	2.85	23.84	49.29	61.13	71.61
2500	2.64	25.33	53.00	66.01	73.20
3000	3.26	26.32	54.92	68.26	79.27



5.4.4 Test 13

Test 13	NIELSEN [2006]				
	1:4 slope	1:6 slope	1:8 slope	1:10 slope	1:12 slope
100	0.03	0.12	0.23	0.07	0.00
200	0.07	0.31	0.37	0.09	0.04
300	0.08	0.49	0.43	0.23	0.18
400	0.35	0.76	0.42	0.28	0.19
500	0.46	0.80	0.57	0.31	0.16
1000	0.92	1.17	1.19	0.46	0.90
1500	1.07	1.69	1.54	0.81	0.91
2000	1.71	2.01	1.87	1.05	1.18
2500	2.06	2.50	2.31	1.85	1.38
3000	2.22	2.57	2.35	1.66	1.42

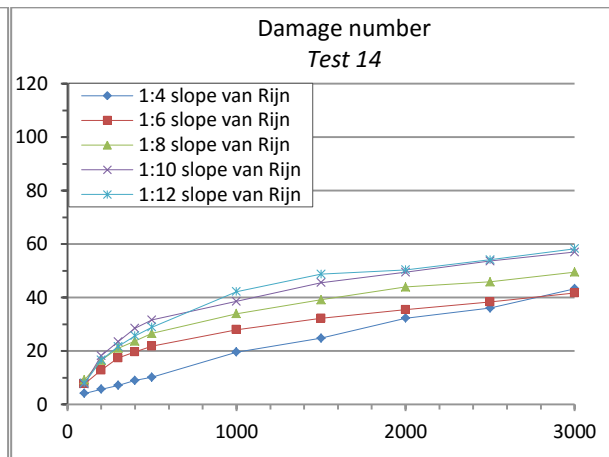
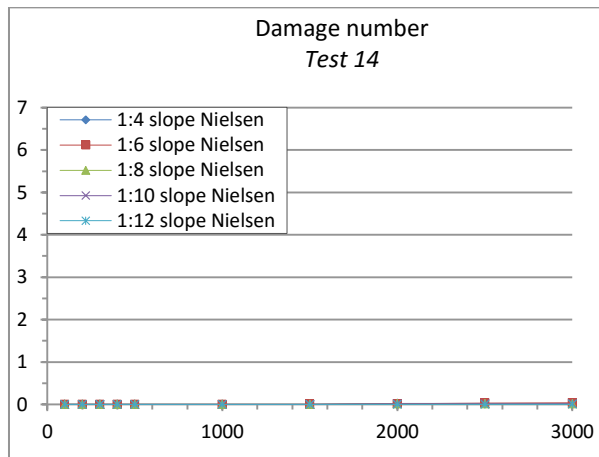
Test 13	VAN RIJN [2007]				
	1:4 slope	1:6 slope	1:8 slope	1:10 slope	1:12 slope
100	5.81	13.43	15.51	15.21	14.04
200	6.63	20.91	28.30	28.08	27.49
300	7.75	23.10	34.01	34.86	37.97
400	7.23	29.13	40.40	39.87	43.88
500	7.25	31.24	44.08	44.80	49.41
1000	9.21	38.42	53.62	62.39	66.01
1500	11.73	42.63	59.99	73.09	76.92
2000	12.36	46.12	64.16	77.46	87.29
2500	13.25	47.42	69.15	81.28	96.49
3000	12.92	48.53	70.80	86.19	99.62



5.4.5 Test 14

Test 14	NIELSEN [2006]				
	1:4 slope	1:6 slope	1:8 slope	1:10 slope	1:12 slope
100	0	0	0	0	0
200	0	0	0	0	0
300	0	0	0	0	0
400	0	0	0	0	0
500	0	0	0	0	0
1000	0	0	0	0	0
1500	0	0	0	0	0
2000	0.02	0.01	0.01	0.02	0
2500	0.02	0.03	0.01	0.02	0
3000	0.02	0.04	0.01	0.02	0.00

Test 14	VAN RIJN [2007]				
	1:4 slope	1:6 slope	1:8 slope	1:10 slope	1:12 slope
100	4.10	7.72	9.16	7.68	7.95
200	5.70	12.78	16.50	18.21	16.56
300	7.13	17.35	20.98	23.46	21.64
400	8.98	19.61	23.69	28.52	25.68
500	10.16	21.80	26.57	31.61	28.91
1000	19.54	27.95	33.94	38.56	42.20
1500	24.79	32.19	39.16	45.57	48.71
2000	32.25	35.44	43.92	49.48	50.34
2500	36.02	38.31	45.87	53.64	54.15
3000	43.27	41.66	49.49	56.99	58.25



Appendix F

*Results of the Varied parameters –
Test Series B*

APPENDIX F: RESULTS OF THE VARIED PARAMETERS – TEST SERIES B

6.1 Different Layer thickness (0.04m)

6.1.1 Damage number

Damage										
VAN RIJN [2007]	Impermeable $t_{layer} = 0.04 m$					homogeneous				
	1:4	1:6	1:8	1:10	1:12	1:4	1:6	1:8	1:10	1:12
Test 10	13.77	55.88	80.92	98.67	115.69					
Test 11	10.66	43.79	66.30	80.93	96.52					
Test 12	7.54	35.67	55.26	67.94	76.62					
Test 13	17.43	49.57	70.55	86.18	96.58					
Test 14	56.21	43.98	54.09	58.46	60.48					

Damage										
NIELSEN [2006]	Impermeable $t_{layer} = 0.04 m$					homogeneous				
	1:4	1:6	1:8	1:10	1:12	1:4	1:6	1:8	1:10	1:12
Test 10	46.36	7.20	4.32	4.12	2.11					
Test 11	64.62	45.91	4.57	2.94	2.10					
Test 12	40.25	47.15	6.29	3.72	2.34					
Test 13	40.26	18.96	1.76	1.33	0.73					
Test 14	34.20	0.02	0.01	0.01	0.01					

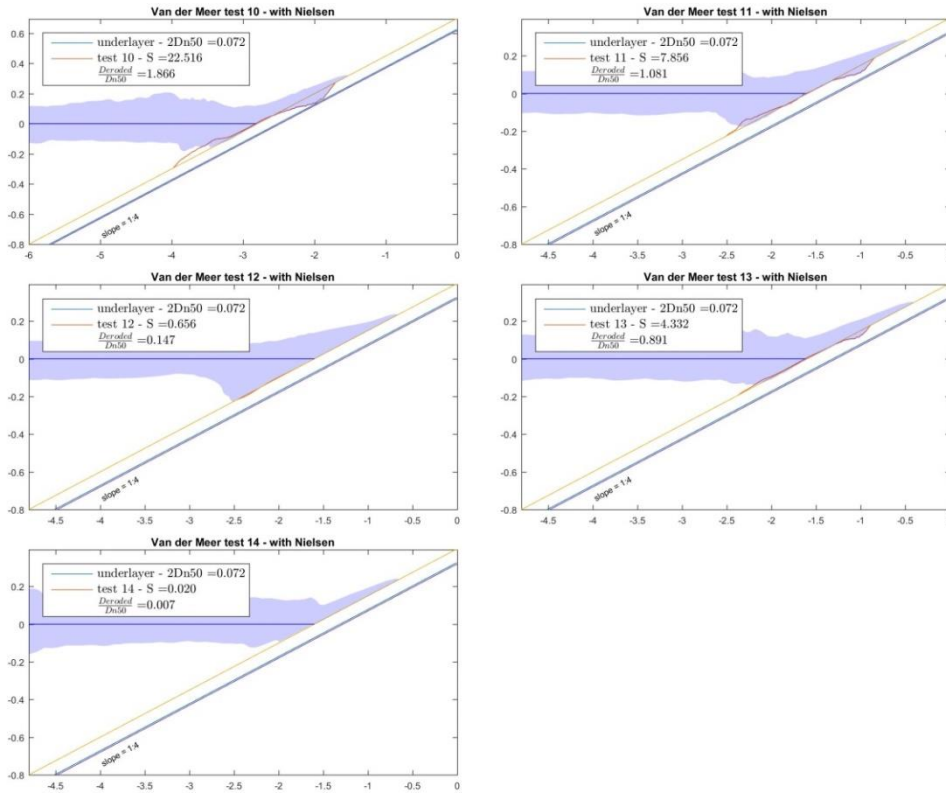
6.1.2 Relative Erosion Depth

Rel. erosion depth $\frac{d_e}{D_{n50}}$										
VAN RIJN [2007]	Impermeable $t_{layer} = 0.04 m$					homogeneous				
	1:4	1:6	1:8	1:10	1:12	1:4	1:6	1:8	1:10	1:12
Test 10	0.70	1.76	2.09	2.16	2.12					
Test 11	0.67	1.84	2.21	2.33	2.29					
Test 12	0.57	1.70	2.09	2.23	2.24					
Test 13	0.73	1.53	1.78	1.83	1.85					
Test 14	1.90	1.44	1.46	1.43	1.33					

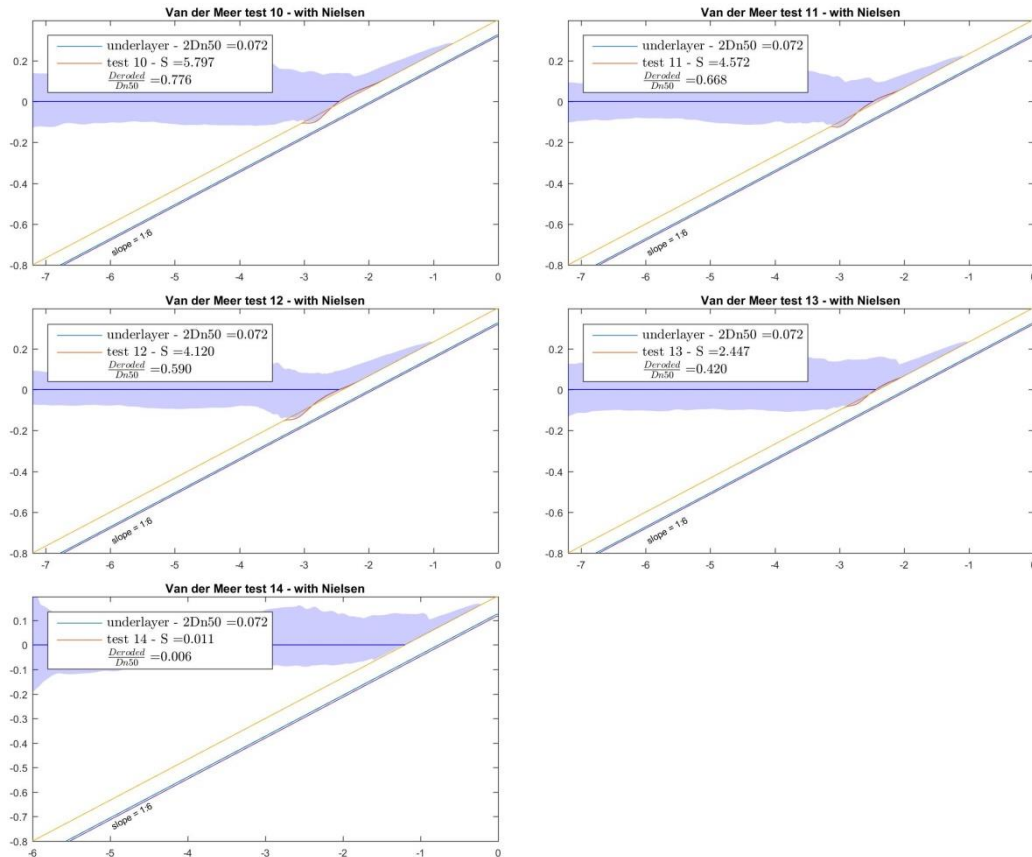
Relative Erosion Depth										
NIELSEN [2006]	Impermeable $t_{layer} = 0.04 m$					homogeneous				
	1:4	1:6	1:8	1:10	1:12	1:4	1:6	1:8	1:10	1:12
Test 10	1.75	0.69	0.62	0.53	0.28					
Test 11	1.92	1.61	0.62	0.38	0.31					
Test 12	1.65	1.50	0.52	0.52	0.37					
Test 13	1.74	1.10	0.28	0.18	0.09					
Test 14	1.71	0.01	0.01	0.01	0.01					

6.1.3 Formed erosion profile

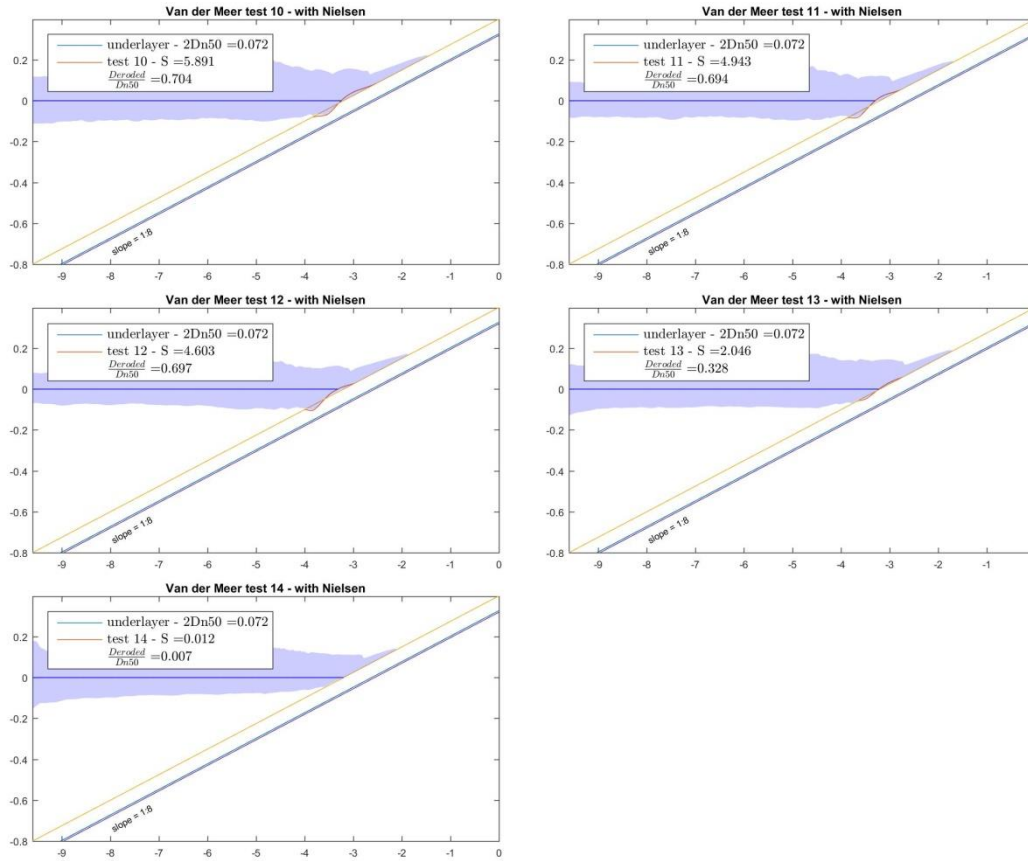
NIELSEN [2006] - Layer Thickness = 0.04m - 1:4 slope



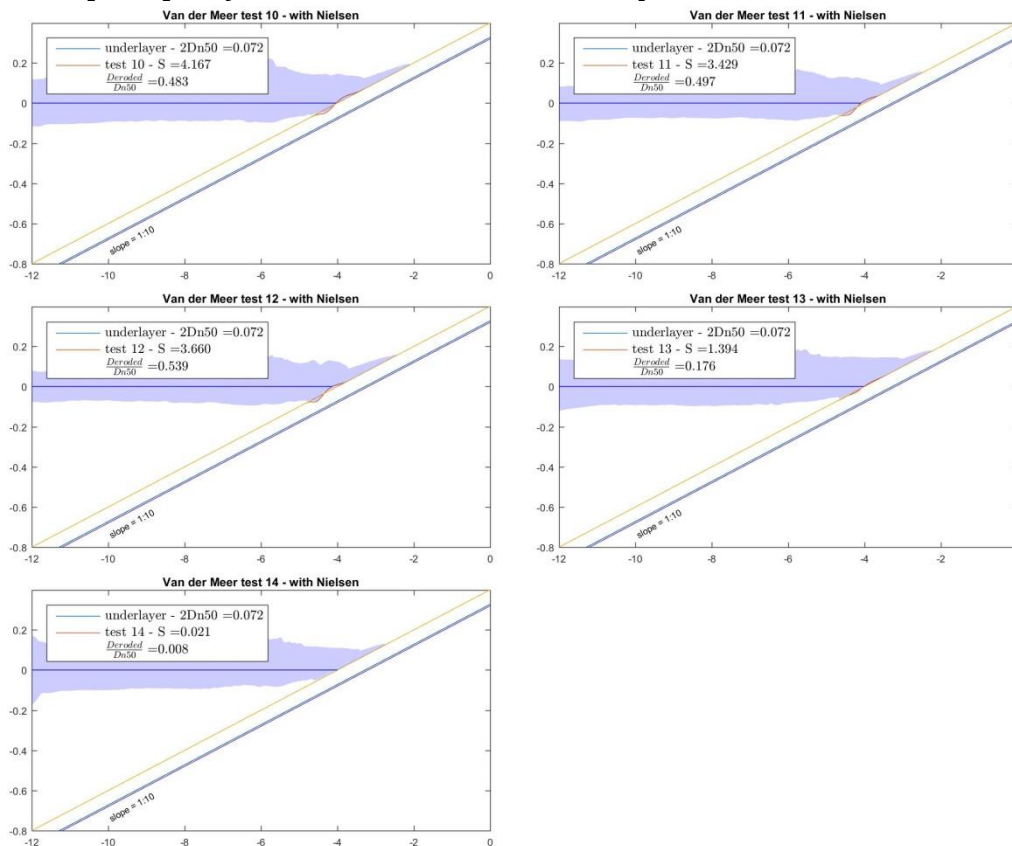
NIELSEN [2006] - Layer Thickness = 0.04m - 1:6 slope



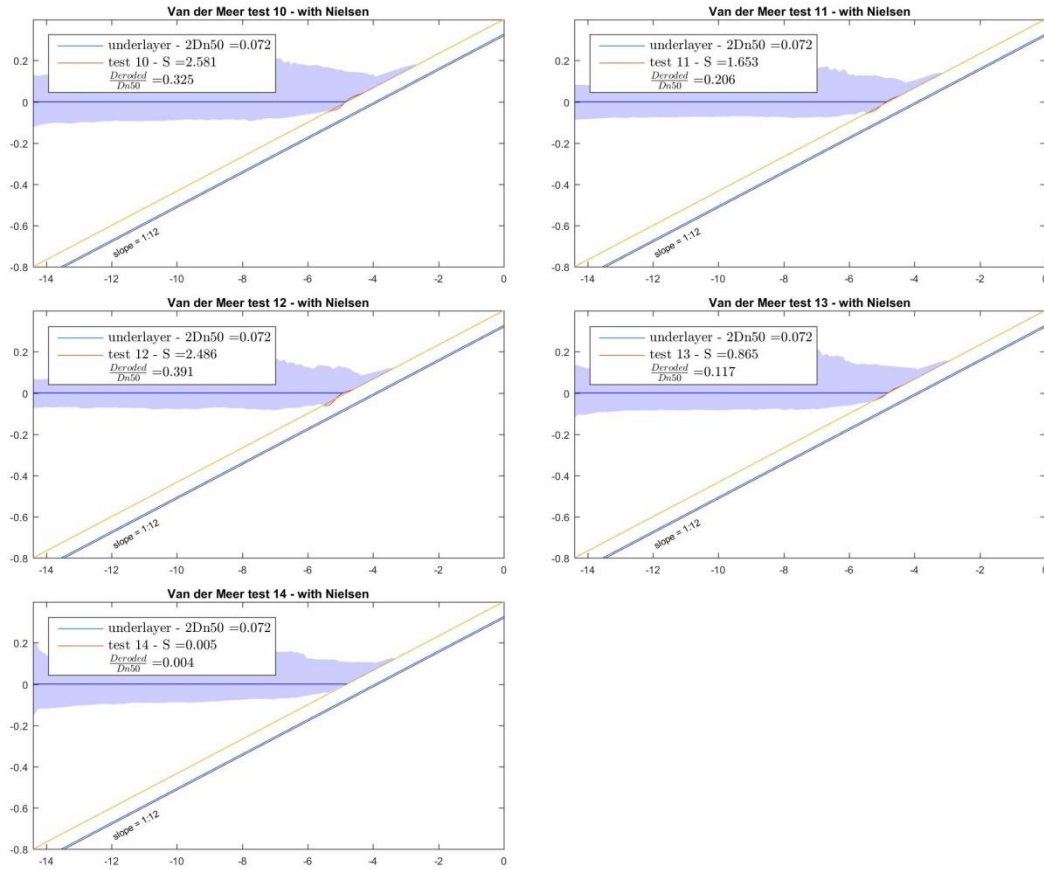
NIELSEN [2006] -Layer Thickness =0.04m - 1:8 slope



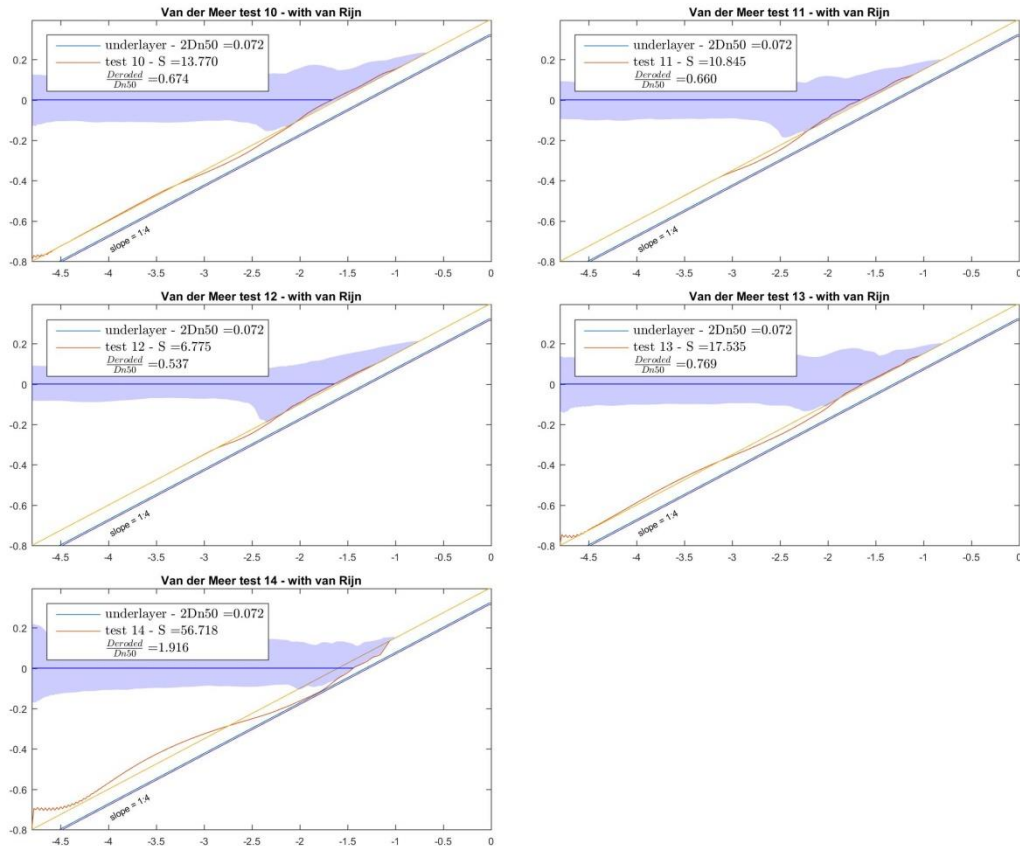
NIELSEN [2006] -Layer Thickness =0.04m - 1:10 slope



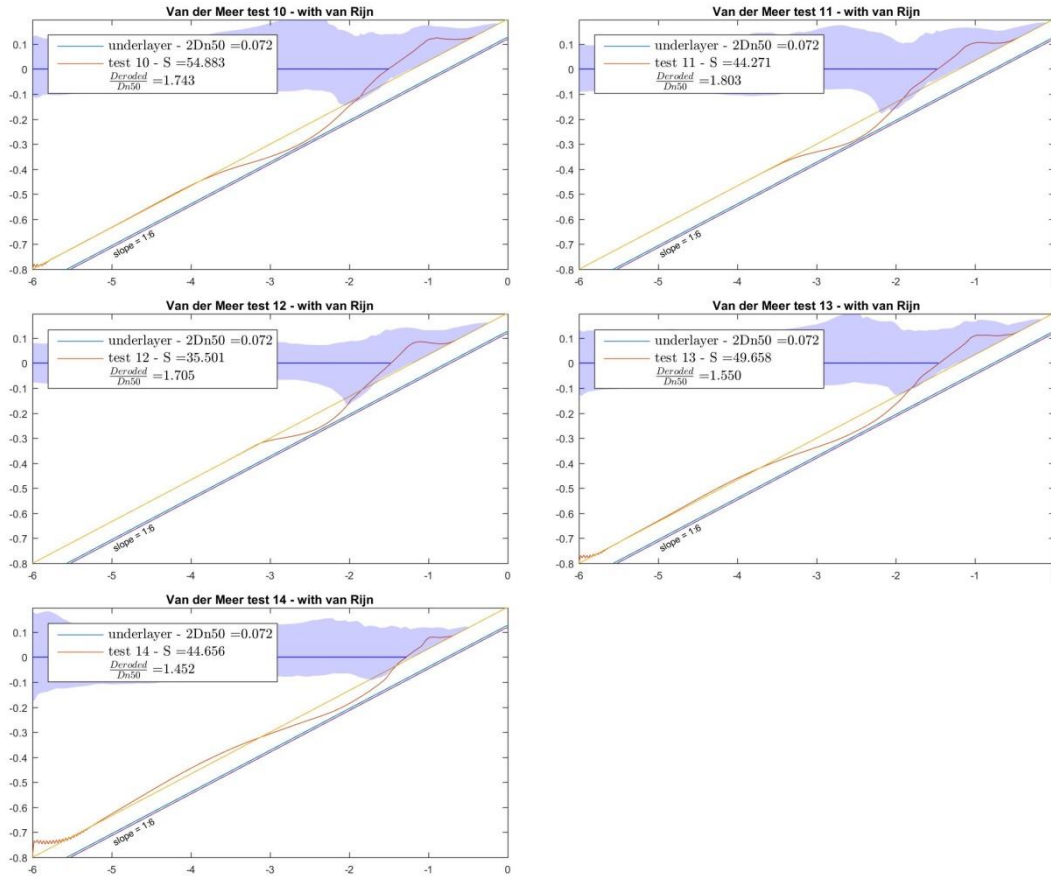
NIELSEN [2006] - Layer Thickness = 0.04m - 1:12 slope



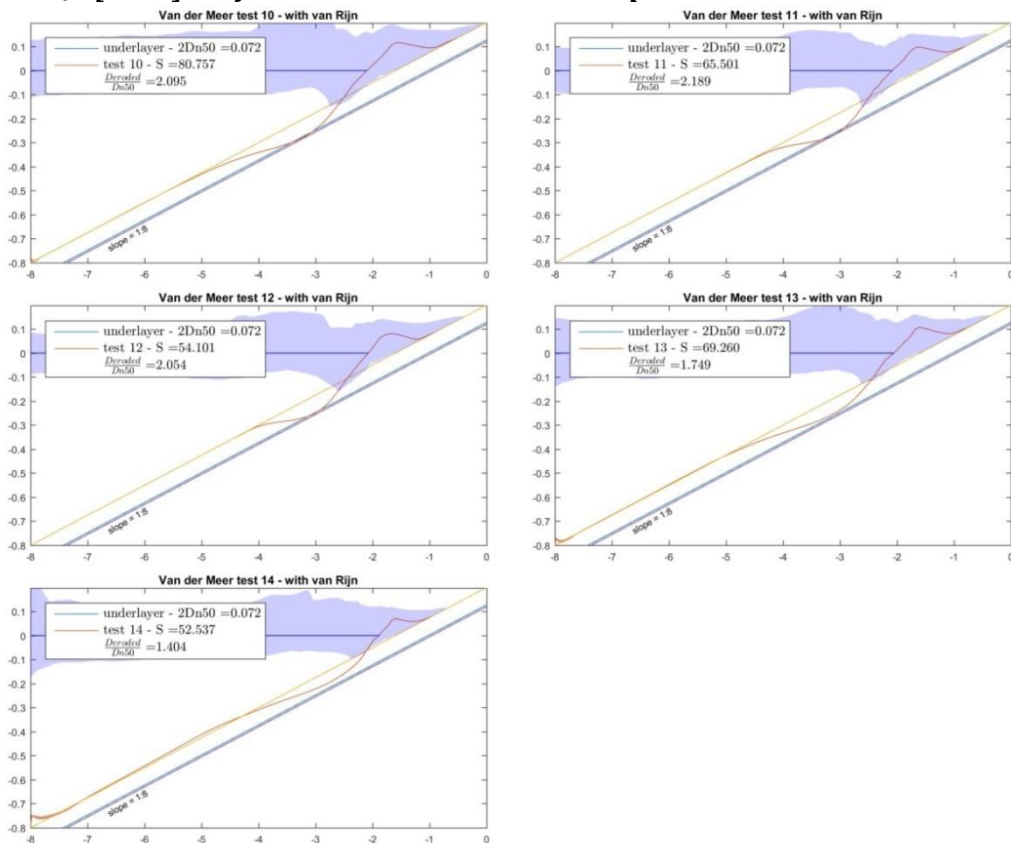
VAN RIJN [2007] - Layer Thickness = 0.04m - 1:4 slope



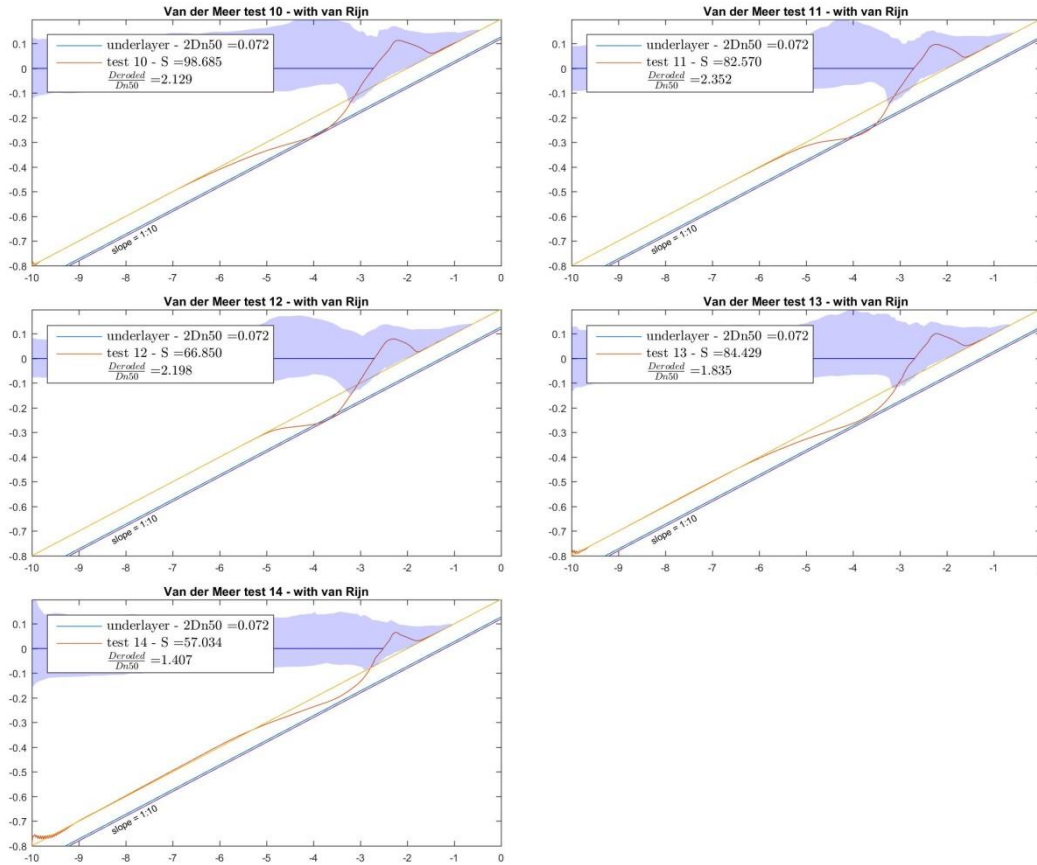
VAN RIJN [2007] - Layer Thickness = 0.04m - 1:6 slope



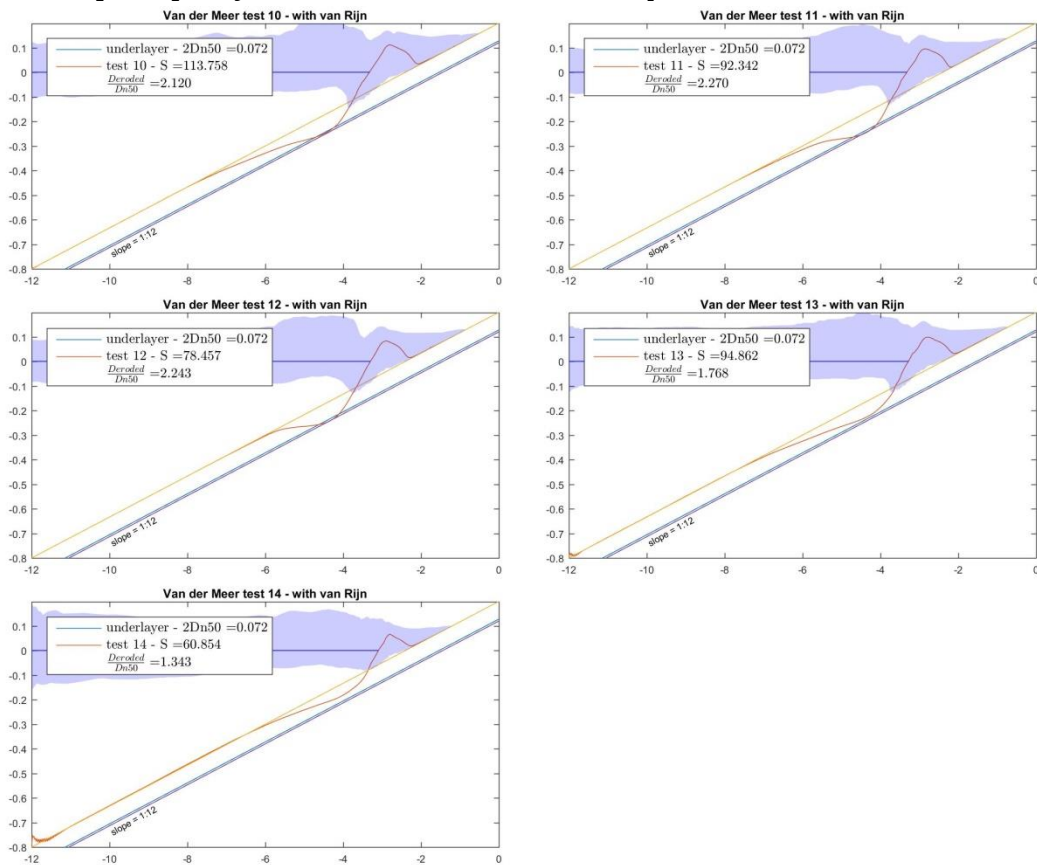
VAN RIJN [2007] - Layer Thickness = 0.04m - 1:8 slope



VAN RIJN [2007] - Layer Thickness = 0.04m - 1:10 slope



VAN RIJN [2007] - Layer Thickness = 0.04m - 1:12 slope



6.2 Different Stone size

6.2.1 Damage number

Damage										
VAN RIJN [2007]	Impermeable					Homogeneous				
	1:4	1:6	1:8	1:10	1:12	1:4	1:6	1:8	1:10	1:12
Test 10: Dn50=0.02m						27.96	156.31	254.81	314.44	355.85
Test 11: Dn50=0.02m						18.19	125.18	205.97	261.28	300.02
Test 12: Dn50=0.02m						13.20	105.18	175.40	223.05	262.56
Test 13: Dn50=0.02m						35.72	146.50	221.57	268.09	308.52
Test 14: Dn50=0.02m						112.16	122.48	159.39	185.11	197.55
NIELSEN [2006]	Impermeable					Homogeneous				
	1:4	1:6	1:8	1:10	1:12	1:4	1:6	1:8	1:10	1:12
Test 10: Dn50=0.02m						74.23	56.49	66.71	66.76	55.69
Test 11: Dn50=0.02m						49.63	35.99	60.90	52.64	43.26
Test 12: Dn50=0.02m						8.05	15.05	46.13	49.71	43.38
Test 13: Dn50=0.02m						66.22	37.16	43.09	40.25	34.94
Test 14: Dn50=0.02m						5.49	6.18	3.98	2.151	2.54

Damage										
VAN RIJN [2007]	Impermeable					Homogeneous				
	1:4	1:6	1:8	1:10	1:12	1:4	1:6	1:8	1:10	1:12
Test 10: Dn50=0.05m						9.58	28.53	41.34	50.03	57.61
Test 11: Dn50=0.05m						6.67	23.04	33.73	40.44	45.83
Test 12: Dn50=0.05m						5.95	17.15	26.62	32.48	36.87
Test 13: Dn50=0.05m						10.11	25.80	35.95	43.04	49.21
Test 14: Dn50=0.05m						34.05	25.58	27.03	29.15	30.73
NIELSEN [2006]	Impermeable					Homogeneous				
	1:4	1:6	1:8	1:10	1:12	1:4	1:6	1:8	1:10	1:12
Test 10: Dn50=0.05m						0.14	0.34	0.44	0.19	0.28
Test 11: Dn50=0.05m						0.05	0.43	0.30	0.27	0.16
Test 12: Dn50=0.05m						0.01	0.41	0.71	0.22	0.24
Test 13: Dn50=0.05m						0.02	0.09	0.04	0.07	0.06
Test 14: Dn50=0.05m						0	0	0	0	0

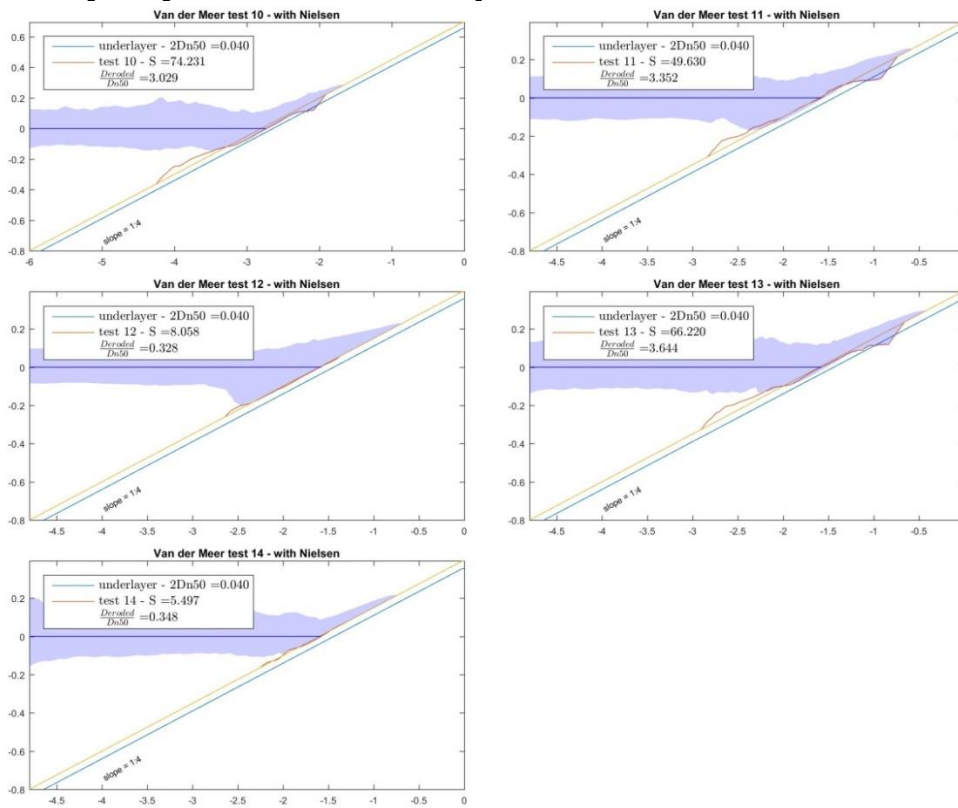
6.2.2 Relative Erosion Depth

Rel. erosion depth $\frac{d_e}{D_{n50}}$										
VAN RIJN [2007]	Impermeable					Homogeneous				
	1:4	1:6	1:8	1:10	1:12	1:4	1:6	1:8	1:10	1:12
Test 10: Dn50=0.02m						-0.014	-0.060	-0.075	-0.078	-0.077
Test 11: Dn50=0.02m						-0.011	-0.062	-0.081	-0.084	-0.083
Test 12: Dn50=0.02m						-0.013	-0.058	-0.076	-0.083	-0.084
Test 13: Dn50=0.02m						-0.021	-0.054	-0.066	-0.066	-0.066
Test 14: Dn50=0.02m						-0.042	-0.050	-0.053	-0.054	-0.051
NIELSEN [2006]	Impermeable					Homogeneous				
	1:4	1:6	1:8	1:10	1:12	1:4	1:6	1:8	1:10	1:12
Test 10: Dn50=0.02m						-0.060	-0.048	-0.052	-0.046	-0.036
Test 11: Dn50=0.02m						-0.067	-0.035	-0.047	-0.041	-0.034
Test 12: Dn50=0.02m						-0.006	-0.014	-0.037	-0.040	-0.034
Test 13: Dn50=0.02m						-0.073	-0.044	-0.042	-0.035	-0.028
Test 14: Dn50=0.02m						-0.007	-0.013	-0.007	-0.004	-0.004

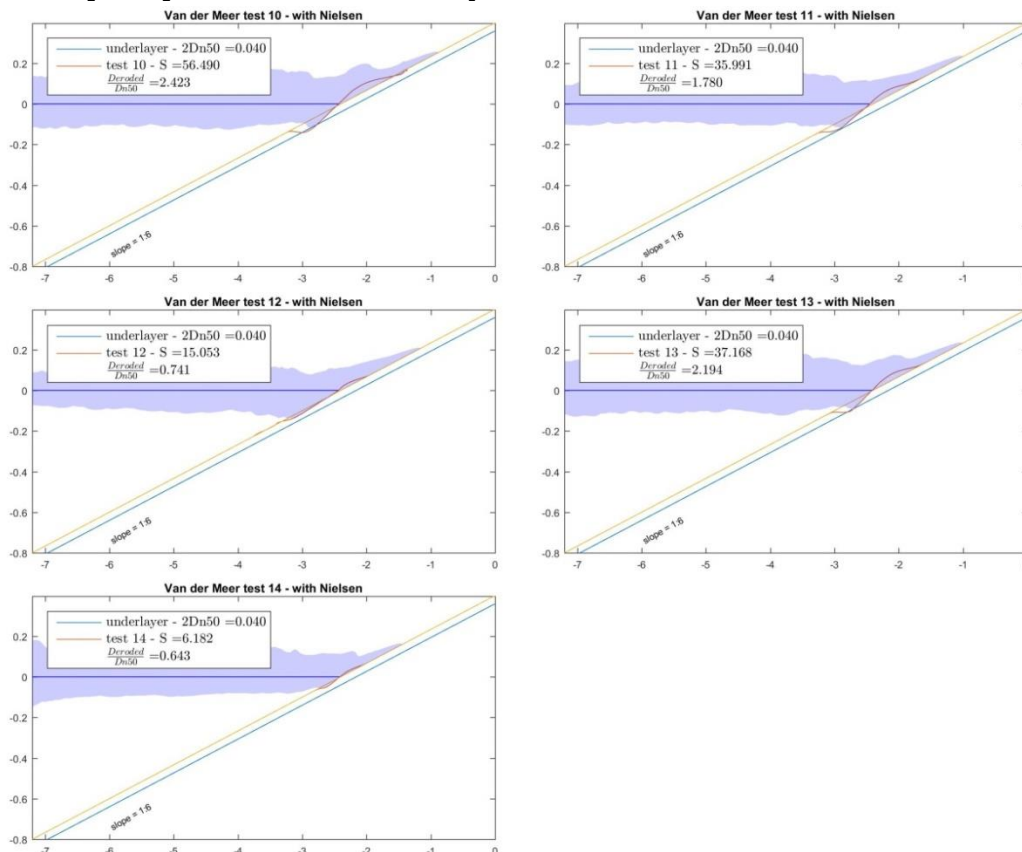
Rel. erosion depth $\frac{d_e}{D_{n50}}$										
VAN RIJN [2007]	Impermeable					Homogeneous				
	1:4	1:6	1:8	1:10	1:12	1:4	1:6	1:8	1:10	1:12
Test 10: Dn50=0.05m						-0.026	-0.060	-0.070	-0.073	-0.073
Test 11: Dn50=0.05m						-0.029	-0.065	-0.078	-0.079	-0.077
Test 12: Dn50=0.05m						-0.029	-0.057	-0.071	-0.075	-0.074
Test 13: Dn50=0.05m						-0.032	-0.054	-0.060	-0.063	-0.061
Test 14: Dn50=0.05m						-0.080	-0.055	-0.048	-0.047	-0.045
NIELSEN [2006]	Impermeable					Homogeneous				
	1:4	1:6	1:8	1:10	1:12	1:4	1:6	1:8	1:10	1:12
Test 10: Dn50=0.05m						-0.0021	-0.0042	-0.0046	-0.0017	-0.0029
Test 11: Dn50=0.05m						-0.0007	-0.0052	-0.0041	-0.0034	-0.0021
Test 12: Dn50=0.05m						-0.0004	-0.0054	-0.0095	-0.003	-0.0032
Test 13: Dn50=0.05m						-0.0004	-0.0012	-0.0008	-0.0006	-0.0009
Test 14: Dn50=0.05m						0	0	0	0	0

6.2.3 Formed erosion profile

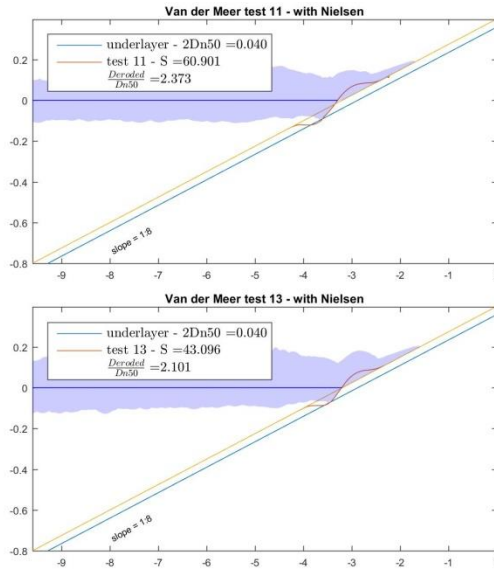
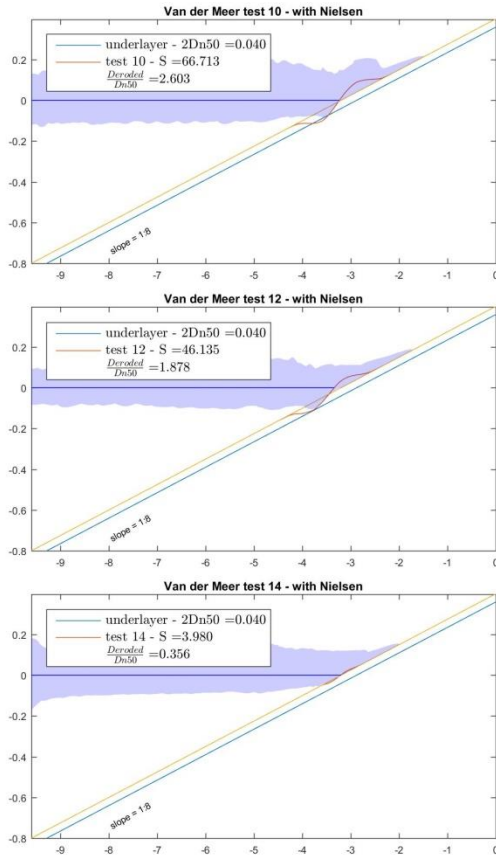
NIELSEN [2006] - $D_{n50}=0.02m$ - 1:4 slope



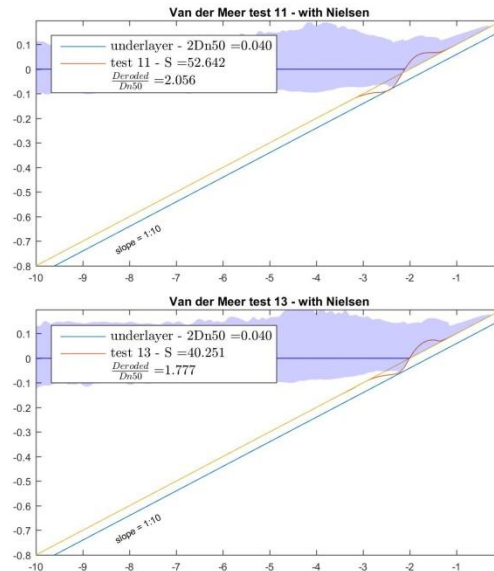
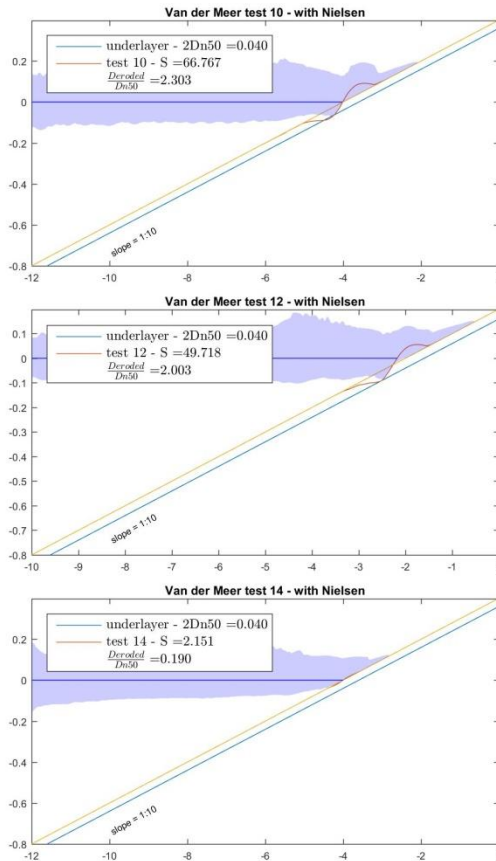
NIELSEN [2006] - $D_{n50}=0.02m$ - 1:6 slope



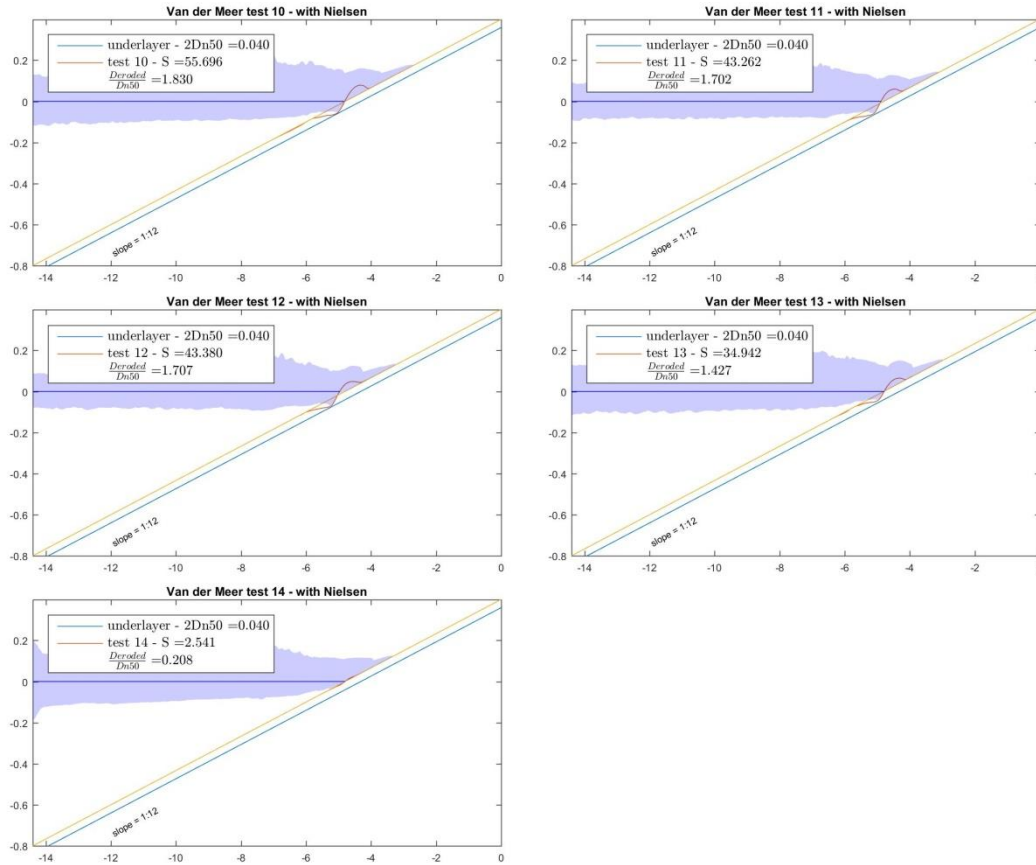
NIELSEN [2006] - $D_{n50}=0.02m$ - 1:8 slope



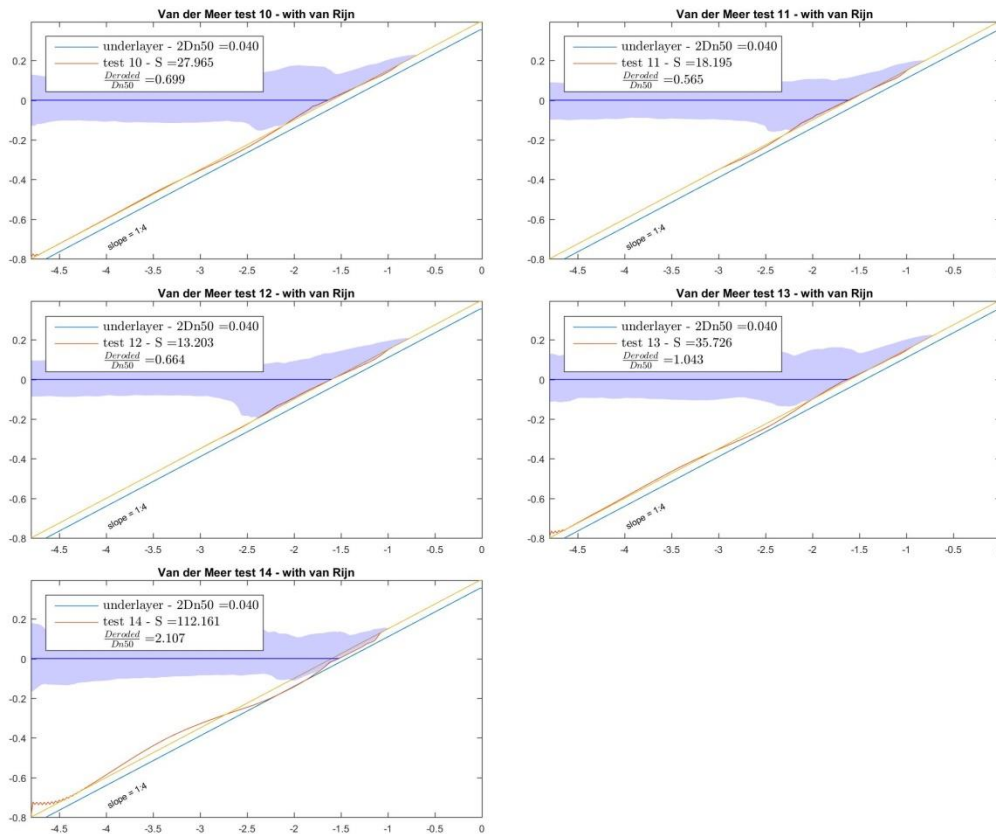
NIELSEN [2006] - $D_{n50}=0.02m$ - 1:10 slope



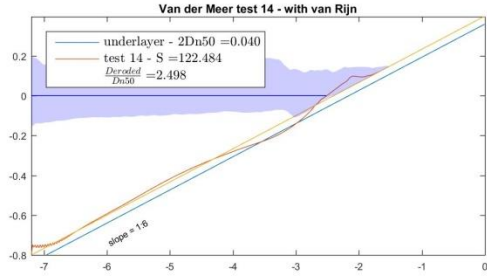
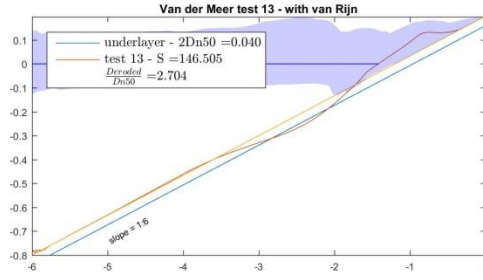
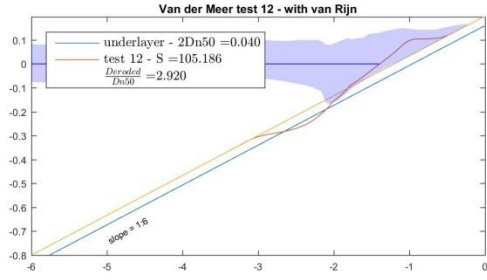
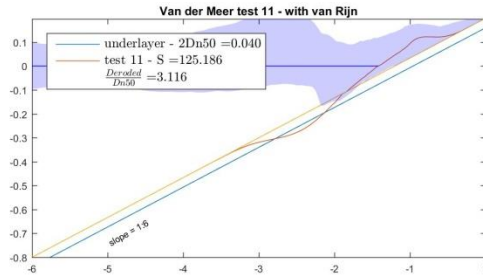
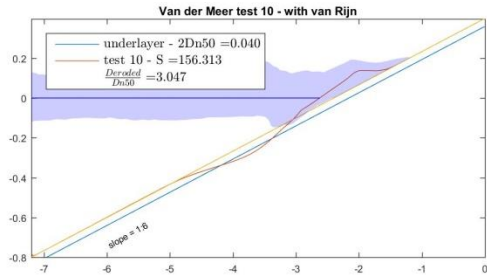
NIELSEN [2006] - Dn50=0.02m- 1:12 slope



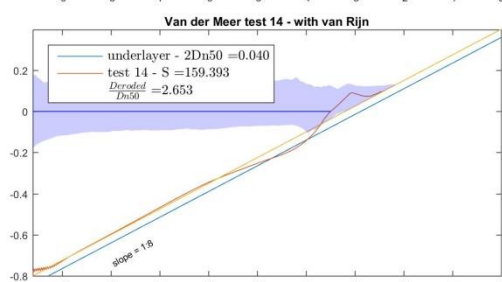
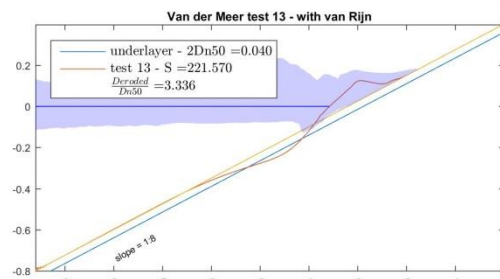
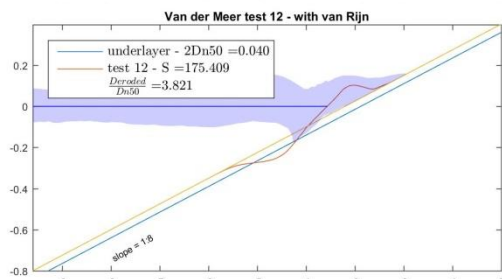
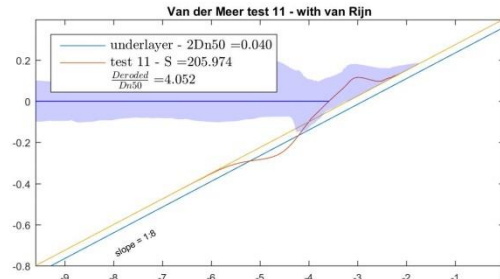
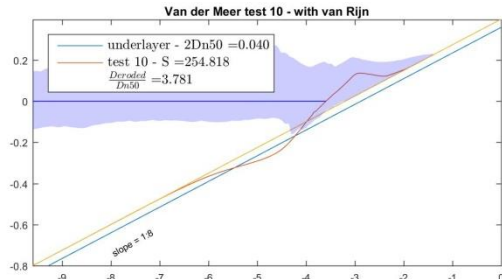
VAN RIJN [2007] - Dn50=0.02m- 1:4 slope



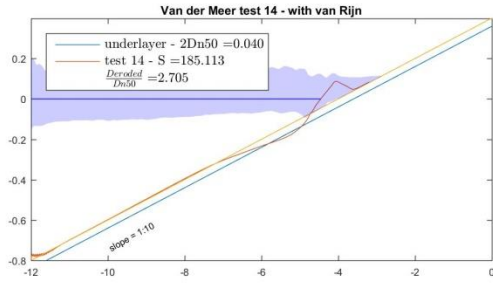
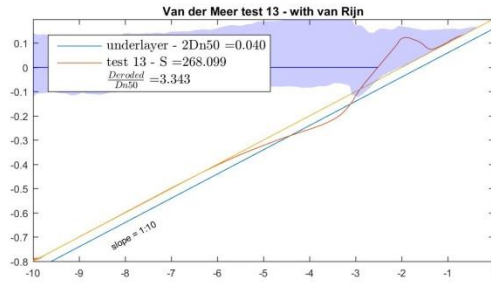
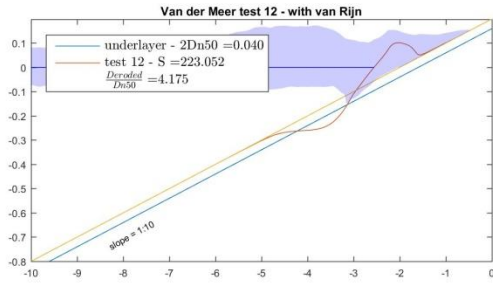
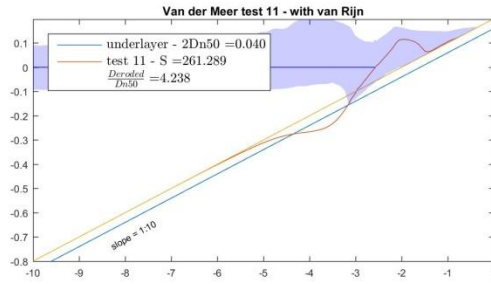
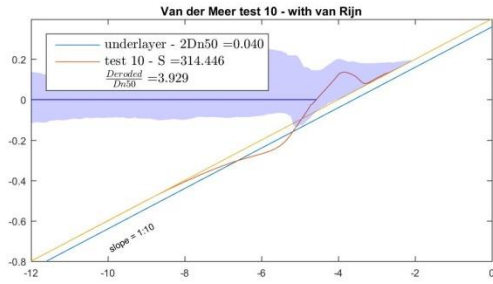
VAN RIJN [2007] - $D_{n50}=0.02m$ - 1:6 slope



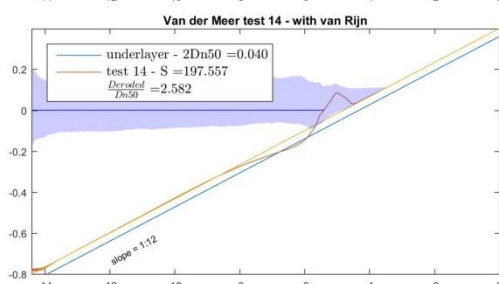
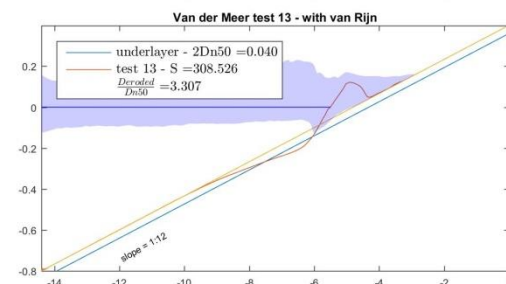
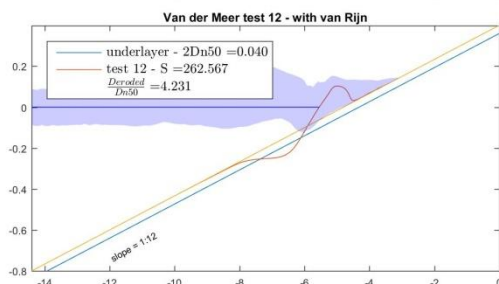
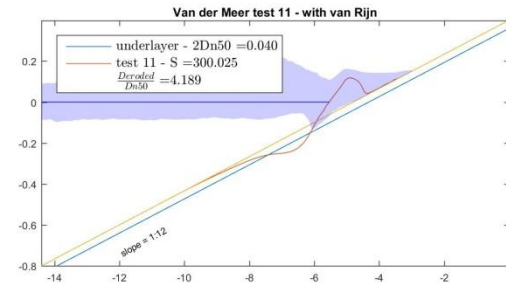
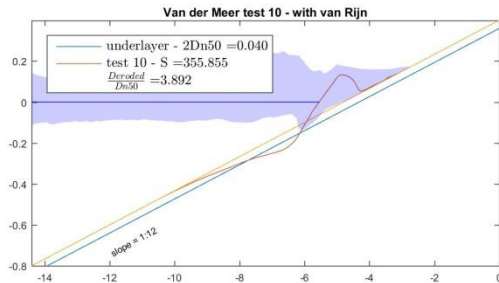
VAN RIJN [2007] - $D_{n50}=0.02m$ - 1:8 slope



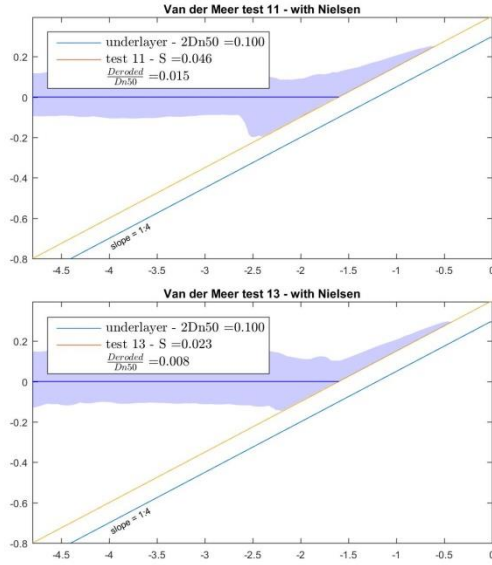
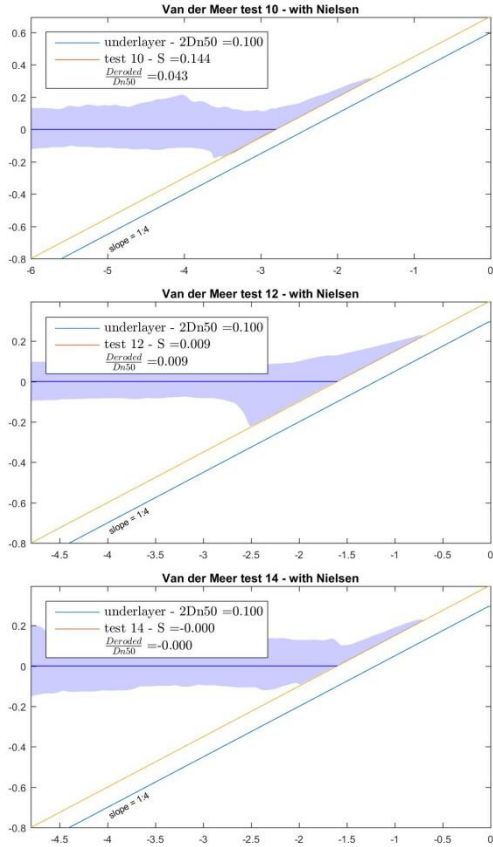
VAN RIJN [2007] - $D_{n50}=0.02m$ - 1:10 slope



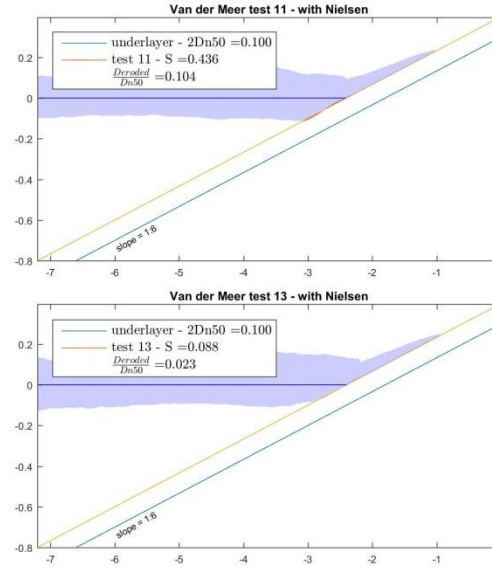
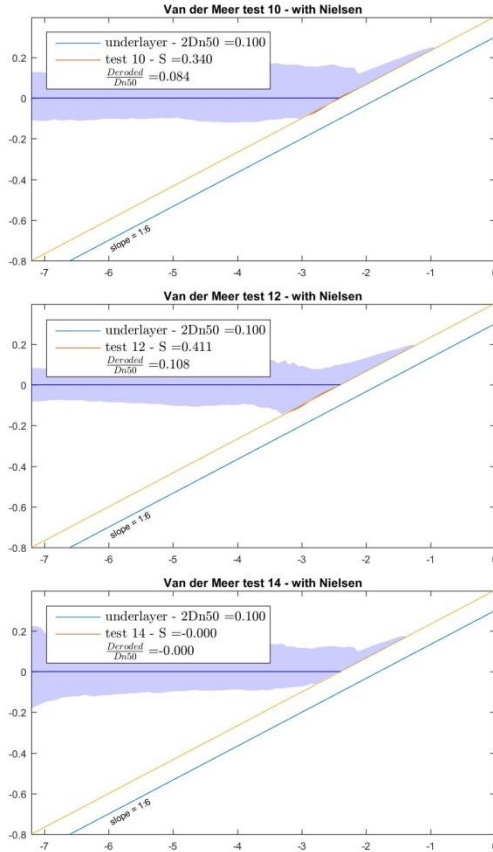
VAN RIJN [2007] - $D_{n50}=0.02m$ - 1:12 slope



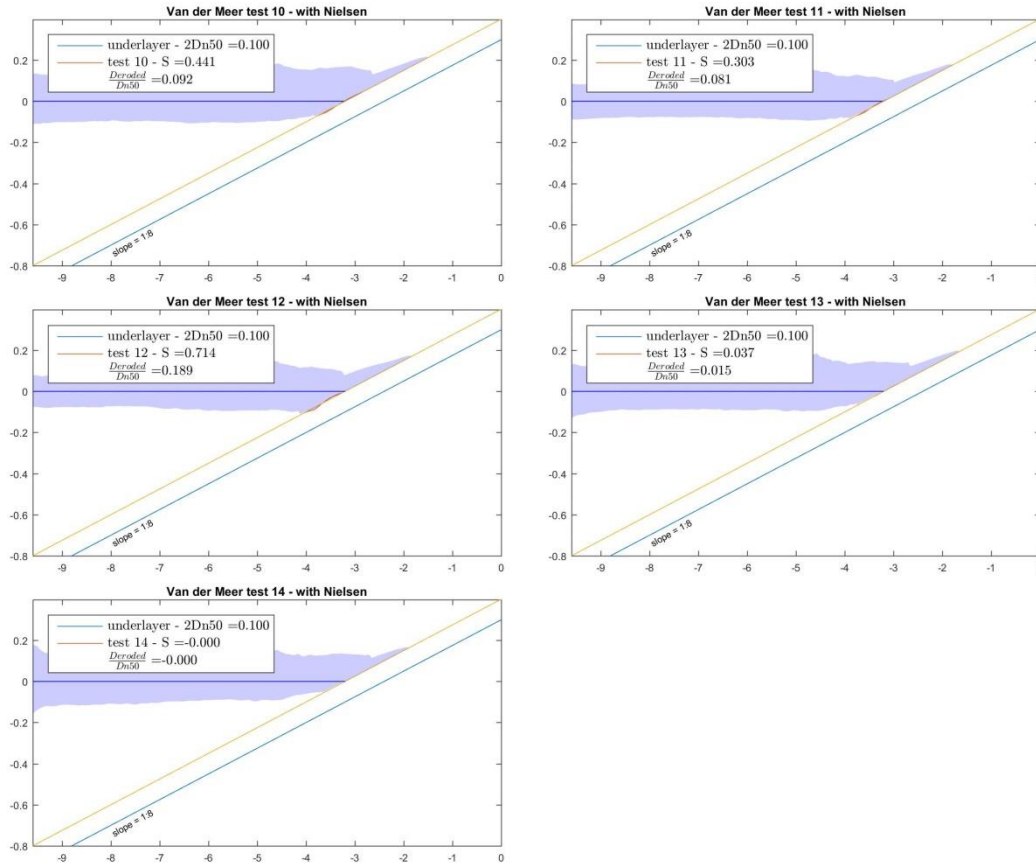
NIELSEN [2006] - Dn50=0.05m - 1:4 slope



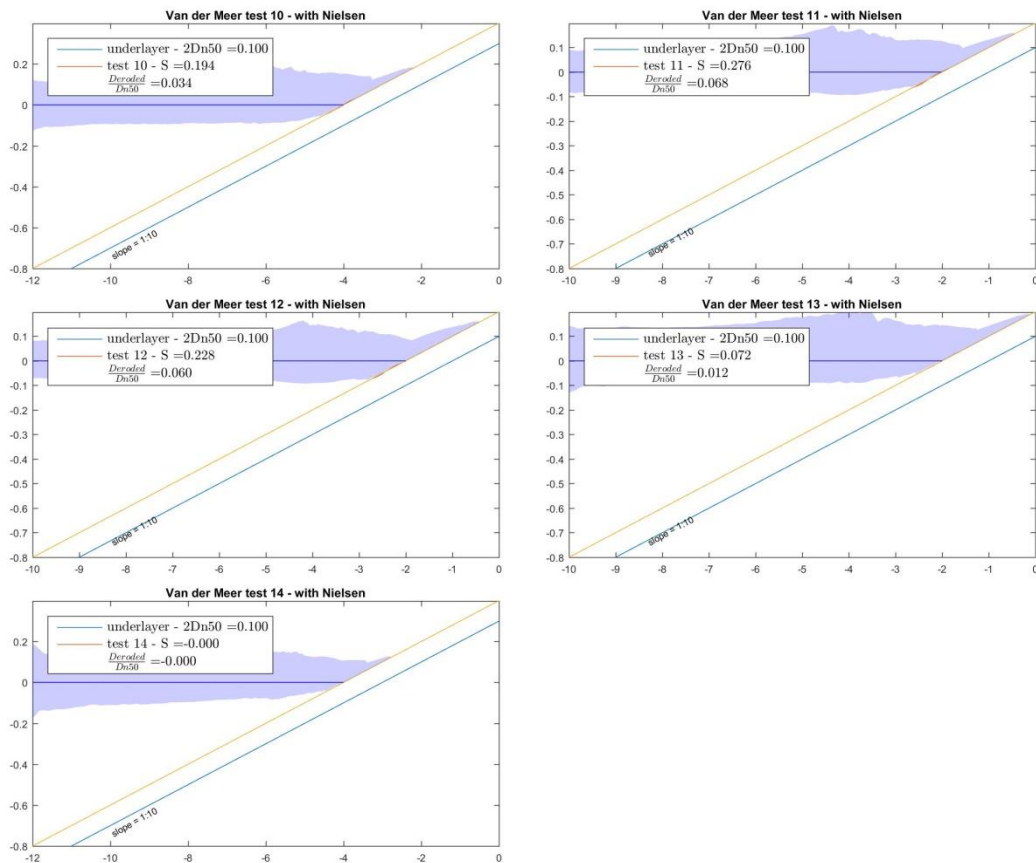
NIELSEN [2006] - Dn50=0.05m - 1:6 slope



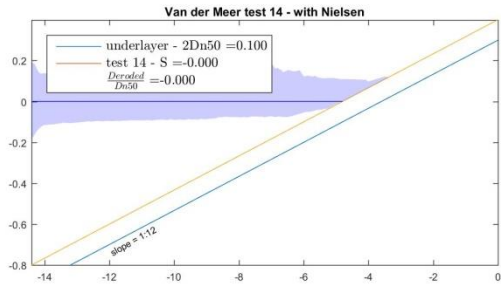
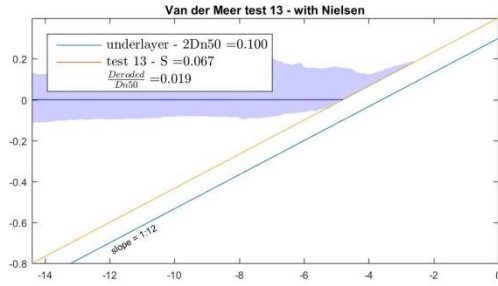
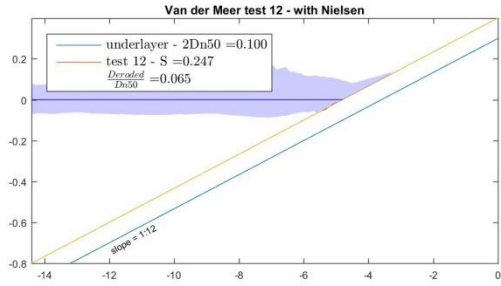
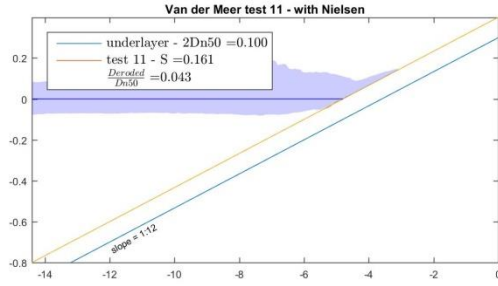
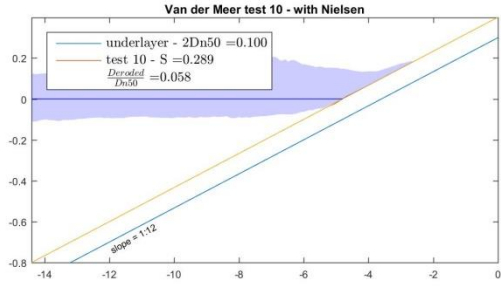
NIELSEN [2006] - Dn50=0.05m - 1:8 slope



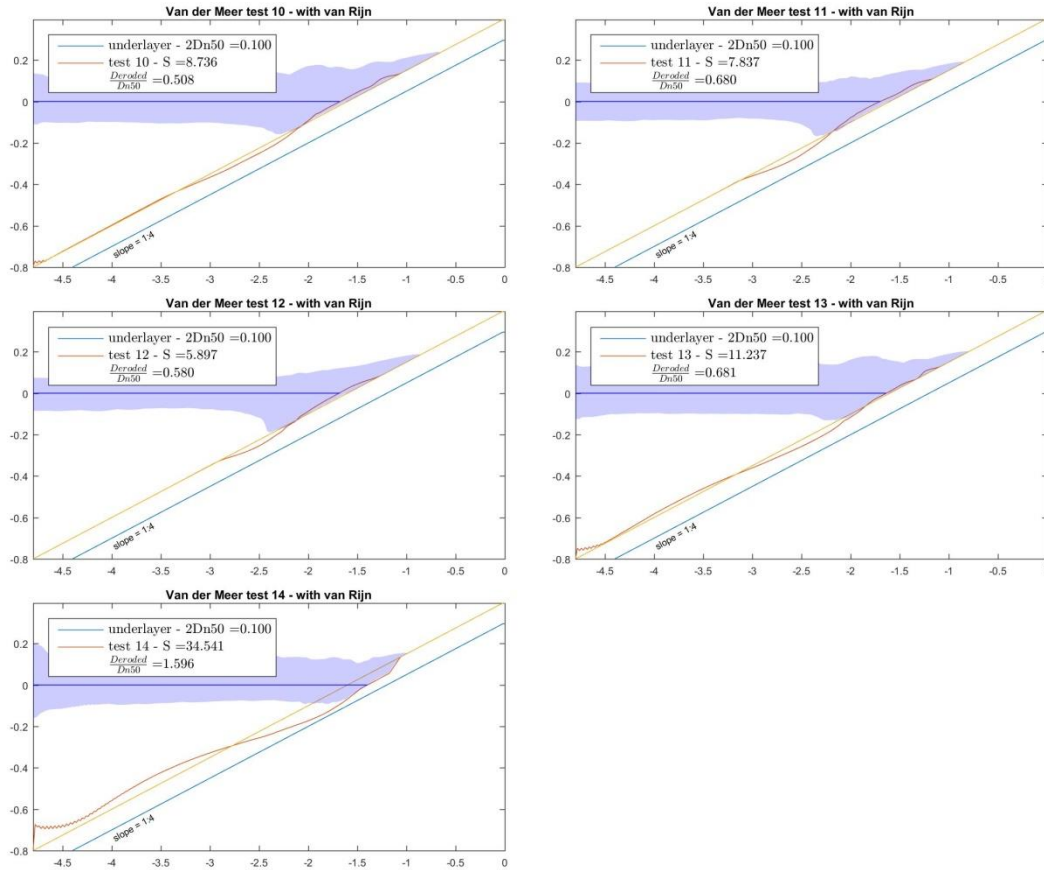
NIELSEN [2006] - Dn50=0.05m - 1:10 slope



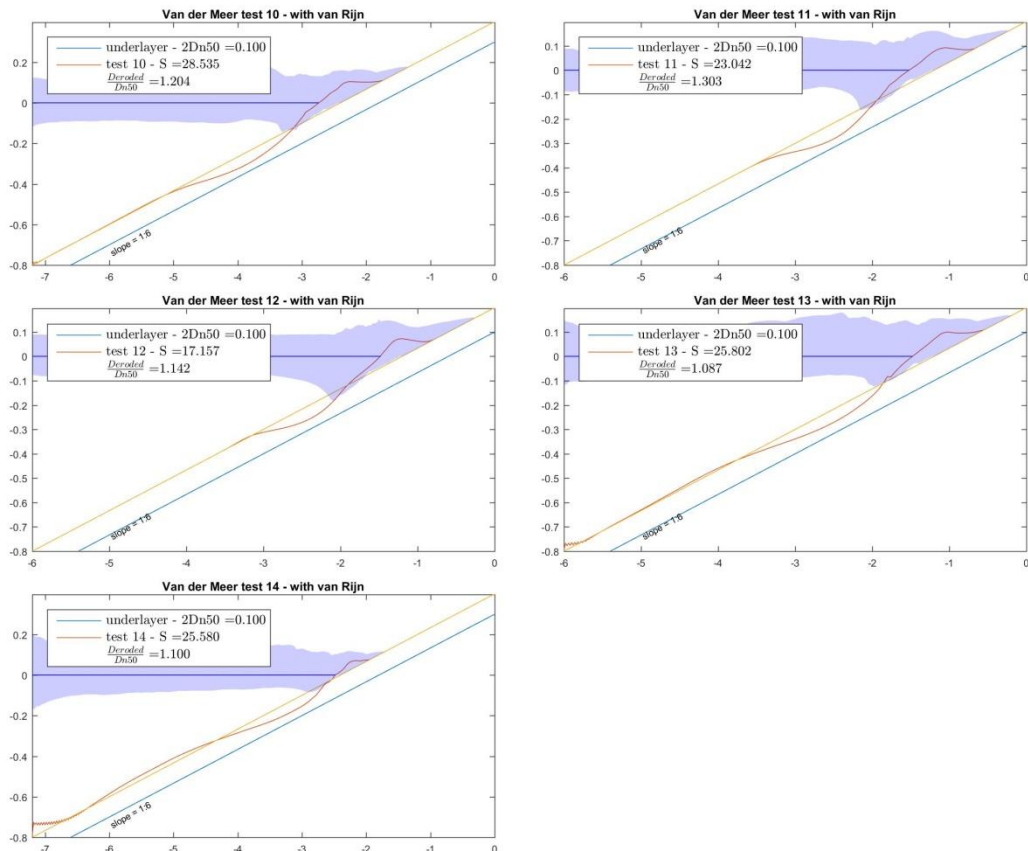
NIELSEN [2006] - Dn50=0.05m - 1:12 slope



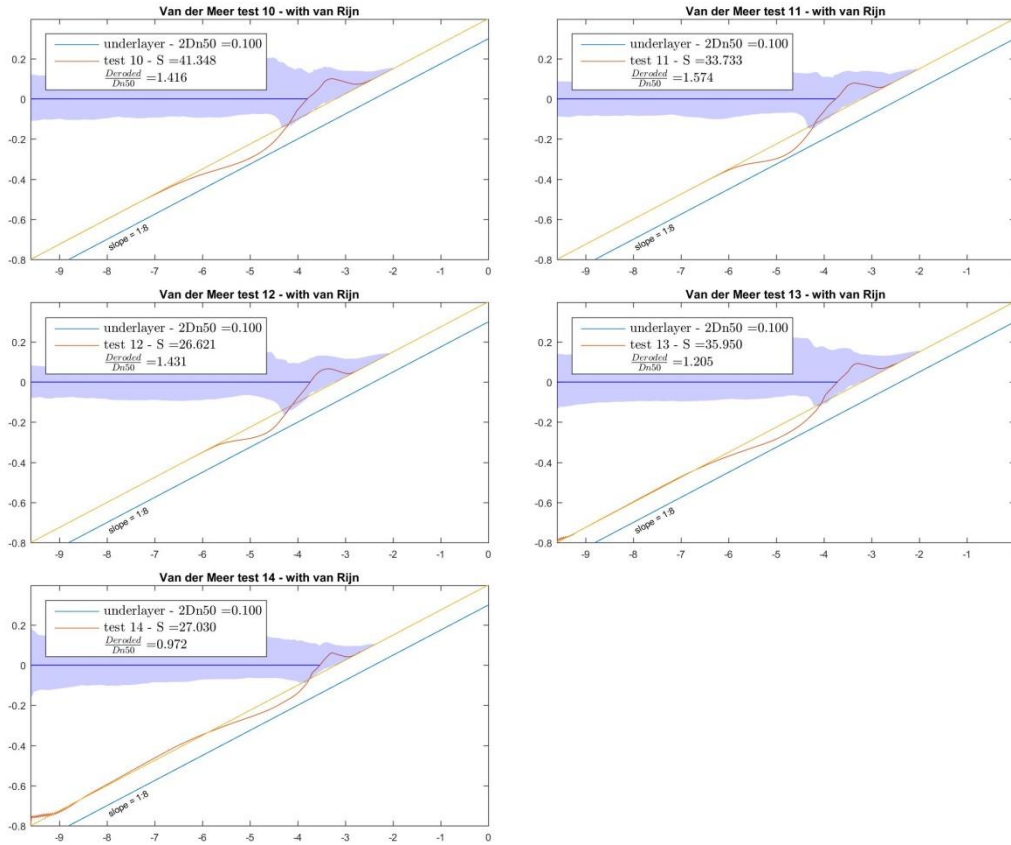
VAN RIJN [2007] - $Dn50=0.05m$ - 1:4 slope



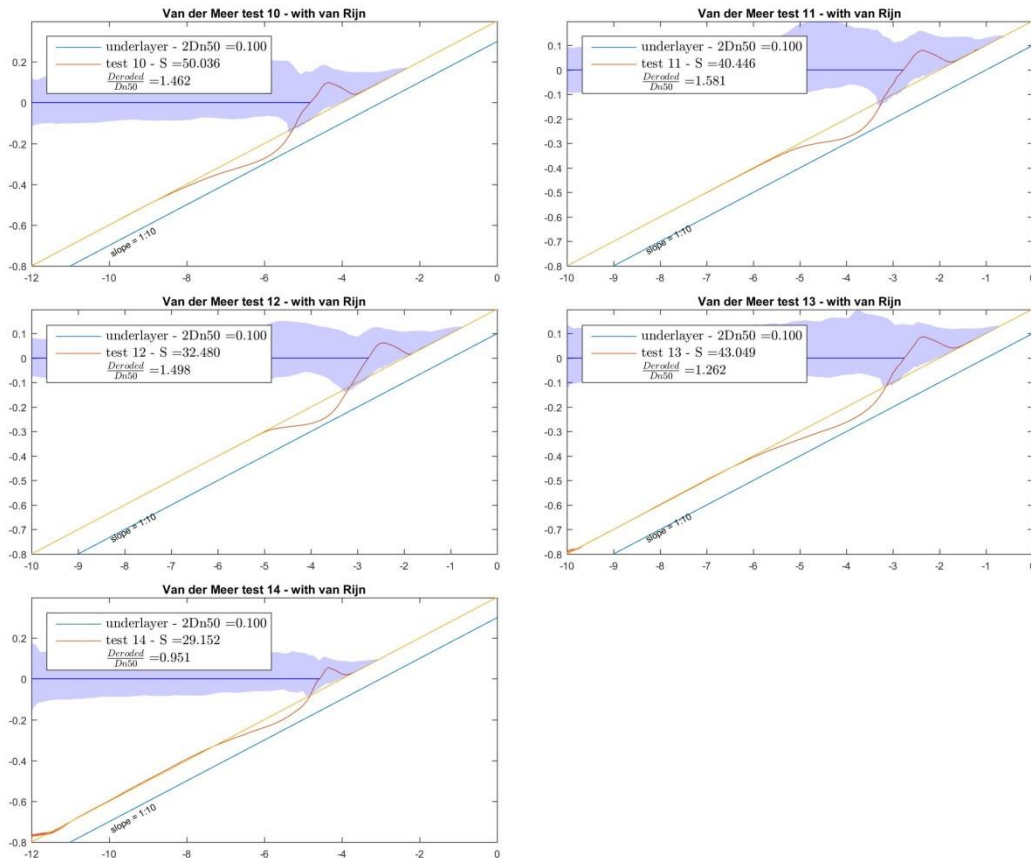
VAN RIJN [2007] - $Dn50=0.05m$ - 1:6 slope



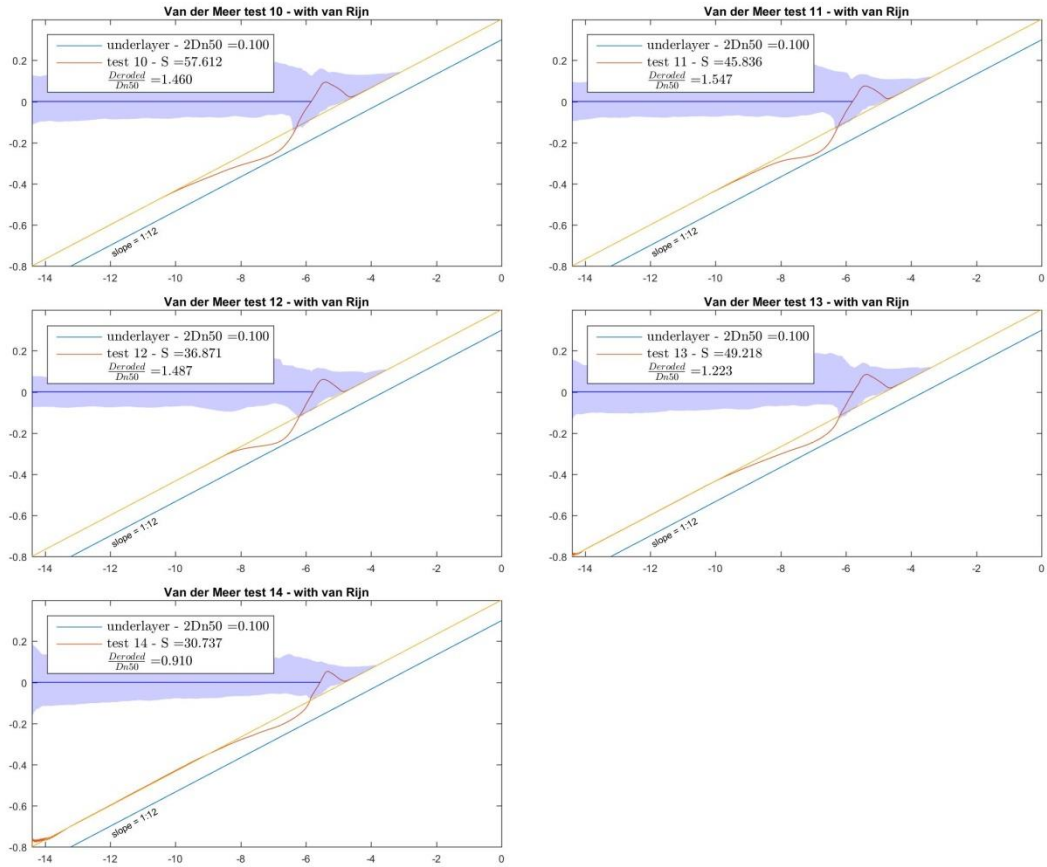
VAN RIJN [2007] - $D_{n50}=0.05m$ - 1:8 slope



VAN RIJN [2007] - $D_{n50}=0.05m$ - 1:10 slope



VAN RIJN [2007] - $D_{n50}=0.05m$ - 1:12 slope



6.3 Different Phase lag angle

6.3.1 Damage number

Erosion Depth										
VAN RIJN [2007]	Impermeable					homogeneous				
	1:4	1:6	1:8	1:10	1:12	1:4	1:6	1:8	1:10	1:12
Test 10 $\varphi = 35^\circ$										
Test 11 $\varphi = 35^\circ$										
Test 12 $\varphi = 35^\circ$										
Test 13 $\varphi = 35^\circ$										
Test 14 $\varphi = 35^\circ$										

NIELSEN [2006]	Impermeable					homogeneous				
	1:4	1:6	1:8	1:10	1:12	1:4	1:6	1:8	1:10	1:12
Test 10 $\varphi = 35^\circ$						14.98	55.81	27.95	24.95	24.86
Test 11 $\varphi = 35^\circ$						37.67	35.72	25.93	23.79	20.25
Test 12 $\varphi = 35^\circ$						3.90	18.31	24.96	27.34	22.78
Test 13 $\varphi = 35^\circ$						61.34	29.68	17.91	16.60	14.15
Test 14 $\varphi = 35^\circ$						3.58	4.43	3.05	1.30	0.85

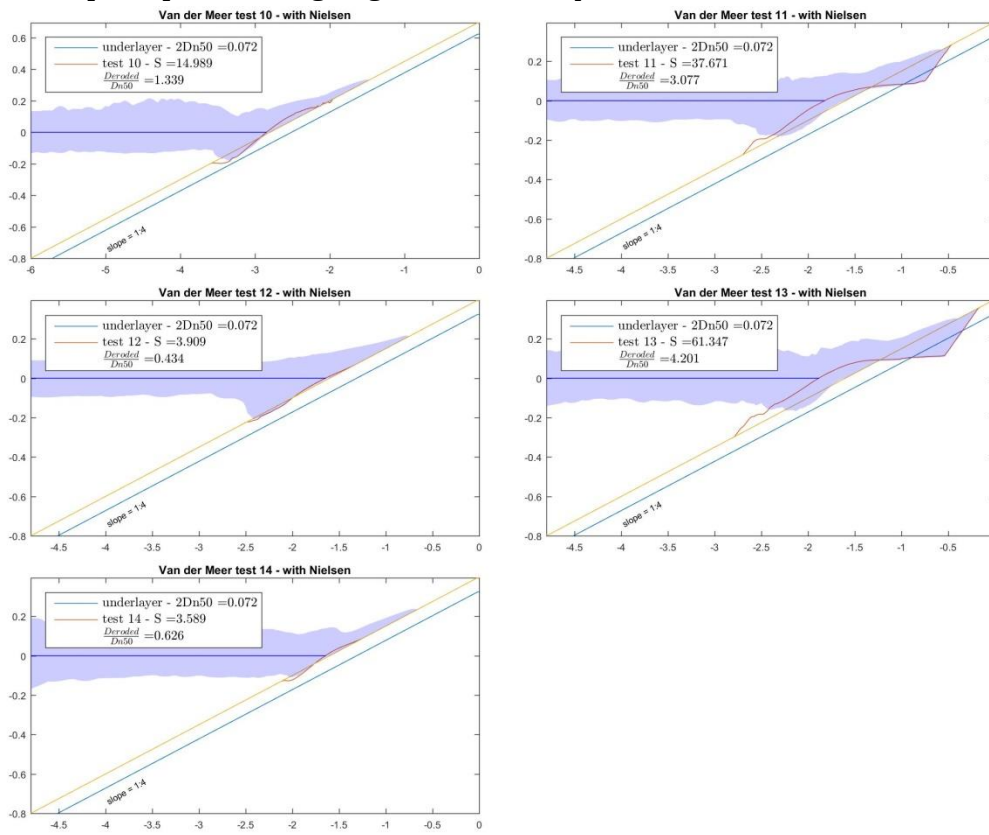
6.3.2 Relative Erosion Depth

Rel. erosion depth $\frac{d_e}{D_{n50}}$										
VAN RIJN [2007]	Impermeable					homogeneous				
	1:4	1:6	1:8	1:10	1:12	1:4	1:6	1:8	1:10	1:12
Test 10 $\varphi = 35^\circ$										
Test 11 $\varphi = 35^\circ$										
Test 12 $\varphi = 35^\circ$										
Test 13 $\varphi = 35^\circ$										
Test 14 $\varphi = 35^\circ$										

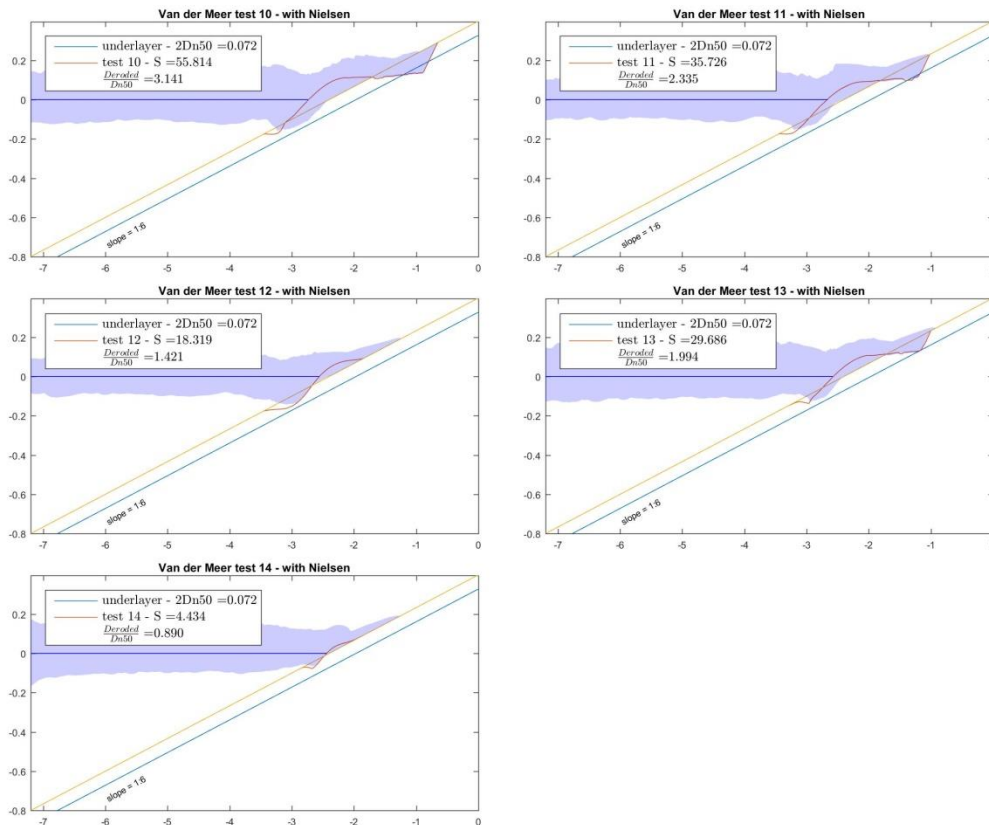
NIELSEN [2006]	Impermeable					homogeneous				
	1:4	1:6	1:8	1:10	1:12	1:4	1:6	1:8	1:10	1:12
Test 10 $\varphi = 35^\circ$						1.34	3.14	1.73	1.52	1.27
Test 11 $\varphi = 35^\circ$						3.08	2.34	1.60	1.41	1.13
Test 12 $\varphi = 35^\circ$						0.43	1.42	1.72	1.57	1.23
Test 13 $\varphi = 35^\circ$						4.20	1.99	1.33	1.19	0.97
Test 14 $\varphi = 35^\circ$						0.63	0.89	0.56	0.18	0.12

6.3.3 Formed erosion profile

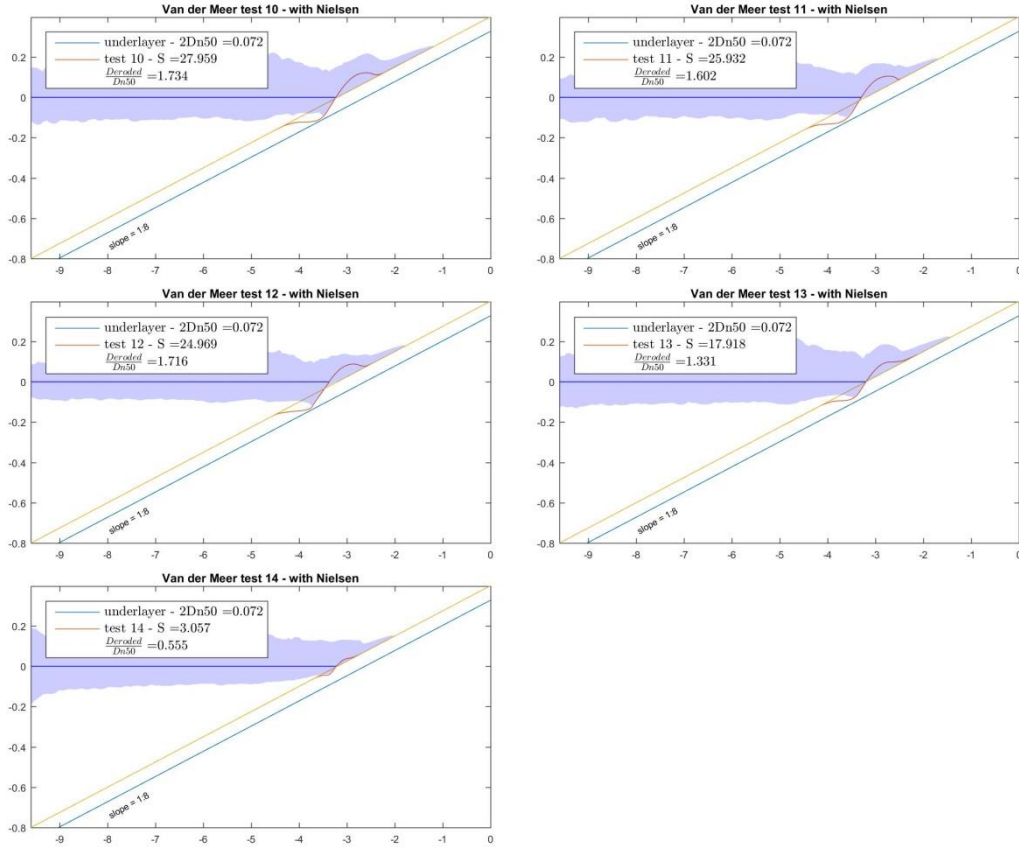
NIELSEN [2006] - Phase lag angle =35 - 1:4 slope



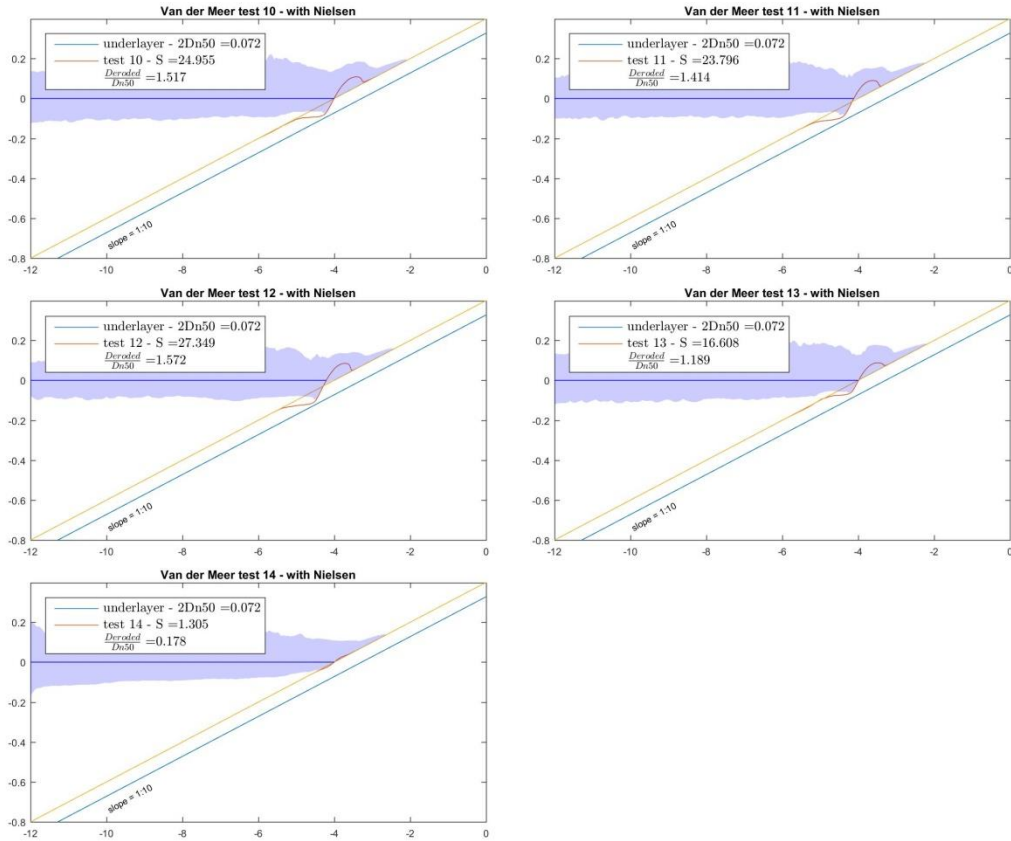
NIELSEN [2006] - Phase lag angle =35 - 1:6 slope



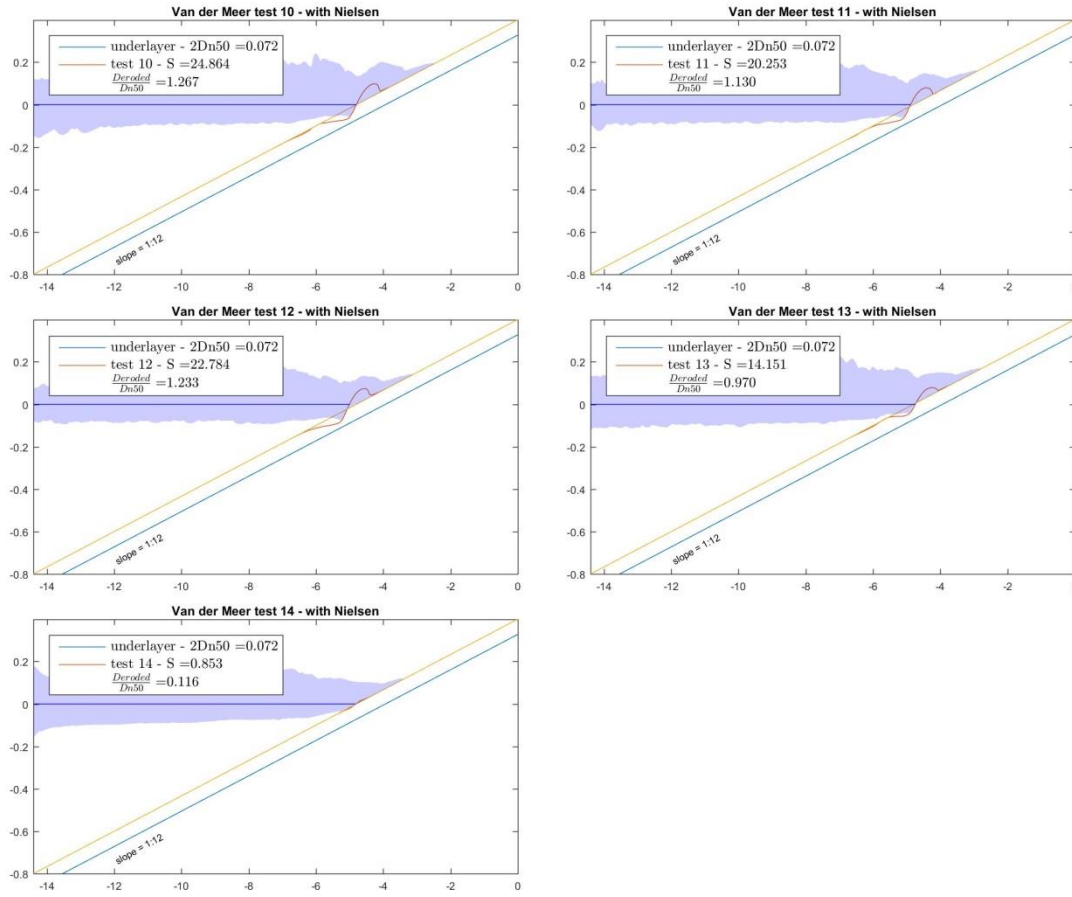
NIELSEN [2006] - Phase lag angle =35 - 1:8 slope



NIELSEN [2006] - Phase lag angle =35 - 1:10 slope



NIELSEN [2006] - Phase lag angle =35 - 1:12 slope



6.4 Different Phase lag angle run 2

6.4.1 Damage number

Erosion Depth										
VAN RIJN [2007]	Impermeable					homogeneous				
	1:4	1:6	1:8	1:10	1:12	1:4	1:6	1:8	1:10	1:12
Test 10 $\varphi = 35^\circ$										
Test 11 $\varphi = 35^\circ$										
Test 12 $\varphi = 35^\circ$										
Test 13 $\varphi = 35^\circ$										
Test 14 $\varphi = 35^\circ$										

NIELSEN [2006]	Impermeable					homogeneous				
	1:4	1:6	1:8	1:10	1:12	1:4	1:6	1:8	1:10	1:12
Test 10 $\varphi = 35^\circ$						56.31	43.13	28.53	24.26	
Test 11 $\varphi = 35^\circ$						30.03	32.43	27.31	24.22	
Test 12 $\varphi = 35^\circ$						4.18	19.25	24.54	26.52	
Test 13 $\varphi = 35^\circ$						32.34	18.04	18.26	16.28	
Test 14 $\varphi = 35^\circ$						3.72	4.36	2.94	1.32	

6.4.2 Relative Erosion Depth

Rel. erosion depth $\frac{d_e}{D_{n50}}$										
VAN RIJN [2007]	Impermeable					homogeneous				
	1:4	1:6	1:8	1:10	1:12	1:4	1:6	1:8	1:10	1:12
Test 10 $\varphi = 35^\circ$										
Test 11 $\varphi = 35^\circ$										
Test 12 $\varphi = 35^\circ$										
Test 13 $\varphi = 35^\circ$										
Test 14 $\varphi = 35^\circ$										

NIELSEN [2006]	Impermeable					homogeneous				
	1:4	1:6	1:8	1:10	1:12	1:4	1:6	1:8	1:10	1:12
Test 10 $\varphi = 35^\circ$						3.87	2.46	1.75	1.41	
Test 11 $\varphi = 35^\circ$						2.62	2.01	1.71	1.46	
Test 12 $\varphi = 35^\circ$						0.38	1.63	1.60	1.49	
Test 13 $\varphi = 35^\circ$						2.89	1.55	1.38	1.14	
Test 14 $\varphi = 35^\circ$						0.61	0.83	0.53	0.19	

6.5 Different Hydraulic Conductivity

6.5.1 Damage number

Erosion Depth										
VAN RIJN [2007]	Impermeable					homogeneous				
	1:4	1:6	1:8	1:10	1:12	1:4	1:6	1:8	1:10	1:12
Test 10 $\varphi = 35^\circ$										
Test 11 $\varphi = 35^\circ$										
Test 12 $\varphi = 35^\circ$										
Test 13 $\varphi = 35^\circ$										
Test 14 $\varphi = 35^\circ$										

NIELSEN [2006]	Impermeable					homogeneous				
	1:4	1:6	1:8	1:10	1:12	1:4	1:6	1:8	1:10	1:12
Test 10 $\varphi = 35^\circ$						4.25	6.16	5.36	4.07	3.29
Test 11 $\varphi = 35^\circ$						1.97	4.80	5.19	3.70	2.21
Test 12 $\varphi = 35^\circ$						0.15	4.43	4.56	3.40	2.60
Test 13 $\varphi = 35^\circ$						1.92	3.06	2.50	1.34	0.91
Test 14 $\varphi = 35^\circ$						0.01	0.02	0.03	0.00	0.00

6.5.2 Relative Erosion Depth

Rel. erosion depth $\frac{d_e}{D_{n50}}$										
VAN RIJN [2007]	Impermeable					homogeneous				
	1:4	1:6	1:8	1:10	1:12	1:4	1:6	1:8	1:10	1:12
Test 10 $\varphi = 35^\circ$										
Test 11 $\varphi = 35^\circ$										
Test 12 $\varphi = 35^\circ$										
Test 13 $\varphi = 35^\circ$										
Test 14 $\varphi = 35^\circ$										

NIELSEN [2006]	Impermeable					homogeneous				
	1:4	1:6	1:8	1:10	1:12	1:4	1:6	1:8	1:10	1:12
Test 10 $\varphi = 35^\circ$						0.61	0.86	0.69	0.53	-0.43
Test 11 $\varphi = 35^\circ$						0.37	0.67	0.70	0.51	-0.31
Test 12 $\varphi = 35^\circ$						0.03	0.61	0.66	0.50	-0.38
Test 13 $\varphi = 35^\circ$						0.36	0.44	0.36	0.15	-0.11
Test 14 $\varphi = 35^\circ$						0.00	0.01	0.01	0.00	0.00

Appendix G 1

Results Hydrodynamics

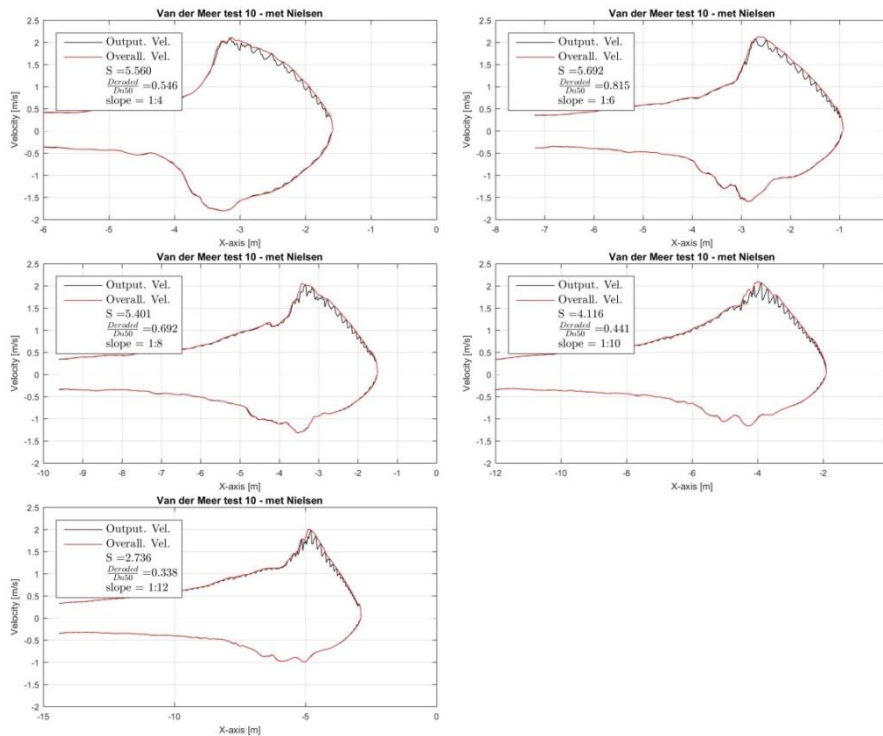
Test Series B

APPENDIX G.1: RESULTS

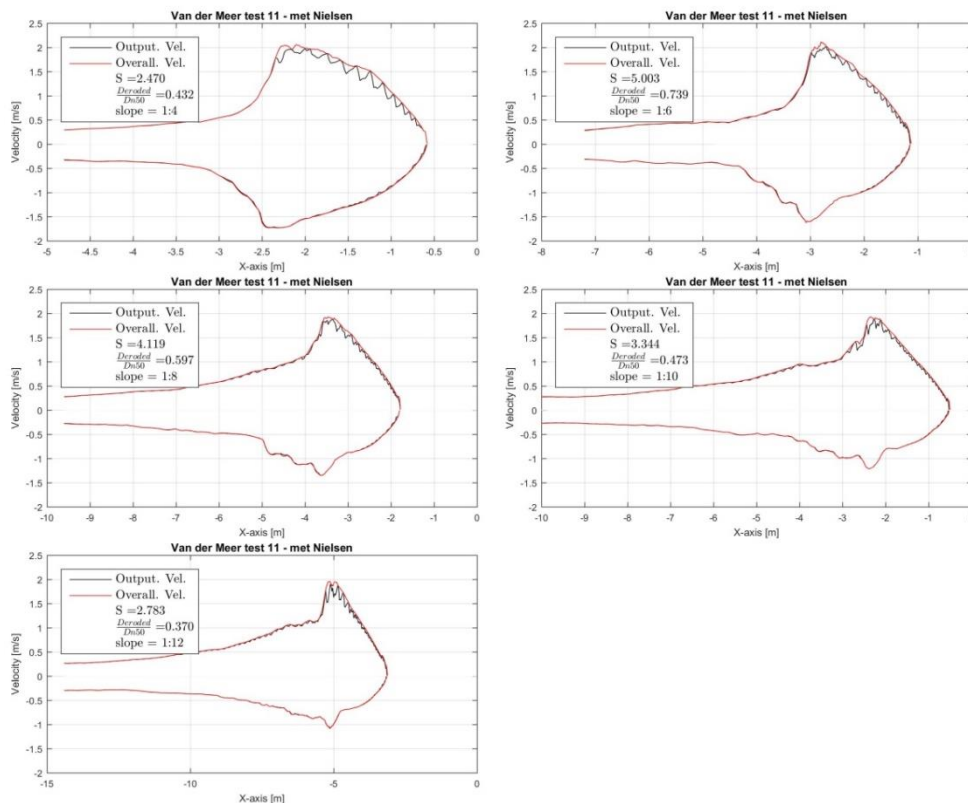
HYDRODYNAMICS – TEST SERIES B

7.1 Velocity

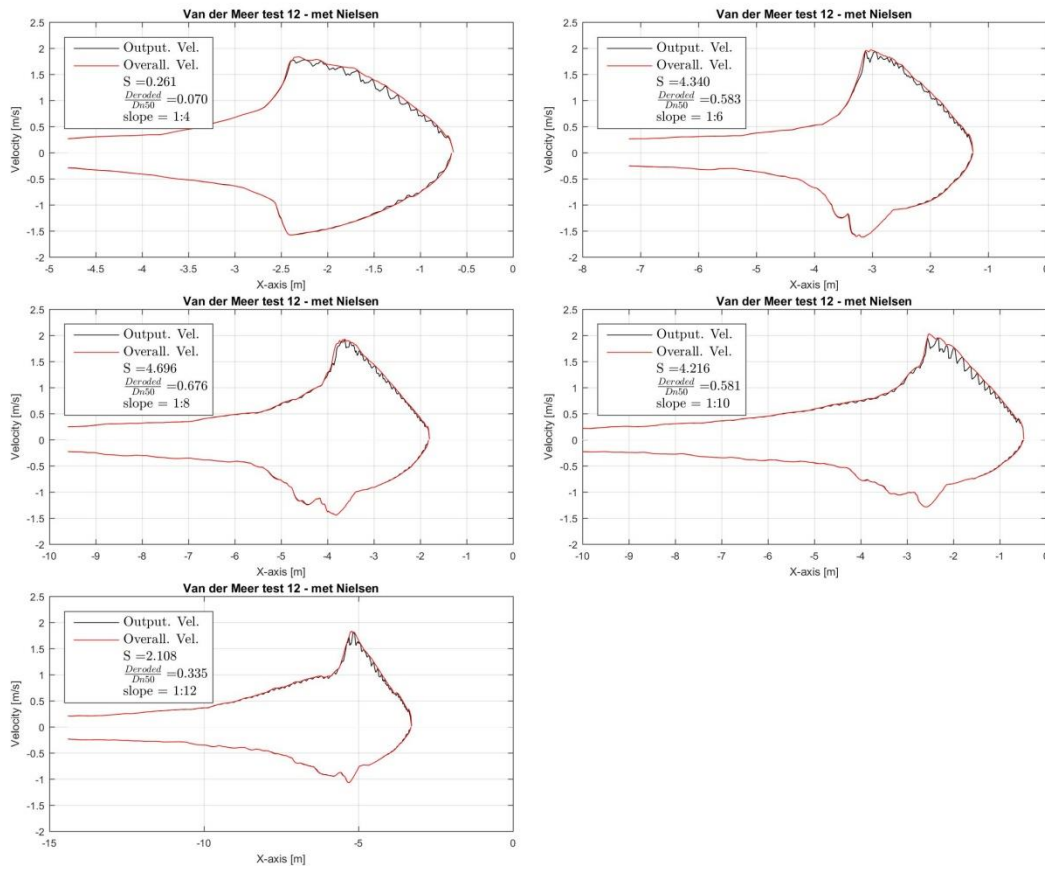
7.1.1 NIELSEN [2006] test 10 - velocity



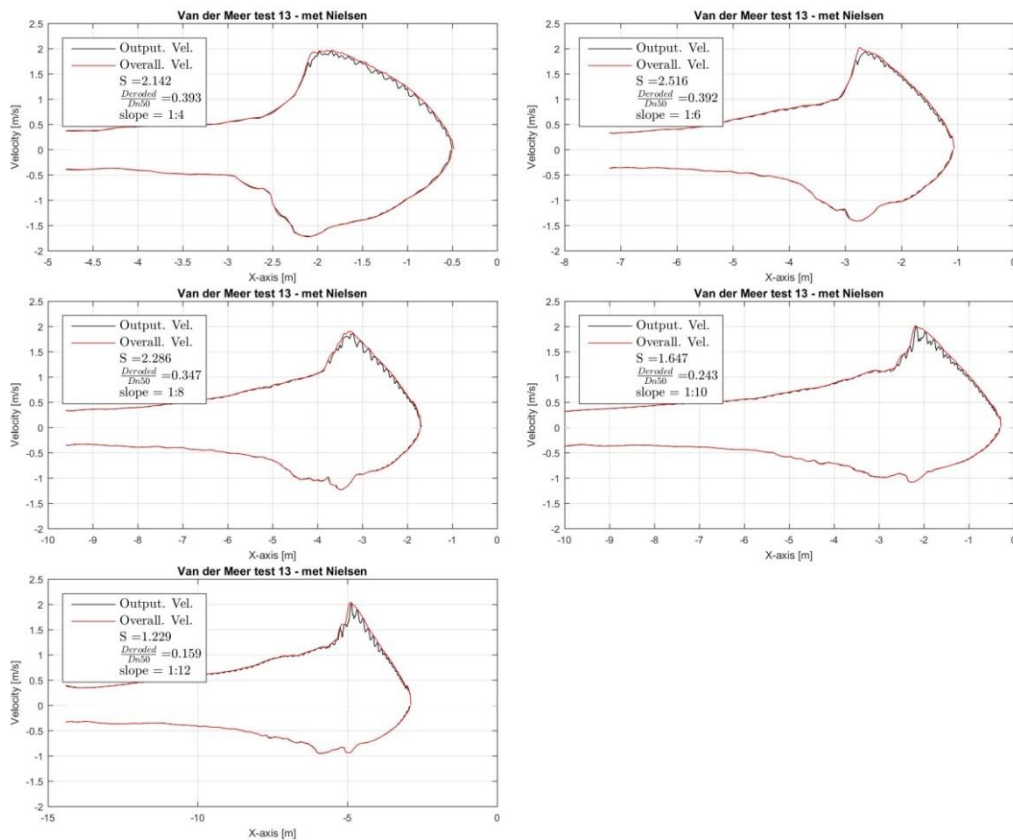
7.1.2 NIELSEN [2006] test 11 - velocity



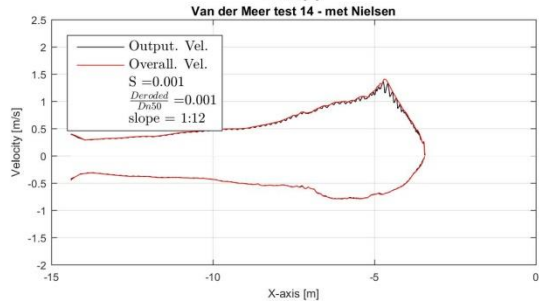
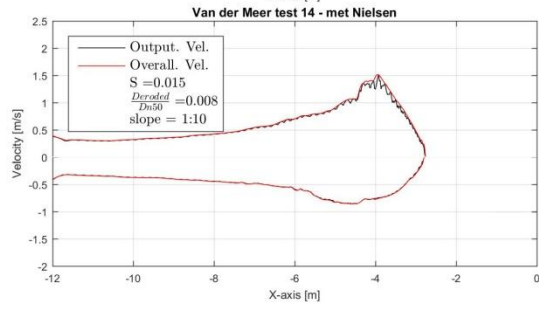
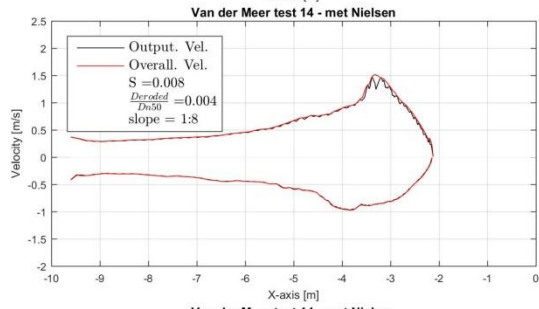
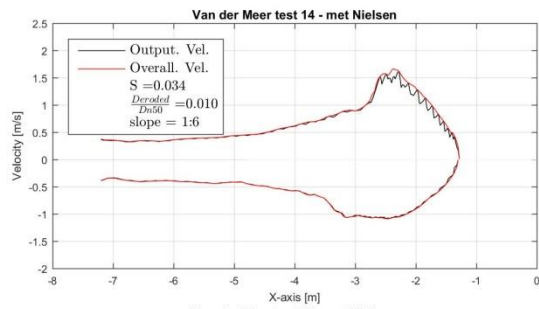
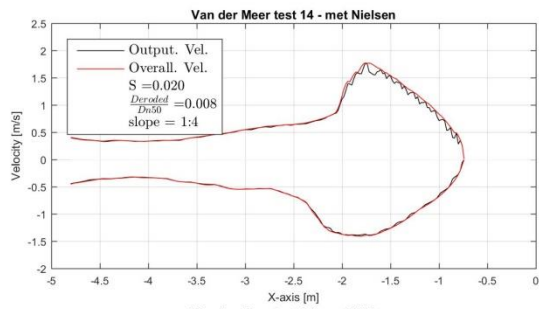
7.1.3 NIELSEN [2006] test 12 - velocity



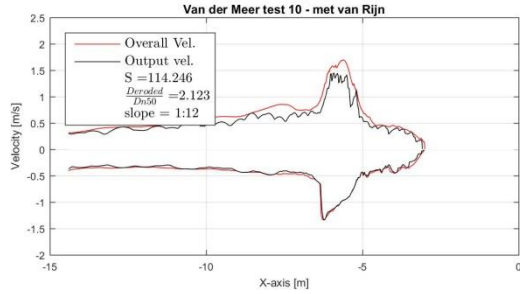
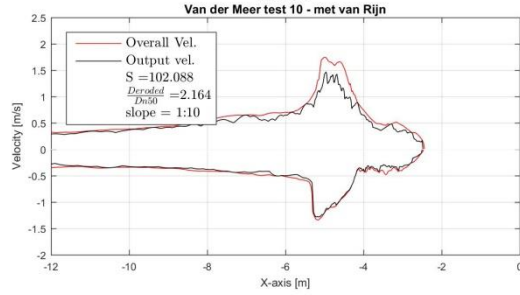
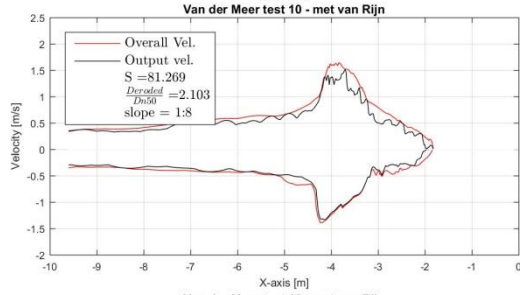
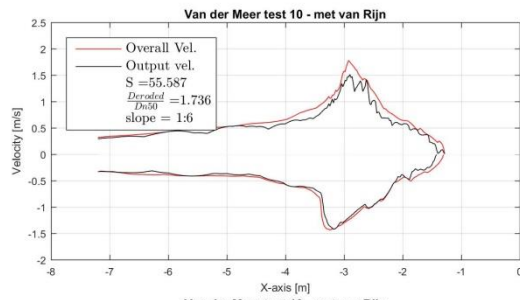
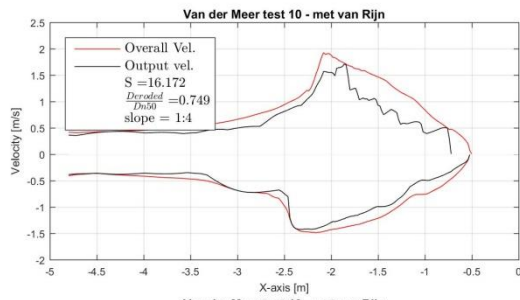
7.1.4 NIELSEN [2006] test 13 - velocity



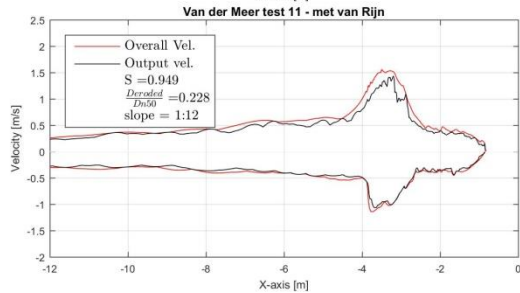
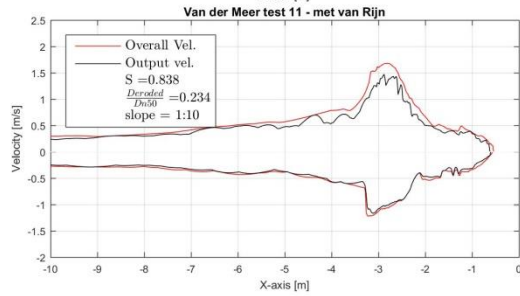
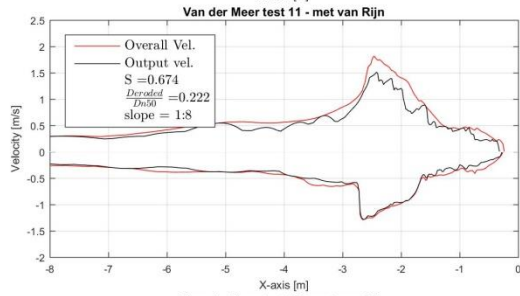
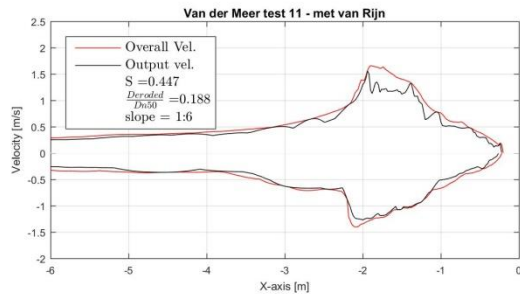
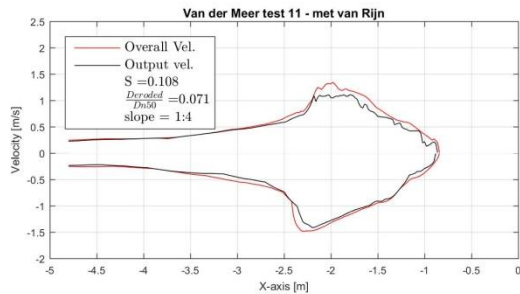
7.1.5 NIELSEN [2006] test 14 - velocity



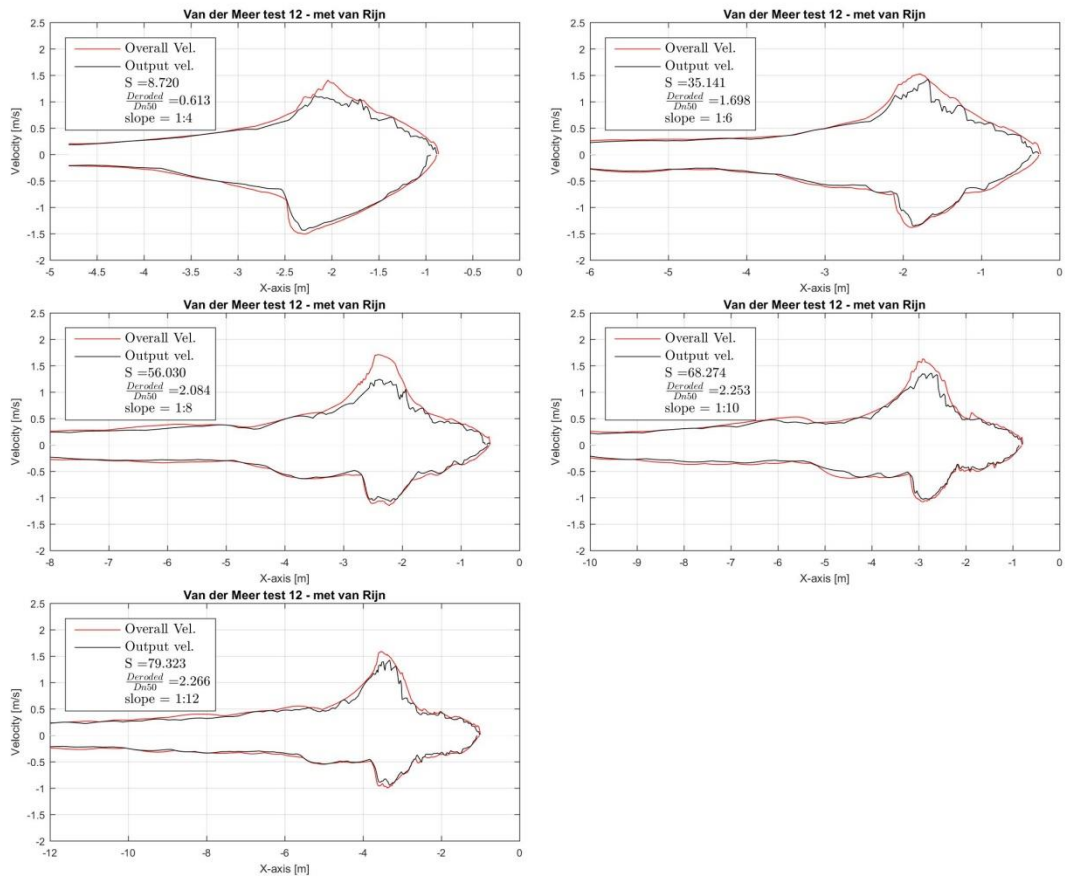
7.1.6 VAN RIJN [2007] test 10 - velocity



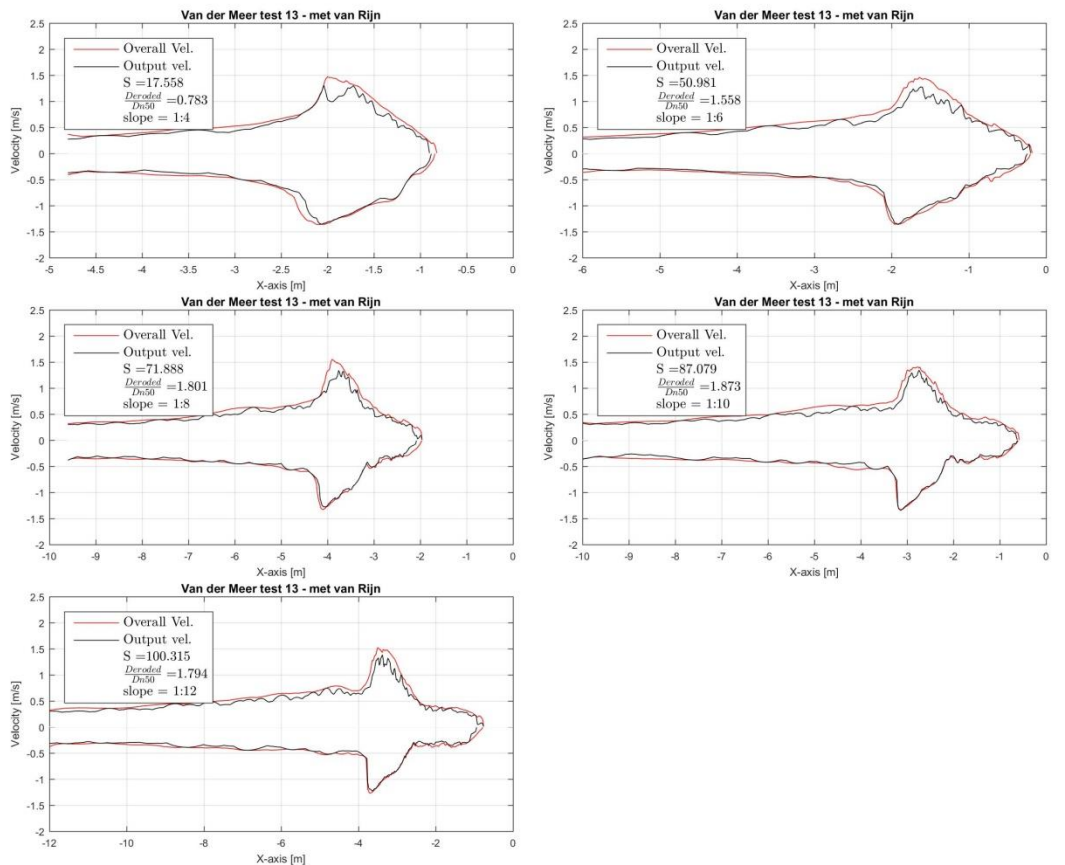
7.1.7 VAN RIJN [2007] test 11 - velocity



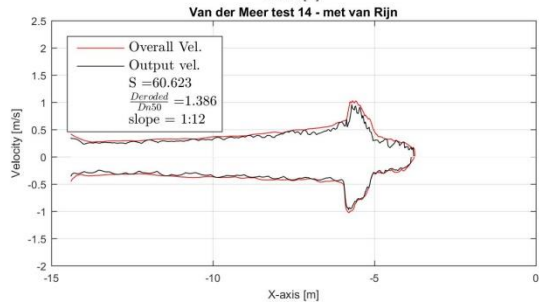
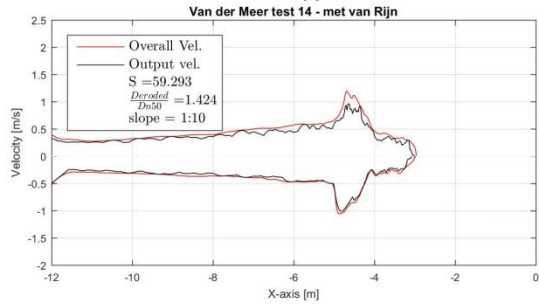
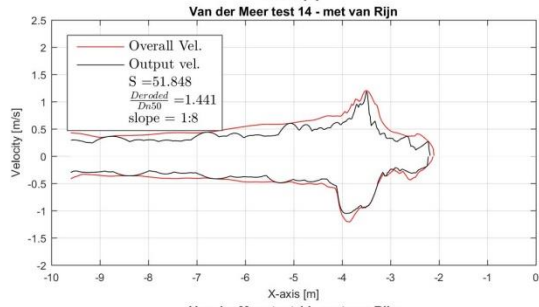
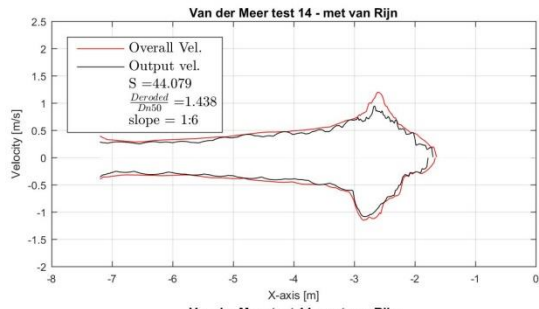
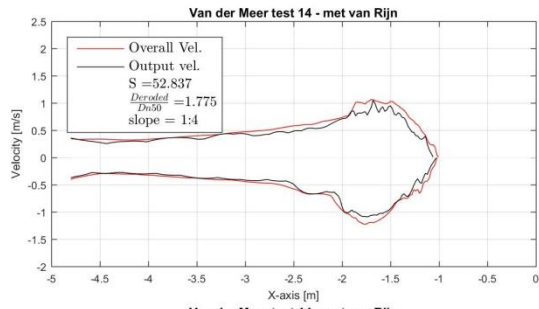
7.1.8 VAN RIJN [2007] test 12 - velocity



7.1.9 VAN RIJN [2007] test 13 - velocity

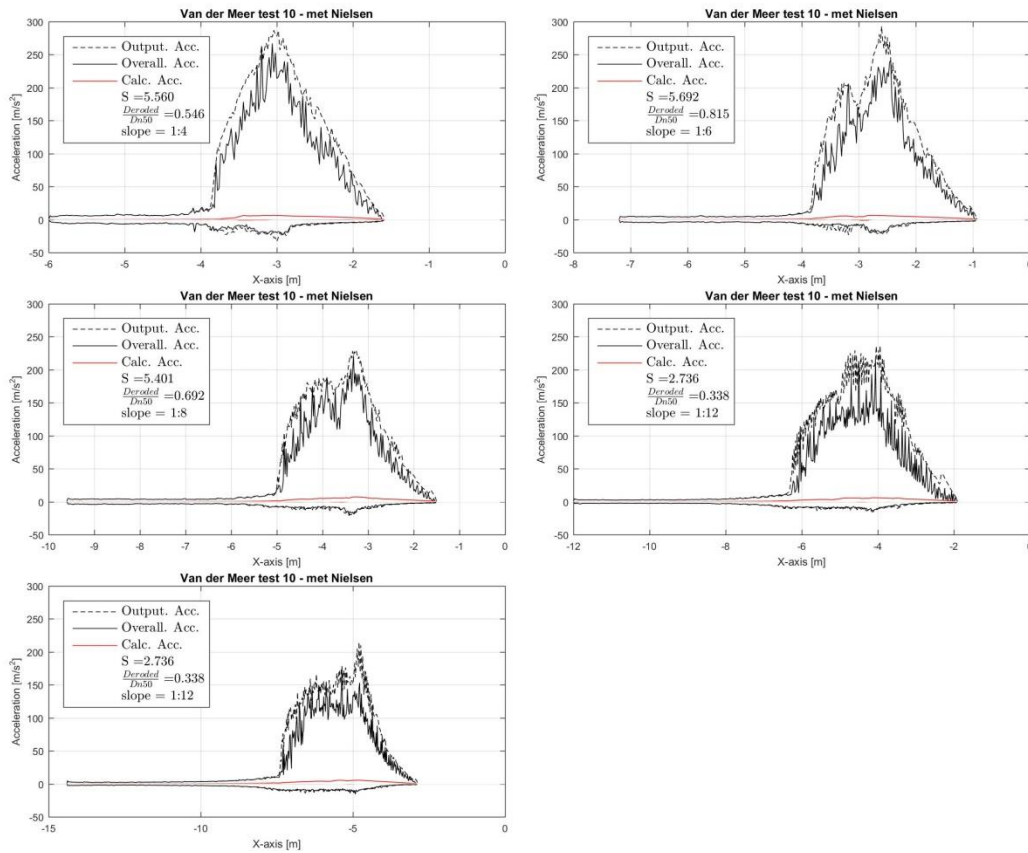


7.1.10 VAN RIJN [2007] test 14 - velocity

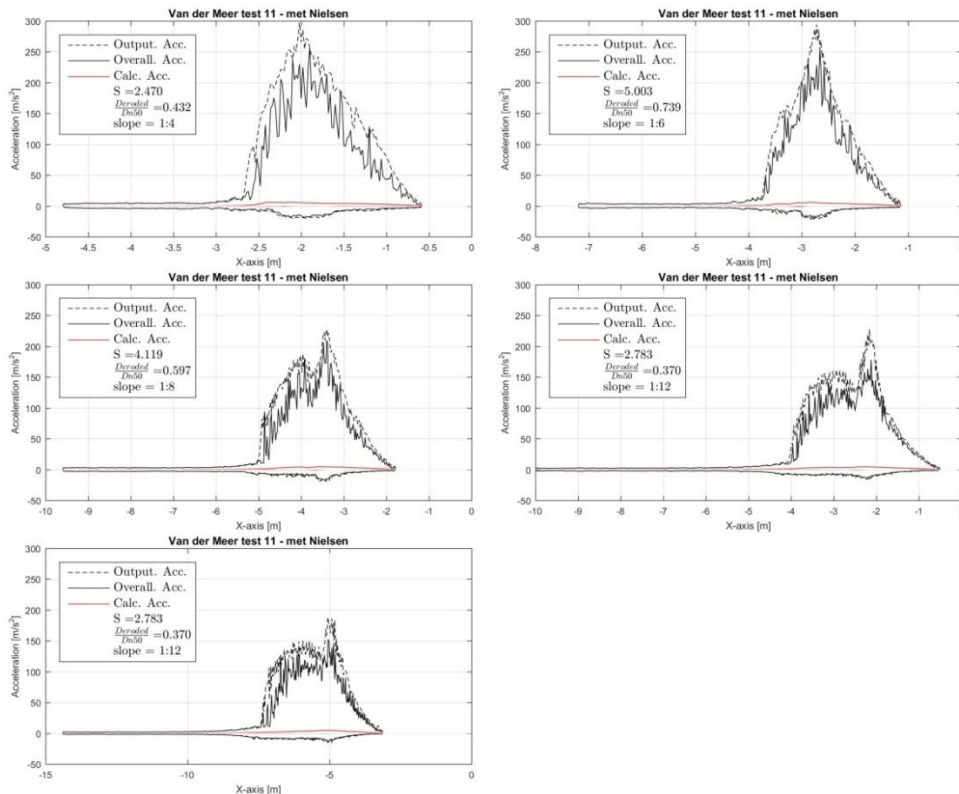


7.2 Acceleration

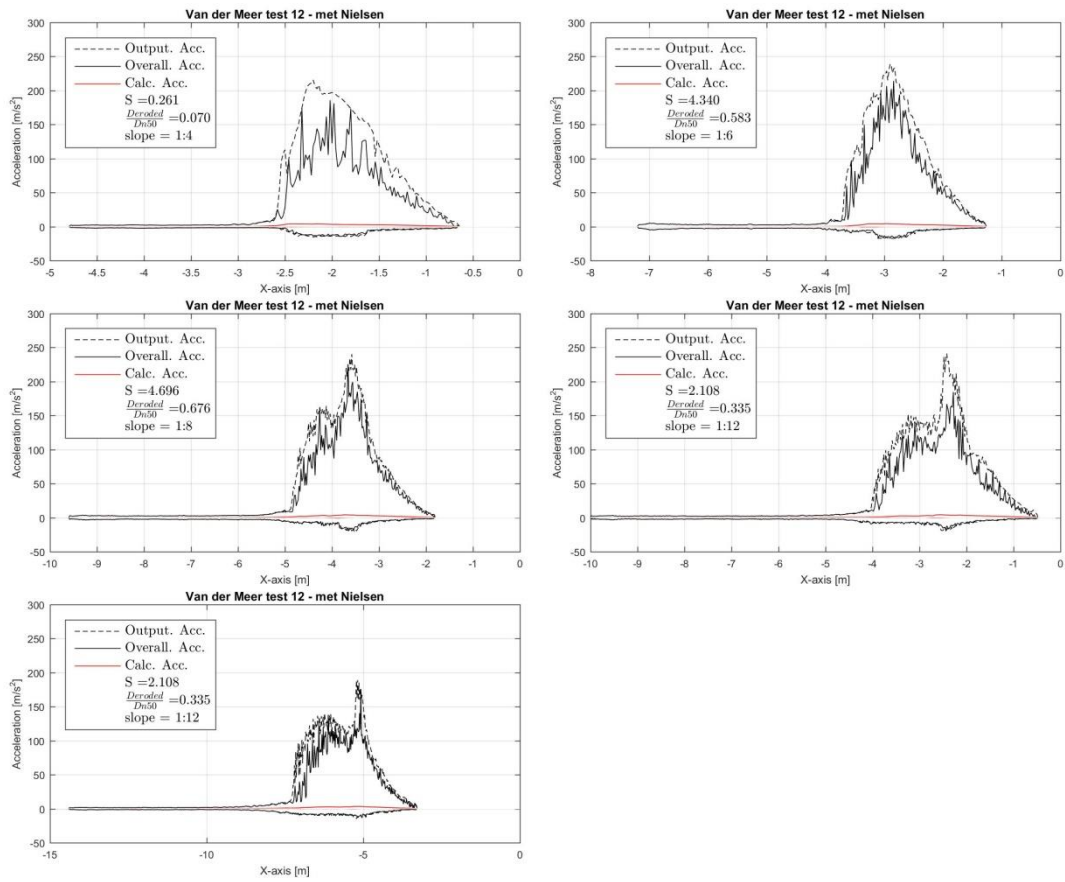
7.2.1 NIELSEN [2006] test 10 - Acceleration



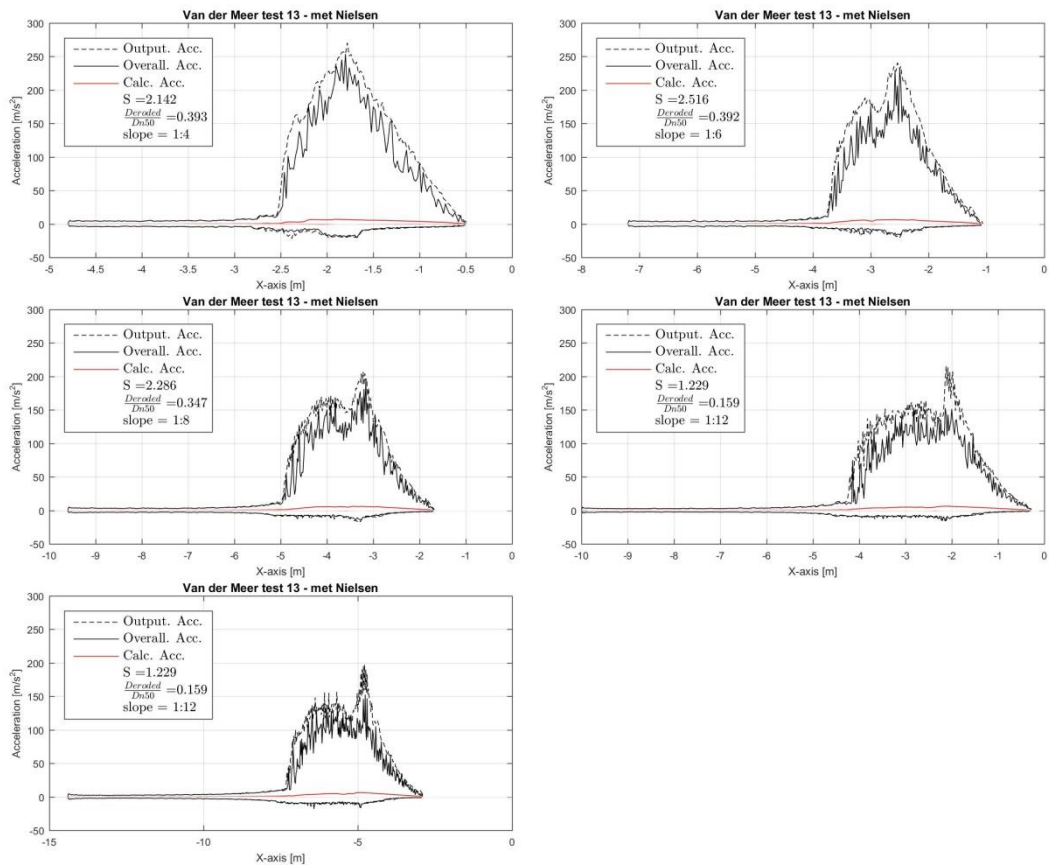
7.2.2 NIELSEN [2006] test 11 - Acceleration



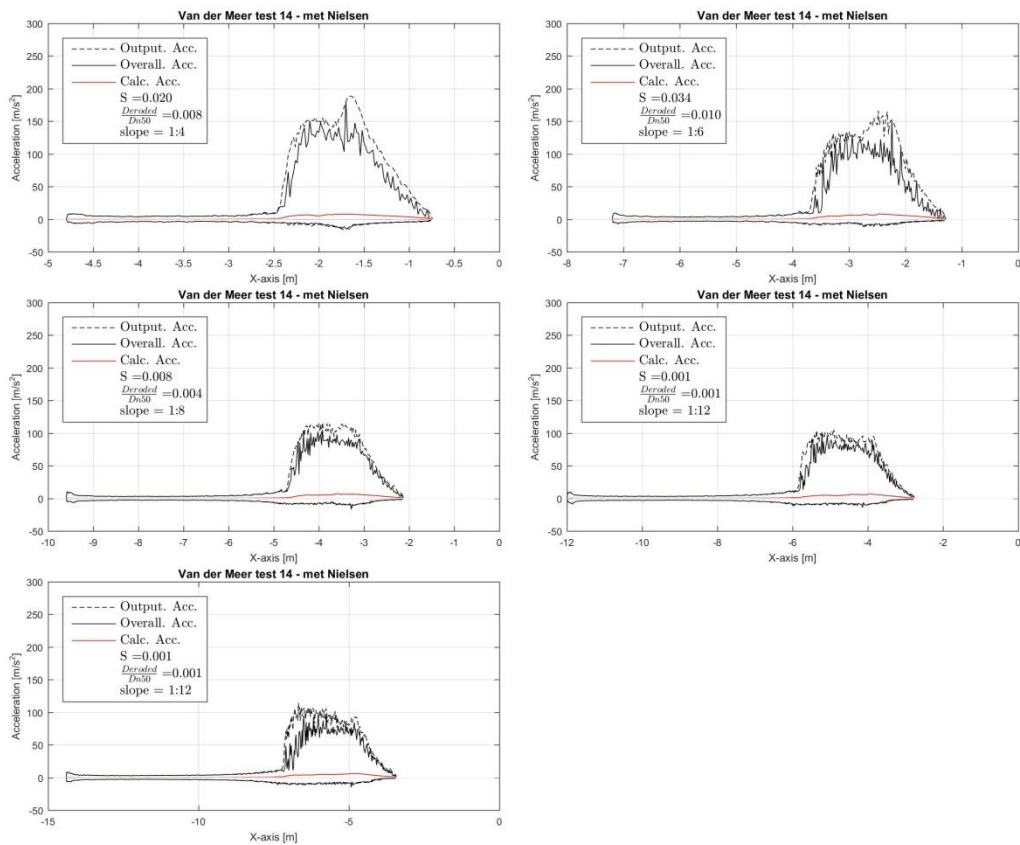
7.2.3 NIELSEN [2006] test 12 - Acceleration



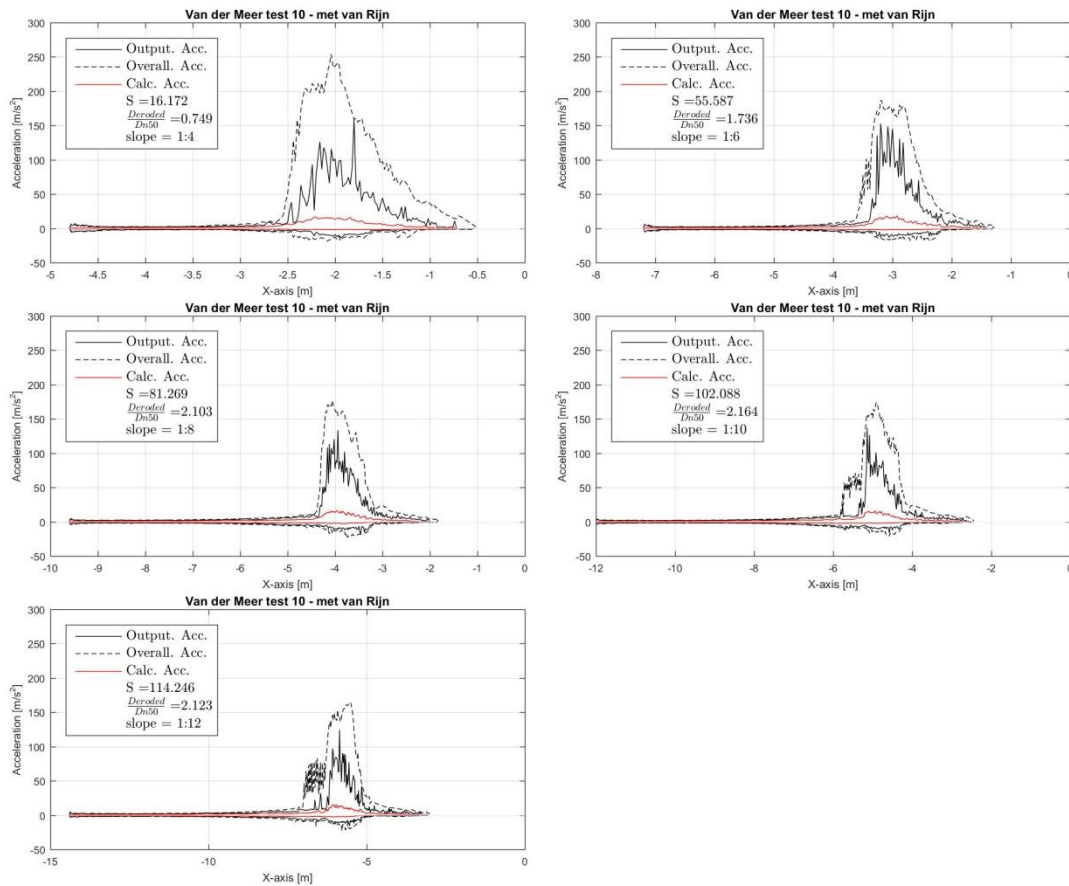
7.2.4 NIELSEN [2006] test 13 - Acceleration



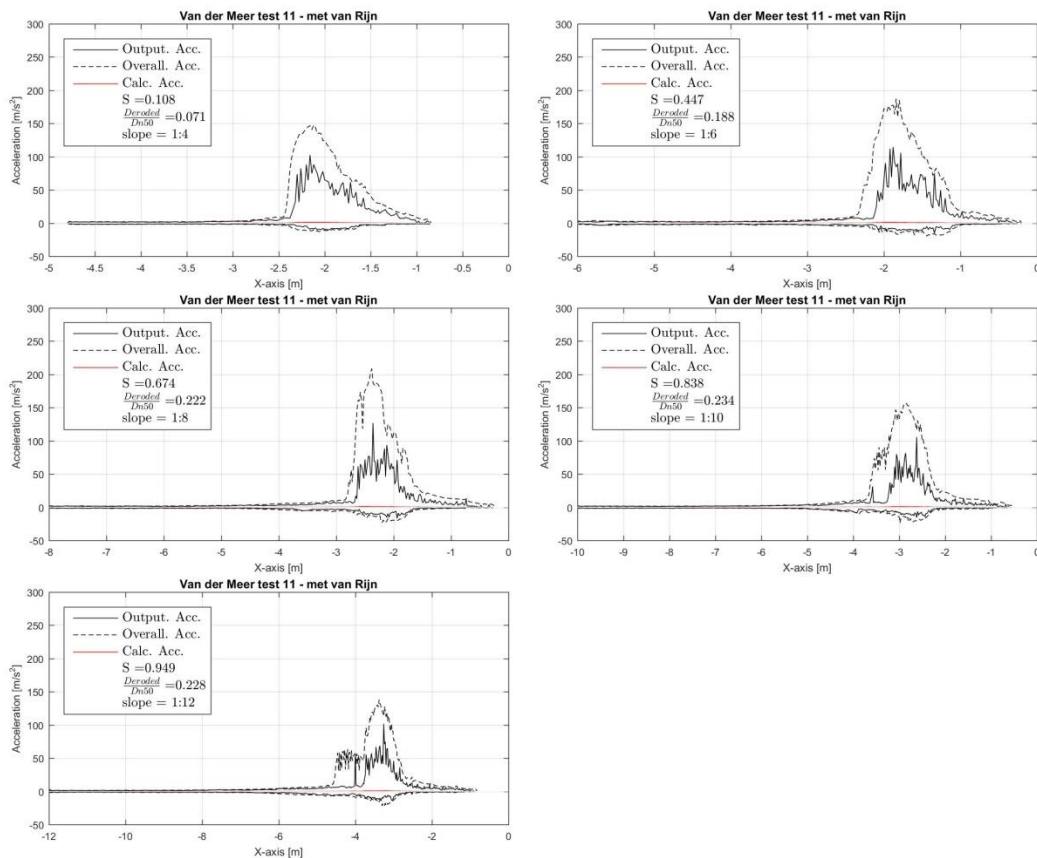
7.2.5 NIELSEN [2006] test 14 - Acceleration



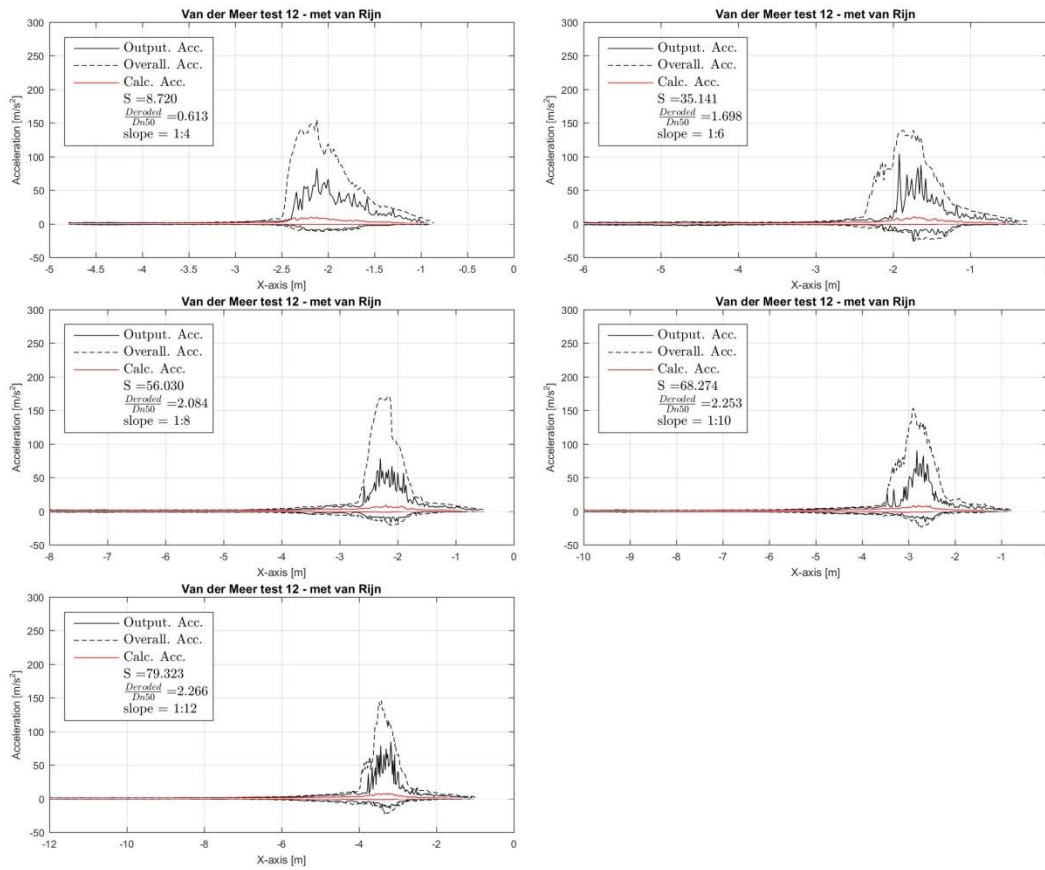
7.2.6 VAN RIJN [2007] test 10 - Acceleration



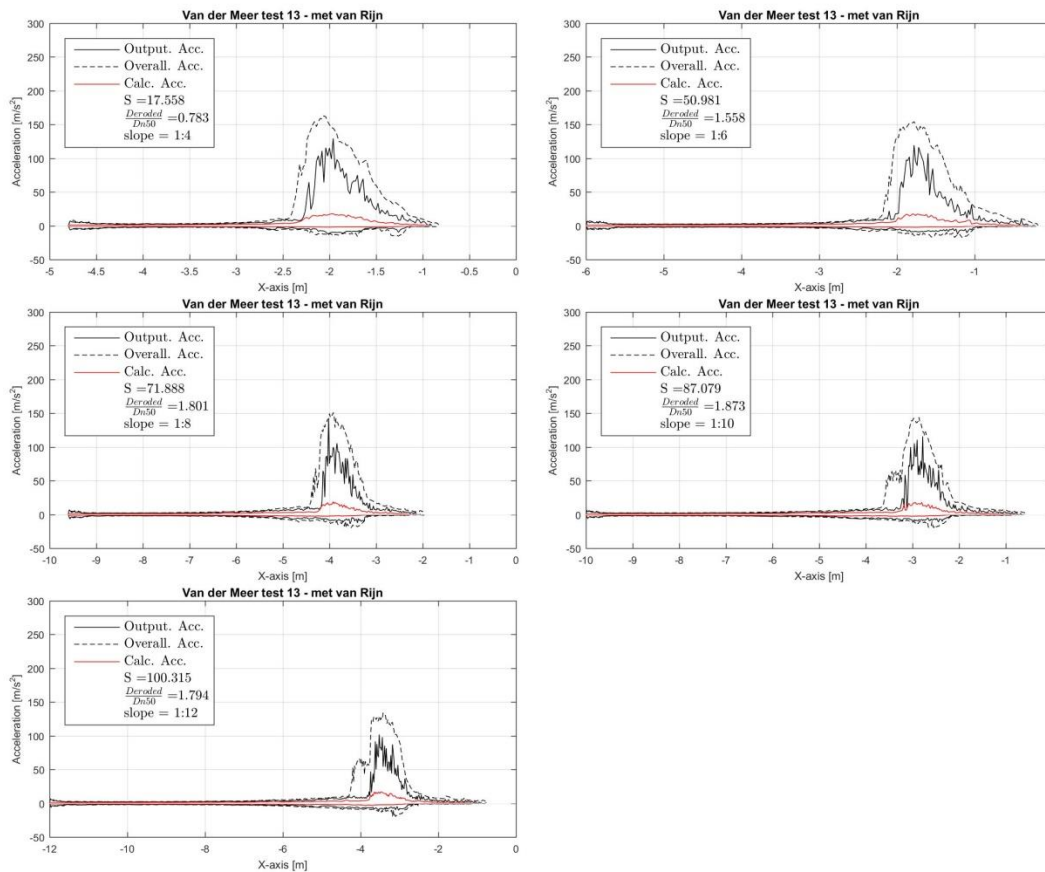
7.2.7 VAN RIJN [2007] test 11 - Acceleration



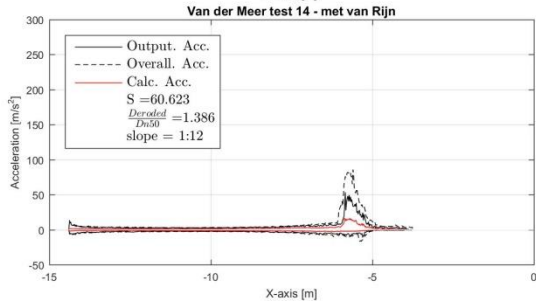
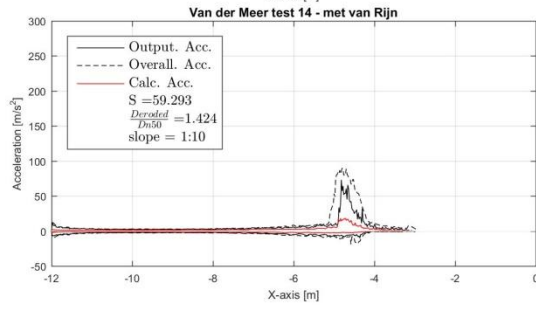
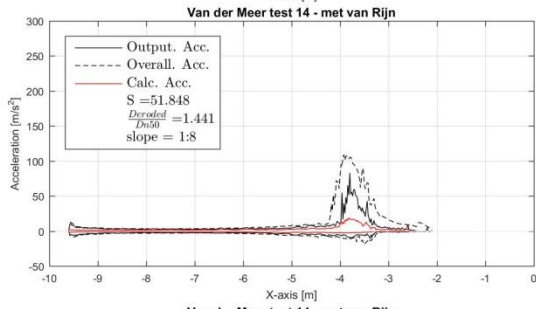
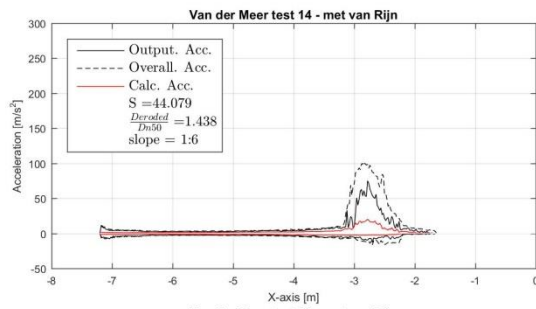
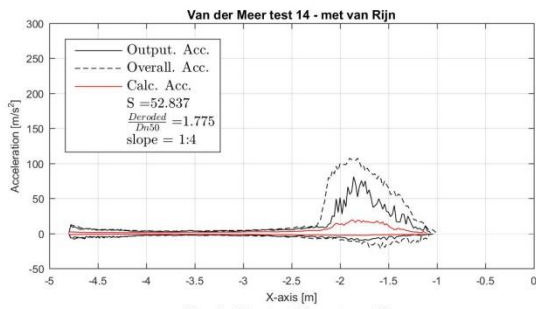
7.2.8 VAN RIJN [2007] test 12 - Acceleration



7.2.9 VAN RIJN [2007] test 13 - Acceleration

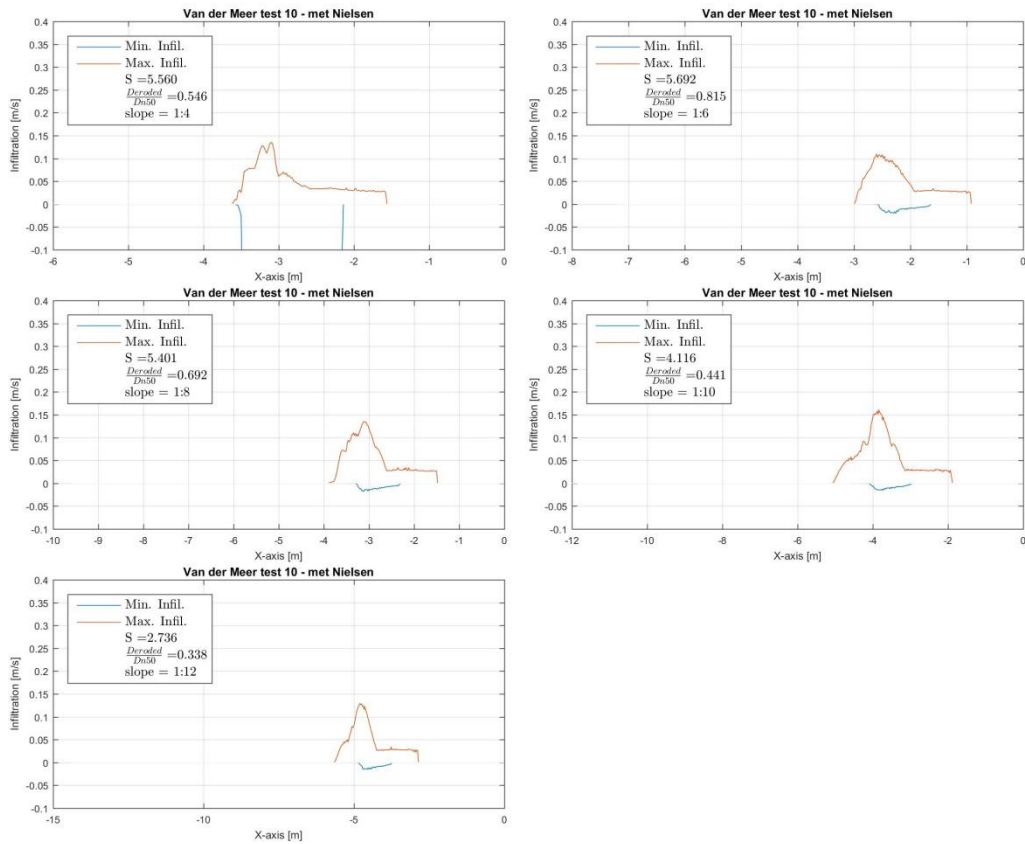


7.2.10 VAN RIJN [2007] test 14 - Acceleration

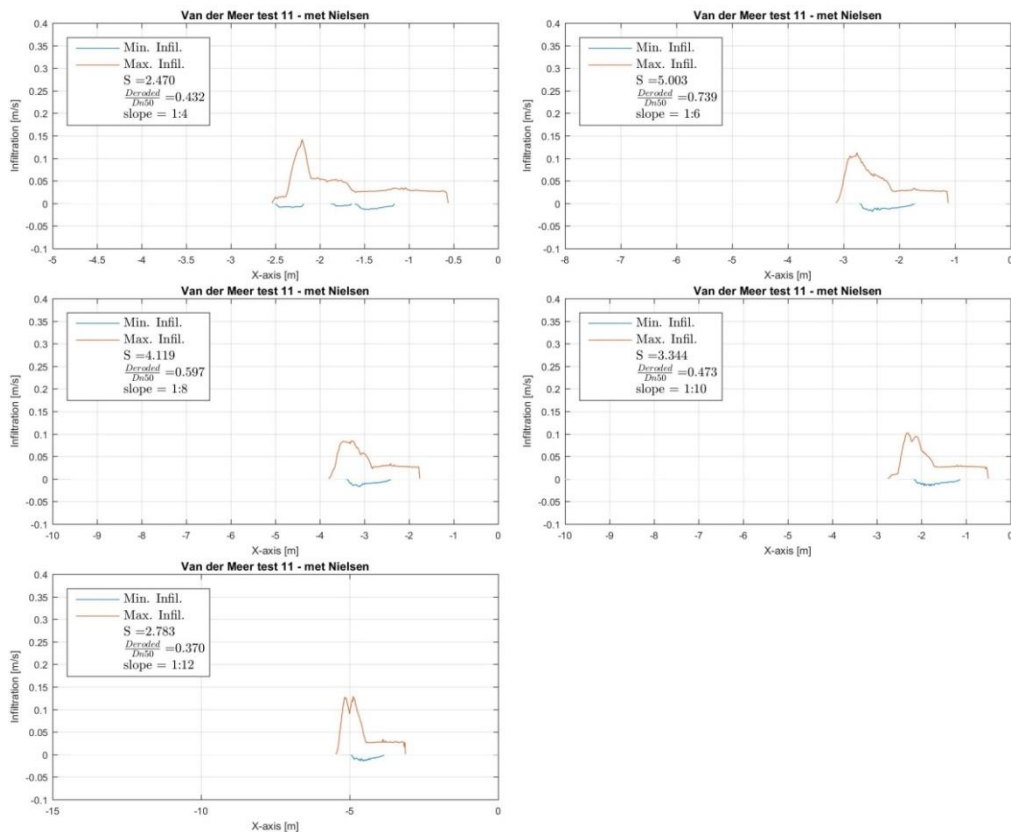


7.3 Infiltration

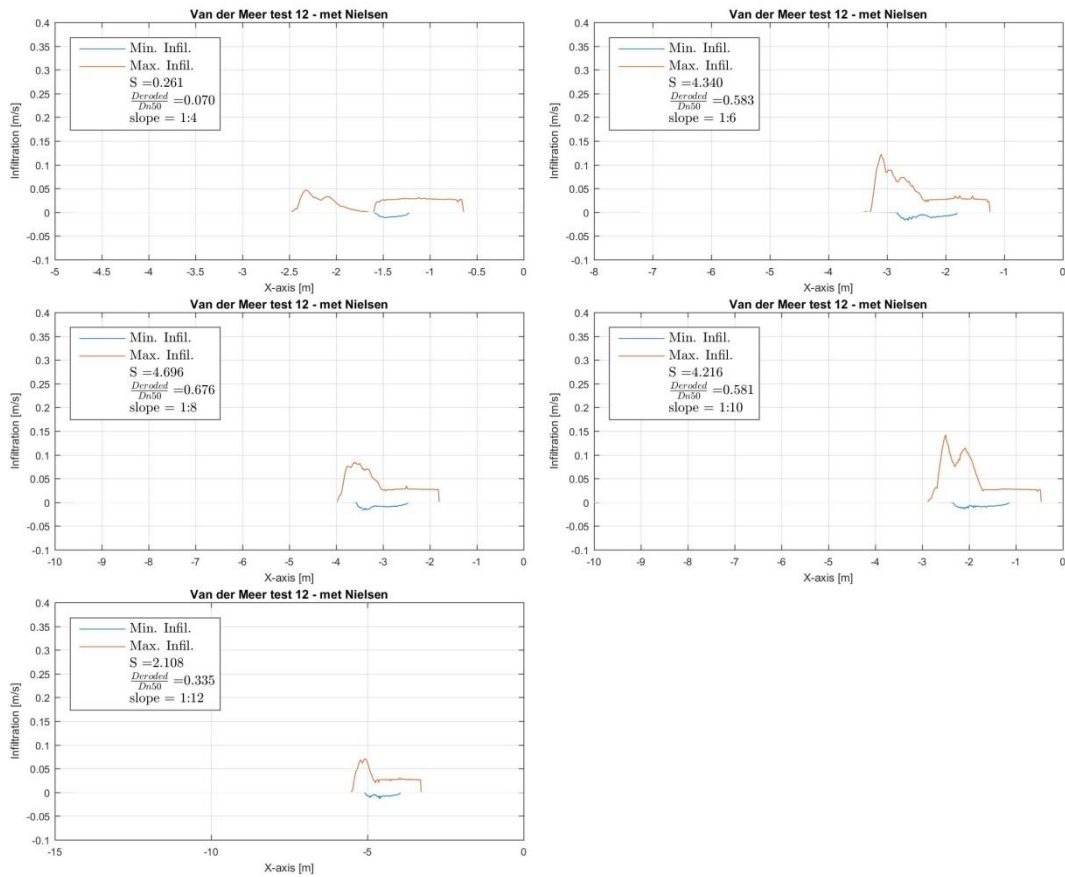
7.3.1 NIELSEN [2006] test 10 - Infiltration



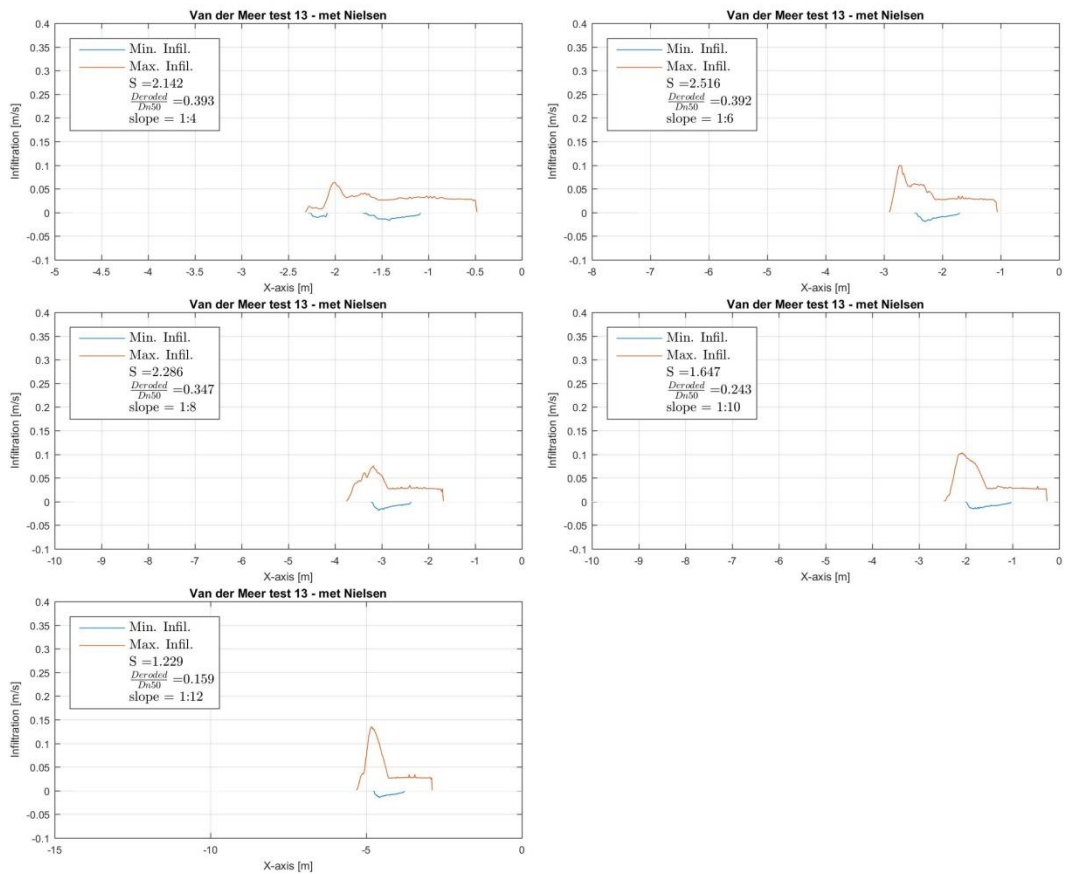
7.3.2 NIELSEN [2006] test 11 - Infiltration



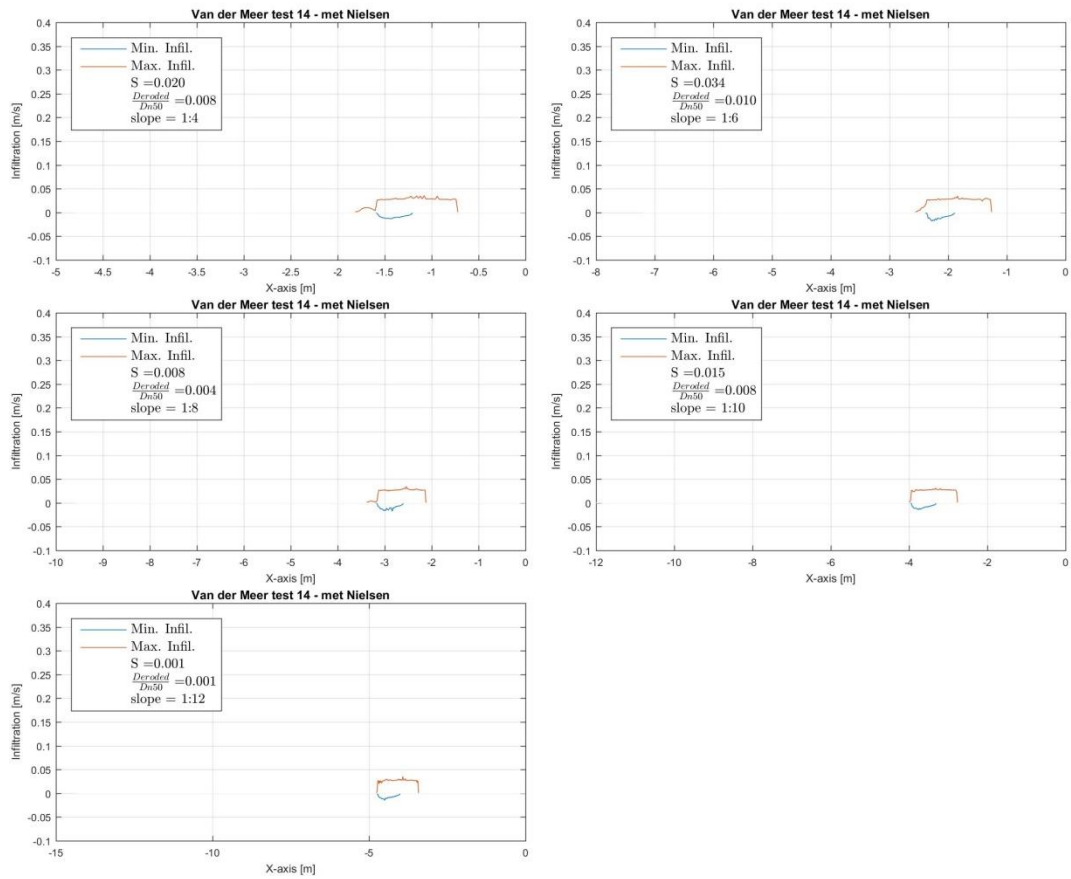
7.3.3 NIELSEN [2006] test 12 - Infiltration



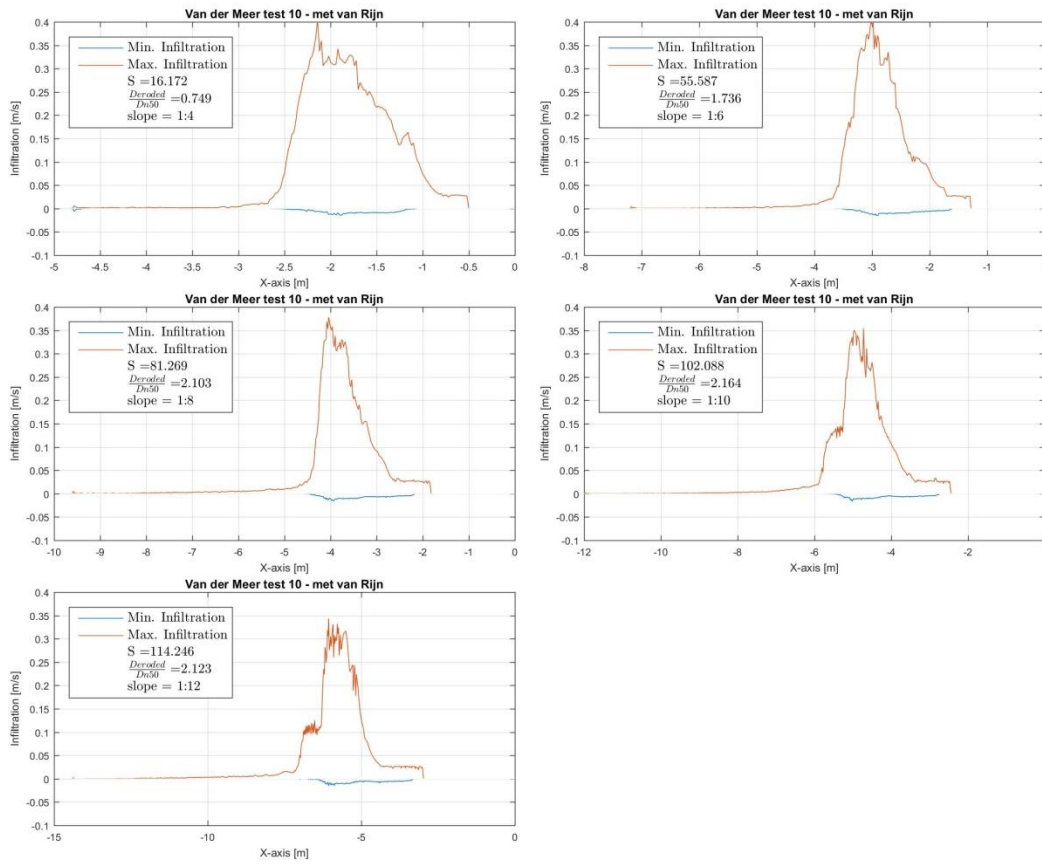
7.3.4 NIELSEN [2006] test 13 - Infiltration



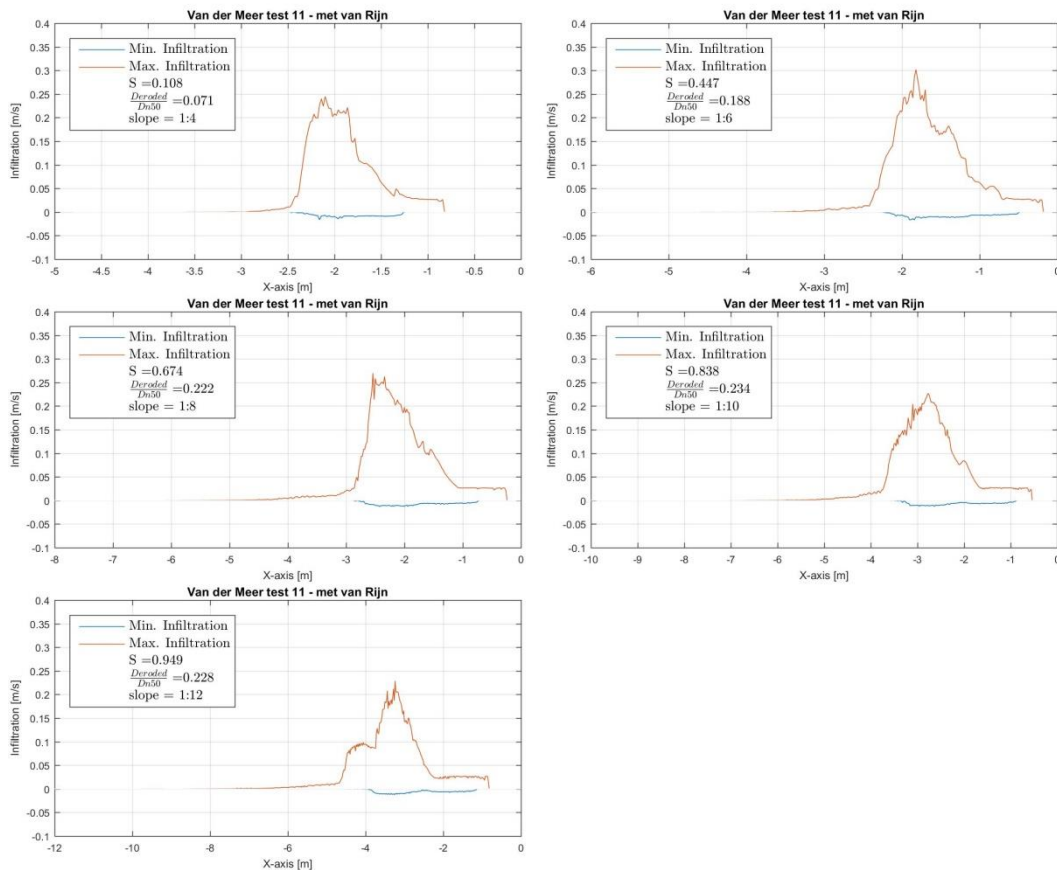
7.3.5 NIELSEN [2006] test 14 - Infiltration



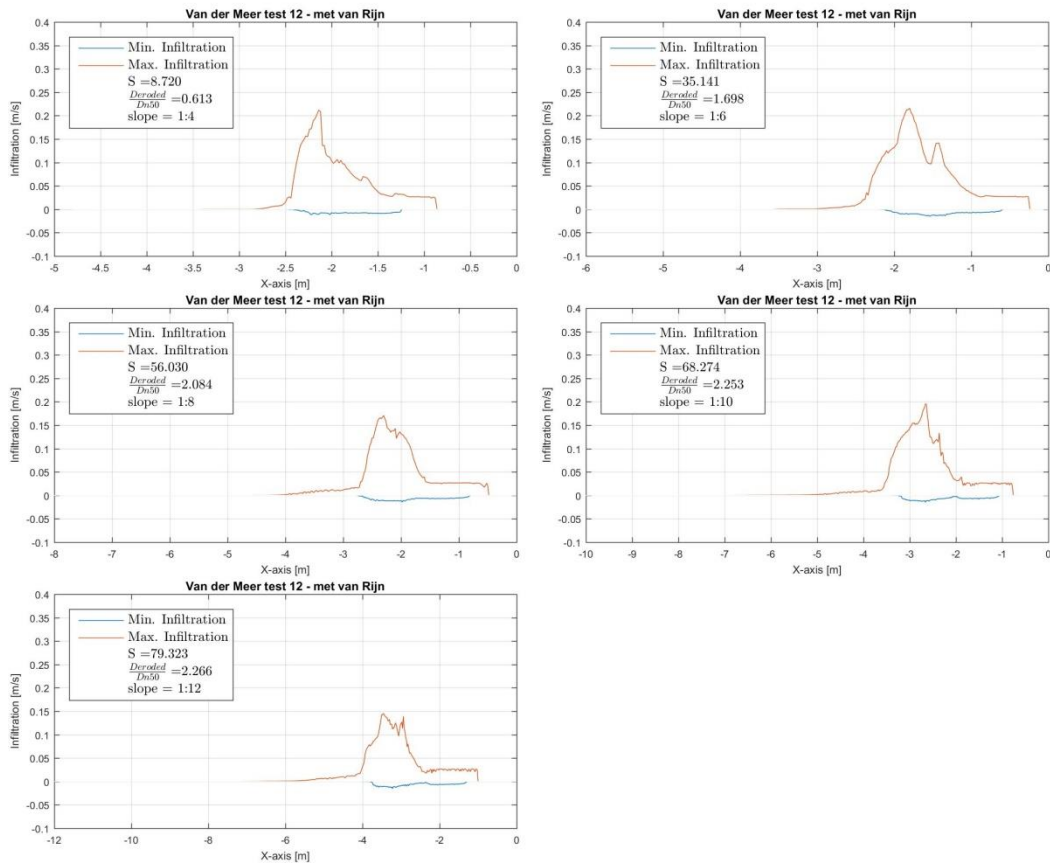
7.3.6 VAN RIJN [2007] test 10 - Infiltration



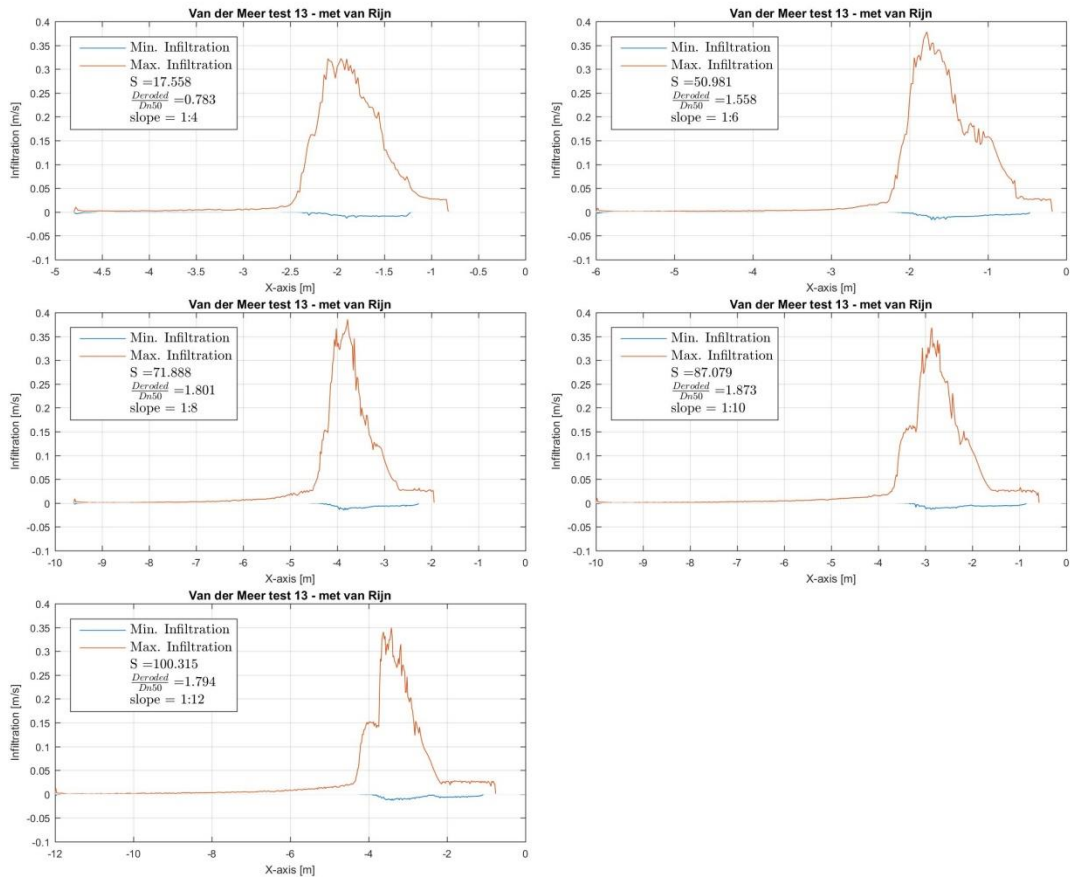
7.3.7 VAN RIJN [2007] test 11 - Infiltration



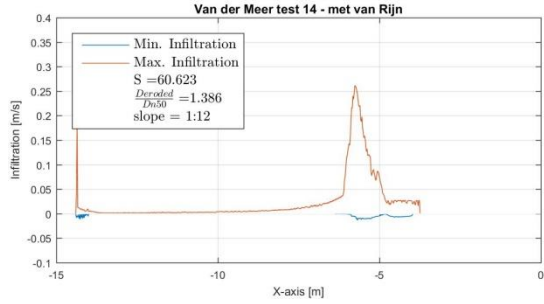
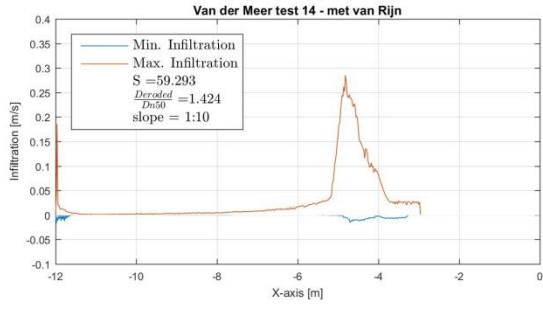
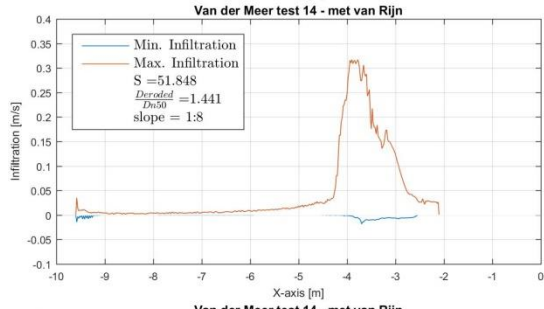
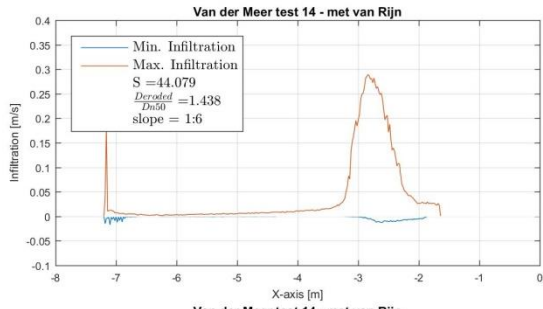
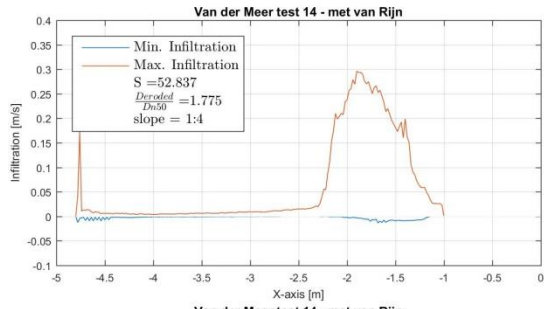
7.3.8 VAN RIJN [2007] test 12 - Infiltration



7.3.9 VAN RIJN [2007] test 13 - Infiltration



7.3.10 VAN RIJN [2007] test 14 - Infiltration



Appendix G2

Results Morphodynamics

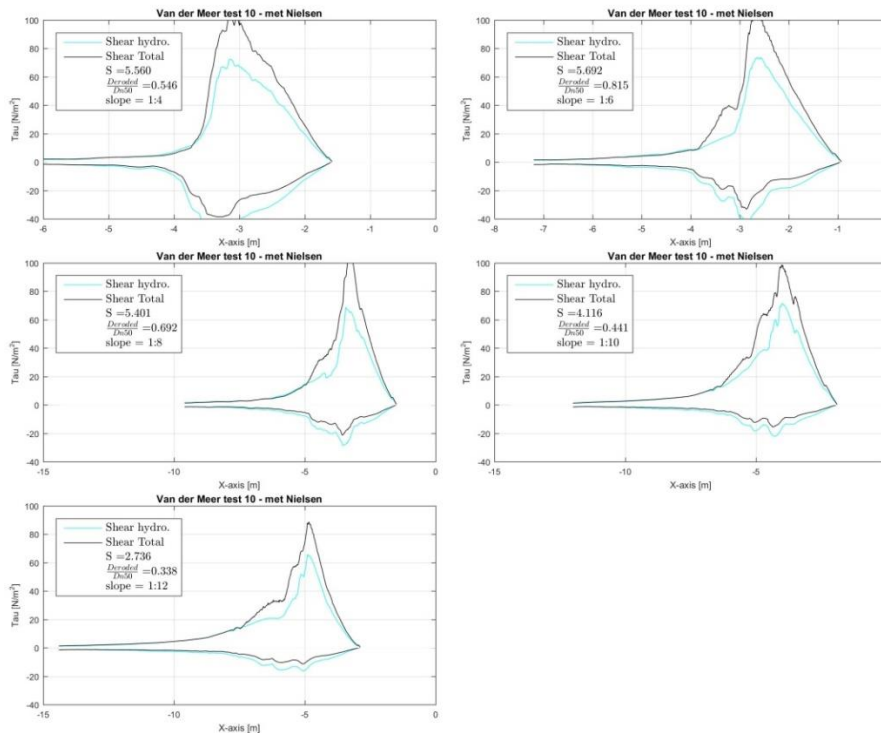
Test Series B

APPENDIX G.2: RESULTS

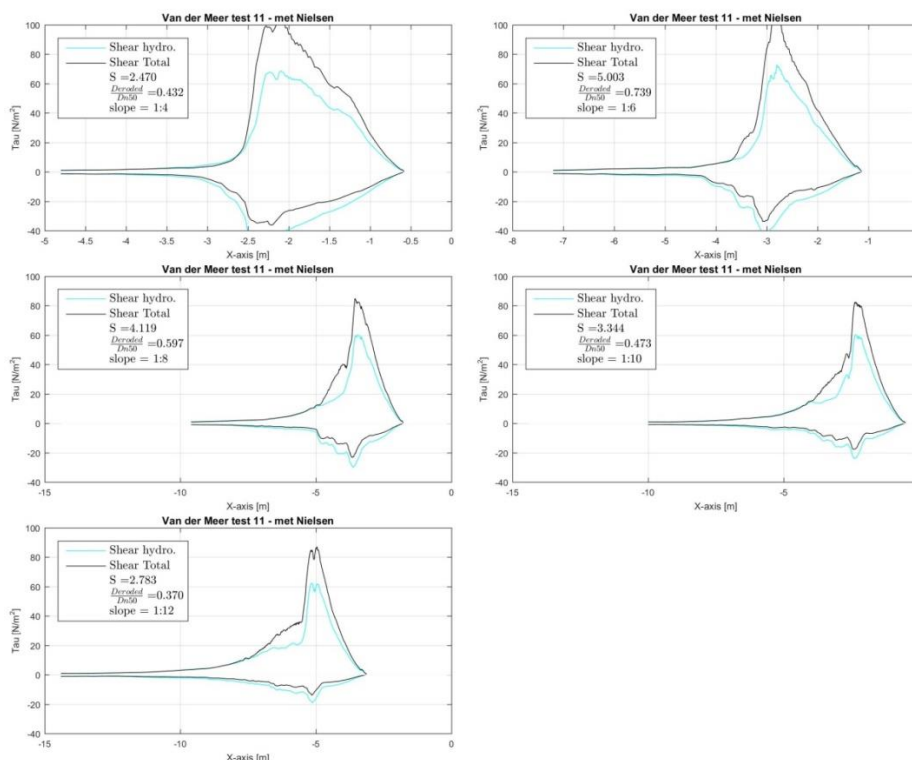
MORPHODYNAMICS – TEST SERIES B

8.1 Shear stress

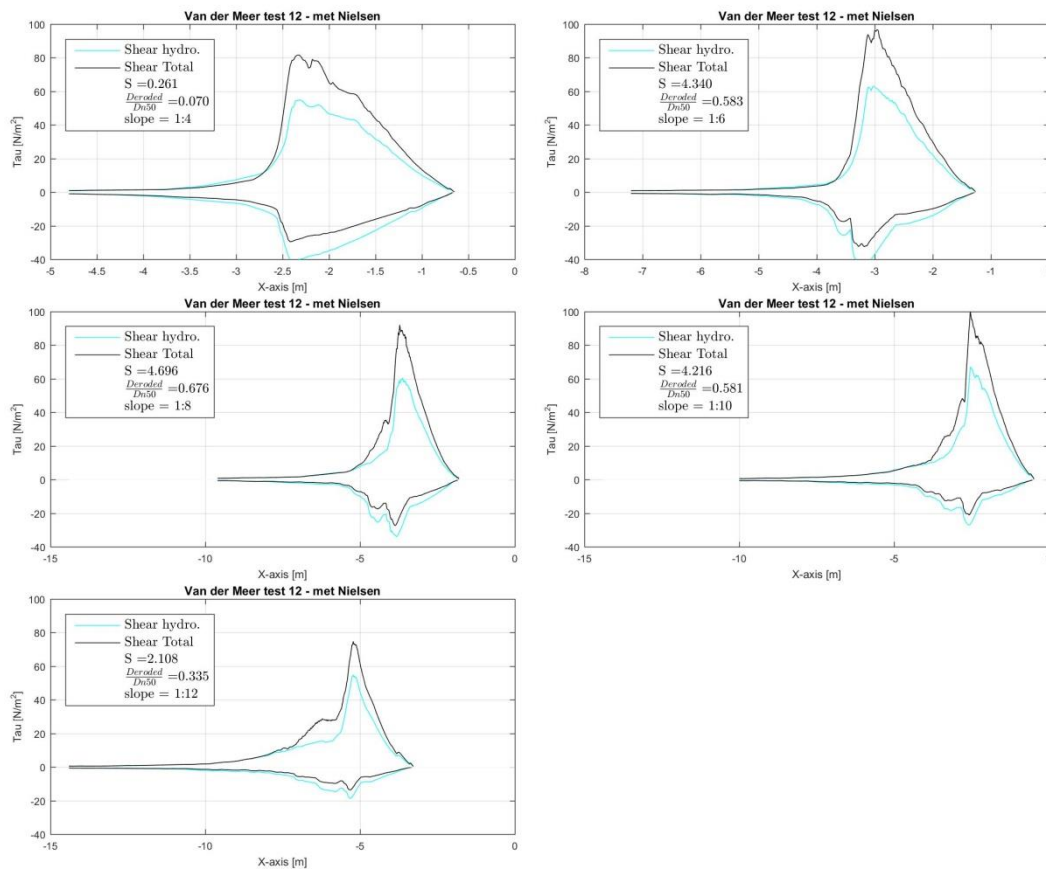
8.1.1 NIELSEN [2006] test 10 – Shear stress



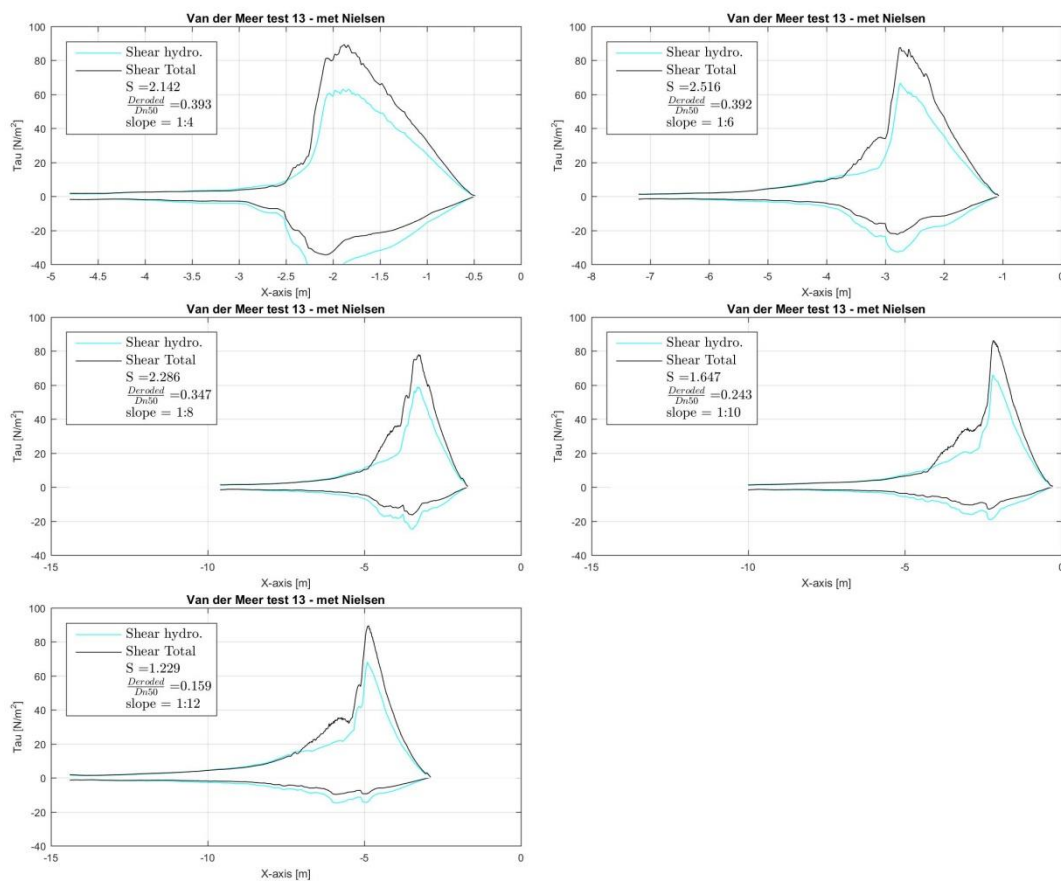
8.1.2 NIELSEN [2006] test 11 – Shear stress



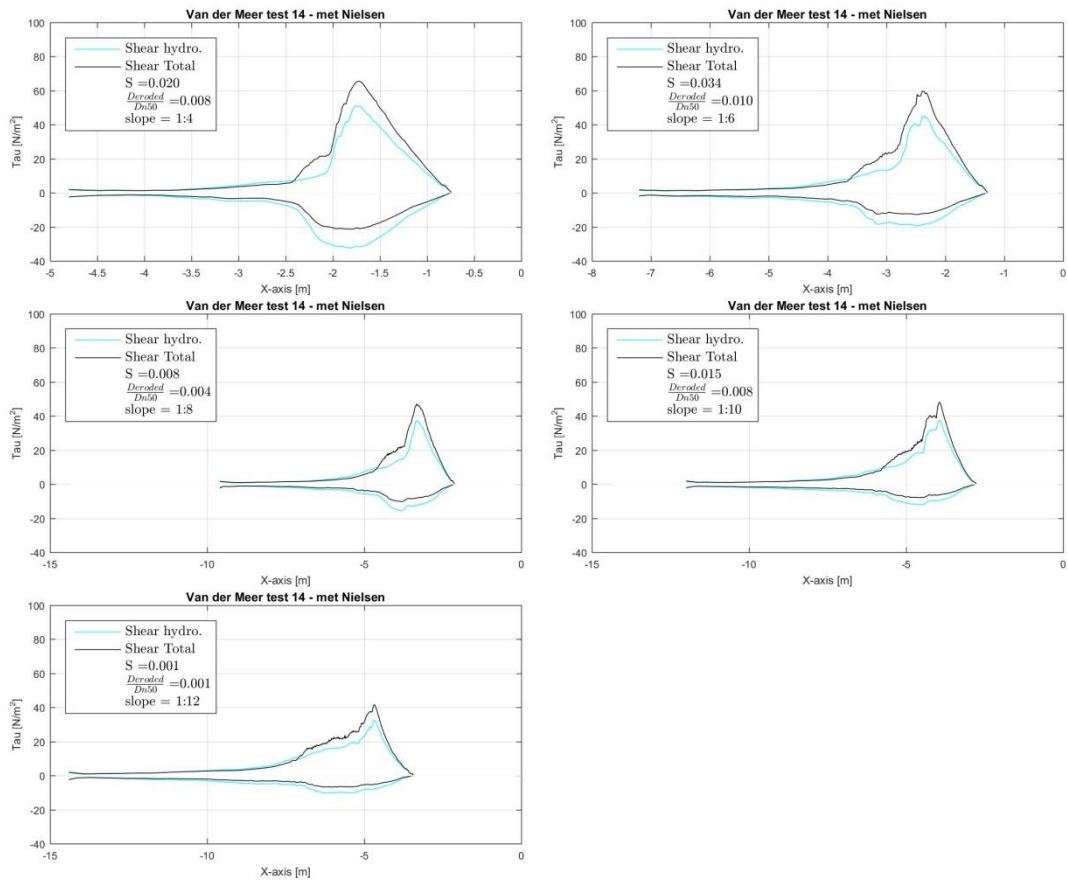
8.1.3 NIELSEN [2006] test 12 - Shear stress



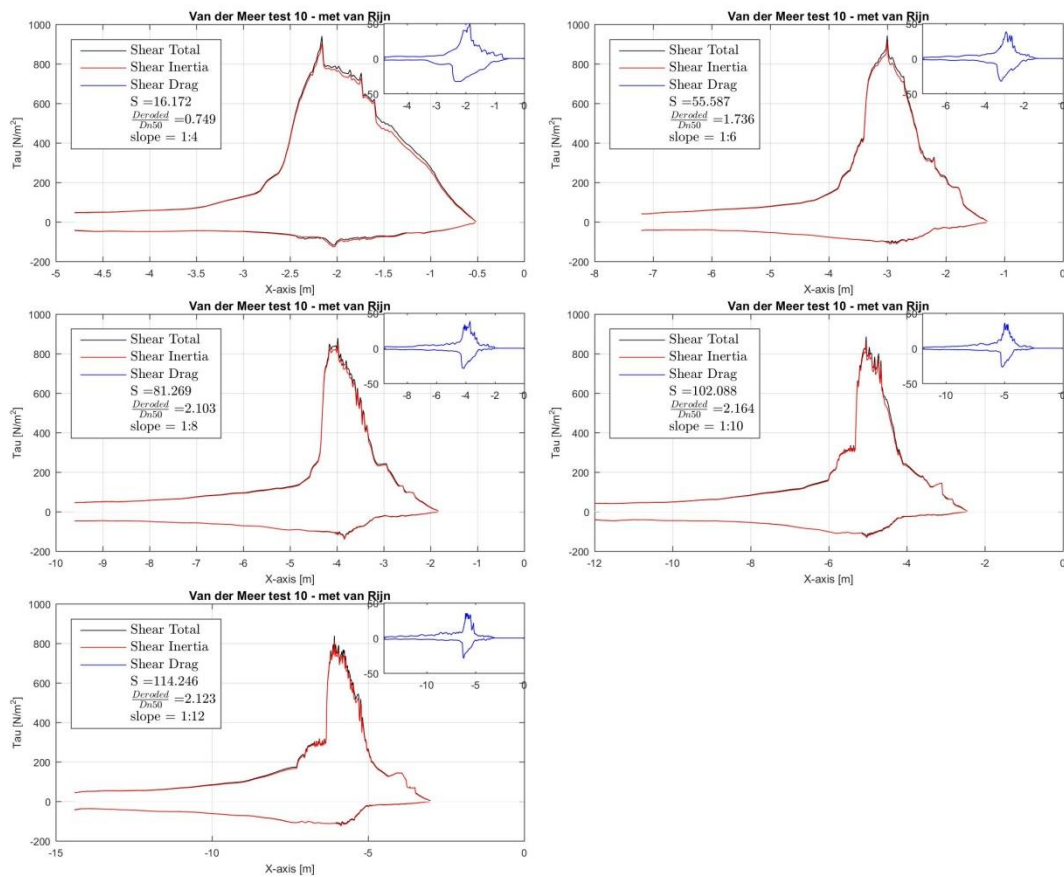
8.1.4 NIELSEN [2006] test 13 - Shear stress



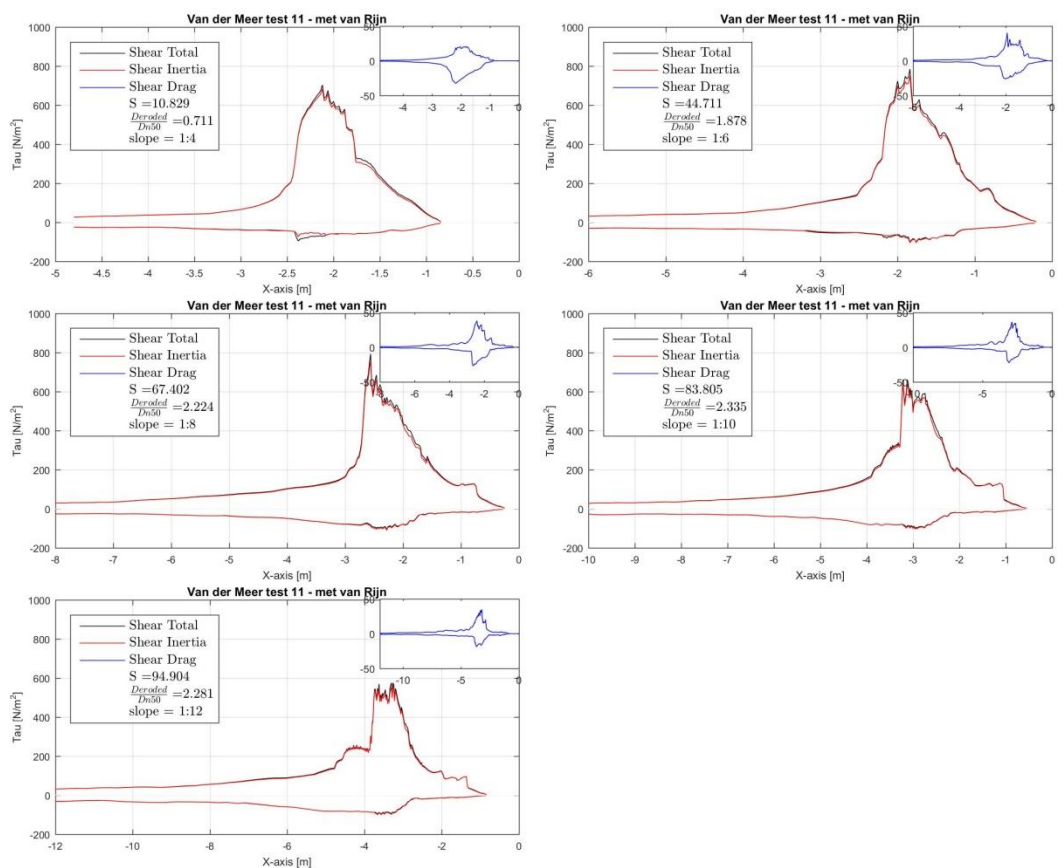
8.1.5 NIELSEN [2006] test 14 - Shear stress



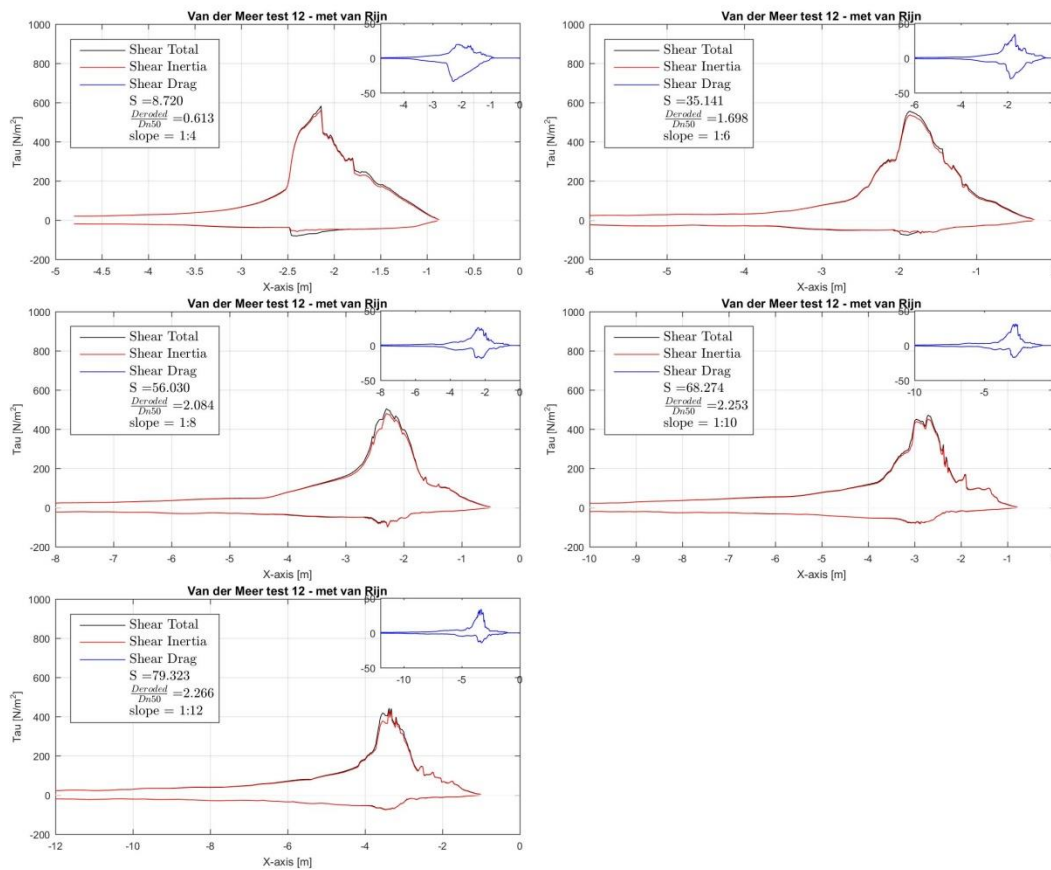
8.1.6 VAN RIJN [2007] test 10 – Shear stress



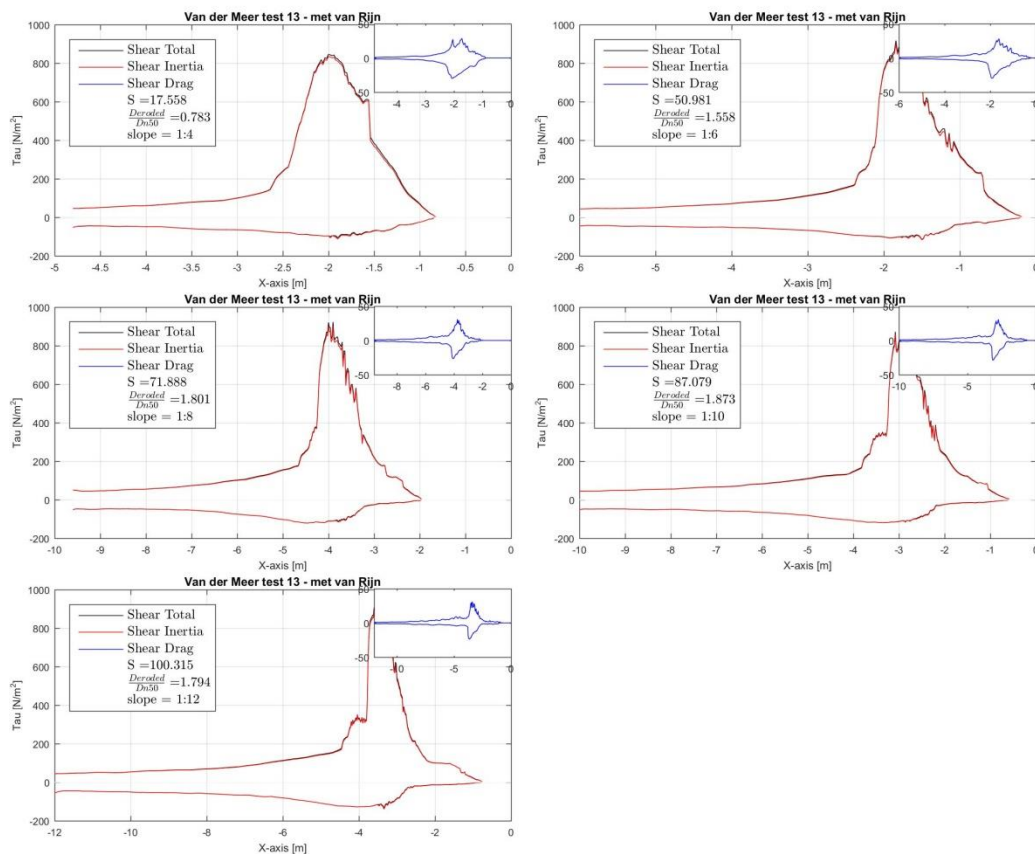
8.1.7 VAN RIJN [2007] test 11 – Shear stress



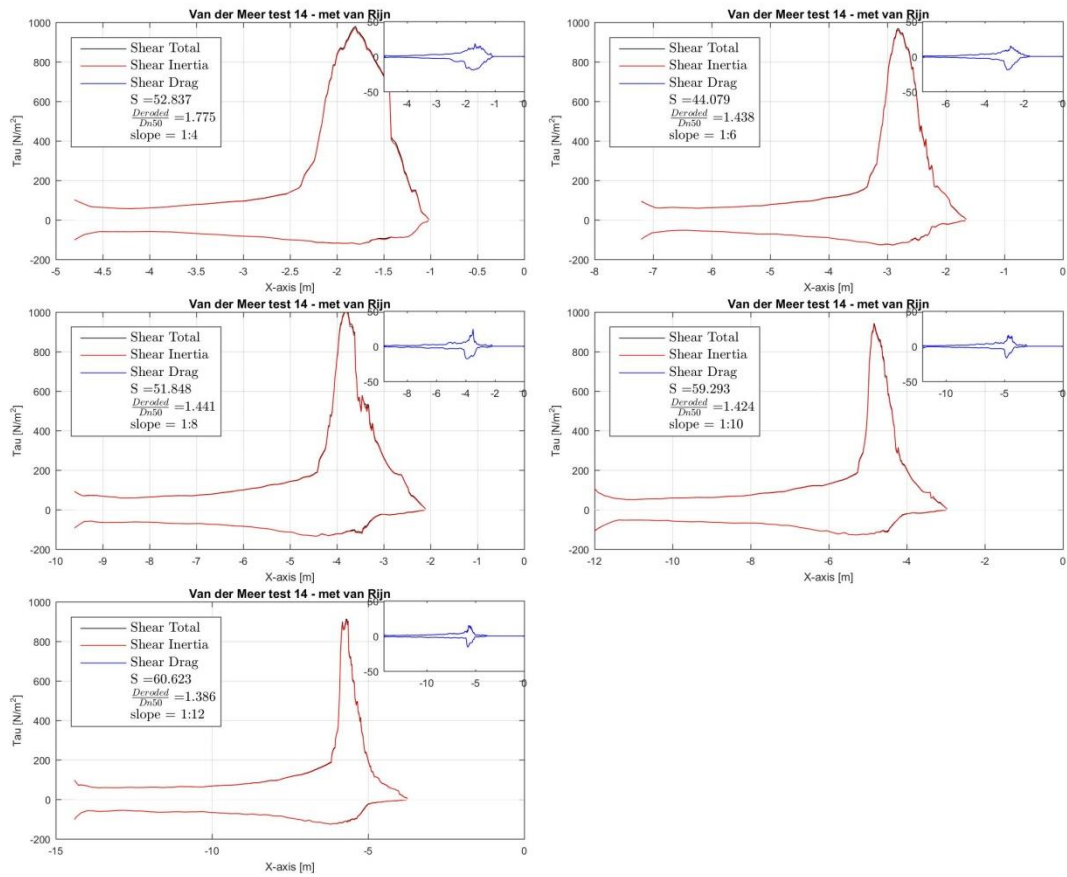
8.1.8 VAN RIJN [2007] test 12 – Shear stress



8.1.9 VAN RIJN [2007] test 13 – Shear stress

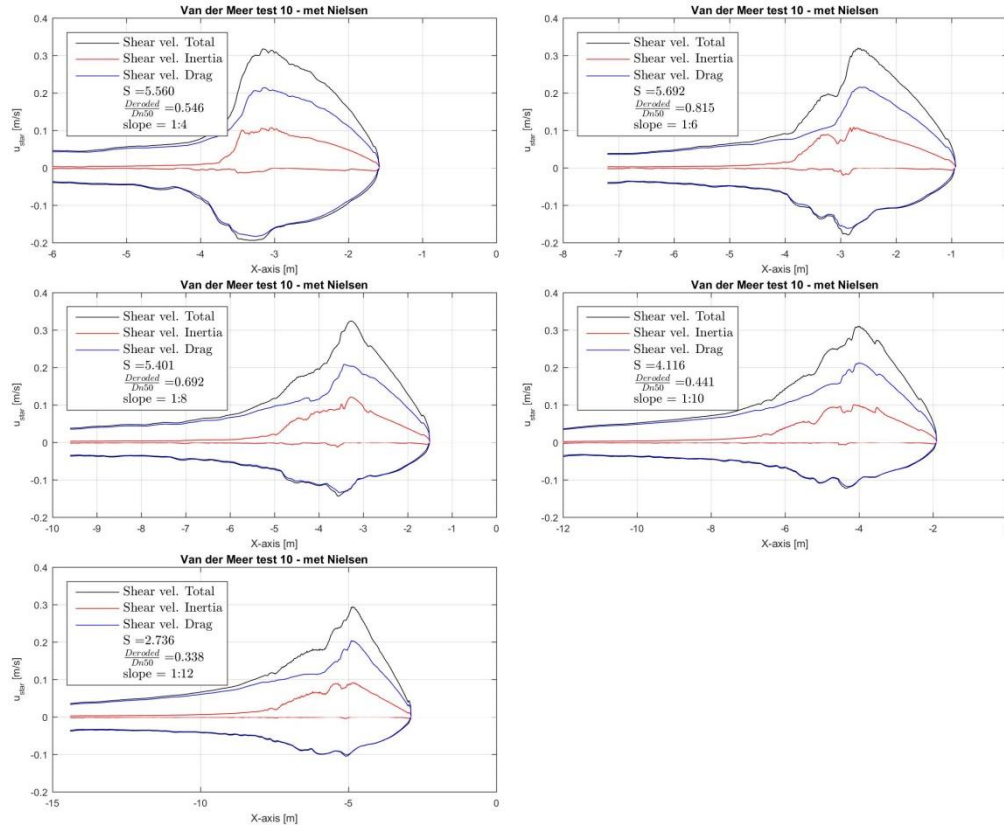


8.1.10 VAN RIJN [2007] test 14 – Shear stress

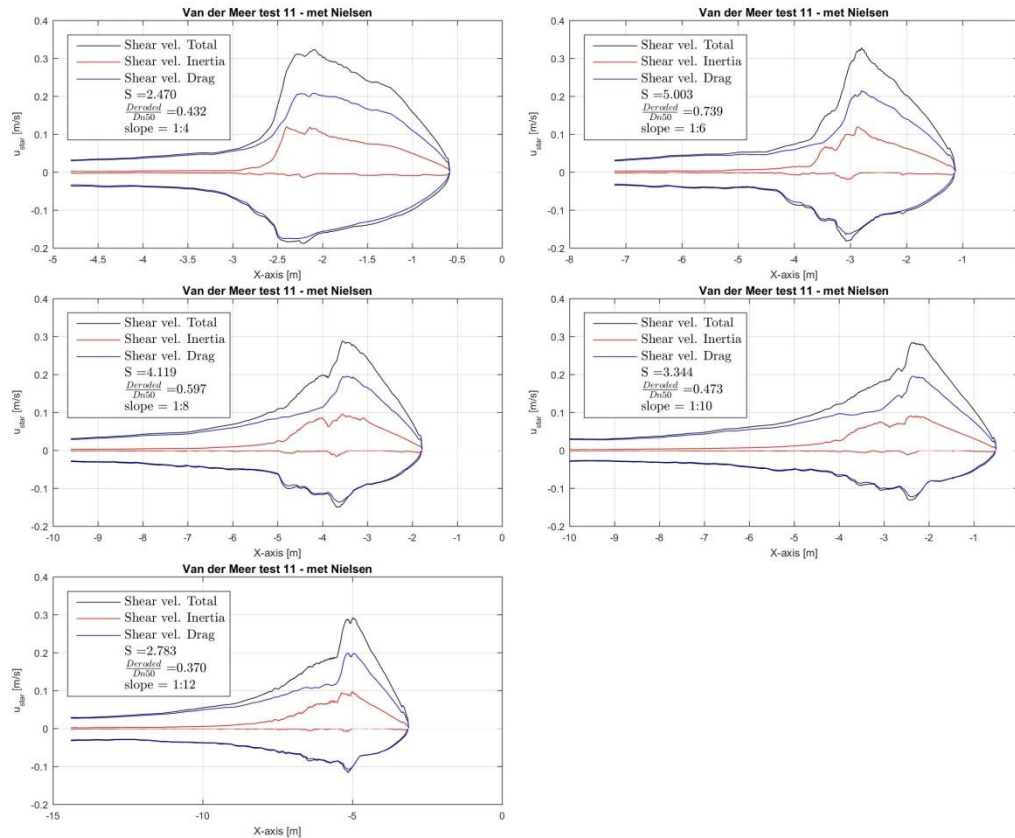


8.2 Shear velocity

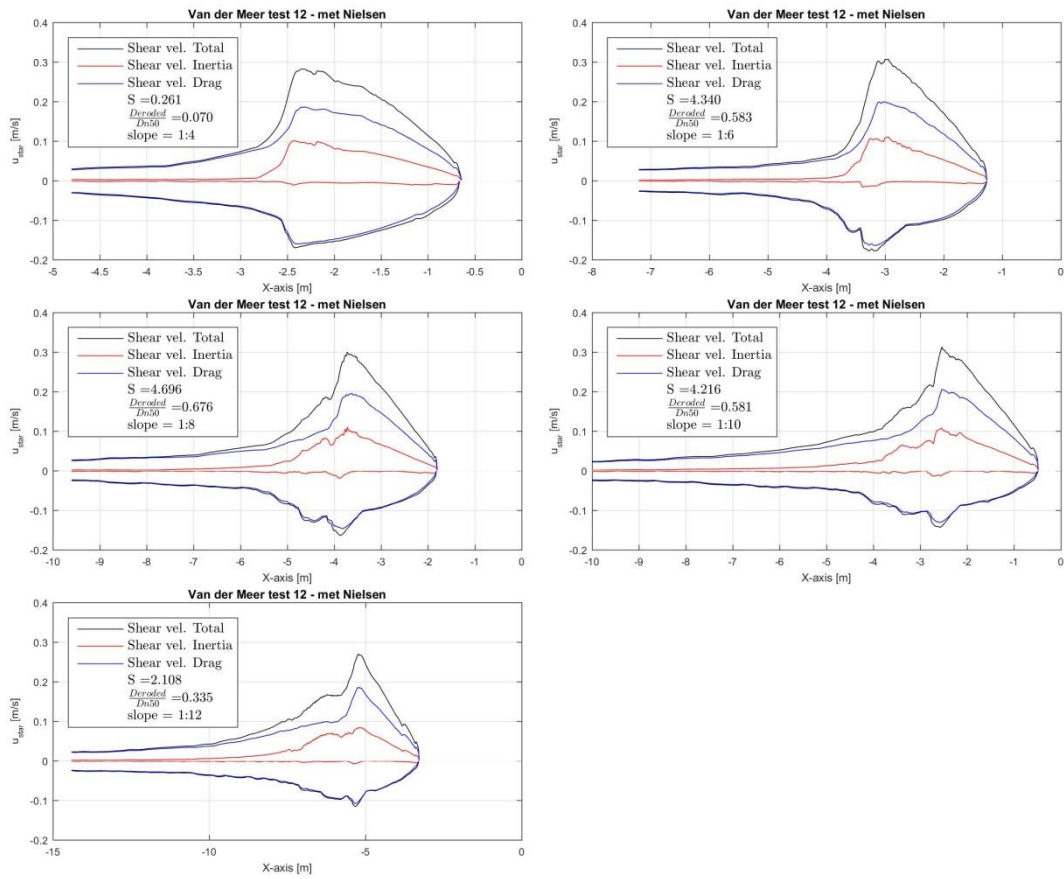
8.2.1 NIELSEN [2006] test 10 – Shear velocity



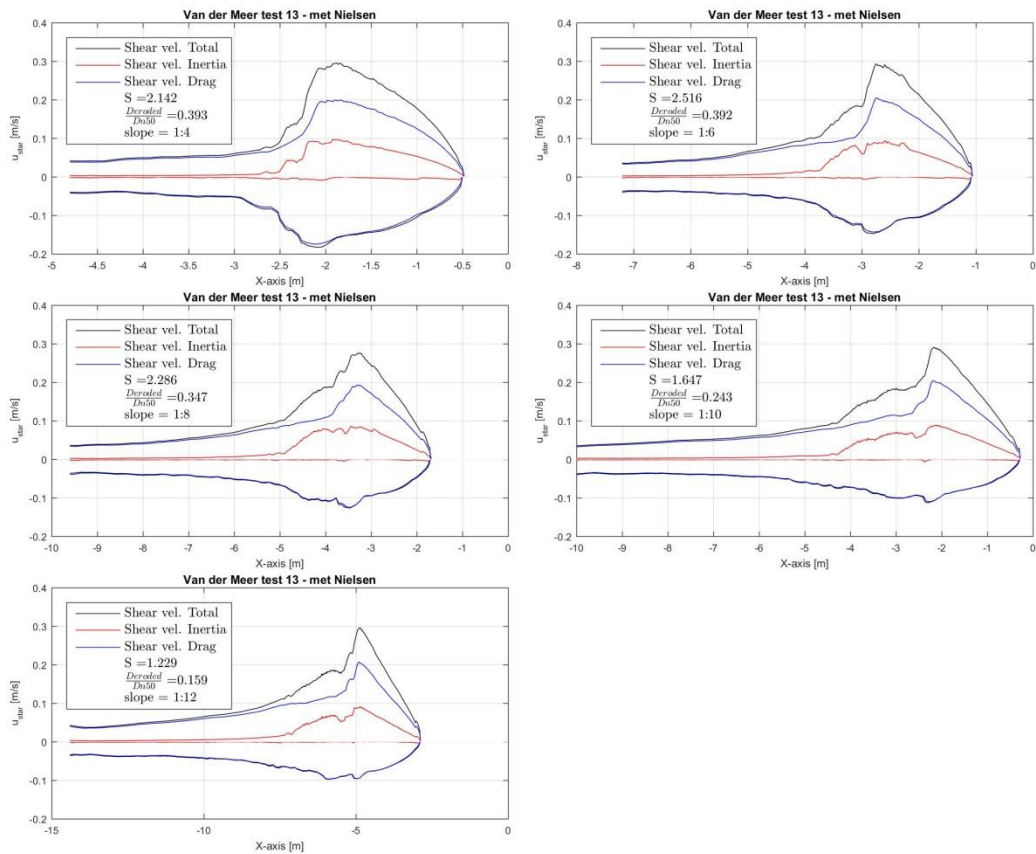
8.2.2 NIELSEN [2006] test 11 – Shear velocity



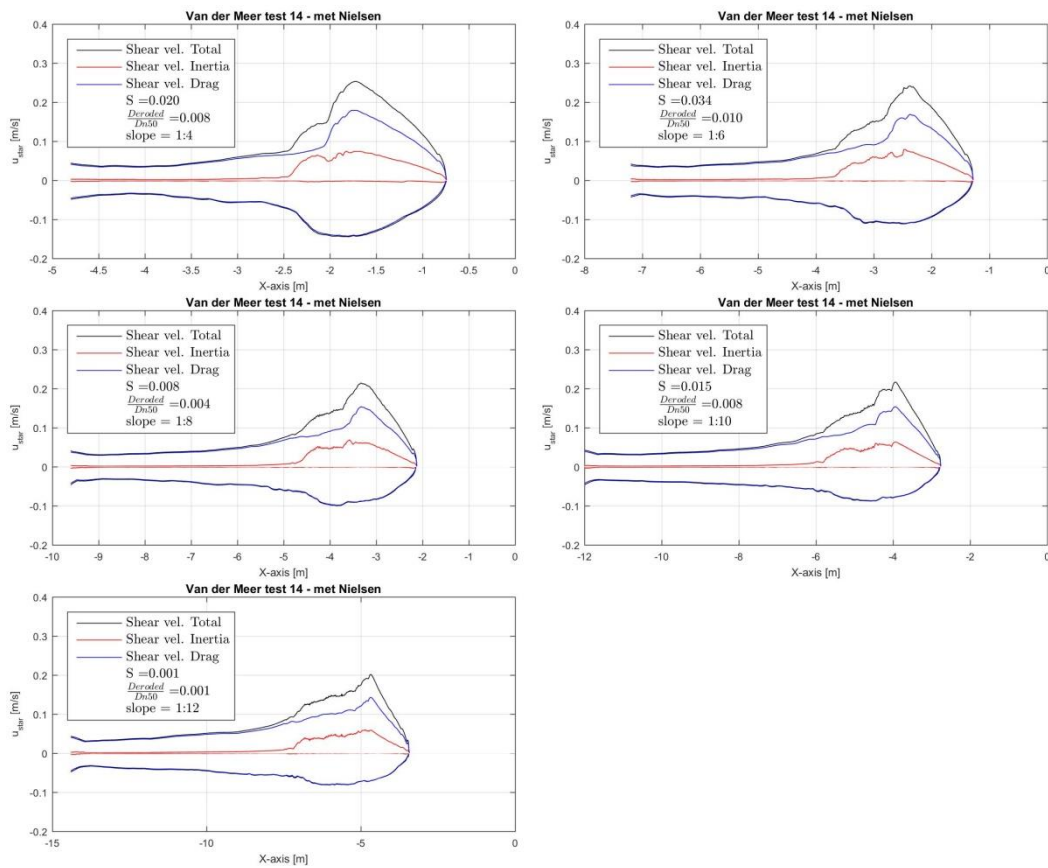
8.2.3 NIELSEN [2006] test 12 - Shear velocity



8.2.4 NIELSEN [2006] test 13 - Shear velocity

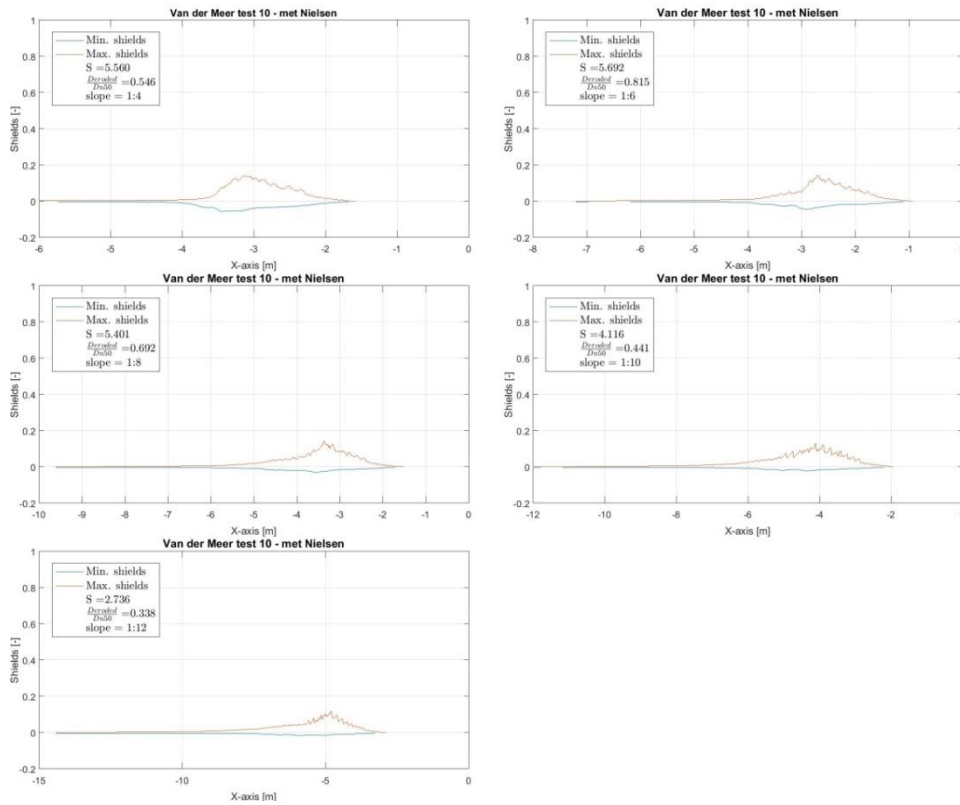


8.2.5 NIELSEN [2006] test 14 – Shear velocity

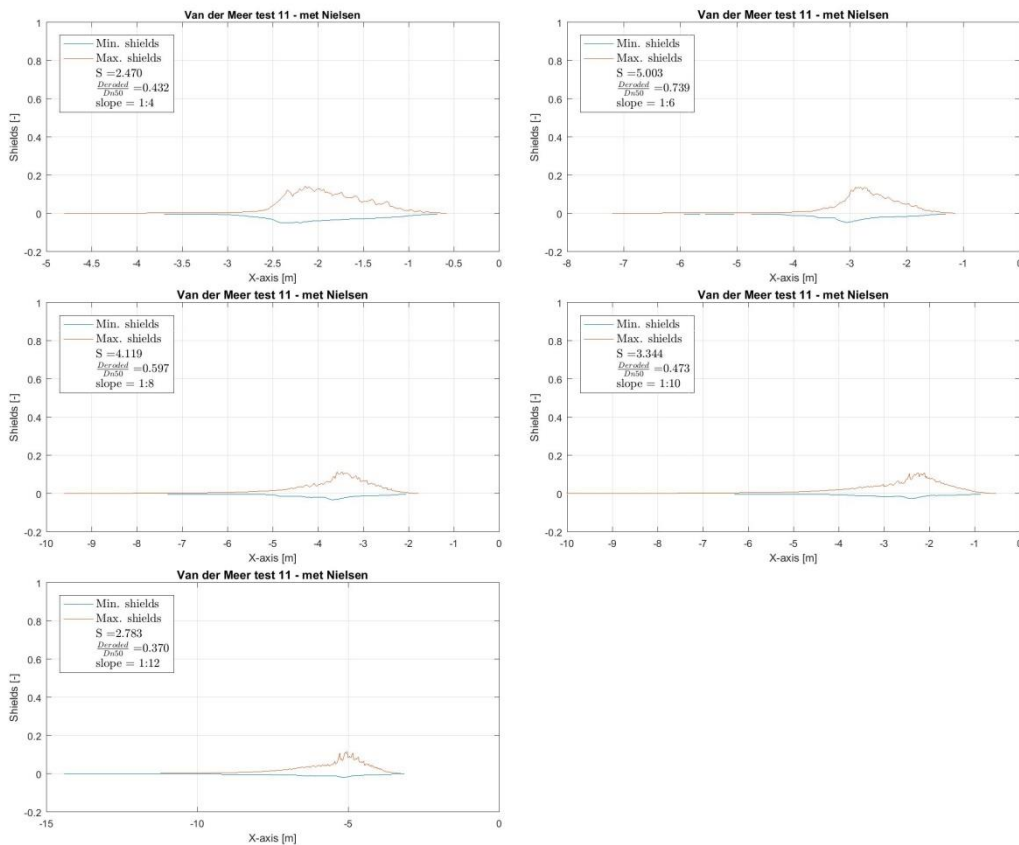


8.3 Shields

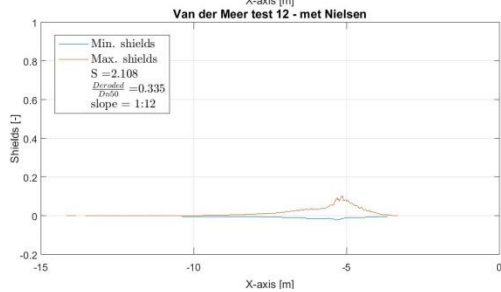
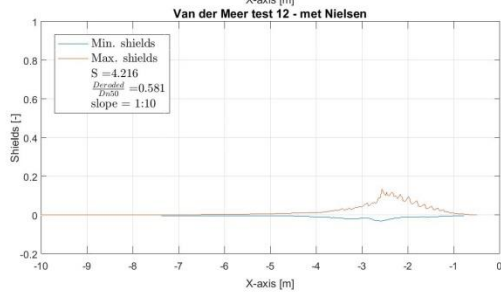
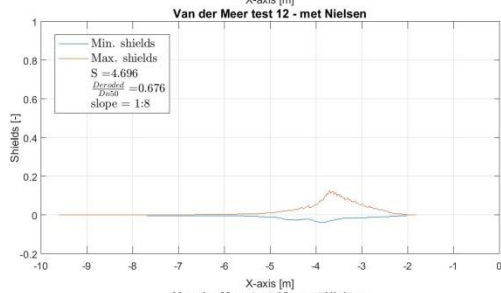
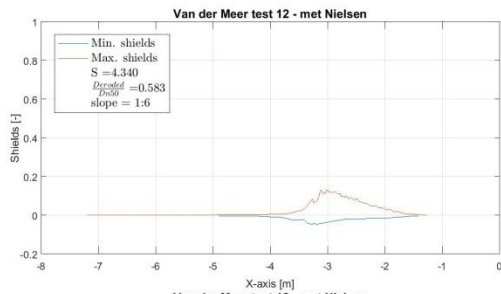
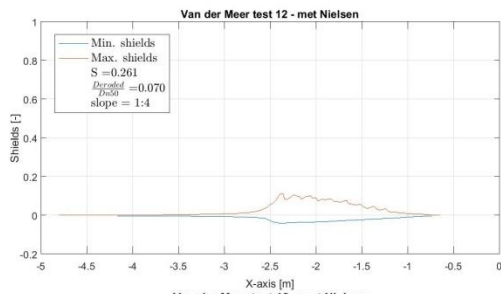
8.3.1 NIELSEN [2006] test 10 - Shields



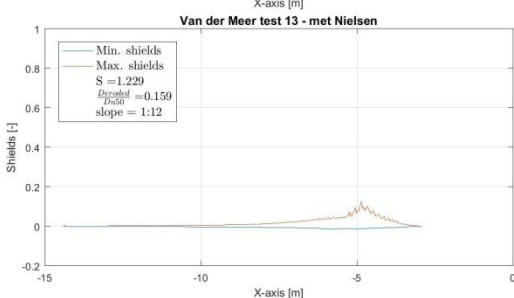
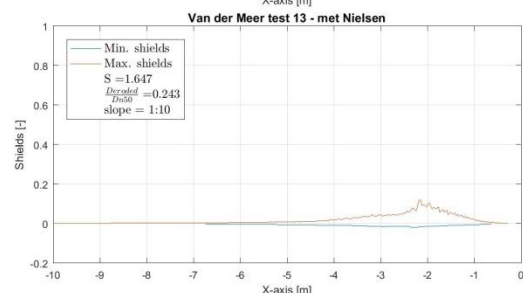
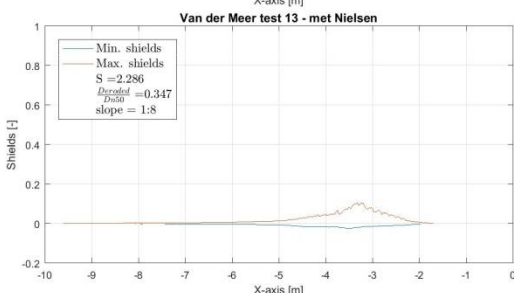
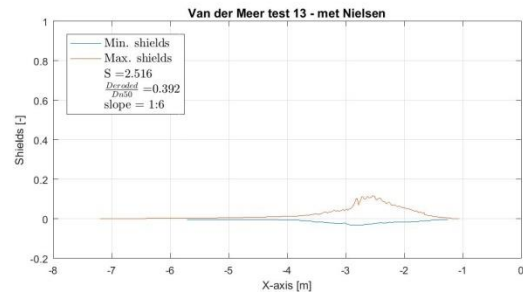
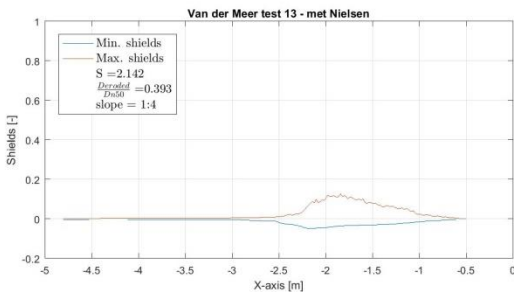
8.3.2 NIELSEN [2006] test 11 - Shields



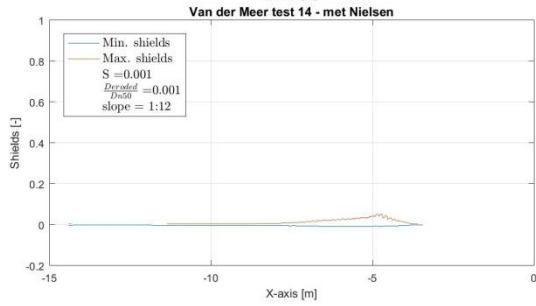
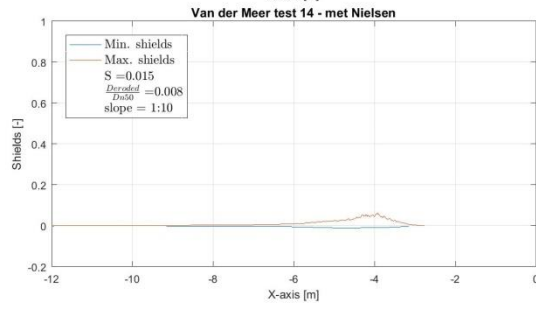
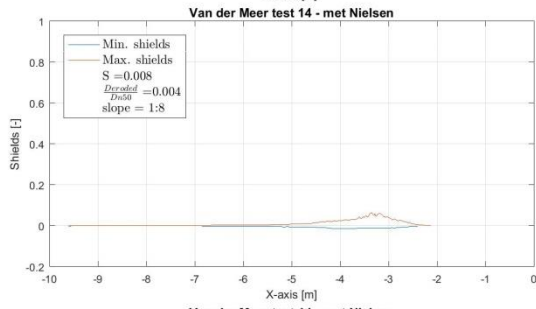
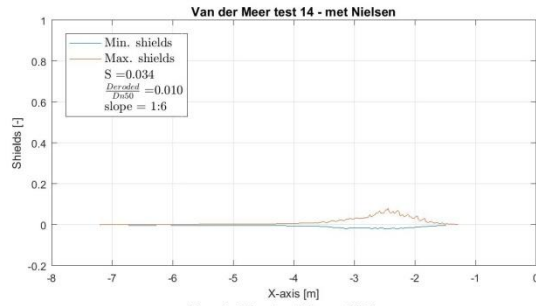
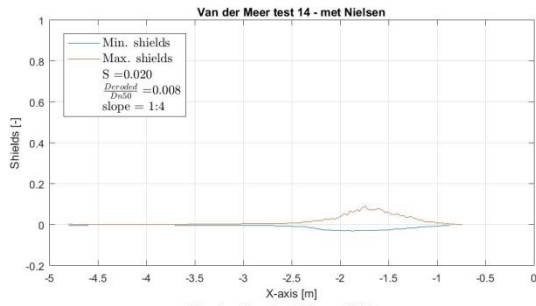
8.3.3 NIELSEN [2006] test 12 - Shields



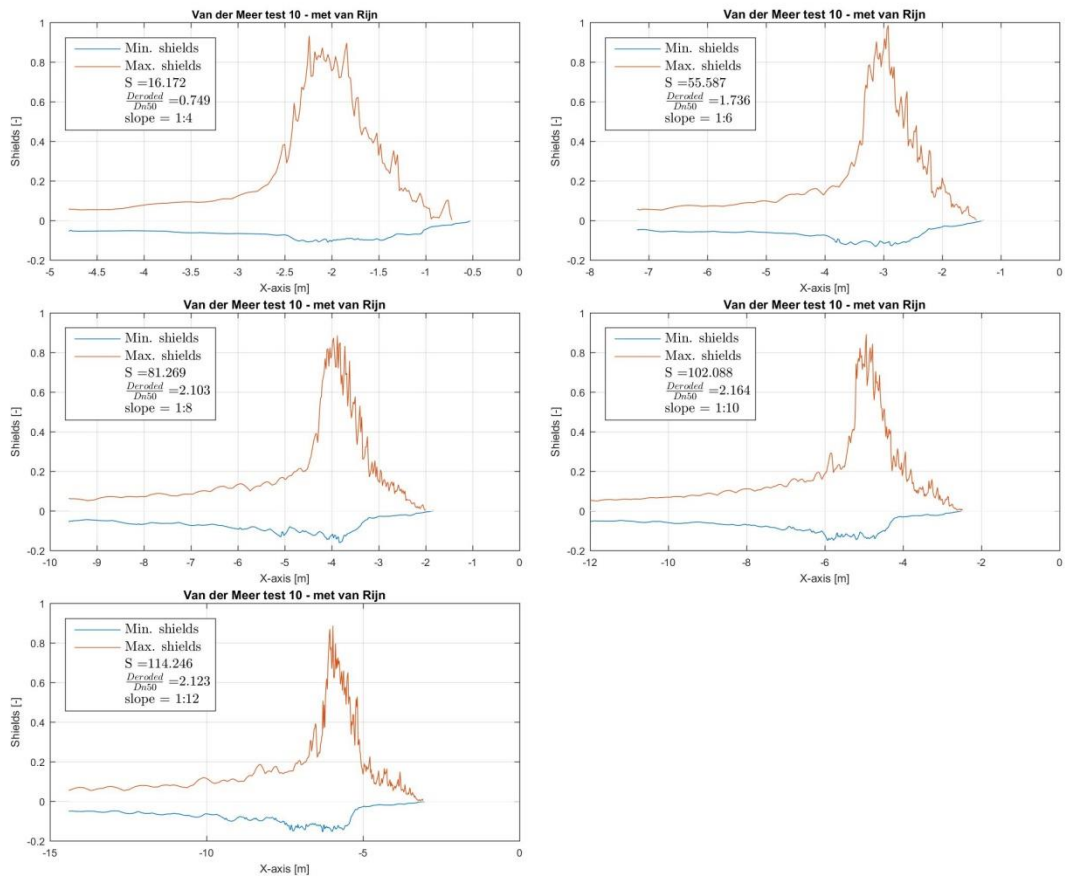
8.3.4 NIELSEN [2006] test 13 - Shields



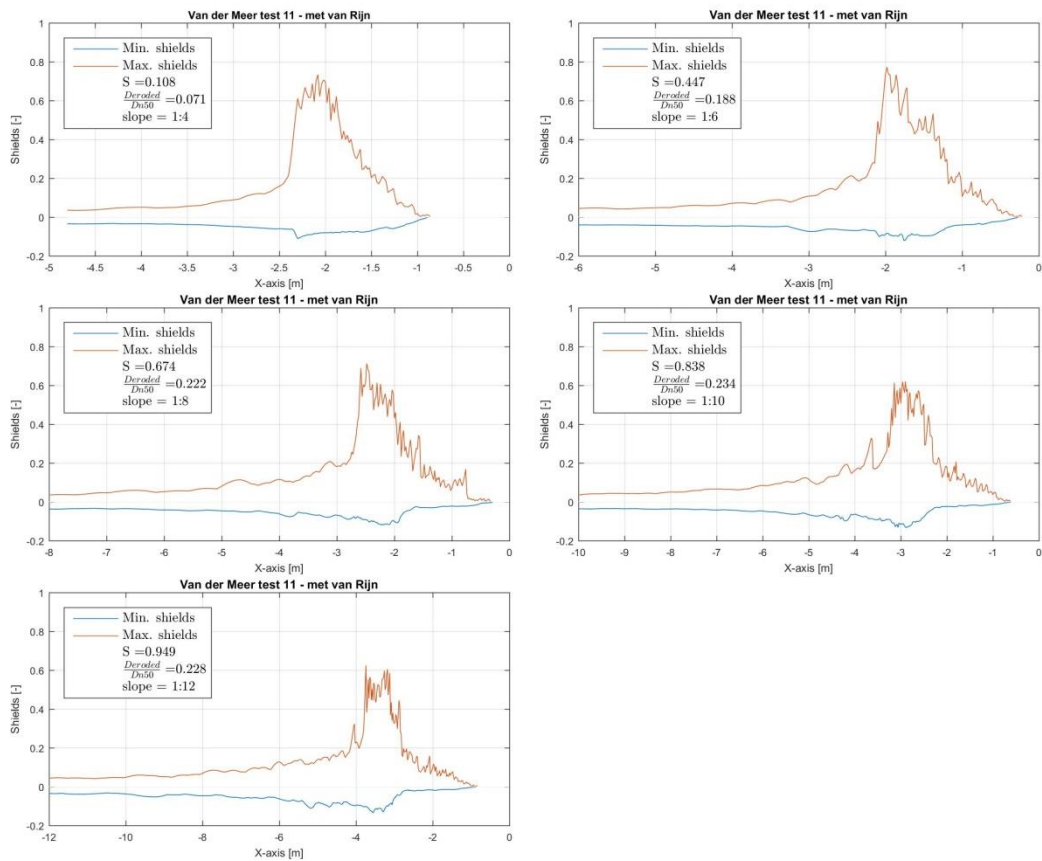
8.3.5 NIELSEN [2006] test 14 - Shields



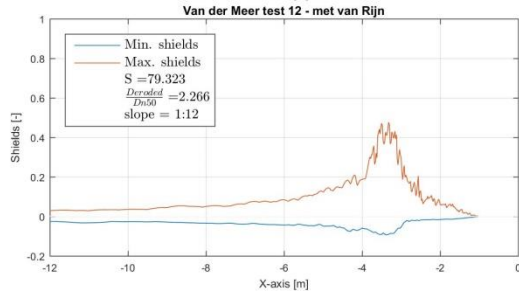
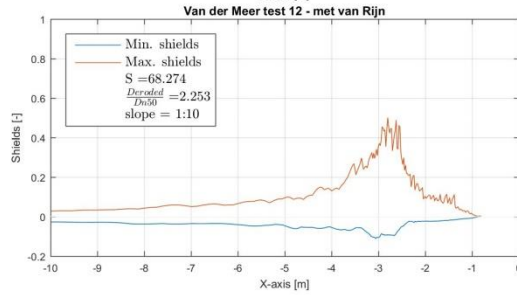
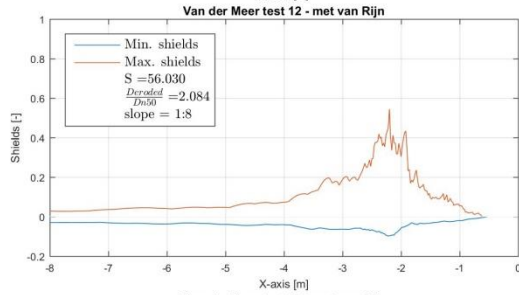
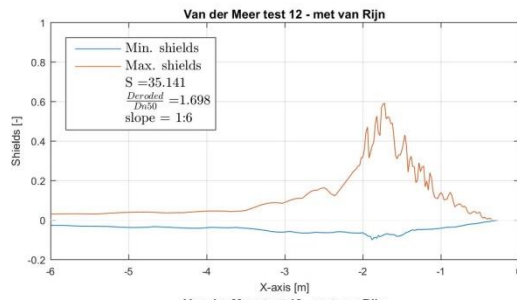
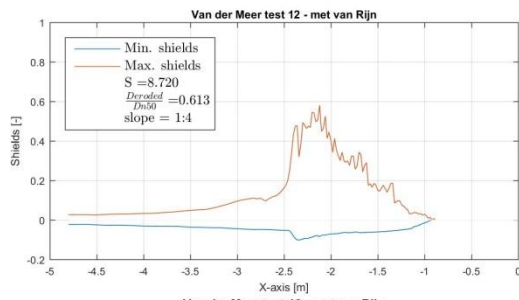
8.3.6 VAN RIJN [2007] test 10 – Shields



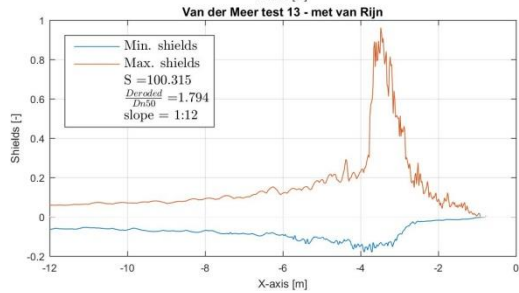
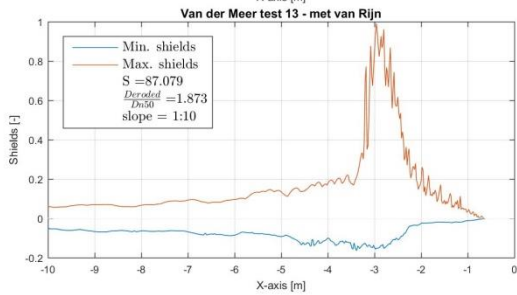
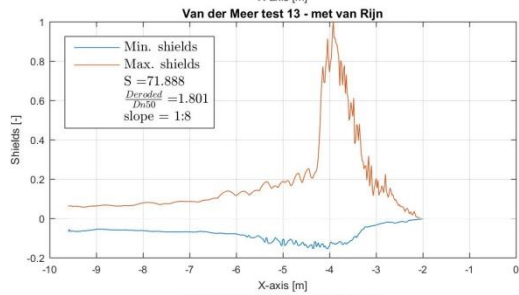
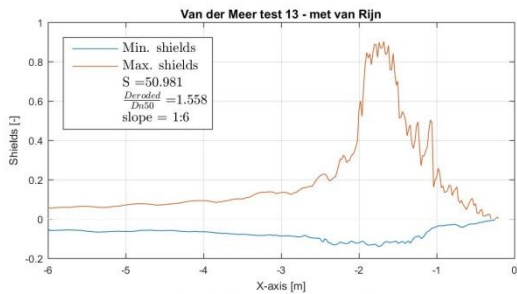
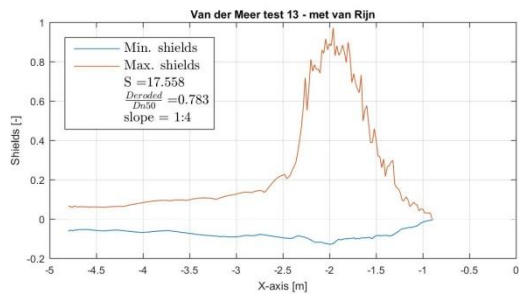
8.3.7 VAN RIJN [2007] test 11 – Shields



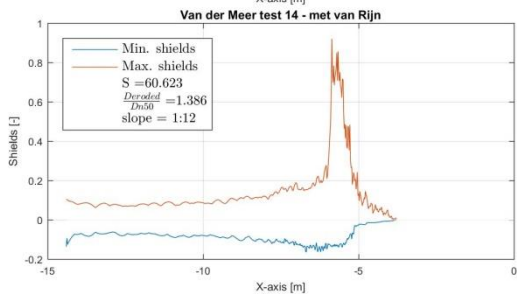
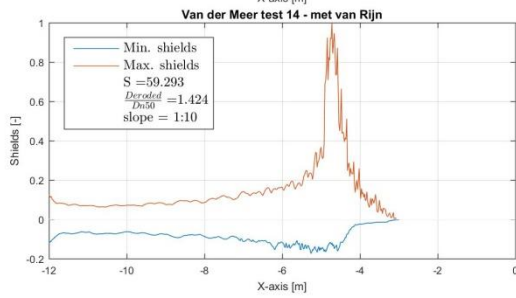
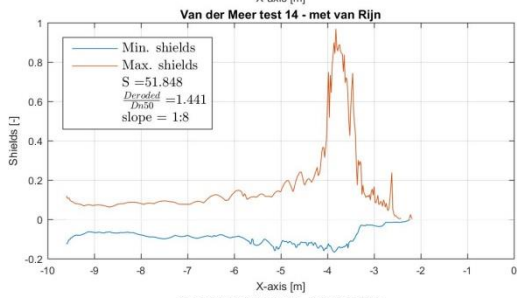
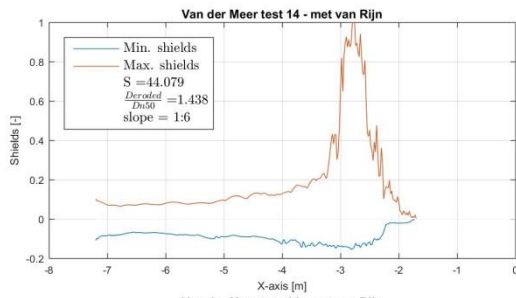
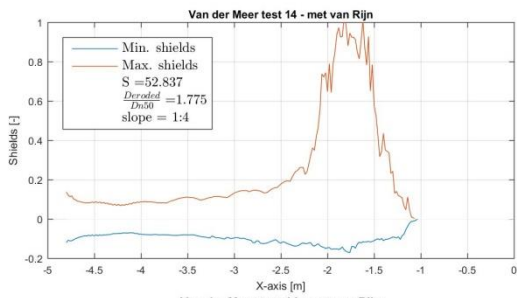
8.3.8 VAN RIJN [2007] test 12 - Shields



8.3.9 VAN RIJN [2007] test 13 - Shields

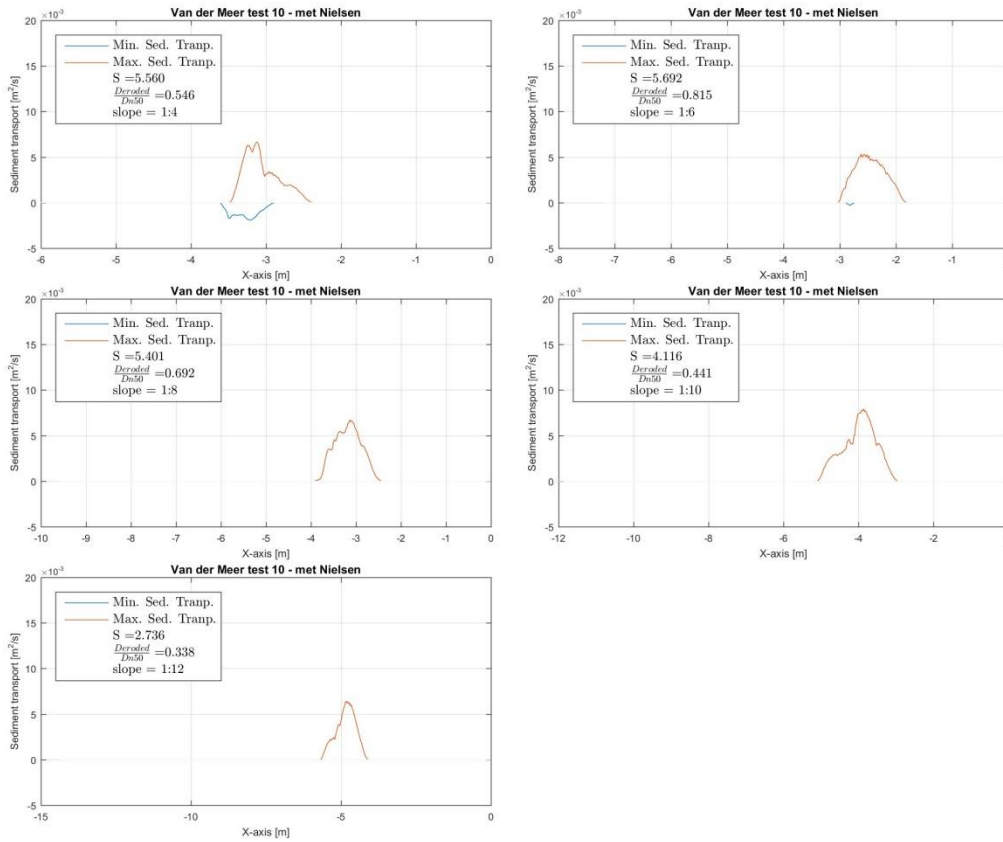


8.3.10 VAN RIJN [2007] test 14 – Shields

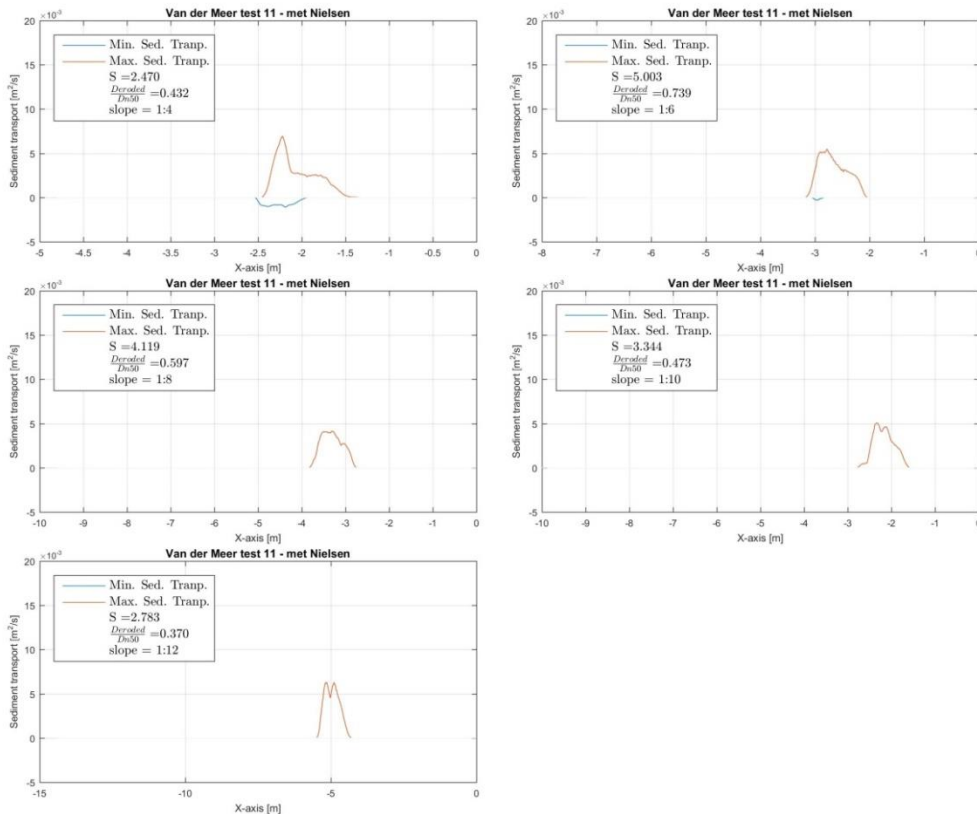


8.4 Sediment transport

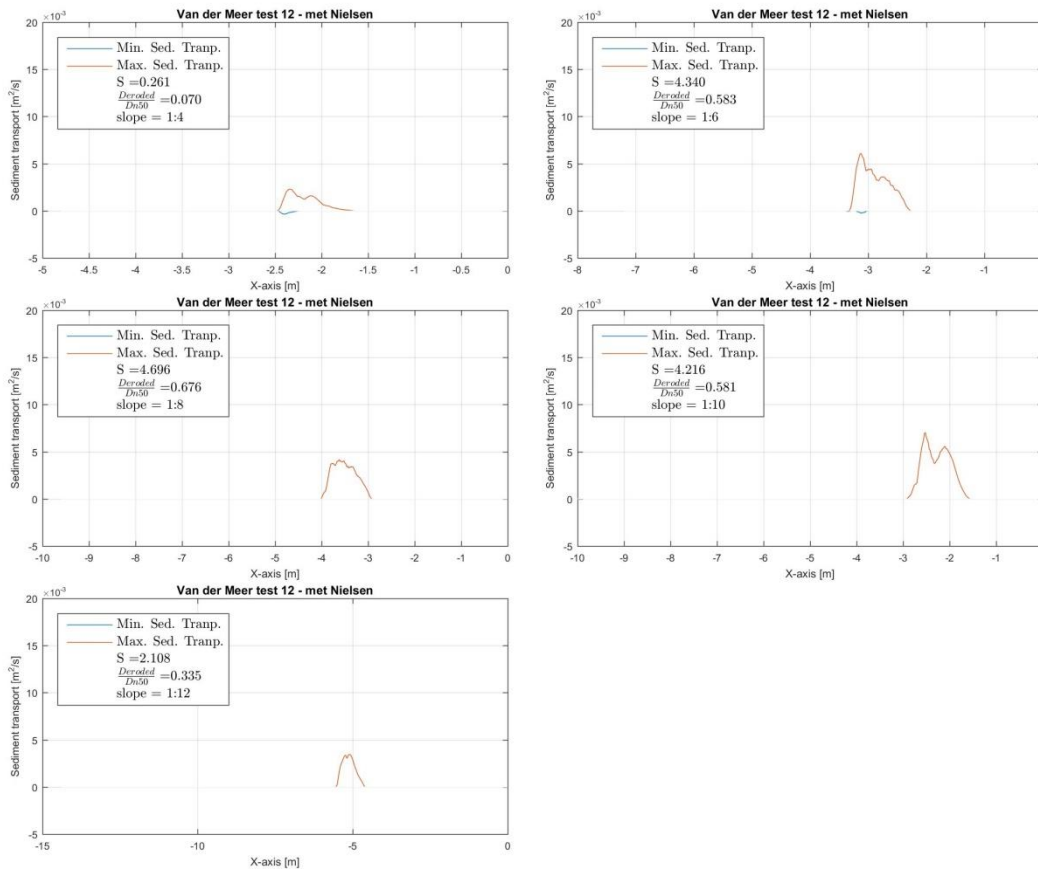
8.4.1 NIELSEN [2006] test 10 – Sediment Transport



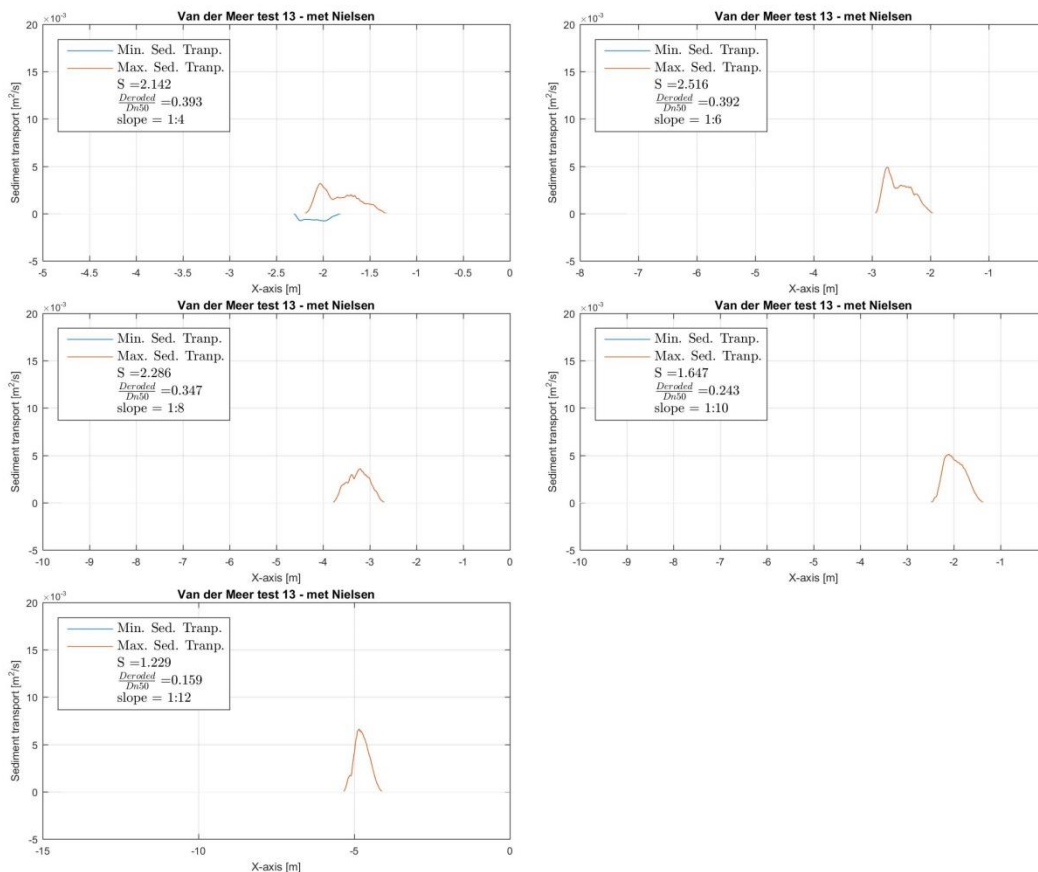
8.4.2 NIELSEN [2006] test 11 – Sediment Transport



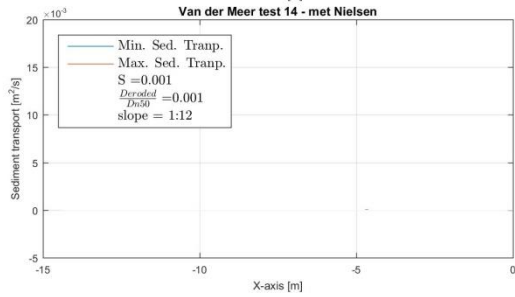
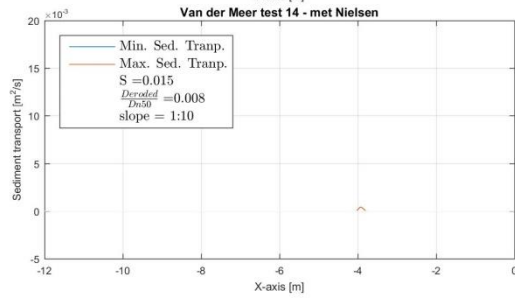
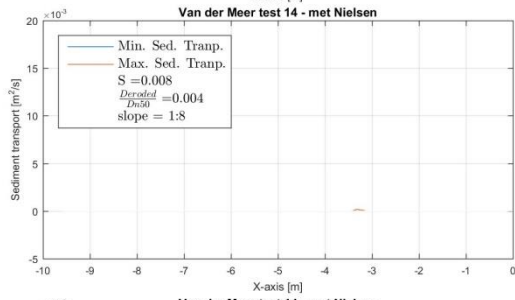
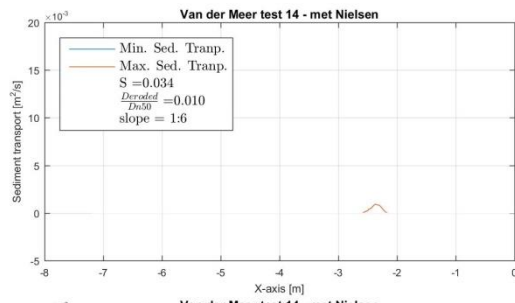
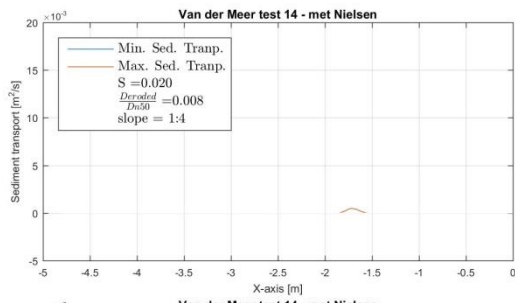
8.4.3 NIELSEN [2006] test 12 – Sediment Transport



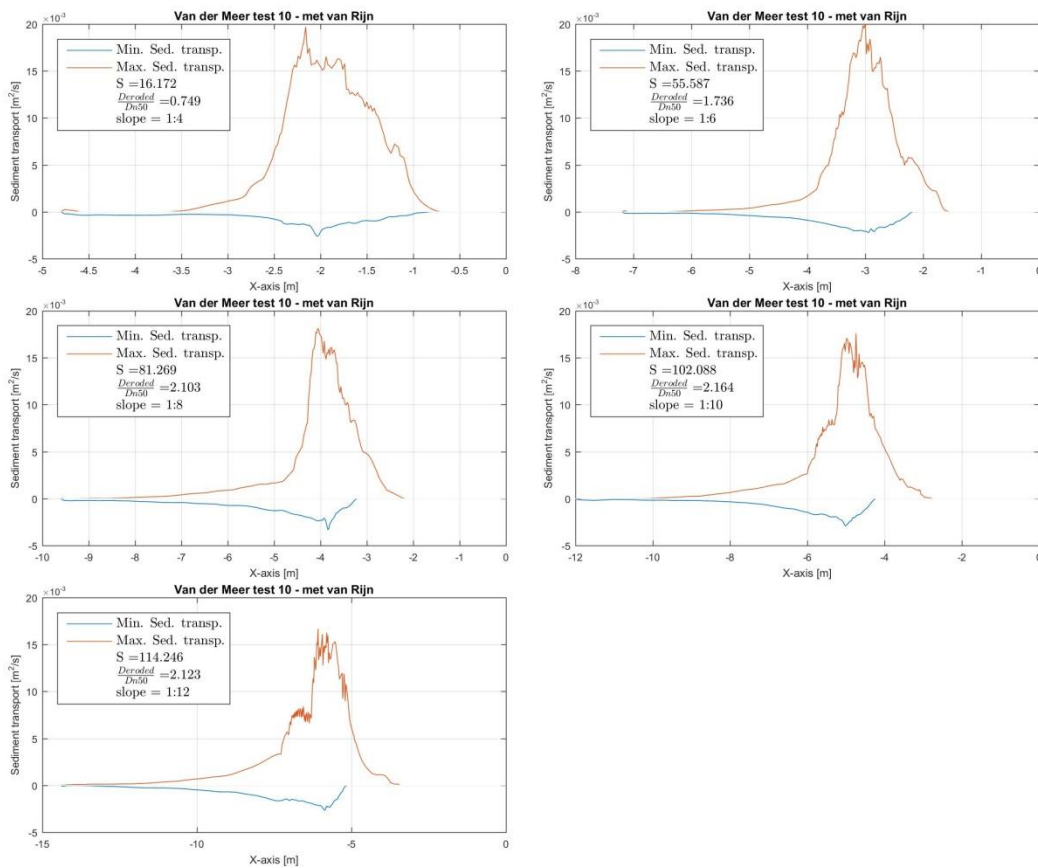
8.4.4 NIELSEN [2006] test 13 – Sediment Transport



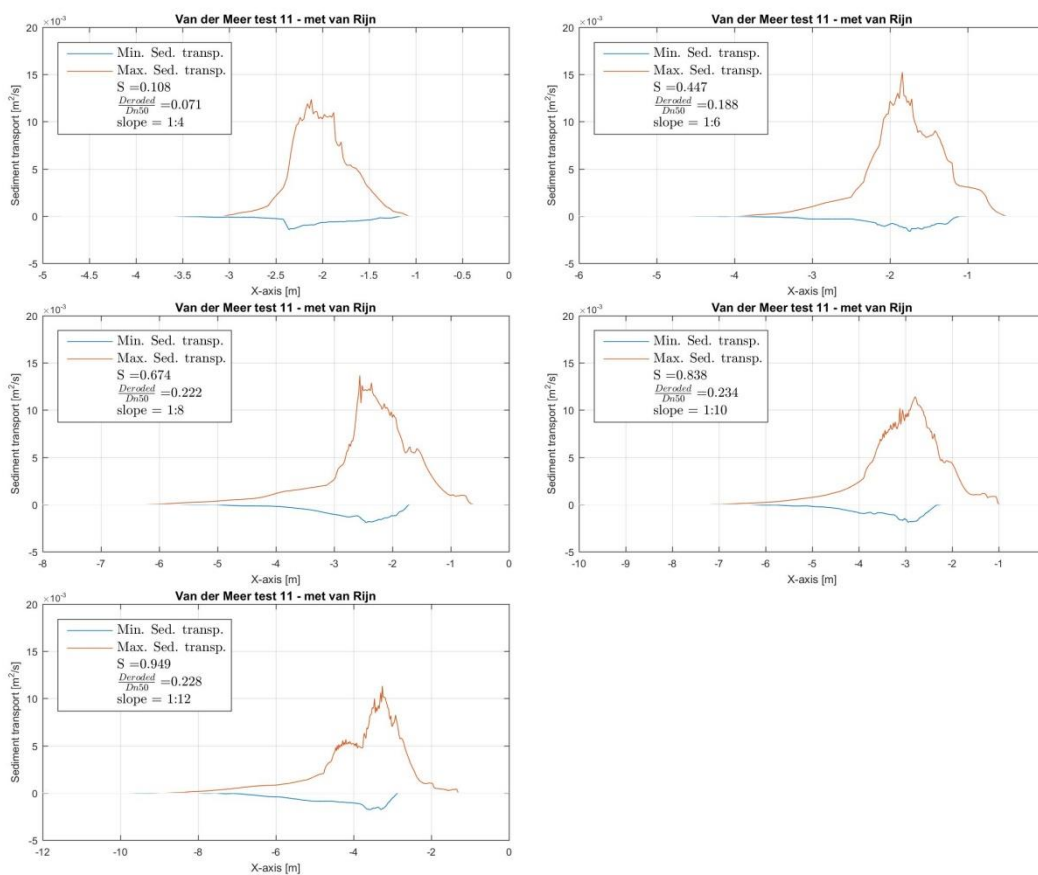
8.4.5 NIELSEN [2006] test 14 - Sediment Transport



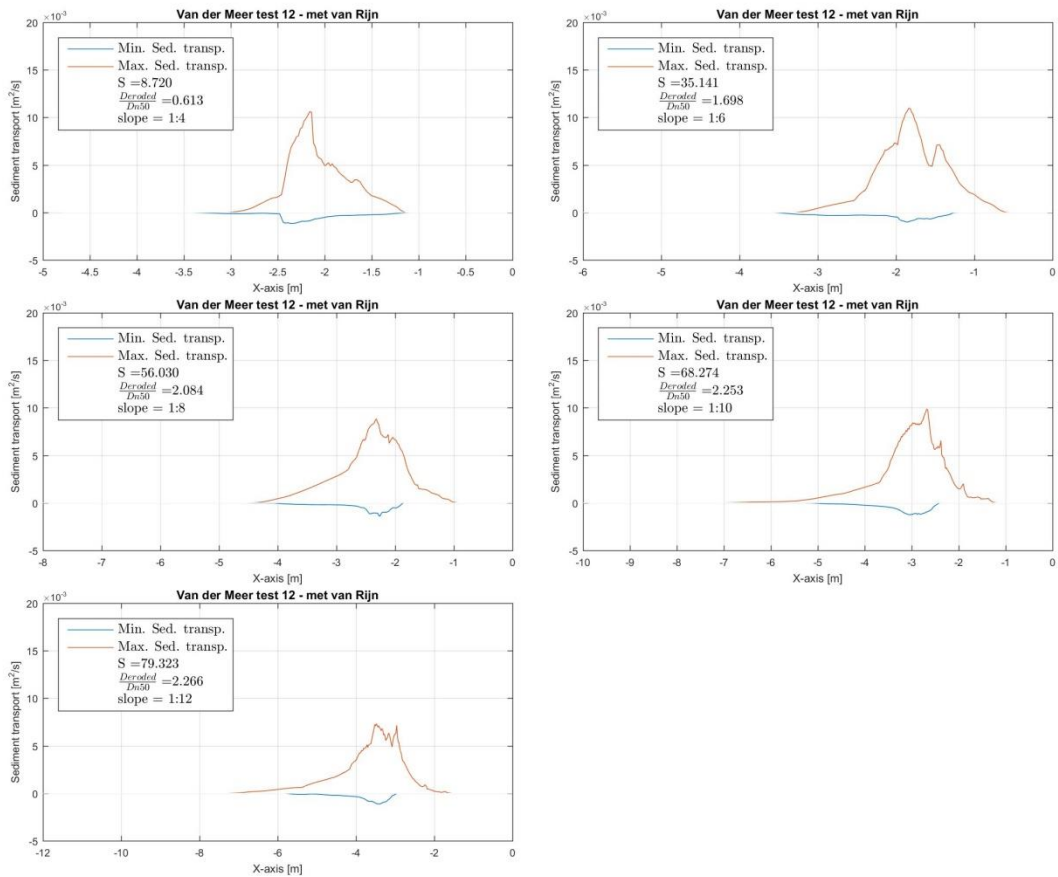
8.4.6 VAN RIJN [2007] test 10 – Sediment Transport



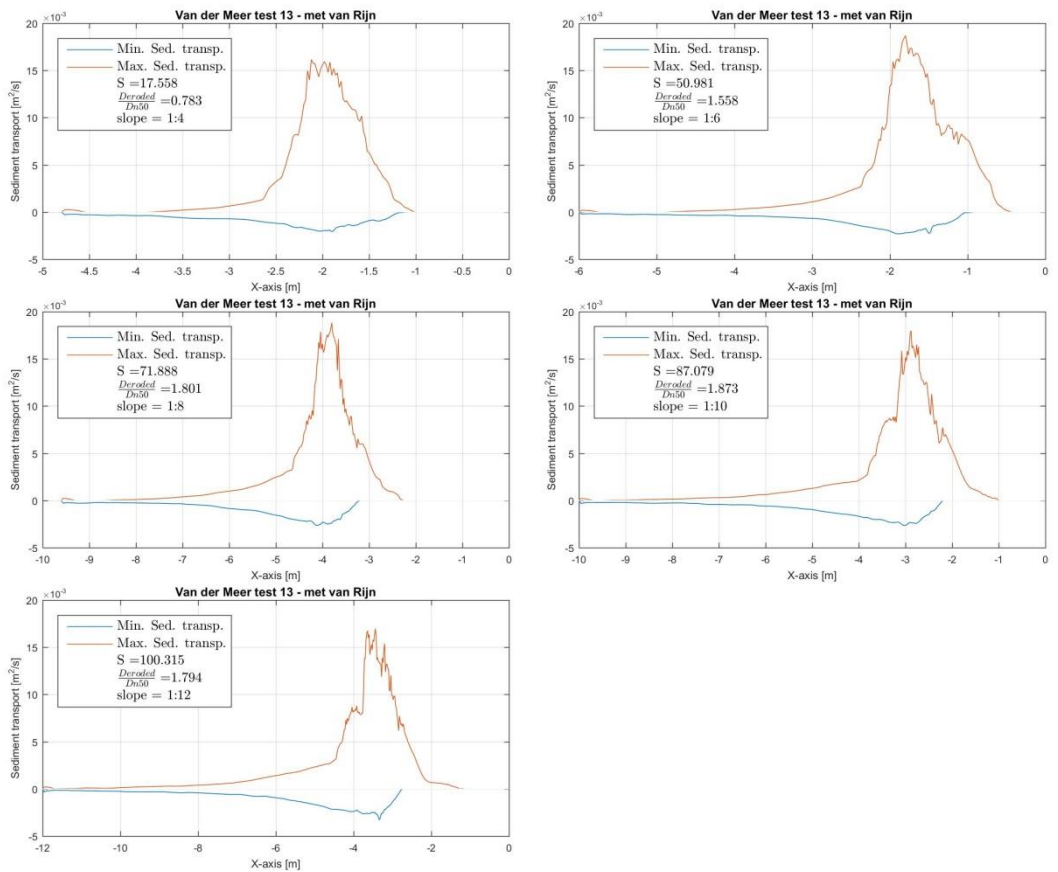
8.4.7 VAN RIJN [2007] test 11 – Sediment Transport



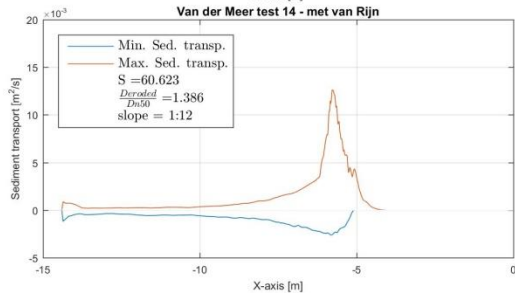
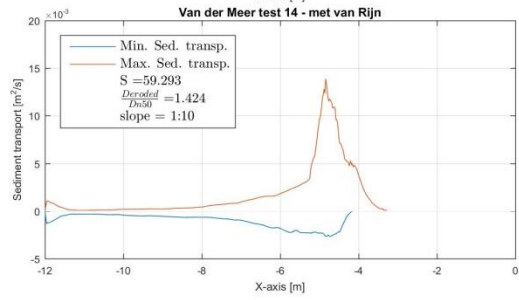
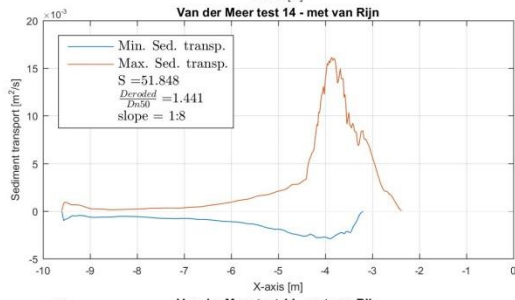
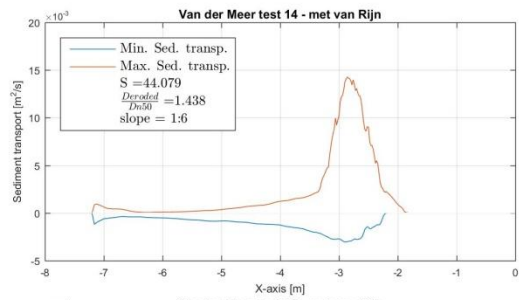
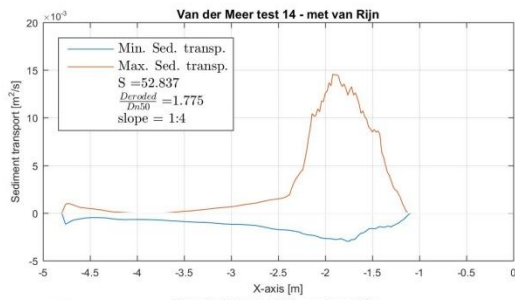
8.4.8 VAN RIJN [2007] test 12 – Sediment Transport

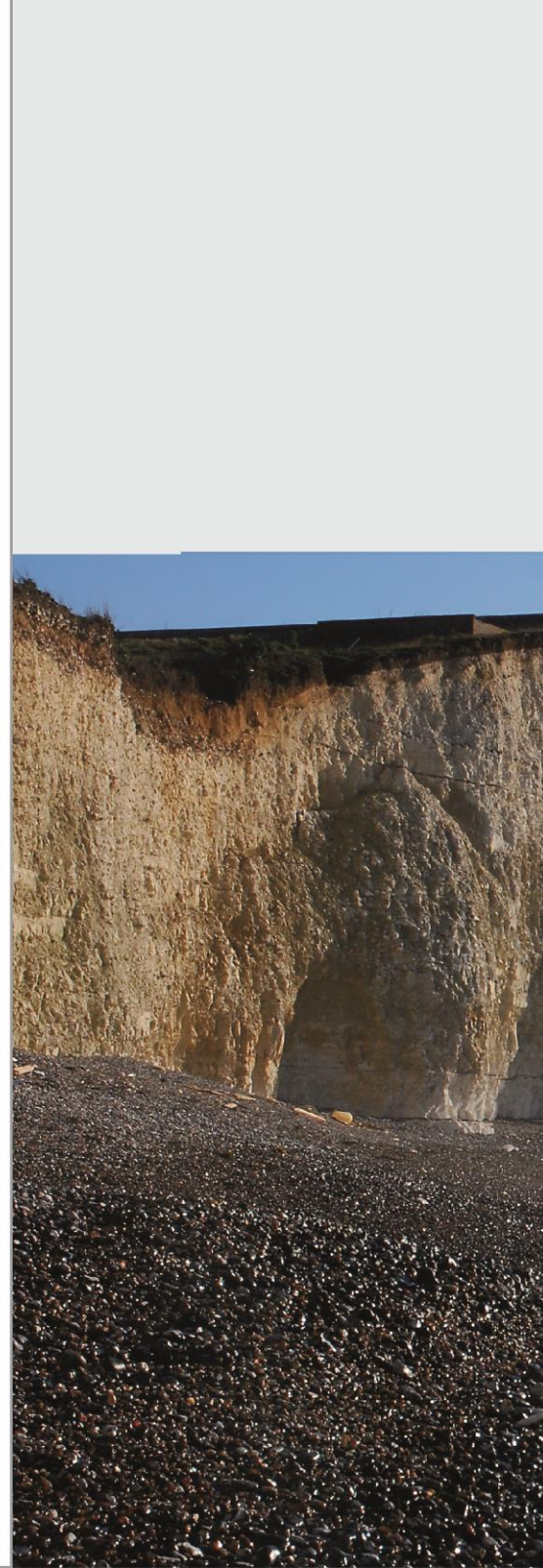


8.4.9 VAN RIJN [2007] test 13 – Sediment Transport



8.4.10 VAN RIJN [2007] test 14 – Sediment Transport





Master of Science Thesis

Title: XBeach-G as a Design Tool for Rock on mild slopes under wave loading.

University: TU Delft - Faculty Civil Engineering and Geoscience

Author: Dhr. M.G. Postma

Year: 1 July 2016

Publisher: TU Delft Repository